Universidade do Minho
Escola de Medicina

Mariana Rodrigues Resende da Silva

Assembly of granulomas during mycobacterial infections in mice: cellular and molecular dynamics

outubro de 2018

Assembly of granulomas during mycobacterial infections in mice: cellular and molecular dynamics
Mariana Rodrigues Resende da Silva
UMinho | 2018

FCT Fundação para a Ciência e a Tecnologia
MINISTÉRIO DA EDUCAÇÃO E CIÊNCIA
COMPETE 2020
NORTE2020 PROGRAMA OPERACIONAL REGIONAL DO NORTE
PORTUGAL 2020
UNIÃO EUROPEIA
Fundo Europeu de Desenvolvimento Regional

Universidade do Minho
Escola de Medicina

Mariana Rodrigues Resende da Silva

Assembly of granulomas during mycobacterial infections in mice: cellular and molecular dynamics

Tese de Doutoramento em Ciências da Saúde

Trabalho efetuado sob a orientação do
Doutor António Gil Castro
e do
Doutor Rui Appelberg

outubro de 2018

STATEMENT OF INTEGRITY

I hereby declare having conducted my thesis with integrity. I confirm that I have not used plagiarism or any form of falsification of results in the process of the thesis elaboration.

I further declare that I have fully acknowledged the Code of Ethical Conduct of the University of Minho.

University of Minho, October 10, 2018

Full name:

Mariana Rodrigues Resende da Silva

Signature: Mariana Rodrigues Resende da Silva

The work presented in this thesis was developed at:

Microbiology and Infection Research Domain,

Life and Health Science Research Institute (ICVS),

School of Medicine, University of Minho, Braga, Portugal

ICVS/3B's
Associate Laboratory

Universidade do Minho
Escola de Medicina

I3s - Instituto de Investigação e Inovação em Saúde.

IBMC - Instituto de Biologia Molecular e Celular,

Universiade do Porto, Porto, Portugal

INSTITUTO DE INVESTIGAÇÃO
E INOVAÇÃO EM SAÚDE
UNIVERSIDADE DO PORTO

IBMC
INSTITUTO DE BIOLOGIA MOLECULAR E CELULAR
INSTITUTE FOR MOLECULAR AND CELL BIOLOGY

Trudeau Institute, Saranac Lake, NY 12983, USA

TRUDEAU INSTITUTE
IMPROVING HEALTH THROUGH MEDICAL RESEARCH

The work presented in this thesis was funded by:

Fundação para a Ciência e Tecnologia (FCT) through the PhD fellowship SFRH/BD/89871/2012.

Structured program on bioengineered therapies for infectious diseases and tissue regeneration (Grant NORTE-01-0145-FEDER-000012) supported by Norte Portugal Regional Operational Programme (NORTE 2020, under the Portugal 2020 Partnership Agreement, through the European Regional Development Fund).

FEDER - Fundo Europeu de Desenvolvimento Regional funds through the COMPETE 2020 – Operacional Programme for Competitiveness and Internationalisation (POCI), Portugal 2020; and by Portuguese funds through FCT/Ministério da Ciência in the framework of the project "Institute for Research and Innovation in Health Sciences" (Grant POCI-01-0145-FEDER-007274).

AKNOWLEDGMENTS

I first want to acknowledge my advisors Rui Appelberg and Gil Castro. Rui, it was a tremendous privilege to work with you and to learn from you. I want to thank you for your availability, your ruthless honesty and your support (although sometimes difficult to hear it). Five years ago I would never guess I would have so much fun. Gil, I end up not spending much time at your lab, but it was a pleasure to work with you and I would like to thank for your support and advice.

To Andrea Cooper, although you were not a formal advisor you were a true mentor. Thank you for receiving me so well. Both at the Cooper lab and the Appelberg lab I was given the opportunity to chase my own ideas, and to feel the adrenaline and the rush of testing my own hypothesis (sometimes involving a lot of mice). I have learned so much, even when I failed. It was essential for my engagement and my thrill with science. I realize now that this opportunity is not so common.

During these last years I have worked with different people in different institutes:

At Trudeau institute I felt really welcomed for everyone. I want to acknowledge everybody form the Cooper lab: John; Jeff, who was a pivotal help for all the in vivo experiments; and Mingfeng, my labmate and roommate with whom I lived some of the most unbelievable stories. I want to thank everyone from the campus, particularly to Bill, Liz, Anju and their families. I miss those barbecue nights. I specially want to thank Jen and Chris, the most awesome lumberjack family, and to Frank and Eve. Your help and companion during my time in Saranac Lake were really important. I will nourish our friendship forever.

At ICVS I want to acknowledge everybody from the MIRD where I always felt welcomed. In particular I want to thank Egídio Torrado (my brain still retains the smell of fresh coffee in the morning, and the dinners you cooked during those 2 weeks we share the house in SL), Catarina Ferreira, Inês Mesquita, and Joana Gaifem my personal keeper of the pc charger. I want to acknowledge Ricardo Silvestre who not only helped me with the bureaucracy of ICVS, but was my first scientific mentor. I learned a lot from you and we had so much fun doing science!

At IBMC/i3s I want first to thank to former members of the LMII lab. Lília Pinela, the breakdance queen, and Marisa Teixeira, the lab got much more fun with you. Marcos Cardoso, the cell counting god, you know how important you were to this thesis. Without you the experiments would not have happened. It is a pleasure to work with you, and we also have lot of fun working together. I want to acknowledge everyone form the TDF group but in particular to

Nuno Alves for the support and to Ana Rosalina, friend and companion of countless late nights in the lab. You also rule on breakdancing! During these years I had the luck to work with generous colleagues and friends who were always available to help and to support me. I want to thank everyone from the MP group, particularly to Tânia "primer designer" Cruz, and Ana Georgina, the brigadeiro supplier! A huge thanks to Margarida Duarte. For the friendship, the endless hours talking gibberish, but also talking about science. I learned a lot with you. I almost enjoy to listening about mitochondria.... (or not)! I won't forget your daily calls to check on my sanity while I was writing this thesis. I am really grateful to everyone from the Immunobiology group, where I felt welcomed since day 1. I particularly want to acknowledge Manuel Vilanova for all the support. It has been pleasure to spend this time in your lab. Alexandra Correia you have been a tremendous support, there is no words to express my gratitude. Ricardo Fróis, the artist also known as "young grasshopper, master of design and ppt figures, looser of all esferopong games". My favorite person to bully! I want to thank you for your help and your invigorating enthusiasm. You made the lab a much funnier place. I want to thank Tânia Lima, companion of all twixs, Rita Pedro, Carla, and Filipa Gláucia who is always willing to move to the "bad" flow chamber just because of me!

From older times I want to thank colleagues and friends that were equally important during my scientific pathway: Diana Moreira, Joana Cunha, Nuno Santarém, Sofia Costa-Lima, Carine Gonçalves, Mafalda Santos, and Catarina Leitão. Despite the distance your friendship and understanding were essential during different times. Lúcia Teixeira, friend and travel companion, I want to thank you for your scientific consulting services via whatsapp, and most important for your friendship. Rita Seabra, old friend, although we are no longer in the same institute you were particularly important in the first years of this journey. Finally I want to acknowledge Ana Seixas for the constant support (despite the occasional bullying), for the endless conversations, science discussions, and most important for the unconditional friendship.

On a personal note I want to thank all my family, particularly my parents for your unconditional support and continued belief in me. To Pedro, I know it wasn't always easy but it was much better because it was with you. I am truly thankful for your belief in me, and most important for your patience. Finally I would love to tell all my direct and extended family that from now on, the endless waiting times and the consequent late night dinners are over. But we all know that won't be true!

Thank you.

ABSTRACT

Granulomas are organized accumulations of inflammatory cells typically found during mycobacterial infections. Although for a long time believed to confer protection to an infected host, recent evidence has challenged this idea, and raises the possibility that granulomas may provide a sanctuary for the microbe by facilitating its proliferation in the infected animal. Thus it is essential to understand the genesis of this inflammation type and elucidate its role in the development of protective immunity. Here we dissect the dynamics of granuloma formation and its impact in the development of protective immunity during distinct phases of the immune response to mycobacterial infections: from the early innate mechanisms behind granuloma initiation, through the adaptive immunity and its action on macrophages necessary for granuloma development, to the final steps leading to granuloma necrosis.

IFN-γ is directly implicated in the most important microbicidal mechanisms, playing a central role during both innate and adaptive immune response against mycobacteria. This cytokine, also known to be required for granuloma development, is mostly produced by NK cells during the innate immune response and by T cells at the onset of the adaptive immunity. However, evidence from animal models lacking adaptive immunity suggests the involvement of a non-NK innate cell source of IFN-γ required for resistance to mycobacteria. We have identified a rare population of IFN-γ-expressing $CD45^+$ $Thy1.2^+$ cells that are independent of the common-γ chain of the IL-2 receptor and are of a nonlymphoid, nonmyeloid and non-NK lineage. Moreover we provide evidence that these cells localize within the mycobacterial granuloma and can provide partial protection to *Mycobacterium avium* infected-immunocompromised mice. We have further explored the role of IFN-γ on the onset of the adaptive immunity. The impact of IFN-γ has been widely attributed to its action on macrophages, particularly in the context of pathogens like mycobacteria which have this cell as their main target. We used the MIIG mouse model, whose macrophages are unresponsive to IFN-γ to explore the specific relevance of the IFN-γ-mediated macrophage activation in vivo. We confirmed the requirement of IFN-γ inducing resistance to *M. avium* infection and observed the unexpected result that macrophage activation by this cytokine is not pivotal for such protective immunity or for granuloma development. Additionally we found that TNF-α may compensate for the lack of IFN-γ-signaling on macrophages, thus contributing for the resistance to *M. avium* infection.

Granuloma central necrosis is associated with more severe forms of mycobacterial infection since it compromises tissue integrity and can facilitate bacterial spread. In a previous work from

our lab we have provided evidence that granulomas become hypoxic before the onset of the necrotic process and that the hypoxia adaptor molecule HIF-1α plays a central role in preventing the earlier development of liver granuloma necrosis in a *M. avium* infection context. Here we assessed how the transcription factor HIF-1α may impact granuloma development in the lungs of *Mycobacterium tuberculosis* (Mtb)-infected C57BL/6 mice. Our data suggests that while Mtb-infected mice do not develop granuloma necrosis in the lung, HIF-1α is absolutely required to limit the pulmonary inflammatory response.

In summary, the findings presented in this thesis contribute to a better understanding of the mechanisms behind granuloma development and the protective immunity to mycobacterial infections. We provide novel data that may be useful to delineate new approaches to cope with mycobacterial infection.

RESUMO

Os granulomas são estruturas constituídas por acumulações de células inflamatórias que se desenvolvem durante a resposta a infecções por micobactérias. Apesar de, durante muito tempo se acreditar que estas estruturas conferem protecção ao hospedeiro, recentemente surgiram evidências que desafiam esta ideia, colocando em hipótese que os granulomas possam funcionar como um santuário para as bactérias facilitando a sua proliferação no animal infectado. Assim, é essencial comprender a génese deste tipo de inflamação e elucidar o seu papel no desenvolvimento da imunidade protectora. Nesta tese dissecamos a dinâmica de formação do granuloma e o seu impacto no desenvolvimento da imunidade protectora ao longo de diferentes fases da resposta imune a infecções micobacterianas: começando pelos mecanismo inatos que estão por trás da formação inicial do granuloma, passando pelo imapcto da resposta adaptativa na activação dos macrófagos e desenvolvimento do granuloma, até aos processos finais que podem levar à necrose central do granuloma.

O IFN-γ está directamente implicado na activação dos mecanismos microbicidas mais importantes da célula, desempenhando um papel fundamental tanto durante a resposta inata como na resposta adaptativa contra a infecção por micobactérias. Esta citoquina, que também é requerida para o desenvolvimento do granuloma, é maioritariamente produzida por células NK durante a imunidade inata e por células T durante a imunidade adaptativa. No entanto, a partir de modelos animais que não têm imunidade adaptativa, têm surgido evidências do envolvimento de uma fonte celular inata produtora de IFN-γ, que não as células NK, necessárias na resistência à micobactéria. De facto, nós identificamos uma população rara de células $CD45^+$ $Thy1.2^+$ capazes de expressar IFN-γ e que são independentes da cadeia γ pertencendo a uma linhagem de céluas não-linfoide, não-mieloide e não-NK. Além disso, mostramos eviências de que estas células se localizam no granuloma micobacteriano e proporcionam um protecção parcial em murganhos imunocomprometidos infectados com *Mycobacterium avium*. Nesta tese também aprofundamos o estudo do papel do IFN-γ durante a imunidade inata. O impacto do IFN-γ tem sido na generalidade atribuído à sua acção sob os macrófagos, particularmente na resposta a patogénios como a micobactéria que têm esta célula como principal alvo. Para explorar, *in vivo*, a relevância da activação específica do macrófago mediada pelo IFN-γ, usamos o modelo de murganho MIIG cujos os macrófagos não respondem ao IFN-γ. Confirmamos assim que o IFN-γ é necessário para a indução de resistência à infecção por *M. avium* e mostramos, inesperadamente, que a activação dos macrófagos por esta citoquina não é essencial para a

imunidade protectora nem para o desenvolvimento do granuloma. Além disso, mostramos também que o TNF-α pode compensar a ausência da sinalização do IFN-γ no macrófago, contribuindo assim para a resistência à infecção com *M. avium*.

A necrose central nos granulomas está associada a formas mais severas da infecção micobacteriana uma vez que compromete a integridade do tecido, podendo facilitar a disseminação da bactéria. Num trabalho prévio do nosso grupo, mostramos evidências que os granulomas se tornam hipóxicos antes do início do processo necrótico, e que a molécula adaptadora à hipóxia HIF-1α desempenha um papel importante na prevenção do desenvolvimento da necrose em granulomas do fígado numa infecção por *M. avium*. Nesta tese, mostramos como é que o factor de transcrição HIF-1α pode afectar o desenvolvimento do granuloma em pulmões de murganhos C57BL/6 infectados com *Mycobacterium tuberculosis* (Mtb). Os nosso resultados sugerem que, embora os murganhos infectados com Mtb não desenvolvam necrose nos granulomas, o HIF-1α é necessário para limitar uma resposta inflamatória excessiva nos pulmões.

Em conclusão, os resultados apresentados nesta tese contribuem para uma melhor compreensão dos mecanismos adjacentes ao desenvolvimento do granulomas e à resposta imune protectora contra infecções por micobactérias. Adicionamos assim novos dados que poderão ser utéis no desenho de novas estratégias para lidar com a infeccção por micobactérias.

TABLE OF CONTENTS

LIST OF ABBREVIATIONS

AHR	Aryl Hydrocarbon Receptor
AIDS	Acquired Immune Deficiency Syndrome
AA	Arachidonic Acid
CD	Cluster of Differentiation
CFU	Colony Forming Units
CGD	Chronic Granulomatous Disease
CHILP	Common Helper-like Innate Progenitor
CILP	Common Innate Lymphoid Progenitor
CLP	Common Lymphoid Progenitor
COX	Cyclooxygenase
CR	Complement Receptor
Dpi	Days post infection
BCG	Bacillus Calmette Guerin
DCs	Dendritic Cells
dpi	days post infection
EOMES	Eomesodermin
ESX-1	Early secretory antigenic target (ESAT-6) secretion system-1
FCγR	Fcγ Receptor
FMO	Fluorescence Minus One
GATA3	GATA-binding protein 3
IFN	Interferon
Ig	Immunoglobulin
IL-	Interleukin
ILC	Innate Lymphoid Cell
iNOS	inducible Nitric Oxide Synthesis
Lin	Lineage
LTi	Lymphoid Tissue inducer
MHC	Major Histocompatibility Complex
MyD88	Myeloid differentiation primary response 88
Mtb	*Mycobacterium tuberculosis*

MSMD	Mendelian Susceptibility to Mycobacterial Disease
NFIL3	Nuclear Factor Interleukin-3 regulated
NK	Natural Killer
NO	Nitric Oxide
NOXs	NADPH oxidases
NRAMP1	Natural resistance-associated macrophage protein 1
NTM	Nontuberculous mycobacteria
PAMP	Pathogen Associated Molecular Pattern
PGE_2	Prostaglandin E2
PLZF	Promyelocytic Leukemia Zinc Finger
PRR	Pattern Recognition Receptor
RAG	Recombination Activating Gene
RNS	Reactive Nitrogen species
RORα	Retinoic acid-related Orphan Receptor alpha
RORγt	Retinoic acid-related Orphan Receptor gamma
ROS	Reactive Oxygen Species
Sca-1	Stem Cells Antigen-1
SCID	Severe Combined Immunodeficient
TB	Tuberculosis
TCR	T Cell Receptor
TFR	Transferrin Receptor
Th	T helper
TLR	Toll-Like Receptor
TNF	Tumor Necrosis Factor
TRAIL	TNF-related apoptosis-inducing ligand
Treg	regulatory T
TSLP	Thymic Stromal Lymphopoietin
WT	Wild Type
YFP	Yellow Fluorescent Protein
αLP	alpha Lymphoid Progenitor
γc	gamma chain

List of Manuscripts

The work presented in this thesis collects the following original scientific manuscripts:

1. **Resende M**[#], Cardoso MS, Ribeiro AR, Flórido M, Borges M, Castro AG, Alves NL, Cooper AM, Appelber R. (2017). Innate IFN-γ-producing cells developing in the absence of IL-2 Receptor common γ-chain. ***J Immunol*** 199:1429-1439 [*Thesis Chapter II*]

[#]manuscript written by the first author and edited by all other authors

2. **Resende M**[#], Cardoso MS, Fróis-Martins R, Borges M, Jordan MB, Castro AG, Appelberg R. (2018). TNF-mediated compensatory immunity to *Mycobacterium avium* in the absence of macrophage activation by IFN-γ. ***(Under preparation)***. [*Thesis Chapter III*]

[#]manuscript written by the first author and edited by all other authors

3. **Resende M***, Ferreira CM*, Barbosa AM, Cardoso MS, Sousa J, Silvestre R, Castro AG, Appelberg R, Torrado E[#]. (2018). Hif-1α activity in the myeloid compartment regulates pulmonary inflammation and susceptibility to *Mycobacterium tuberculosis* infection. ***(Submitted for publication)***. [*Thesis Chapter IV*]

*These authors have contributed equally to this work

[#]manuscript written by the last author and edited by all other authors

Chapter I

GENERAL INTRODUCTION

1. Mycobacterial infections

Bacteria from the genus *Mycobacterium* are highly diverse encompassing more than 160 species and subspecies (1). These organisms are characterized by a thick cell wall mainly composed by a mycolyl-arabinogalactosyl-peptidoglycan mycolic acid core (2, 3). This lipid rich cell wall provides them high hydrophobicity and acid- alcohol-fast features, making these bacteria weakly gram positive, only identified through the Ziehl-Neelsen staining method (4). Importantly due to their specific cell wall, mycobacteria are particularly resistant to therapeutic agents and resistant to chemical disinfectants, making it difficult to prevent transmission (2, 5). The mycobacterium bacillus is also characterized by its easy aerosolization, a feature also due to their high hydrophobicity (6).

Although most mycobacteria are non-pathogenic or conditionally pathogenic environmental saprophytes found in soil and water sources (1, 5), *M. tuberculosis* (Mtb) the foremost pathogenic species of mycobacteria for the human host, is a facultative intracellular pathogen that has never been identified in the environment (7, 8). The Mtb bacillus, first identified by Robert Koch (4, 9), is the etiological agent for tuberculosis (TB) known to be spread through aerosolized particles in a human-to-human contact basis (4). TB manifestations are mostly pulmonary but the bacillus can disseminate to other organs (4). The high morbidity and mortality associated with TB renders the Mtb bacillus of great interest to the scientific community. On the other hand, nontuberculous mycobacteria (NTM) or atypical mycobacteria are ubiquitous in nature but can also be found in animal hosts. One of such microbe is *M. avium* which preferentially infects immunocompromised individuals, although human-to-human transmission is not documented (10, 11). Instead the most likely source of human infections is from contaminated water sources. In the urban environment *M. avium* has been mostly found in tap water and in hospitals hot water distribution systems as these bacteria can survive to temperatures above 50°C, pH changes, and to the most commonly used disinfectants (5). *M. avium* is seen as an opportunistic infectious agent affecting mainly humans with compromised immunity such as individuals with primary genetic immune deficiencies, AIDS, cancer, and individuals undergoing chemotherapy or immunosuppressive treatments. Local compromised immunity, as pulmonary emphysema, and chronic bronchitis, are also risk factors (5, 12). *M. avium* invades the human host via either the respiratory tract through the inhalation of aerosols containing bacteria (as Mtb), or through the intestinal track (1, 12). The number of NMT infections reported has been increasing which might be directly related with increased number of

individuals under immunosuppressive treatments, general ageing of the human population but also better diagnosis due to greater awareness by the clinicians to NTM infections (5, 11). In opposition TB incidence is decreasing worldwide though the number of multidrug-resistant patients is rising (4).

Both Mtb and *M. avium* are slowly-growing mycobacteria (4, 5) and although pathogenic (or opportunistically pathogenic), exposure to these organisms only rarely results in development of disease. Hence it is believed that the majority of the infected individuals either eliminate the bacillus or contain it in a latent state (4). It is estimated that less than 10% of the Mtb-infected individuals develop disease (4, 8). This holds true also for immunocompromised people infected with less virulent species. Indeed only 1/3 of SCID children, (T and B cell-deficient), vaccinated with BCG (the attenuated *M. bovis* Bacillus Calmette Guérin) develops disseminated disease (7, 13). It is therefore conceivable that in most of the infections innate immunity may be sufficient to control the infection with poor or no development of memory T cell immunity (14). As the majority of the diagnostic tests commonly used to detect Mtb infections relies in the adaptive memory T cell response, this suggests that even the number of cases of infection might be underestimated.

Experimental infection by the Mtb bacillus is by obvious reasons the main focus of the scientific community. However other species of mycobacteria are also used to gain comprehension on the pathogenesis of mycobacterial disease. *M. avium* and BCG are such examples. These bacteria share many features with the Mtb-induced host immune response, namely the development of granuloma structures (a complex aggregate of immune cells, discussed in detail below). More recently the zebrafish embryo-*M. marinum* infection model has been increasingly used in fundamental research. *M. marinum* is an environmental bacterium residing in water that infects fishes although it can also induce skin lesions in humans (15). Given its transparency and easily amenable gene manipulation the zebrafish embryo has become a powerful tool to study the innate immune response, namely the first steps of granuloma formation (15). All the examples given above do not require level 3 laboratory facilities, an enormous advantage over Mtb in terms of lab manipulation.

This thesis encompasses details of the host immune response and granuloma development in the mouse model using either *M. avium* or Mtb, therefore the following sections are focused on these two species of mycobacteria.

2. Immune response to mycobacterial infections

The mouse model of mycobacterial infection shares several features with the host immune response in humans although it does not completely mimic it (16). Still, given to the easy handling, affordable costs, availability of a wide range of reagents and accessibility to inbred and to genetically modified strains, the mouse model is extensively used by the scientific community (8). Indeed, the current knowledge that we have about mycobacterial induced immune response derives largely from this animal model. Using the mouse model we must be aware that the outcome of the infection relies in a combination of factors such as host genetic background, virulence of the mycobacterial strain, dose and route of inoculation.

C57BL/6, the mouse strain used in the work enclosed in this thesis, while being considered a resistant mouse model to Mtb infection (16) it is susceptible to infection by *M. avium* (17) (the NRAMP protein underlies this difference, discussed in detail in section 2.1.3). Despite these variations, both mycobacteria grow exponentially up to the first 3 to 4 weeks of infection reaching a plateau afterwards. In the case of Mtb infection, C57BL/6 mice eventually succumb after several months of infection (8). The beginning of the stationary phase, hence the control of bacterial replication, coincides with the onset of adaptive immune response (18). Indeed a pro-inflammatory adaptive response is required to activate the bactericidal mechanisms of mycobacterial-infected macrophages. Nevertheless if the inflammatory response is too strong it can become detrimental to the host (18, 19). The perfect immune response is able to clear the pathogen without leading to excessive immunopathology, which is achieved through a delicate balance between pro-inflammatory and anti-inflammatory mechanisms. The development of granuloma structures during mycobacterial infections promotes a continuous interaction between innate and adaptive immunity (20, 21).

2.1. Innate Immune Response

Macrophages are major effectors of the innate immune system and the main target of mycobacteria. For this reason the outcome of a mycobacterial infection depends tightly on the balance between the host ability to activate the macrophage killing mechanisms and the capacity of the bacteria to evade it (discussed throughout the next chapters). Neutrophils and Dendritic Cells (DCs) can also ingest mycobacteria and play major roles during the immune response (described in detail in chapter 2.1.4). Other innate cells include Innate Lymphoid Cells (ILCs) and Natural Killer (NK) cells, Natural Killer T cells (NKT), γδ T cells and Mucosal Associated Invariant T (MAIT) cells. Although these cells are known to respond rapidly to infection, their role in the

mycobacterial-induced immune response is not well established. The specific contribution of each one of these cellular populations is probably overcome by the action of the adaptive immunity making it more difficult to infer their role in the overall picture. Since the role of ILCs and NK cells in the immune response to mycobacterial infection is addressed in one of the works included in this thesis, these cells are discussed in detail later on (chapter 4).

2.1.1 Mycobacterial recognition by the innate cells

Host cells express specific receptors termed Pattern Recognition Receptors (PRRs) that recognize conserved molecules expressed by pathogens designated Pathogen Associated Molecular Patterns (PAMPs). This initial interaction between mycobacterial PAMPs and PRRs can facilitate phagocytosis of the bacteria into the host cell and shapes the subsequent immune response (22). The ability to activate different PRRs relies greatly in the mycobacteria cell wall composition which varies considerably among different species. Mycobacteria internalization into the host cell is known to be mediated by different receptors: mannose receptors (MR), type A scavenger receptors, complement receptors (CR), and Fcγ receptors (FcγR) (23). The relevance of a particular receptor engagement relies in the signals induced by each one of them. For instance, binding to CR3 fails to initiate a respiratory burst, while IgG coated mycobacteria bound to FcγR triggers the cell respiratory burst in a NOX2-dependent manner (reviewed in (23)).

Apart from phagocytosis, mycobacteria are also recognized by other receptors which drive cytokine signals that influence mycobacterial clearance. Toll-like Receptors (TLRs) are one of such class of receptors. Both *M. avium* and Mtb exhibit increased susceptibility in TLR2- (24-27) and TLR9-deficent mice when compared to the corresponding WT controls (28, 29). In the absence of MyD88, an intracellular adaptor molecule required for signaling of most TLRs, mice susceptibility to these two pathogens is even more pronounced (25, 29). These data suggests that other TLRs might also be involved in the innate recognition of both mycobacterial species. According to this, Bafica showed that during Mtb infection, MyD88-deficient mice still exhibited enhanced susceptibility when compared to TLR2/9-doube deficient animals (29). In contrast, the work of Hölscher showed TLR2/4/9 triple deficient mice to be equally susceptible to Mtb as WT mice (30). Alternatively the small effect from individual TLR-deficiency when compared to MyD88$^{-/-}$ mice might rely on signaling through IL-1 Receptor (IL-1R). This receptor also signals through MyD88 and in fact mice deficient in IL-1R are highly susceptible to Mtb (nearly indistinguishable from MyD88$^{-/-}$ mice) (31, 32). The same was not observed for *M. avium* where IL-1R$^{-/-}$ infected mice displayed similar bacterial loads as the control group (25). Hence in vivo data on TLR

contribution to Mtb susceptibility in the mouse model is somehow controversial. Nevertheless there are several in vitro studies showing the capacity of mycobacteria to activate the immune response upon engagement with different TLRs. Carmona and colleagues reported that activation via TLR2 or TLR4 varies according to the Mtb strain which might be critical for the consequent immune response (33). Besides TLRs, Mtb can also engage with other PRRs, such as c-type lectin receptors, NOD and NOD-like receptors (NLRs), either at cell surface or intracellularly (23, 34). Again although these receptors are involved in recognition and induction of the immune response, they do not contribute much to protection most likely due to a high degree of redundancy between all PRRs (35-37).

2.1.2 Phagocytosis and intracellular trafficking

Besides the variability of mycobacterial PAMPs among different species, PRRs are also differentially expressed by the different innate cells. Mycobacteria can infect neutrophils and DCs, but mainly infect macrophages where they reside and can replicate. For this reason the immune response to mycobacterial infections is highly centered on this cell. Upon recognition by PRRs the bacillus is engulfed by the macrophage and encapsulated in a membrane bound vacuole termed phagosome. Usually this vacuole would mature and fuse with the lysosome, an acidic organelle rich in hydrolytic enzymes capable of degrading the material within the phagosome. Mycobacteria however, developed mechanisms to escape the phagolysosome killing machinery. Both Mtb and *M. avium* can prevent phagosome-lysosome fusion and inhibit the acidification of the vacuole allowing the survival of the bacteria (38-42). This strategy allows mycobacteria to escape proteolytic degradation and avoid the consequent loading of processed peptides required for antigen presentation and initiation of the adaptive immune response. *Mycobacterium*-containing phagosomes actively interact with endosomes allowing extracellular nutrients, to reach the phagosome, hence the bacteria (43, 44). Interestingly it has been observed that the Mtb bacillus can evade from the phagolysosome into the cytosol where it has free access to nutrients, and it can replicate. This evasion mechanism was found to be dependent on the ESX-1 secretion system (45, 46) which is absent in *M. avium* species. It is believed that *M. avium* stays longer within the phagosome than the more pathogenic Mtb relying in the endosome-carrying nutrients to survive (1). One of such pivotal nutrients is iron which is transported into the phagosomes by the transferrin bound-transferrin receptor (TF-TFR) in the endosome membrane (47, 48).

Despite mycobacterial early evasion mechanisms, it is well established that IFNγ, a major cytokine produced by some innate immune cell populations but mostly produced by T cells,

inhibits the phagosome-endosome interactions on the infected macrophage (impairing iron availability), and promotes phagosome maturation creating a more hostile environment to the bacteria (48, 49). IFN-γ-inducible small GTPases have been demonstrated to be required for the fusion of the *Mycobacterium*-containing phagosome with lysosomes thus being critical to contain Mtb growth (50). These data illustrate the ability of the host immune response to overcome the bacterial modulation of the phagosome.

2.1.3 Killing mechanisms

In addition to acidification of the bacteria-containing vacuole, macrophages have other microbicidal mechanisms. Through the production of reactive species of nitrogen and oxygen within the cell, pathogens like mycobacteria are subjected to oxidative stress (RNS and ROS, respectively). In murine macrophages besides the PRR signals induced by the pathogen, the generation of such toxic intracellular environment is highly dependent on the action of IFN-γ and enhanced by the production of TNF-α. As a result these microbicidal mechanisms are highly amplified during the adaptive immune response (discussed in detail below).

Nitric Oxide (NO) and its metabolites are produced by the enzyme inducible NO synthase (iNOS or NOS2) which competes with Arginase-1 for the same substrate, L-arginine (51, 52). Upon infection, IFN-γ production results in elevated and sustained expression of iNOS (52). Supporting this notion, there is a direct correlation between iNOS and IFN-γ expression during the response to Mtb, both peaking around 20 dpi coinciding with the onset of IFN-γ^{+}CD4^{+} T cells in the lung (53). However there can be circumstances where IFN-γ is not the main inducer of iNOS. Recently Moreira-Teixeira and colleagues have shown that in the absence of IFN-γ signaling, type I IFN can induce iNOS expression in macrophage cultures infected with a highly virulent Mtb strain (54). Importantly, both NOS2-deficient and IFN-γ signaling-deficient mice (therefore with impaired NO production) are highly susceptible to Mtb and eventually succumb to infection (55-58). These data show that NO production through iNOS is essential for an efficient immune response and control of Mtb infection. On the other side of the spectrum, in the response to *M. avium* infection NO production can be detrimental to the host. Although in the absence of IFN-γ signaling, mice infected with *M. avium* also exhibit increased susceptibility, the same is not observed in mice lacking NO production. Indeed *M. avium*-infected NOS2-deficient mice are able to control bacterial proliferation to the same extent as the WT controls, or even better at longer time points of infection (59, 60). The control of *M. avium* replication in NOS2-deficient mice is

accompanied by an increase in the inflammatory response with larger granulomas and increased cellular influx particularly of T cells (60, 61). These data suggest that NO is important to restrict the inflammatory response namely by limiting T cell numbers as proposed by Cooper and colleagues (61).

The production of ROS (superoxide, hydrogen peroxide singlet oxygen, and others) is another effective anti-microbial mechanism. Mitochondrial respiratory chain and NADPH oxidases (NOXs) are two of the main sources of ROS. Free iron and cooper ions, haem groups and metal storage proteins can also contribute to increase ROS production (62). While a role for NO in response to mycobacterial infections in humans is not clear (51), there is a correlation between patients with impaired respiratory burst in macrophages and mycobacterial infections. Bustamante and colleagues have shown that Chronic Granulomatous Disease (CGD) patients, who owing to mutations in the gene *CYBB* encoding for gp91phox a subunit of the NOX2 enzyme, have deficient ROS production in all phagocytes, have increased predisposition to mycobacterial disease. The same was observed in patients with macrophage-specific *CYBB* mutations (63, 64). NOX2 is a multiprotein complex residing on plasma or phagosome membranes of phagocytes which upon activation releases ROS to the extracellular environment or to the vacuolar space. This complex is composed by 5 subunits which includes the cell membrane subunit gp91phox and the cytosolic protein p47phox (65).The assembly of phox subunits into the bacteria-containing phagosome is promoted by IFN-γ-induced GTPases activation (66) and signaling via TNF-Receptor 1 (TNFR1) is required for NOX localization into the phagosome and p47phox phosphorylation (67-69). In the mouse model of mycobacterial infection the role for NOX2 is not clear. Following Mtb infection, while one report showed a transient increase in lung bacterial loads at early time points in Phox-deficient mice (70), others have reported no differences in Mtb growth between the genetic-deficient mice and the WT counterparts (71, 72). In contrast, both *BCG* and *M. marinum* infection revealed increased bacterial proliferation and more severe disease in mice lacking the p47phox subunit (73, 74). In the *M. avium* infection model, whereas WT and Phox-deficient mice were shown to be equally resistant to an intravenous infection of a virulent strain of *M. avium*, Fujita ad colleagues reported gp91phox-deficient mice to be more susceptible to a clinically isolated strain of *M. avium* inoculated through the intratracheal route than WT animals (75, 76). In vitro, it was shown that macrophages infected with *M. avium* can produce superoxide, which is produced in increased amounts by low virulent strains in a process dependent on TNF-α. These data suggest that, due to the consequent decrease of ROS

production, inhibition of TNF-α might be an evasion mechanism from *M. avium* virulent strains (77, 78). Despite the unclear role of NOX2 activation in the control of mycobacterial replication in mice, a common consequence observed with the different mycobacterial species in Phox-deficient mice was the increase infiltration of inflammatory cells in the infected tissues (70, 72-74, 76).

Other way to limit bacterial growth is achieved by depriving the pathogens of essential nutrients like iron which is pivotal for mycobacterial replication within the cell. In fact, the host immune response has different mechanisms to limit the access of iron to the bacteria. In response to inflammatory signals namely IFN-γ, macrophages downregulate TFR expression, limiting iron import to the phagosome via endosome interaction (79). Iron and other divalent cations can also be actively removed from the bacteria-containing phagosome via the natural resistance-associated macrophage protein 1 (Nramp1) in a process induced by pro-inflammatory cytokines as IFN-γ, TNF-α or IL-1 (17). *Nramp1* (or *Slc11a1*) has two alleles that occur naturally in laboratory mouse strains, the R or the S allele encoding for a functional or a non-functional protein respectively (80). Mouse models like BALB/c or C57BL/6 are homozygous for *Nramp1*^{s} and display increased bacterial burdens upon infection with *M. avium* when compared to *Nramp1*^{r} mouse strains (17, 79, 81). These data are consistent with the thought that in the non-functional Nramp1, phagosomes are deprived of a mechanism that allows iron to be pumped out, thereby not restricting iron availability from the bacteria. Mtb induced susceptibility in mouse models was not found to be dependent on NRAMP1 (82), and so far a *NRAMP1* allele analogous to murine *Nramp1*^{s} in humans has not been described (1, 12).

2.1.4 Innate cells immunity

Recognition of mycobacterial products by specific receptors on phagocytic cells leads to internalization of the bacteria and to the activation of the host cells. This mycobacterial-induced activated state is translated into the production of several cytokines as IL-12, TNF, IL-6 and IL-1 by macrophages and DCs (reviewed in (83)), reflecting a pro-inflammatory status of the cell pivotal for activation of the adaptive immunity. In addition these cytokines promptly stimulate NK cells and other innate lymphoid cells (ILCs) to produce IFN-γ (discussed in detail on chapter 4). In addition TNF-α can act in an autocrine fashion over the infected cells and together with IFN-γ is able to induce the microbicidal machinery of the host cells. This early IFN-γ production by

innate cells is thought to be important to restrain bacterial replication before the adaptive immune response ensues.

The host immune response to mycobacteria is centered on macrophages as these cells are the main targets of the bacteria. In addition to the aforementioned microbicidal mechanisms that macrophages are equipped with and from which the bacillus tries to evade, the death pathway of the infected macrophages either by necrosis or apoptosis was shown to be pivotal in the outcome of the infection (84). Necrosis occurs via cell lysis which is beneficial to the mycobacteria since it enables the release of the microbe avoiding host defenses and allowing the spread to the neighboring cells. Apoptosis on the other hand, maintains the plasma membrane integrity intact enabling the restriction of bacterial growth (84). The cytokine IL-1 was found to induce the production of prostaglandin E2 (PGE_2) on macrophages (85) which protects cells from necrosis facilitating the repair of the plasma membrane (86, 87). The eicosanoid PGE_2 is a lipid mediator derived from arachidonic acid (AA) by the action of cyclooxygenases (COXs) and in its absence Mtb-infected mice are more susceptible to infection (86, 87). On the other hand, animals deficient in the 5-lipoxygenase, an enzyme that competes for the AA substrate to generate lipoxins and leukotrienes, are more resistant to infection (87). Taken together these data indicate that products of lipoxygenase promote Mtb growth via necrosis of the infected macrophage, while the IL-1 induced COX-dependent PGE_2 confers resistance to the infection by promoting apoptosis of the infected macrophage. IL-1 is thus an important mediator of the eicosanoids balance, contributing to host protection by influencing the cell death outcome of the infected macrophages (88). IL-1 encompasses IL-1α and IL-1β, both are pro-inflammatory cytokines and are produced by mycobacterial-infected macrophages (89). During the immune response to mycobacteria, most macrophages acquired a pro-inflammatory phenotype termed M1 in opposition to the more anti-inflammatory profile, M2. It is now known that this dualistic model of macrophage activation profiles is rather simplistic, and *in vivo* the different macrophage profiles represent a spectrum of activations status with M1 and M2 classifications representing extremes of this spectrum (90, 91). For ease of discussion the M1/M2 terminology is widely used although one must be careful to not oversimplify the reality. M1 activation is stimulated by TLR ligands and IFN-γ which is extensively produced during the immune response to mycobacteria infection particularly in the onset of the adaptive immunity (90, 91) (discussed in detail in chapter 2.2.1). On the other hand M2 activation is stimulated by IL-4 and IL-13 (90, 91) which are poorly induced during the host response to mycobacteria. Briefly, M1 macrophages are characterized by increased expression of

IL-1β, TNF-α and iNOS (among other important molecules) being thus related to the macrophage microbicidal mechanisms and a pro-inflammatory status. M2 activation on the other hand is characterized by down-regulation of the M1-related molecules and increased expression of arginase (among other molecules), being thus associated to a more anti-inflammatory profile and tissue remodeling (90, 91). An excessive pro-inflammatory response can often occur during the host immune response to mycobacterial infections and M1 macrophages can contribute to excessive pathology and disease exacerbation (92).

DCs are considered professional antigen presenting cells (APCs) and an essential key to trigger adaptive immunity. Upon infection, DCs activation is accompanied by the increased surface expression of MHC-II and the co-stimulatory molecules CD80, and CD86 which together with mycobacterial processed antigens equips host cells for antigen presentation. In a process dependent on CCR7 and IL-12p40, both induced by mycobacterial infection, DCs migrate to the draining lymph nodes (93, 94) where they are capable to present mycobacterial antigens to naïve T cells triggering an adaptive immune response (95, 96). CCR7 expression guides DCs toward the homeostatic chemokine CCL-21 expressed by the lymphatic endothelium while CCL-19 and CCL-21, expressed by cells in the lymph node, guide DCs to this organ (97). The time required for DCs to reach the lymph nodes and prime T cells is thought to contribute to susceptibility. The longer it takes the longer will be the uncontrolled bacterial growth period. Mtb susceptible mouse strains exhibit late T cell activation when compared to resistant strains, which might be a reflex of delayed DC-lymph node trafficking (98, 99). Recently, the group of Jean-Laurent Casanova has shown that patients with a particular mutation leading to decreased numbers of a conventional DC subset exhibit increased susceptibility to mycobacterial infections (100). This data illustrates the fundamental role of DCs in the anti-mycobacterial immunity.

In addition to macrophages and DCs, upon mycobacterial inoculation neutrophils are also readily recruited to the local of infection. Neutrophil anti-microbial mechanisms comprise rapid production of ROS and NO, production of proteolytic enzymes, antimicrobial peptides and molecules that sequester iron (101). An additional antimicrobial mechanism elicited by these cells is the development of neutrophil extracellular traps (NETs) which induce cell killing. The only evidence for the involvement of NETs during mycobacterial infection come from human samples and so far it has not been confirmed in the mouse model (102). Neutrophils have a protective effect in the beginning of mycobacterial infections. Several reports have shown that depletion of neutrophils before or during the first days of infection results in increased mycobacterial growth

(103, 104). In line with this, experiments with neutrophil transfer into infected hosts improved host outcome (103). The antimicrobial machinery of neutrophils is highly efficient however these cells are short-lived. Neutrophils usually die by apoptosis avoiding an inflammatory response. In the late 80's it was shown that macrophages from mycobacterial infected mice ingest neutrophil apoptotic cells and acquire some of their cytotoxic content, revealing a probable mechanism whereby macrophages enhance their antimicrobial activity (105). Later on, in vitro experiments confirmed this hypothesis showing that uptake of apoptotic neutrophils or granule contents by macrophages decreases Mtb growth (106). In a similar apoptosis- dependent process it has been shown that infected neutrophils can transfer mycobacteria or mycobacterial antigens to DCs, accelerating DC migration into the lymph nodes and the subsequent T cell activation (107). In a follow-up work, using pro-apoptotic Mtb mutants, the same authors have shown that Mtb can manipulate the immune response by avoiding neutrophil apoptosis and thereby delaying the adaptive immune response (108). Neutrophils produce an array of cytokines that also modulate the immune response. Production of IL-12, TNF-α and IL-1β by infected neutrophils amplifies the pro-inflammatory signals influencing T cell activation. On the other hand neutrophils also produce IL-10 which is essential to control mycobacterial-induced inflammation (109). In fact during chronic infection, increased neutrophilia is detrimental to the host due to excess of immunopathology (109, 110) (discussed in detail in chapter 2.3).

2.2. Adaptive Immune Response

Activation of the adaptive immune response is essential to control mycobacterial growth, particularly when innate immunity alone does not suffice. The mouse model shows us that restriction of bacterial growth is dependent on the onset of the adaptive immunity (18). In addition SCID children and people infected with HIV which have deficient adaptive immunity are more susceptible to mycobacterial infection and usually present disseminated disease in opposition to immunocompetent individuals where the disease is primarily pulmonary (6).

The role of B cells during mycobacterial infections has been neglected. In response to Mtb infection it is known that B cells can modulate T cell and cytokine response, accumulate in the granuloma structure and influence inflammation. However the overall contribution to the outcome of the infection remains poorly understood (111-113).

The adaptive immune response to mycobacterial infections is highly centered on T cells. Upon interaction with APCs carrying mycobacterial antigens, $CD4^+$ T and $CD8^+$ T cells are activated and mount antigen specific responses. $CD4^+$ T cells are critical in the outcome of the infection

whereas less is known on the role of $CD8^+$ T cell-mediated immunity. In response to mycobacteria, $CD8^+$ T cells are activated through MHC-I antigen restricted presentation and become capable of exerting cytotoxic mediated cell lysis and to produce TNF-α and IFN-γ (114). The protective role of these cells during Mtb infection has been demonstrated by the use of antibody-mediated depletion or genetic-ablated mice with impaired $CD8^+$ T cell response, where mice develop increased susceptibility and decreased survival when compared to the WT controls (115-118). Moreover adoptive transfer of Mtb-infected $CD8^+$ T cells into previously irradiated hosts enhanced resistance to Mtb (119). Despite the evident protective role of $CD8^+$ T cells in the response to Mtb the same is not observed during *M. avium* infection where the control of bacterial growth is similar in WT and $CD8^+$ T cell-depleted mice (120, 121). Still, $CD8^+$ T cells are recruited and accumulate in the granulomata induced either by Mtb or *M. avium*. It has become evident that $CD8^+$ T cells are required for optimal immunity particularly against Mtb, however the protective role of $CD4^+$ T cells is far more obvious.

The evidence from the fundamental role of $CD4^+$ T cells in the control of mycobacterial growth derives both from humans and the mouse model. In humans, the most illustrative example comes from AIDS patients, who have low $CD4^+$ T cell numbers, and are highly susceptible to develop mycobacterial disease induced by Mtb but also by poorly pathogenic species as *M. avium* (6, 122). In the mouse model, animals with deficient CD4 T cell immunity either by means of genetic ablation or antibody-mediated depletion exhibit increased bacterial burdens with mice succumbing to Mtb infection much earlier than mice with deficient CD8 T cell immunity or the WT controls. (117, 123). Infection by *M. avium* also exhibit increased bacterial loads in mice lacking $CD4^+$ T cells when compared to the WT controls, despite the increased bacterial growth mice did not succumb during the time that the experiments lasted (120, 121). The absence of $CD4^+$ T cells in *M. avium*-infected animals results in poor granuloma formation with smaller size and few lymphoid cells (124). Likewise, in the first weeks after Mtb infection, CD4-deficient mice exhibit poor granulomata though at later time points these granulomas become heavily infiltrated by granulocytes (123). $CD4^+$ T cell priming occurs in the lymph node through T cell receptor (TCR) interaction with DCs carrying mycobacterial antigenic peptides in a MHC-II restricted process (18, 125). For full T cell polarization besides the TCR-peptide-MHC-II interaction, co-stimulatory molecules and adequate cytokine signaling are required (18). Depending on the context, naive $CD4^+$ T cell can be polarized into different phenotypes. Th1 cells are driven by IL12 signaling and produce IFN-γ and TNF-α, Th2 cells are dependent on IL-4 and produce IL-4,

IL-5 and IL-13, and Th17 cells which driven by TGF-β, IL-6 and IL-1β, produce IL-17 (126). In the immune response to mycobacterial infections, $CD4^+$ T cells mainly polarize into Th1 cells but also into Th17 cells (both discussed in detail in the next sections). Regulatory T (Treg) cells are suppressive cells developed upon infection that might prevent inflammation but can also delay the onset of the adaptive response (127).

2.2.1. Th1 cells and the IL-12/IFN-γ axis

Th1 cells are characterized by the expression of the transcription factor T-bet and therefore IFN-γ is their signature cytokine. Once recruited to the site of infection, IFN-γ^+-producing Th1 cells act on infected macrophages to increase their anti-microbial activity which includes promotion of phagosome maturation, and production of RNIs and ROS. In addition Th1 cells also produce TNF-α which has a major role in enhancing the IFN-γ-induced microbicidal mechanisms. Deficiencies in IFN-γ signaling both in humans or the mouse model revealed the essential requirement of Th1 cells for the outcome of mycobacterial infections. These includes deficiencies in IL-12, the cytokine driving Th1 polarization, deficiencies in IFN-γ production by Th1 cells, deficiencies in the IFN-γ receptor particularly in macrophages, and deficiencies downstream of IFN-γ signaling in macrophages, such as in the transcription factor STAT-1, or in IRF8 which binds to IFN-stimulated response elements. In humans these deficiencies are categorized in a condition termed Mendelian susceptibility to mycobacterial disease (MSMD) (128). These patients have increased predisposition to develop clinical disease manifestations caused by BCG and by nontuberculous mycobacteria such as *M. avium*. For the same reason these patients are at high risk of developing tuberculosis (128). Alterations in the IL-12/IFN-γ axis in the mouse model also reveal the key role of Th1 cells. IL-12 neutralization leads to increased bacterial growth in Mtb and *M. avium* infection as well as a reduction in granuloma integrity (129-131). On the other way exogenous IL-12 induces increased resistance to Mtb with prolonged survival of WT mice (129, 132). A similar IL-12 treatment in IFN-γ deficient animals did not confer any protection suggesting that IL-12 protective effect is dependent on IFN-γ (132). *M. avium* infection of T cell-deficient SCID mice revealed that, while they are more susceptible than WT mice, neutralization of either IL-12 or IFN-γ in SCID animals greatly increases their susceptibility to *M. avium* infection (131, 133). These data suggest that in the absence of T cells, *M. avium* growth might be controlled by IFN-γ from sources other than T cells. The high susceptibility to Mtb infection in mice with deficient IFN-γ signaling has been widely attributed to the impairment of iNOS

production. However in the response to *M. avium*, while IFN-γ is necessary to control bacterial growth, NO can be detrimental (as already discussed in chapter 2.1.3). IFN-γ can activate or enhance different anti-microbial mechanisms, but how exactly IFN-γ affords protection in *M. avium* infection in mice is not yet known. In humans, while there is no established role for NO in the response to mycobacterial infections, deficient ROS expression is associated with increased predisposition to mycobacterial disease. However in the mouse model the role for ROS-induced mycobacterial proliferation control is not clear (see chapter 2.1.3). One might expect that the different IFN-γ induced anti-mycobacterial mechanisms may be redundant, which given the multiple effects of IFN-γ it might be difficult to assess. One report has shown that NOS2/gp91phox-double deficient mice were no more susceptible to Mtb infection than NOS2-deficient animals (71), but that was never explored during *M. avium* infections where iNOS does not afford protection. TNF-α produced either by Th1 cells or by the infected macrophage acting in an autocrine way, can also induce the anti-microbial machinery increasing the redundancy of the immune response. Besides IFN-γ direct role in macrophage activation, this cytokine also plays important roles in limiting inflammation, namely by restricting neutrophil recruitment through Th17 suppression (19) (discussed in detail in chapter 2.3).

Despite the IFN-γ pivotal role for anti-mycobacterial mediated immunity, different studies have reported the existence of IFN-γ independent $CD4^+$ T cell mediated protection. Gallegos and colleagues showed that the transfer of Th1 skewed cells incapable of producing IFN-γ (T-$bet^{-/-}$) provided protection against Mtb infected mice to the same extent as the transfer of WT Th1-sekwed cells. Transfer of Th2- or Th17-skewed cells was less efficient in conferring protection than Th1 skewed cells, suggesting a strong role for Th1 mediated immunity not necessarily via IFN-γ (134). A different model where naïve $CD4^+$ T cells isolated from WT or IFN-$\gamma^{-/-}$ mice were transferred into Mtb-infected $Rag1^{-/-}$ animals showed that while IFN-γ-producing $CD4^+$ T cells were absolutely essential to control the infection in the spleen, these cells had a small role in the control of Mtb growth in the lung. This work suggests that IFN-γ^+CD4^+ T cells are particularly important in the control of extrapulmonary TB (135). Recently, another work from the same group suggests that in addition to IFN-γ, Mtb growth restriction in the lung requires $CD4^+$ T cells expressing CD153, a molecule belonging to the TNF superfamily (136). Similarly Flórido et al had previously shown CD153/CD30 interactions to be required for optimal immunity to *M. avium* (137). The study of new anti-mycobacterial T cell-mediated protection mechanisms is

fundamental to devise new vaccination strategies, as the ones seeking to increase IFN-γ production by Mtb-specific CD4+ T cells are not corresponding to the expectations.

2.2.2. Th2 cells

Th2 cells are driven by the expression of IL-4 and are characterized by the up-regulation of the transcription factor GATA3 and secretion of IL-4, IL-5 and IL-13. Th2 cells are particularly relevant in allergic responses, in the protection against helminth infections, and tissue repair (138). Mycobacterial-induced immune response is clearly Th1-driven and in fact, depletion of either one or both the Th2 signature cytokines, IL-4 or IL-13, in Mtb infected mice has a small impact in the bacterial burdens with conflicting results raging from decreased bacterial loads (139), to no impact in the infection (140, 141), and increased Mtb growth only at late time points (141). Th2 cells can polarize macrophages to an alternatively activated state, characterized by the expression of Arginase (and decrease of NO production) and can thus be responsible for increased collagen synthesis eliciting a fibrotic encapsulation over the granuloma structure (142) (discussed in detail in chapter 3.1).

2.2.3. Th17 cells

In the immune response to mycobacterial infections, CD4+ T cells are also polarized towards a Th17 phenotype. These cells are driven by the expression of IL-6, TGF-β, and IL-1β, and expanded by the action of IL-23. Th17 cells are characterized by RORγ expression and in addition to IL-17, these cells also produce IL-22, IL-21, TNF-α and GM-CSF. IL-17, the signature cytokine of Th17 cells, can also be produced by other immune cells such as γδ T cells, group 3 ILCs, iNKT and NK cells (reviewed in (143)). The role of IL-17 in the immune response to mycobacterial infections is not clear. Data from human studies is contradictory, while in some studies increase IL-17 expression is associated with active TB patients, in others is associated with latent TB patients and healthy controls (143). In the mouse model, IL-17 appears to be dispensable for the control of infection by lab adapted Mtb strains, such as H37Rv, or less virulent Mtb clinical isolates, as the absence of IL-17 did not impact bacterial growth (144, 145). The same was not true for one hyper-virulent Mtb clinical isolate strain, where IL-17-deficient mice displayed increased bacterial burdens accompanied by less organized granuloma formation (144). BCG-infected IL-17-deficient mice were also reported to exhibit impaired granuloma formation despite the lack of impact in bacterial growth (146, 147). IL-17 has been shown to induce neutrophil accumulation at the site of infection (146, 148) but also to enhance Th1 cells,

as shown by their decreased numbers in infected IL-17-deficient mice (146). In addition following vaccination with a mycobacterial peptide, IL-17 was also shown to be required for an earlier recruitment of IFN-γ-producing $CD4^+$ T cells into the lung upon Mtb challenge (149). On the other hand IFN-γ-producing cells can limit the expansion of Th17 cells and the subsequent neutrophil increase, as shown with mice deficient for IFN-γ signaling infected either with BCG or Mtb (19, 150). A balance between Th1 and Th17 cells seems to be important in regulating mycobacterial-induced immunopathology.

2.3 Immunopathology

The mycobacterial-induced immune response is mostly a pro-inflammatory response dominated by the production of IFN-γ and TNF-α. Inflammation is thus required for bacterial growth restriction but it can also be detrimental to the host. An excessive inflammatory response or unrestrained inflammation can induce cell damage and eventually tissue destruction. Indeed, despite the protective role of IFN-γ, it was shown that from a certain threshold increasing the levels of this cytokine can lead to early death of the Mtb-infected host despite controlling bacterial proliferation (135). At the same time too little inflammation might not be sufficient to restrain or kill the bacteria. The immune system has mechanisms of self-regulation. One such example is the balance between Th1 and Th17 cells. IL-17 can recruit neutrophils, which in excess can be detrimental to the host (146, 148). At the same time IL-17 also enhances Th1 cells and IFN-γ can limit Th17 expansion and thus block neutrophil recruitment (19, 146, 149, 150). Although neutrophils can be protective in the early onset of the infection (103, 104), later on they can become detrimental to the host. Indeed neutrophilia has been correlated with the severity of the infection: cavitating pulmonary TB (upon granuloma central necrosis and liquefaction of the tissue) is characterized by extremely high numbers of neutrophils (151); and in patients with established TB disease high neutrophil numbers have been found to correlate with poor outcome and increased risk of mortality (152). Likewise, increased numbers of neutrophils are found in lungs of susceptible mouse strains and neutrophil depletion leads to prolonged survival of the susceptible mice but not the resistant (153, 154). Using the mouse model it has been found that neutrophil-antibody mediated depletion studies resulted in increased susceptibility to mycobacteria but only when neutrophils were depleted in the early onset of the infection (as discussed above on chapter 2.1.4). Studies where neutrophils were depleted late in infection either did not impact Mtb or *M. avium* growth (104, 155) or even decreased bacterial loads of Mtb infected mice when assessed at a later time point (156). These data suggest that neutrophils

have a dual role during mycobacterial infection: protective immediately after exposure where neutrophils are able to kill the bacteria and influence the immune response; and deleterious in the chronic phase of the infection where neutrophils contribute to the immunopathology. Different studies have shown that in the absence of IFN-γ signaling, mice display increased neutrophil accumulation at the infection site. IFN-γ, a cytokine mostly classified as pro-inflammatory, can thus also exert an anti-inflammatory role by blocking neutrophil recruitment in a chronic situation. Upon infection, neutrophils are relevant producers of IL-10 (156), which is an immunosuppressive cytokine and may underlie the detrimental role of neutrophils during the chronic stage. Immunosuppression of an inflammatory response is required to limit host damage, but it has to be tightly balanced in order not to dampen the protective immunity. In fact high levels of IL-10 may overcome the protective immune response promoting chronic infection, whereas low levels of IL-10 may allow an excessive immune response leading to host pathology. Beside neutrophils, IL-10 can be produced by other immune cells such macrophages, DCs, T cells, and B cells (157). During the immune response to mycobacteria, IL10 can directly act on macrophages and DCs to block pro-inflammatory cytokines as TNF-α and IL-12, and down-regulate surface MHCII expression, inhibiting antigen presentation and delaying the onset of the adaptive immune response and Th1 polarization. IL-10 can also inhibit several anti-microbial mechanisms as phagosome maturation, production of ROS and RNI (reviewed in (158)). It has been proposed that mycobacteria can use IL-10 to manipulate and subvert the host immune response in their own profit, as suggested by the early induction of IL-10 by hyper-virulent Mtb clinical isolate strains. The immune system is equipped with other mechanisms to prevent immunopathology such as Treg cells, which can limit accumulation of effector T cells in the response to Mtb infection, although it is not clear whether this suppression is mediated by IL-10. A successful immune response has to restrict bacterial growth while avoiding an excessive inflammation which is achieved by a tight balance between the pro- and anti-inflammatory mechanisms of the immune response.

3. Granuloma

Granuloma formation is the hallmark of mycobacterial diseases. Granulomas develop in response to chronic antigen stimulation and can be developed in response to other infectious diseases such as schistosomiasis and leishmaniasis but also to pathologies with no infectious origin as sarcoidosis and Crohn's disease (142). Mycobacterial-induced granuloma "grows" around infected macrophages and is composed by an aggregate of macrophages and other

innate cells surrounded by a lymphocytic cuff that later on can be enclosed by a fibrotic capsule. Under certain circumstances, granulomas undergo central necrosis (termed caseation) allowing the spread of the microbe to other locations of the host but it can also facilitate person-to-person transmission by leaking bacteria into the airways (159). The formation of granuloma structures in response to mycobacterial infections is a conundrum to the scientific community in the sense that while capable of restricting bacterial growth it also provides a niche for mycobacteria to survive and eventually disseminate. In addition to allow cell-to-cell interaction hence continuous immune regulation, the granuloma structure also walls off bacteria preventing dissemination. For this reason granulomas were viewed for a long time as essential to provide protection to an infected host. On the other side, granulomas are often unable to completely eliminate bacteria, which might remain in a latent state until an opportunity arises for escaping from the granuloma. In addition, recent evidence from the *M. marinum*-induced innate-like granuloma in zebrafish embryo, support the thought that granulomas may provide a sanctuary for the bacillus allowing its proliferation (160). The authors reported that the recruitment of macrophages to the nascent granuloma ends up by providing new targets for bacteria and that infected macrophages have the ability to egress from innate granulomas establishing secondary granulomas (160). A more integrative view however argues that while granulomas are crucial to limit bacterial growth and restrain inflammation into specific foci, they are required for mycobacteria life cycle uncovering a dynamic balance between two opponents, the bacteria and the host immune response. Still, the debate whether granulomas are "good or evil" remains open. Mycobacteria may profit from granuloma formation but there are ample evidence for a protective view of the mature granuloma that are pivotal for infection control: innate granulomas (lacking immune adaptive cells) do not eliminate mycobacteria efficiently; in the absence of T cells, innate sources of IFN-γ are not sufficient to provide full protection, particularly during Mtb infection; and T cell transfer has been shown to enhance protection and granuloma formation (reviewed in (159)). In addition it is well established that the initiation of the adaptive response which leads to the formation of the mature granuloma correlates with bacterial growth control (18). AIDS and SCID patients that do not develop well-structured granulomas usually present disseminated mycobacterial infection, while in immunocompetent individuals capable of developing mature granulomas, infection is mostly pulmonary, suggesting that granulomas are important to restrict the disease to the lung. Regardless the role of granuloma is still a matter of debate. To fully understand mycobacterial

disease is fundamental to know in depth how and which cells, molecules and signals underlie the granuloma development.

3.1. Granuloma development

Mycobacteria internalization by a macrophage triggers a localized proinflammatory response with production of cytokines and chemokines that attract additional innate cells from the neighboring blood vessels. Neutrophils, monocyte-derived macrophages, DCs, NK cells, γδ T cells and other innate cells are therefore recruited (innate granuloma, Fig 1) and constitute the first stage of the granuloma which is thought to promote cell activation and antigen upload by APCs, while at the same time inadvertently providing a niche for the bacteria to infect other cells and propagate (160). Infected or antigen loaded DCs migrate to the lymph nodes where T cells are primed and differentiate mostly into Th1 and Th17 phenotypes as well as cytotoxic CD8 T cells (18, 114, 161). Activated T cells undergo clonal proliferation and, together with B cells, are guided through a chemokine gradient exiting from the lymph node and homing to the infected tissue where they form a rim surrounding the innate cells (15, 162). This structure (mature granuloma, Fig. 1) is thought to be optimal for cell interaction and activation of the infected cells by cytokines such as IFN-γ and TNF-α which in turn enhance the macrophage microbicidal machinery while promoting additional inflammatory cell infiltration (163, 164). Fibrotic encapsulation of the granuloma can be observed at later stages of granuloma development (chronic granuloma, Fig. 1). Fibrosis is triggered by the excess of deposition of extracellular matrix components such as collagen and although it is known to occur in response to the Th2 cytokines IL-4 and IL-13 or in response to TGF-β, a cytokine that can be secreted by macrophages and DCs but also by Treg cells, the signals underlying fibrosis in mycobacterial-induced granulomas are not established (142). Collagen synthesis is mediated by the expression of arginase which uses the same substrate as iNOS for the production of NO, L-arginine. Indeed a previous work from our lab has shown that upon *M. avium* infection collagen deposition was increased in granulomas of mice lacking iNOS expression (165). While the fibrotic process allows for encapsulation of the lesion, excessive fibrosis can compromise organ function (142).

Within the granuloma structure, macrophages undergo dramatic morphological changes over time. A significant portion of these cells acquire an epithelioid appearance characterized by extended cytoplasm and interdigitated cell membranes that tightly link adjacent cells (166). Recently it was shown that these macrophages actually undergo an epithelial reprograming where cell-to-cell adhesion is driven by the expression of E-cadherin (167). Interfering with the

function of E-cadherin in macrophages resulted in more diffuse and disorganized granulomas (167). Occasionally epithelioid macrophages can fuse together forming multinucleated giant cells or suffer deficient cytokinesis resulting in polyploidization (168, 169). These cells possess the nuclei organized in a horseshoe pattern aligned along the cell border and are called Langhans cells in honor of the scientist that first described them (142, 170). Although commonly observed in human granulomas, such giant cells are seldom described in murine granulomas (171). Another common feature of mycobacterial granulomas is the presence of foamy macrophages (172). These cells are characterized by a high content of lipid bodies which are thought to function as a major nutrient source to the bacillus (172, 173). Indeed foamy macrophages are heavily infected cells, and lipid bodies are found to be in close association with phagosomes containing Mtb or *M. avium* as shown by electron microscopy (174, 175). Foamy macrophages are highly represented in granulomas undergoing necrosis (discussed in detailed in the next chapter) and are located in the interface region between the necrotic area and the epithelioid macrophages suggesting an active role of foamy cells during the necrotizing process (172, 174).

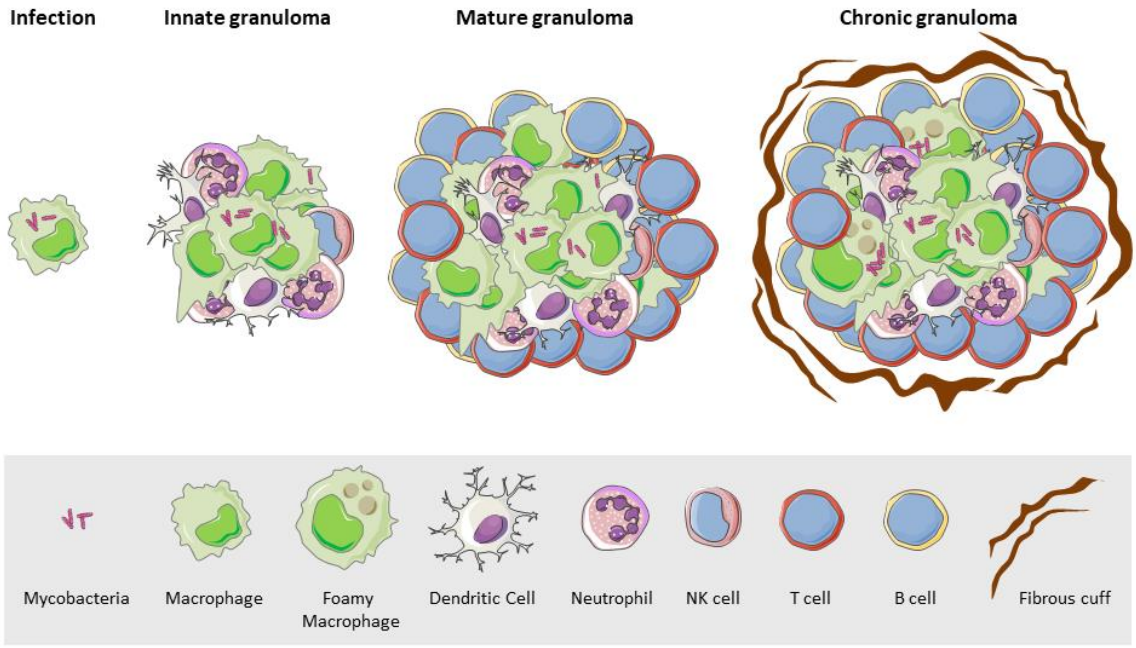

Figure 1. Different stages of granuloma development. Upon mycobacterial internalization the immune system responds through the recruitment of several cell populations that surround the infected macrophages. Figure based on Shaler et al., 2013 (162).

An established granuloma is not a static structure. Using real-time imaging of *M. marinum* infected-zebrafish embryos, Davis and Ramakrishnan have shown macrophages to be highly motile in the early (innate) granuloma (160). In contrast, using intravital microscopy in BCG-

infected mice, the Germain lab showed that macrophages in mature granulomas are largely immobile whereas T cells exhibit rapid motility yet restrained within the granuloma boundaries (20). This study also highlighted the requirement of TNF-α for maintenance of the granuloma structure as upon its neutralization granuloma size decreased mainly due to the loss of uninfected macrophages (20). Cellular recruitment towards the granuloma structure is highly dependent on cytokine expression and on chemokine gradients created through the differential expression of several chemokines and their receptors by different cells beginning on infected macrophages. In the early stages of granuloma assembly, accumulation of innate cells is particularly dependent on chemokines binding to CCR2 such as CCL-2/MCP-1, CCL-12 and -13 which are responsible for the recruitment of monocytes, DCs and NK cells. Chemokines binding to CCR4 and CCR5 can also be responsible for innate cell recruitment. Neutrophils and NK cells can additionally be recruited through the binding of CXCR2 to the ligands CXCL-3 and CXCL-5 which are up-regulated upon infection. CXCL-8 secreted by cells as monocytes, macrophages and endothelial cells is also an important chemoattractant of neutrophils through CXCR1/2 binding (reviewed in (89, 97, 171)). T cell activation in the lymph nodes is accompanied by up-regulation of chemokine receptors such as CXCR3 and CCR5 which trigger their migratory capacity towards the inflamed tissue where their ligands are highly expressed (CXCL-9, -10 and -11 for CXCR3 and CCL-3, -4, -5 and -8 for CCR5) (89, 97, 171). The expression of these ligands is up-regulated by the signature Th1 cytokines IFN-γ and TNF-α (89, 171). Additionally CCR2, CCR4 and CCR6 are also involved in T cell recruitment to the granuloma (89, 97, 171). It has become evident that chemokine-guided recruitment both of innate and adaptive immune cells exhibit significant redundancy (89, 171).

Granuloma development and fate are dependent on the balance of several immune mediators, however two cytokines, IFN-γ and TNF-α, stand out due to their role in the assembly and maintenance of the granulomatous structure and both are addressed in works included in this thesis. The relevance of these cytokines during granuloma development cannot be dissociated from their role in activating macrophages and microbicidal mechanisms which has been thoroughly described along the previous chapters.

IFN-γ is absolutely required for immune-mediated protection as in its absence both humans and mice display increased susceptibility to mycobacterial disease which can be often fatal (described in section 2.2.1). The IFN-γ relevance to the secretion of the chemokines CXCL-9, -10 and -11 is best illustrated by their alternative names: monokine induced by Interferon-gamma (for

CXCL-9), Interferon-gamma-inducible protein 10 (for CXCL-10) and Interferon-inducible T cell alpha chemoattractant (for CXCL-11) (176). These chemokines bind to CXCR3 which is upregulated on Th1 cells as its expression is dependent on T-bet (176). Besides affecting T cell recruitment, IFN-γ might affect innate cell recruitment as well. IFN-γ-deficient mice infected with *M. avium* exhibit poor granulomata constituted by small accumulations of lymphoid cells without an evident inner core of innate cells (177). Similarly, IFN-γ monoclonal antibody depletion of *M. avium*-infected SCID mice (therefore lacking adaptive immunity) exhibit reduced cellular recruitment with small and fewer lesions than the isotype-treated control group (163). Although IFN-γ is mostly produced by T cells, it can also be secreted by innate cells such as NKT cells, γδT cells, NK cells and other ILCs. Hence it is believed that these early sources of IFN-γ might activate the infected macrophages and influence the cellular recruitment pattern. The effect of Mtb infection over the granulomata of IFN-γ-deficient mice is different: large cellular accumulations almost exclusively constituted by neutrophils undergoing central necrosis can be observed (57, 58). Importantly, due to the absence of IFN-γ, these granuloma-like structures are also practically devoid of mononuclear cells (57, 58).

TNF-α is an important cytokine for macrophage activation exhibiting synergistic effects with IFN-γ (121). The absence of TNF-α either through antibody-mediated depletion or genetic-disruption leads to a moderate increase of mycobacterial burdens (Mtb or *M. avium*) yet mice succumb early in infection (164, 178, 179). These TNF-α-deficient infected animals exhibit decreased or delayed expression of chemokines (178) which is translated into delayed cellular recruitment and less defined granuloma structures that might underlie their decreased survival (89, 171, 178). Moreover, TNF-α neutralization of chronically Mtb-infected mice induced a modest increase in Mtb growth (although not to levels that usually cause the death of mice) that was accompanied by disintegration of the previously formed granulomas and animal death (180). Similarly it was observed that patients with autoimmune or chronic diseases undergoing TNF-α neutralizing therapies exhibited a high incidence of TB as well as high rates of extra-pulmonary and disseminated TB (181-184). These results reveal the requirement of TNF-α in maintaining the structure of previously formed granulomas highlighting its role in preventing reactivation of the disease. Summing up, TNF-α produced by infected macrophages and later on by T cells is pivotal to maintain the elevated levels of chemokines that mediate cell recruitment and allow the maintenance of the granuloma structure (89, 171).

The fate of mycobacteria-induced granulomas depends on a balance between the bacteria and the host immune response. While the granuloma can wall-off the bacteria and efficiently kill the pathogen it can also allow for the bacillus to persist in a latent form until an opportunity emerges allowing reactivation and dissemination.

3.2. Caseous necrosis

Caseous granulomas have a "cheese-like" appearance in the center of the structure due to extensive tissue necrosis that eventually can progress to cavitation (Fig. 2). It is generally accepted that caseation plays a major role in dissemination of the infection and in facilitating bacterial spread by coughing. The mechanisms underlying caseous necrosis are poorly understood though some evidence-based hypotheses have been proposed. Transcriptional analyses of microdissected human granulomas have correlate caseation with an increase in lipid metabolism (185), which is consistent with the role of foamy macrophages in the development of the central necrosis. Given the elevated proportion of neutrophils in granulomas undergoing central necrosis it is likely for these cells to be involved in caseation development (124, 151). Neutrophils have an elevated content of cytotoxic molecules which may cause significant tissue destruction. Lack of vascularization has been observed in granulomas undergoing central necrosis, which is believed to cause a hypoxic environment and may underlie the necrotizing process (discussed in detail in the next chapter).

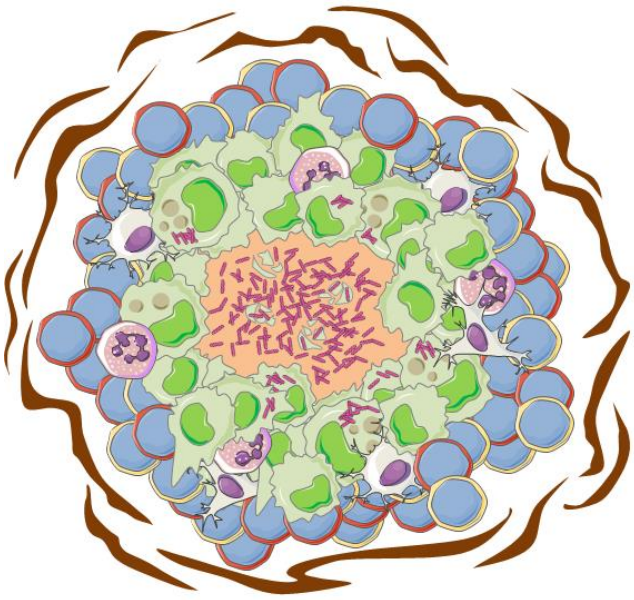

Figure 2. Caseating granuloma. Granuloma undergoes central necrosis that eventually culminates in tissue liquefaction and mycobacterial spread. Figure based on Ramakrishnan, 2012 (15).

Granuloma central necrosis can be found in patients infected with Mtb or with *M. avium*, but is difficult to mimic in the mouse model. Upon Mtb infection both rabbits and guinea pigs develop caseous necrosis and cavitation (186), and in fact these models have been used to study this pathology but restricted to the limited tools available. More recently some mouse strains have been described develop necrotizing lesions and even undergo cavitation, but both Balb/c and C57Bl/6, the most used inbred laboratory strains do not develop necrotizing lesions upon Mtb infection unless using gene-disrupted mice (187). In the early 2000's the Appelberg group developed a model for studying granuloma necrosis in C57BL/6 mice infected intravenously with a low dose (10^2) of a highly virulent *M. avium* strain (124). Central necrosis occurred around 90 days post-infection and it was dependent on CD4, IL-12 and IFN-γ, as mice genetically deficient for these molecules did not develop necrosis. On the other side, CD8, TNFRp55, RNS and NOX-inducible ROS were dispensable for the development of the necrotic lesions (124).

3.2.1. Hypoxia and the role of HIF-1α

Granuloma necrosis has been associated with hypoxic environments in mycobacterial-infected rabbits, guinea pigs, and non-human primates, animal models known to develop granuloma structures resembling the ones in humans (188). The same authors did not find any hypoxic lesions in Mtb-infected Balb/c or C57BL/6 mice, animal models whose granulomas lack central necrosis (188). These data strongly suggest a correlation between hypoxic environment and granuloma central necrosis. In accordance, Mtb-infected C3HeB/FeJ mice develop granuloma central necrosis that was associated with hypoxia (189). Central necrosis has been observed mostly in large granulomas which are thought to be poorly vascularized and therefore likely to be deprived of nutrients and oxygen. In fact this hypothesis has been supported by the absence of endomucin, a marker for vascularization, in the necrotic center of *M. avium*-induced granulomas (190). Cells can adapt to hypoxic conditions, and the transcription factor HIF-1 plays a fundamental role in that sense. HIF-1α, one of the subunits of HIF-1 is stabilized under hypoxic conditions being capable then to dimerize with the constitutively stable subunit HIF-1β. The HIF-1 complex thus binds to the DNA promoting the transcription of several target genes which include the vascular endothelial growth factor, erythropoietin, glycolytic enzymes and glucose transporters. Taking advantage of the *M. avium*-induced granuloma necrosis model, Cardoso et al have used C57BL/6 mice lacking HIF-1α in the myeloid lineage (cells that locate in the lesion center) in order to study the impact of hypoxia in the development of granuloma necrosis in the liver. HIF-1α deficient mice, developed granuloma necrosis earlier than the WT controls and were

more susceptible to infection. These data strongly suggest that a hypoxic environment in the center of granulomas accelerates the necrotizing process.

4. Innate Lymphoid Cells

Innate Lymphoid Cells (ILCs) are a group of heterogeneous immune cells that belong to the lymphoid lineage, do not express the recombination activating gene (RAG) but depend on the γc component of the IL-2 family of receptors (191). This particular chain of the receptor (γc) is shared by several cytokine receptors (Fig. 3A) and is required for the signaling of cytokines like IL-7 and IL-15 which are indispensable for the development of T and B cells but also ILCs (191, 192). In 2013, ILCs were classified in three different populations based on transcription factor expression and the production of signature cytokines: group 1 which include NK cells and type 1 ILCS (ILC1s) are IFNγ producers; group 2 are ILC2s and mainly produce IL-13 and IL-5; and group 3 which comprehends ILC3s and Lymphoid Tissue-inducer (LTi) cells and are IL-17 and IL-22 producers (Fig 3B) (193). It has been suggested that each one of the ILC subsets may be considered an innate counterpart of the different T cell populations. Given the greater capacity to produce cytolytic granules, NK cells would correspond to cytotoxic $CD8^+$ T cells whereas ILC1s, ILC2s, and ILC3s would correspond to Th1, Th2 and Th17 $CD4^+$ T cells (respectively) (194). In contrast to T cells, ILCs are devoid of antigen receptors and do not exhibit clonal expansion capabilities. These cells are considered and arm of the innate immune system, quickly responding to different stimuli as cytokines and other soluble molecules within the microenvironment (193). ILCs are present both in lymphoid and non-lymphoid organs, but are particularly enriched at barrier surfaces which are common sites of colonization or where invasion by pathogens occurs with higher incidence (195, 196). ILCs are particularly important in regulating interactions with microbiota and maintaining immune tolerance, but it is also described that ILCs play active roles in response to allergy, cancer, metabolic regulation and inflammation (195). In addition ILCs are known to be important players in the response to infection, contributing to the resistance to several pathogens (195-197).

Despite their multiple roles in the immune system, non-NK ILCs are scarce in number. With the emergence of new technologies capable to overcome this limitation, these cells have been extensively studied particularly in the past few years. For this reason the ILC field is still poorly understood and is being constantly challenged by different interpretations in light of new data. The following sections are a summary mainly highlighting just some of the more relevant molecules involved in the ILC field from the murine model.

4.1 Development of ILCs

ILCs as well as T and B cells derive from a common lymphoid progenitor (CLP) residing in the bone marrow. Downstream CLP, is the Common Innate Lymphoid Progenitor (CILP) or α Lymphoid Progenitor (αLP), with a restricted differentiation potential that includes all ILCs but not T or B cells (191, 198). This progenitor was described to be dependent on the expression of transcription factor NFIL3 (199) (Fig 3B). However, recent studies have shown that following some infections or specific environment factors, NK cells and some ILCs subsets can overcome the requirement for NFIL3 (200-202). Collectively these data suggest that under certain conditions ILCs can bypass the lack of this master regulator of their development or that these cells may derive from alternative progenitors (203). Downstream the CILP/αLP stage occurs the divergence between the NK cells lineage and the other ILCs. The expression of the transcription factors Id2 and Gata3 is in the origin of the Common Helper-like Innate Progenitor (CHILP) that gives rise to all ILCs except NK cells (204) (Fig 3B). CHILP can give rise to LTi cells or, through the elevated expression of PLZF, can differentiate into the Innate Lymphoid Cell Precursor (ILCP). This cell is the immediate precursor of ILC1s, ILC2s and ILC3s, but not of NK or LTi cells. Interestingly PLZF expression is required for the ILCP stage but is not sustained in the mature ILCs (Fig 3B) (205). The development to mature ILC cells will be discussed in the next section. One major regulator that is differentially expressed in the NK and ILCs lineages is the transcription factor Gata3. In opposition to all the other ILCs, NK cells are Gata3-independent. Id2 is not required for commitment into the NK cell lineage but is necessary for NK cell maturation. On the other hand, Eomes, is a transcription factor exclusively expressed in the NK cell lineage (198) (Fig 3B).

Only recently the ILC development has been studied in detail and therefore is particularly liable to new interpretations. Moreover, data from different experts in the field emphasize the elevated plasticity of these cells which might be a reflection of different pathways not identified so far (203, 206).

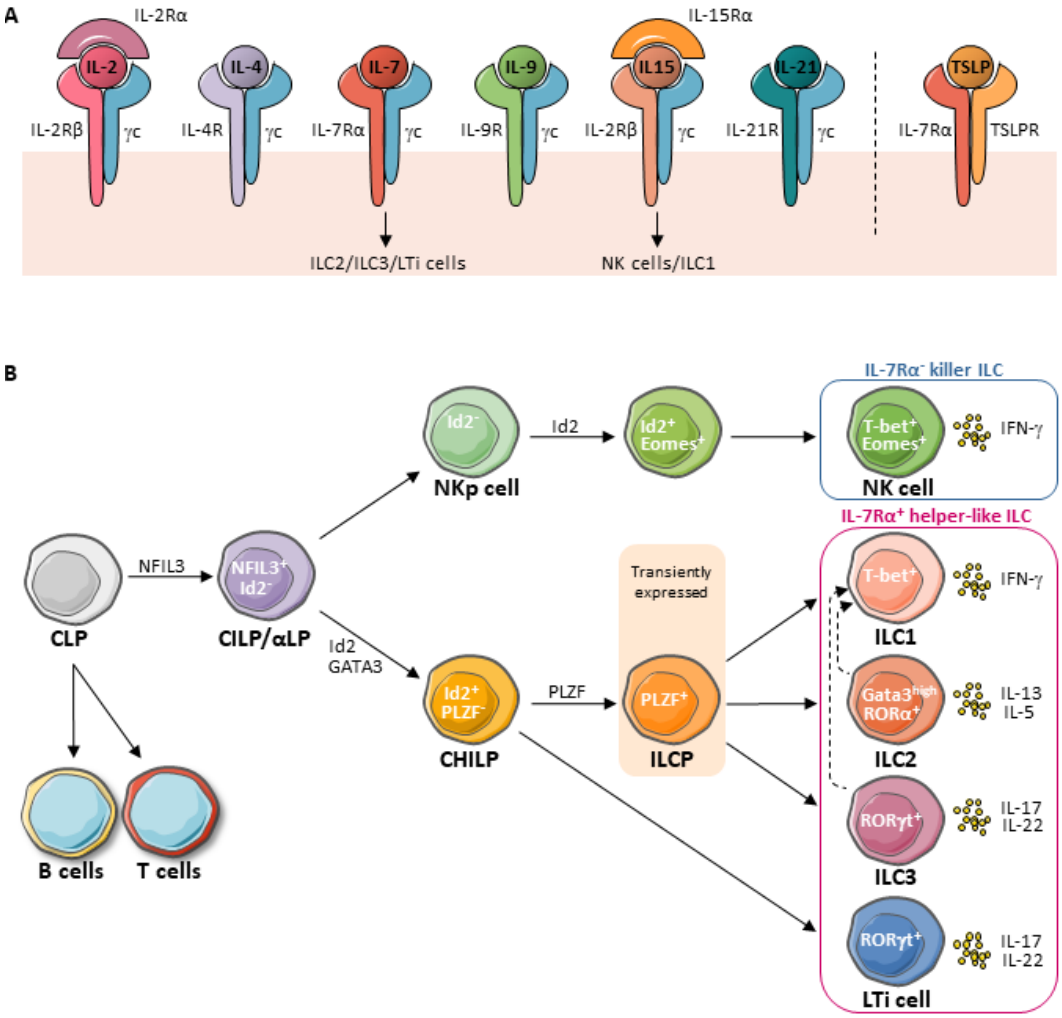

Figure 3. Common γc receptor and ILC development. (A) Receptors for IL-2, IL-4, IL-7, IL-9, IL-15 and IL21 share the common cytokine receptor γ-chain (γc). The receptors for TSLP and for IL-7 share the IL7-Rα chain. IL7 and IL15 signaling is required for ILC development. Figure based on Rochman et al., 2009 (192) **(B)** Mouse ILC development pathway depicting some of the main transcription factors driving ILC development as well as the main cytokines produce by each ILC subset. CLP, common lymphoid progenitor; CILP, common innate lymphoid progenitor; αLP, αLymphoid progenitor; CHILP, common helper-like innate lymphoid progenitor; ILCP, innate lymphoid cell progenitor; NKp NK progenitor cell; iNK immature NK cell. Figure based on Dienfenbach et al., 2014, and Spits et al., 2015 (198, 207).

4.2 ILCs subsets

As mentioned before ILCs are further divided in three subsets reflecting their different transcription factor requirements and cytokine production abilities. Importantly, ILCs do not express any T cell lineage marker (Lin$^-$). Almost all ILCs express the surface molecule Thy1 and, with the exception of NK cells, ILCs are characterized by the expression of IL-7Rα, also named CD127, and by the lack of myeloid phenotypical markers (193, 196). While NK cells recirculate between the blood and tissues, most of the other ILCs are resident cells (203).

4.2.1 Group 1 ILCs

Although NK cells and ILC1s derive from distinct progenitors both cell types belong to the Group 1 ILCs. They depend on T-bet and respond to IL-12 and IL-18 to produce IFNγ (197). Despite being included in the same subset there are some striking differences among these two cell types. In addition to T-bet, mature NK cells depend on the transcription factor Eomes while ILC1s are Eomes$^-$ (197, 203). For this reason, these cells are also called Eomes$^-$ ILC1s and Eomes$^+$ NK cells (203) (Fig 3B). Through the production of granzyme and perforin NK cells exert granule-dependent cytotoxicity, while ILC1s express the death-inducing ligand TRAIL which can induce cell death on cells expressing its receptor (197, 208). In opposition to the majority of other ILCs, both ILC1s and NK cells express NKp46 and NK1.1 (208). Importantly although ILC1s express IL-7Rα, IL-7 is dispensable for their development. In fact both NK cells and ILC1s require IL-15 signaling (203, 204) (Fig 3A).

By downregulation of RORγt (ILC3s master TF) and up-regulation of T-bet, NKp46 and NK1.1, certain ILC3 populations can convert into IFN-γ-producing ILC1s (209, 210). In addition, recent studies have shown that under certain conditions ILC2s can also convert into IFN-γ-producing ILC1s (211, 212). This phenomenon exemplifies well the great plasticity of ILCs (Fig3B).

4.2.2 Group 2 ILCs

These cells, also called nuocytes (213), produce IL-5 and IL-13 upon stimulation with IL-25, IL-33 and TSLP. ILC2s express high levels of Gata3 and are dependent of RORα (Fig 3B) (196). These cells require IL-7 signaling for development, express CD25, Sca1, MHCII and the co-stimulatory molecules CD80 and CD86 (208). Group 2 ILCs play an important role in the immune response to allergies and helminth infections (196, 213).

4.2.3 Group 3 ILCs

Group 3 ILCs encompass both ILC3s and LTi cells. The latter are critical for lymphoid organogenesis (196, 206). Both cell types require IL-7 signaling for their development and produce IL-17 and IL-22 in response to IL-23 and IL-1β (193, 195). ILC3s are dependent on the expression of RORγt and the aryl hydrocarbon receptor (AHR), while LTi cells are reported to be dependent on RORγt but not on AHR (195). Group 3 ILCs are relatively heterogeneous. LTi cells are CCR6$^+$ and can be either CD4$^+$ or CD4$^-$, whereas ILC3s are CCR6$^-$ and comprehends two subsets distinguished by the expression or not of NKp46 (195). As group 2 ILCs, ILC3s also express MHCII (206, 208).

4.3 Role of ILCs during mycobacterial infections

With the exception of NK cells, the role of ILCs during mycobacterial infections is not known. As mentioned before, IFNγ is essential for mycobacterial proliferation control, yet studies with immunodeficient mouse models lacking T cells, the major IFNγ producer cells after infection, have shown resistance to mycobacterial infections. This protection has been associated to NK cells. However it should be highlighted that works involving mycobacterial infections and ILCs were mostly done in the late 1990's and early 2000's, when the only population of ILCs well described was NK cells. For this reason the main conclusions of those works concern only NK cells. It is now known that through the immediate cytokine production different ILCs subsets contribute to the resistance to both extra- and intracellular pathogens, providing a first line of defense (196, 203). It is thus plausible to expect ILCs to impact the immune response during mycobacterial infections.

Mycobacterial infections trigger multiple cells involved both in the innate and adaptive immunity, with T cells playing a major role in the resistance to the pathogen. Hence as adaptive response ensues, T cells might override the relevance of ILCs, making it difficult to study their precise contribution. Indeed in immunocompetent mice Ab-mediated neutralization of NK cells did not impact host resistance to *M. avium* or *M. tuberculosis* (214-216). However in mice lacking and adaptive response (SCID or $Rag^{-/-}$), ILCs were important to control the proliferation of both *Mycobacterium* species. (217, 218). Feng and colleagues have shown that despite being more susceptible to *M. tuberculosis* infection than WT mice, $Rag^{-/-}$–infected animals where more resistant than $Rag^{-/-}$ with disruptive IFNγ signaling, or $Rag^{-/-}\gamma c^{-/-}$ -double deficient mice, which lack all ILC subsets (217). This work strongly suggests an important role for ILCs, either NK cells or not, in the immune response to *M. tuberculosis* via IFN-γ production. On the other hand in the *M. avium* infection model, immunodeficient SCID mice treated with NK cell-depleting antibodies exhibit the same resistance to *M. avium* as the IgG-treated controls (218), supporting a possible protective role for an ILC beside NK cells. The authors also excluded cytolitic activity as source of the protective immunity in these animals (218). It is thus possible to speculate that non-NK ILCs might also provide an early source of IFNγ, perhaps capable of influencing the granuloma assembly and providing some degree of protection particularly when acquired immunity is lacking.

5. Thesis aims

Granuloma formation is a hallmark of mycobacterial infections. Although it has been believed to provide protection, recent evidence raised the possibility that granulomas may provide a sanctuary to microbes. Hence it is crucial to understand the pathogenesis of inflammation and clarify its role in the development of protective immunity. For that it is necessary to unveil the mechanisms behind granuloma initiation, to better understand how macrophages respond to the adaptive immunity and the processes triggering granuloma central necrosis.

Aim 1 – To identify the initial cellular source of IFN-γ.

Although the assembly of mature granulomas certainly requires an efficient adaptive immune response most likely dominated by IFN-γ-producing $CD4^+$ T cells, less structured accumulations of leukocytes mimicking granulomatous structures can be observed in the absence of T cells. This has been observed in AIDS patients, in Rag-deficient animals, and even in zebrafish larvae which still lack adaptive immune mechanisms. This raises the question on whether innate sources of IFN-γ may be responsible for the initial leukocyte recruitment and whether these putative cells may have a role in bacterial growth restriction.

Aim 2 - To study the IFN-γ-mediated macrophage activation in infected mice.

The impact of IFN-γ–dependent resistance to intracellular pathogens has been widely attributed to its action on macrophages, particularly in the case of pathogens that have this cell as their main target. In vivo, this assumption has been extrapolated from experiments using specific antibody-mediated depletions and mice deficient in IFN-γ or its receptor which impact all cellular targets of IFN-γ and not just the macrophage. Whether or not IFN-γ has to act directly on macrophages to establish the organization of the granuloma remains elusive. MIIG mice have macrophages unresponsive to IFN-γ which when infected with the low virulent *M. avium* 2447 strain affords a unique opportunity to study its effects during chronic inflammation.

Aim 3 - To study the role of hypoxia-inducing pathology in mycobacterial infections.

We have already dissected the role of the hypoxia adaptor molecule HIF-1α in delaying the development of liver necrotic lesions in a *M. avium*-induced granuloma necrosis model. Mtb-infected C57BL/6 mice do not develop caseous necrosis. Whether HIF-1α prevents the emergence of necrotizing lesions in Mtb infected C57BL/6 mice and how it can affect the lung immunopathology is not known.

6. References

1. Ignatov, D., E. Kondratieva, T. Azhikina, and A. Apt. 2012. Mycobacterium avium-triggered diseases: pathogenomics. *Cellular microbiology* 14: 808-818.
2. Brennan, P. J., and H. Nikaido. 1995. The envelope of mycobacteria. *Annual review of biochemistry* 64: 29-63.
3. Kaur, D., M. E. Guerin, H. Skovierova, P. J. Brennan, and M. Jackson. 2009. Chapter 2: Biogenesis of the cell wall and other glycoconjugates of Mycobacterium tuberculosis. *Advances in applied microbiology* 69: 23-78.
4. Lawn, S. D., and A. I. Zumla. 2011. Tuberculosis. *Lancet* 378: 57-72.
5. Falkinham, J. O., 3rd. 2009. Surrounded by mycobacteria: nontuberculous mycobacteria in the human environment. *Journal of applied microbiology* 107: 356-367.
6. Falkinham, J. O., 3rd. 1996. Epidemiology of infection by nontuberculous mycobacteria. *Clinical microbiology reviews* 9: 177-215.
7. Casanova, J. L., and L. Abel. 2002. Genetic dissection of immunity to mycobacteria: the human model. *Annual review of immunology* 20: 581-620.
8. North, R. J., and Y. J. Jung. 2004. Immunity to tuberculosis. *Annual review of immunology* 22: 599-623.
9. Daniel, T. M. 2006. The history of tuberculosis. *Respiratory medicine* 100: 1862-1870.
10. Cosma, C. L., D. R. Sherman, and L. Ramakrishnan. 2003. The secret lives of the pathogenic mycobacteria. *Annual review of microbiology* 57: 641-676.
11. Kendall, B. A., and K. L. Winthrop. 2013. Update on the epidemiology of pulmonary nontuberculous mycobacterial infections. *Seminars in respiratory and critical care medicine* 34: 87-94.
12. Appelberg, R. 2006. Pathogenesis of Mycobacterium avium infection: typical responses to an atypical mycobacterium? *Immunologic research* 35: 179-190.
13. Marciano, B. E., C. Y. Huang, G. Joshi, N. Rezaei, B. C. Carvalho, Z. Allwood, A. Ikinciogullari, S. M. Reda, A. Gennery, V. Thon, F. Espinosa-Rosales, W. Al-Herz, O. Porras, A. Shcherbina, A. Szaflarska, S. Kilic, J. L. Franco, A. C. Gomez Raccio, P. Roxo, Jr., I. Esteves, N. Galal, A. S. Grumach, S. Al-Tamemi, A. Yildiran, J. C. Orellana, M. Yamada, T. Morio, D. Liberatore, Y. Ohtsuka, Y. L. Lau, R. Nishikomori, C. Torres-Lozano, J. T. Mazzucchelli, M. M. Vilela, F. S. Tavares, L. Cunha, J. A. Pinto, S. E. Espinosa-Padilla, L. Hernandez-Nieto, R. A. Elfeky, T. Ariga, H. Toshio, F. Dogu, F. Cipe, R.

Formankova, M. E. Nunez-Nunez, L. Bezrodnik, J. G. Marques, M. I. Pereira, V. Listello, M. A. Slatter, Z. Nademi, D. Kowalczyk, T. A. Fleisher, G. Davies, B. Neven, and S. D. Rosenzweig. 2014. BCG vaccination in patients with severe combined immunodeficiency: complications, risks, and vaccination policies. *The Journal of allergy and clinical immunology* 133: 1134-1141.

14. Verrall, A. J., M. G. Netea, B. Alisjahbana, P. C. Hill, and R. van Crevel. 2014. Early clearance of Mycobacterium tuberculosis: a new frontier in prevention. *Immunology* 141: 506-513.
15. Ramakrishnan, L. 2012. Revisiting the role of the granuloma in tuberculosis. *Nature reviews. Immunology* 12: 352-366.
16. Cooper, A. M. 2014. Mouse model of tuberculosis. *Cold Spring Harbor perspectives in medicine* 5: a018556.
17. Gomes, M. S., and R. Appelberg. 1998. Evidence for a link between iron metabolism and Nramp1 gene function in innate resistance against Mycobacterium avium. *Immunology* 95: 165-168.
18. Cooper, A. M. 2009. Cell-mediated immune responses in tuberculosis. *Annual review of immunology* 27: 393-422.
19. Nandi, B., and S. M. Behar. 2011. Regulation of neutrophils by interferon-gamma limits lung inflammation during tuberculosis infection. *The Journal of experimental medicine* 208: 2251-2262.
20. Egen, J. G., A. G. Rothfuchs, C. G. Feng, N. Winter, A. Sher, and R. N. Germain. 2008. Macrophage and T cell dynamics during the development and disintegration of mycobacterial granulomas. *Immunity* 28: 271-284.
21. Russell, D. G. 2007. Who puts the tubercle in tuberculosis? *Nature reviews. Microbiology* 5: 39-47.
22. Medzhitov, R., and C. Janeway, Jr. 2000. Innate immune recognition: mechanisms and pathways. *Immunological reviews* 173: 89-97.
23. Hmama, Z., S. Pena-Diaz, S. Joseph, and Y. Av-Gay. 2015. Immunoevasion and immunosuppression of the macrophage by Mycobacterium tuberculosis. *Immunological reviews* 264: 220-232.

24. Gomes, M. S., M. Florido, J. V. Cordeiro, C. M. Teixeira, O. Takeuchi, S. Akira, and R. Appelberg. 2004. Limited role of the Toll-like receptor-2 in resistance to Mycobacterium avium. *Immunology* 111: 179-185.

25. Feng, C. G., C. A. Scanga, C. M. Collazo-Custodio, A. W. Cheever, S. Hieny, P. Caspar, and A. Sher. 2003. Mice lacking myeloid differentiation factor 88 display profound defects in host resistance and immune responses to Mycobacterium avium infection not exhibited by Toll-like receptor 2 (TLR2)- and TLR4-deficient animals. *Journal of immunology* 171: 4758-4764.

26. Reiling, N., C. Holscher, A. Fehrenbach, S. Kroger, C. J. Kirschning, S. Goyert, and S. Ehlers. 2002. Cutting edge: Toll-like receptor (TLR)2- and TLR4-mediated pathogen recognition in resistance to airborne infection with Mycobacterium tuberculosis. *Journal of immunology* 169: 3480-3484.

27. Drennan, M. B., D. Nicolle, V. J. Quesniaux, M. Jacobs, N. Allie, J. Mpagi, C. Fremond, H. Wagner, C. Kirschning, and B. Ryffel. 2004. Toll-like receptor 2-deficient mice succumb to Mycobacterium tuberculosis infection. *The American journal of pathology* 164: 49-57.

28. Carvalho, N. B., F. S. Oliveira, F. V. Duraes, L. A. de Almeida, M. Florido, L. O. Prata, M. V. Caliari, R. Appelberg, and S. C. Oliveira. 2011. Toll-like receptor 9 is required for full host resistance to Mycobacterium avium infection but plays no role in induction of Th1 responses. *Infection and immunity* 79: 1638-1646.

29. Bafica, A., C. A. Scanga, C. G. Feng, C. Leifer, A. Cheever, and A. Sher. 2005. TLR9 regulates Th1 responses and cooperates with TLR2 in mediating optimal resistance to Mycobacterium tuberculosis. *The Journal of experimental medicine* 202: 1715-1724.

30. Holscher, C., N. Reiling, U. E. Schaible, A. Holscher, C. Bathmann, D. Korbel, I. Lenz, T. Sonntag, S. Kroger, S. Akira, H. Mossmann, C. J. Kirschning, H. Wagner, M. Freudenberg, and S. Ehlers. 2008. Containment of aerogenic Mycobacterium tuberculosis infection in mice does not require MyD88 adaptor function for TLR2, -4 and -9. *European journal of immunology* 38: 680-694.

31. Fremond, C. M., D. Togbe, E. Doz, S. Rose, V. Vasseur, I. Maillet, M. Jacobs, B. Ryffel, and V. F. Quesniaux. 2007. IL-1 receptor-mediated signal is an essential component of MyD88-dependent innate response to Mycobacterium tuberculosis infection. *Journal of immunology* 179: 1178-1189.

32. Mayer-Barber, K. D., D. L. Barber, K. Shenderov, S. D. White, M. S. Wilson, A. Cheever, D. Kugler, S. Hieny, P. Caspar, G. Nunez, D. Schlueter, R. A. Flavell, F. S. Sutterwala, and A. Sher. 2010. Caspase-1 independent IL-1beta production is critical for host resistance to mycobacterium tuberculosis and does not require TLR signaling in vivo. *Journal of immunology* 184: 3326-3330.

33. Carmona, J., A. Cruz, L. Moreira-Teixeira, C. Sousa, J. Sousa, N. S. Osorio, A. L. Saraiva, S. Svenson, G. Kallenius, J. Pedrosa, F. Rodrigues, A. G. Castro, and M. Saraiva. 2013. Mycobacterium tuberculosis Strains Are Differentially Recognized by TLRs with an Impact on the Immune Response. *PloS one* 8: e67277.

34. Stamm, C. E., A. C. Collins, and M. U. Shiloh. 2015. Sensing of Mycobacterium tuberculosis and consequences to both host and bacillus. *Immunological reviews* 264: 204-219.

35. Gandotra, S., S. Jang, P. J. Murray, P. Salgame, and S. Ehrt. 2007. Nucleotide-binding oligomerization domain protein 2-deficient mice control infection with Mycobacterium tuberculosis. *Infection and immunity* 75: 5127-5134.

36. Walter, K., C. Holscher, J. Tschopp, and S. Ehlers. 2010. NALP3 is not necessary for early protection against experimental tuberculosis. *Immunobiology* 215: 804-811.

37. Heitmann, L., H. Schoenen, S. Ehlers, R. Lang, and C. Holscher. 2013. Mincle is not essential for controlling Mycobacterium tuberculosis infection. *Immunobiology* 218: 506-516.

38. Armstrong, J. A., and P. D. Hart. 1971. Response of cultured macrophages to Mycobacterium tuberculosis, with observations on fusion of lysosomes with phagosomes. *The Journal of experimental medicine* 134: 713-740.

39. Frehel, C., C. de Chastellier, T. Lang, and N. Rastogi. 1986. Evidence for inhibition of fusion of lysosomal and prelysosomal compartments with phagosomes in macrophages infected with pathogenic Mycobacterium avium. *Infection and immunity* 52: 252-262.

40. Clemens, D. L., and M. A. Horwitz. 1995. Characterization of the Mycobacterium tuberculosis phagosome and evidence that phagosomal maturation is inhibited. *The Journal of experimental medicine* 181: 257-270.

41. Crowle, A. J., R. Dahl, E. Ross, and M. H. May. 1991. Evidence that vesicles containing living, virulent Mycobacterium tuberculosis or Mycobacterium avium in cultured human macrophages are not acidic. *Infection and immunity* 59: 1823-1831.

42. Sturgill-Koszycki, S., P. H. Schlesinger, P. Chakraborty, P. L. Haddix, H. L. Collins, A. K. Fok, R. D. Allen, S. L. Gluck, J. Heuser, and D. G. Russell. 1994. Lack of acidification in Mycobacterium phagosomes produced by exclusion of the vesicular proton-ATPase. *Science* 263: 678-681.

43. Sturgill-Koszycki, S., U. E. Schaible, and D. G. Russell. 1996. Mycobacterium-containing phagosomes are accessible to early endosomes and reflect a transitional state in normal phagosome biogenesis. *The EMBO journal* 15: 6960-6968.

44. Russell, D. G., J. Dant, and S. Sturgill-Koszycki. 1996. Mycobacterium avium- and Mycobacterium tuberculosis-containing vacuoles are dynamic, fusion-competent vesicles that are accessible to glycosphingolipids from the host cell plasmalemma. *Journal of immunology* 156: 4764-4773.

45. van der Wel, N., D. Hava, D. Houben, D. Fluitsma, M. van Zon, J. Pierson, M. Brenner, and P. J. Peters. 2007. M. tuberculosis and M. leprae translocate from the phagolysosome to the cytosol in myeloid cells. *Cell* 129: 1287-1298.

46. Simeone, R., A. Bobard, J. Lippmann, W. Bitter, L. Majlessi, R. Brosch, and J. Enninga. 2012. Phagosomal rupture by Mycobacterium tuberculosis results in toxicity and host cell death. *PLoS pathogens* 8: e1002507.

47. Clemens, D. L., and M. A. Horwitz. 1996. The Mycobacterium tuberculosis phagosome interacts with early endosomes and is accessible to exogenously administered transferrin. *The Journal of experimental medicine* 184: 1349-1355.

48. Olakanmi, O., L. S. Schlesinger, A. Ahmed, and B. E. Britigan. 2002. Intraphagosomal Mycobacterium tuberculosis acquires iron from both extracellular transferrin and intracellular iron pools. Impact of interferon-gamma and hemochromatosis. *The Journal of biological chemistry* 277: 49727-49734.

49. Schaible, U. E., S. Sturgill-Koszycki, P. H. Schlesinger, and D. G. Russell. 1998. Cytokine activation leads to acidification and increases maturation of Mycobacterium avium-containing phagosomes in murine macrophages. *Journal of immunology* 160: 1290-1296.

50. MacMicking, J. D., G. A. Taylor, and J. D. McKinney. 2003. Immune control of tuberculosis by IFN-gamma-inducible LRG-47. *Science* 302: 654-659.

51. Fang, F. C. 2004. Antimicrobial reactive oxygen and nitrogen species: concepts and controversies. *Nature reviews. Microbiology* 2: 820-832.

52. Bogdan, C. 2015. Nitric oxide synthase in innate and adaptive immunity: an update. *Trends in immunology* 36: 161-178.

53. Shi, L., Y. J. Jung, S. Tyagi, M. L. Gennaro, and R. J. North. 2003. Expression of Th1-mediated immunity in mouse lungs induces a Mycobacterium tuberculosis transcription pattern characteristic of nonreplicating persistence. *Proceedings of the National Academy of Sciences of the United States of America* 100: 241-246.

54. Moreira-Teixeira, L., J. Sousa, F. W. McNab, E. Torrado, F. Cardoso, H. Machado, F. Castro, V. Cardoso, J. Gaifem, X. Wu, R. Appelberg, A. G. Castro, A. O'Garra, and M. Saraiva. 2016. Type I IFN Inhibits Alternative Macrophage Activation during Mycobacterium tuberculosis Infection and Leads to Enhanced Protection in the Absence of IFN-gamma Signaling. *Journal of immunology* 197: 4714-4726.

55. MacMicking, J. D., R. J. North, R. LaCourse, J. S. Mudgett, S. K. Shah, and C. F. Nathan. 1997. Identification of nitric oxide synthase as a protective locus against tuberculosis. *Proceedings of the National Academy of Sciences of the United States of America* 94: 5243-5248.

56. Scanga, C. A., V. P. Mohan, K. Tanaka, D. Alland, J. L. Flynn, and J. Chan. 2001. The inducible nitric oxide synthase locus confers protection against aerogenic challenge of both clinical and laboratory strains of Mycobacterium tuberculosis in mice. *Infection and immunity* 69: 7711-7717.

57. Cooper, A. M., D. K. Dalton, T. A. Stewart, J. P. Griffin, D. G. Russell, and I. M. Orme. 1993. Disseminated tuberculosis in interferon gamma gene-disrupted mice. *The Journal of experimental medicine* 178: 2243-2247.

58. Flynn, J. L., J. Chan, K. J. Triebold, D. K. Dalton, T. A. Stewart, and B. R. Bloom. 1993. An essential role for interferon gamma in resistance to Mycobacterium tuberculosis infection. *The Journal of experimental medicine* 178: 2249-2254.

59. Doherty, T. M., and A. Sher. 1997. Defects in cell-mediated immunity affect chronic, but not innate, resistance of mice to Mycobacterium avium infection. *Journal of immunology* 158: 4822-4831.

60. Gomes, M. S., M. Florido, T. F. Pais, and R. Appelberg. 1999. Improved clearance of Mycobacterium avium upon disruption of the inducible nitric oxide synthase gene. *Journal of immunology* 162: 6734-6739.

61. Cooper, A. M., L. B. Adams, D. K. Dalton, R. Appelberg, and S. Ehlers. 2002. IFN-gamma and NO in mycobacterial disease: new jobs for old hands. *Trends in microbiology* 10: 221-226.

62. Nathan, C., and A. Cunningham-Bussel. 2013. Beyond oxidative stress: an immunologist's guide to reactive oxygen species. *Nature reviews. Immunology* 13: 349-361.

63. Bustamante, J., G. Aksu, G. Vogt, L. de Beaucoudrey, F. Genel, A. Chapgier, O. Filipe-Santos, J. Feinberg, J. F. Emile, N. Kutukculer, and J. L. Casanova. 2007. BCG-osis and tuberculosis in a child with chronic granulomatous disease. *The Journal of allergy and clinical immunology* 120: 32-38.

64. Bustamante, J., A. A. Arias, G. Vogt, C. Picard, L. B. Galicia, C. Prando, A. V. Grant, C. C. Marchal, M. Hubeau, A. Chapgier, L. de Beaucoudrey, A. Puel, J. Feinberg, E. Valinetz, L. Janniere, C. Besse, A. Boland, J. M. Brisseau, S. Blanche, O. Lortholary, C. Fieschi, J. F. Emile, S. Boisson-Dupuis, S. Al-Muhsen, B. Woda, P. E. Newburger, A. Condino-Neto, M. C. Dinauer, L. Abel, and J. L. Casanova. 2011. Germline CYBB mutations that selectively affect macrophages in kindreds with X-linked predisposition to tuberculous mycobacterial disease. *Nature immunology* 12: 213-221.

65. Brandes, R. P., N. Weissmann, and K. Schroder. 2014. Nox family NADPH oxidases: Molecular mechanisms of activation. *Free radical biology & medicine* 76: 208-226.

66. Kim, B. H., A. R. Shenoy, P. Kumar, R. Das, S. Tiwari, and J. D. MacMicking. 2011. A family of IFN-gamma-inducible 65-kD GTPases protects against bacterial infection. *Science* 332: 717-721.

67. Vazquez-Torres, A., G. Fantuzzi, C. K. Edwards, 3rd, C. A. Dinarello, and F. C. Fang. 2001. Defective localization of the NADPH phagocyte oxidase to Salmonella-containing phagosomes in tumor necrosis factor p55 receptor-deficient macrophages. *Proceedings of the National Academy of Sciences of the United States of America* 98: 2561-2565.

68. Yazdanpanah, B., K. Wiegmann, V. Tchikov, O. Krut, C. Pongratz, M. Schramm, A. Kleinridders, T. Wunderlich, H. Kashkar, O. Utermohlen, J. C. Bruning, S. Schutze, and M. Kronke. 2009. Riboflavin kinase couples TNF receptor 1 to NADPH oxidase. *Nature* 460: 1159-1163.

69. Dewas, C., P. M. Dang, M. A. Gougerot-Pocidalo, and J. El-Benna. 2003. TNF-alpha induces phosphorylation of p47(phox) in human neutrophils: partial phosphorylation of

p47phox is a common event of priming of human neutrophils by TNF-alpha and granulocyte-macrophage colony-stimulating factor. *Journal of immunology* 171: 4392-4398.

70. Cooper, A. M., B. H. Segal, A. A. Frank, S. M. Holland, and I. M. Orme. 2000. Transient loss of resistance to pulmonary tuberculosis in p47(phox-/-) mice. *Infection and immunity* 68: 1231-1234.

71. Jung, Y. J., R. LaCourse, L. Ryan, and R. J. North. 2002. Virulent but not avirulent Mycobacterium tuberculosis can evade the growth inhibitory action of a T helper 1-dependent, nitric oxide Synthase 2-independent defense in mice. *The Journal of experimental medicine* 196: 991-998.

72. Olive, A. J., C. M. Smith, M. C. Kiritsy, and C. M. Sassetti. 2018. The Phagocyte Oxidase Controls Tolerance to Mycobacterium tuberculosis Infection. *Journal of immunology*.

73. Deffert, C., M. G. Schappi, J. C. Pache, J. Cachat, D. Vesin, R. Bisig, X. Ma Mulone, T. Kelkka, R. Holmdahl, I. Garcia, M. L. Olleros, and K. H. Krause. 2014. Bacillus calmette-guerin infection in NADPH oxidase deficiency: defective mycobacterial sequestration and granuloma formation. *PLoS pathogens* 10: e1004325.

74. Chao, W. C., C. L. Yen, C. Y. Hsieh, Y. F. Huang, Y. L. Tseng, P. A. Nigrovic, and C. C. Shieh. 2017. Mycobacterial infection induces higher interleukin-1beta and dysregulated lung inflammation in mice with defective leukocyte NADPH oxidase. *PloS one* 12: e0189453.

75. Segal, B. H., T. M. Doherty, T. A. Wynn, A. W. Cheever, A. Sher, and S. M. Holland. 1999. The p47(phox-/-) mouse model of chronic granulomatous disease has normal granuloma formation and cytokine responses to Mycobacterium avium and Schistosoma mansoni eggs. *Infection and immunity* 67: 1659-1665.

76. Fujita, M., E. Harada, T. Matsumoto, Y. Mizuta, S. Ikegame, H. Ouchi, I. Inoshima, S. Yoshida, K. Watanabe, and Y. Nakanishi. 2010. Impaired host defence against Mycobacterium avium in mice with chronic granulomatous disease. *Clinical and experimental immunology* 160: 457-460.

77. Sarmento, A., and R. Appelberg. 1996. Involvement of reactive oxygen intermediates in tumor necrosis factor alpha-dependent bacteriostasis of Mycobacterium avium. *Infection and immunity* 64: 3224-3230.

78. Sarmento, A. M., and R. Appelberg. 1995. Relationship between virulence of Mycobacterium avium strains and induction of tumor necrosis factor alpha production in infected mice and in in vitro-cultured mouse macrophages. *Infection and immunity* 63: 3759-3764.

79. Cassat, J. E., and E. P. Skaar. 2013. Iron in infection and immunity. *Cell host & microbe* 13: 509-519.

80. Wessling-Resnick, M. 2015. Nramp1 and Other Transporters Involved in Metal Withholding during Infection. *The Journal of biological chemistry* 290: 18984-18990.

81. Gomes, M. S., and R. Appelberg. 2002. NRAMP1- or cytokine-induced bacteriostasis of Mycobacterium avium by mouse macrophages is independent of the respiratory burst. *Microbiology* 148: 3155-3160.

82. North, R. J., R. LaCourse, L. Ryan, and P. Gros. 1999. Consequence of Nramp1 deletion to Mycobacterium tuberculosis infection in mice. *Infection and immunity* 67: 5811-5814.

83. Cooper, A. M., K. D. Mayer-Barber, and A. Sher. 2011. Role of innate cytokines in mycobacterial infection. *Mucosal immunology* 4: 252-260.

84. Behar, S. M., C. J. Martin, M. G. Booty, T. Nishimura, X. Zhao, H. X. Gan, M. Divangahi, and H. G. Remold. 2011. Apoptosis is an innate defense function of macrophages against Mycobacterium tuberculosis. *Mucosal immunology* 4: 279-287.

85. Mayer-Barber, K. D., B. B. Andrade, S. D. Oland, E. P. Amaral, D. L. Barber, J. Gonzales, S. C. Derrick, R. Shi, N. P. Kumar, W. Wei, X. Yuan, G. Zhang, Y. Cai, S. Babu, M. Catalfamo, A. M. Salazar, L. E. Via, C. E. Barry, 3rd, and A. Sher. 2014. Host-directed therapy of tuberculosis based on interleukin-1 and type I interferon crosstalk. *Nature* 511: 99-103.

86. Chen, M., M. Divangahi, H. Gan, D. S. Shin, S. Hong, D. M. Lee, C. N. Serhan, S. M. Behar, and H. G. Remold. 2008. Lipid mediators in innate immunity against tuberculosis: opposing roles of PGE2 and LXA4 in the induction of macrophage death. *The Journal of experimental medicine* 205: 2791-2801.

87. Divangahi, M., M. Chen, H. Gan, D. Desjardins, T. T. Hickman, D. M. Lee, S. Fortune, S. M. Behar, and H. G. Remold. 2009. Mycobacterium tuberculosis evades macrophage defenses by inhibiting plasma membrane repair. *Nature immunology* 10: 899-906.

88. Mayer-Barber, K. D., and A. Sher. 2015. Cytokine and lipid mediator networks in tuberculosis. *Immunological reviews* 264: 264-275.

89. Domingo-Gonzalez, R., O. Prince, A. Cooper, and S. A. Khader. 2016. Cytokines and Chemokines in Mycobacterium tuberculosis Infection. *Microbiology spectrum* 4.

90. Sica, A., and A. Mantovani. 2012. Macrophage plasticity and polarization: in vivo veritas. *The Journal of clinical investigation* 122: 787-795.

91. Murray, P. J. 2017. Macrophage Polarization. *Annual review of physiology* 79: 541-566.

92. Flynn, J. L., J. Chan, and P. L. Lin. 2011. Macrophages and control of granulomatous inflammation in tuberculosis. *Mucosal immunology* 4: 271-278.

93. Bhatt, K., S. P. Hickman, and P. Salgame. 2004. Cutting edge: a new approach to modeling early lung immunity in murine tuberculosis. *Journal of immunology* 172: 2748-2751.

94. Khader, S. A., S. Partida-Sanchez, G. Bell, D. M. Jelley-Gibbs, S. Swain, J. E. Pearl, N. Ghilardi, F. J. Desauvage, F. E. Lund, and A. M. Cooper. 2006. Interleukin 12p40 is required for dendritic cell migration and T cell priming after Mycobacterium tuberculosis infection. *The Journal of experimental medicine* 203: 1805-1815.

95. Cooper, A. M., A. Kipnis, J. Turner, J. Magram, J. Ferrante, and I. M. Orme. 2002. Mice lacking bioactive IL-12 can generate protective, antigen-specific cellular responses to mycobacterial infection only if the IL-12 p40 subunit is present. *Journal of immunology* 168: 1322-1327.

96. Feng, C. G., D. Jankovic, M. Kullberg, A. Cheever, C. A. Scanga, S. Hieny, P. Caspar, G. S. Yap, and A. Sher. 2005. Maintenance of pulmonary Th1 effector function in chronic tuberculosis requires persistent IL-12 production. *Journal of immunology* 174: 4185-4192.

97. Monin, L., and S. A. Khader. 2014. Chemokines in tuberculosis: the good, the bad and the ugly. *Seminars in immunology* 26: 552-558.

98. Chackerian, A. A., T. V. Perera, and S. M. Behar. 2001. Gamma interferon-producing CD4+ T lymphocytes in the lung correlate with resistance to infection with Mycobacterium tuberculosis. *Infection and immunity* 69: 2666-2674.

99. Chackerian, A. A., J. M. Alt, T. V. Perera, C. C. Dascher, and S. M. Behar. 2002. Dissemination of Mycobacterium tuberculosis is influenced by host factors and precedes the initiation of T-cell immunity. *Infection and immunity* 70: 4501-4509.

100. Kong, X. F., R. Martinez-Barricarte, J. Kennedy, F. Mele, T. Lazarov, E. K. Deenick, C. S. Ma, G. Breton, K. B. Lucero, D. Langlais, A. Bousfiha, C. Aytekin, J. Markle, C. Trouillet,

F. Jabot-Hanin, C. S. L. Arlehamn, G. Rao, C. Picard, T. Lasseau, D. Latorre, S. Hambleton, C. Deswarte, Y. Itan, K. Abarca, D. Moraes-Vasconcelos, F. Ailal, A. Ikinciogullari, F. Dogu, I. Benhsaien, A. Sette, L. Abel, S. Boisson-Dupuis, B. Schroder, M. C. Nussenzweig, K. Liu, F. Geissmann, S. G. Tangye, P. Gros, F. Sallusto, J. Bustamante, and J. L. Casanova. 2018. Disruption of an antimycobacterial circuit between dendritic and helper T cells in human SPPL2a deficiency. *Nature immunology* 19: 973-985.

101. Segal, A. W. 2005. How neutrophils kill microbes. *Annual review of immunology* 23: 197-223.

102. Ramos-Kichik, V., R. Mondragon-Flores, M. Mondragon-Castelan, S. Gonzalez-Pozos, S. Muniz-Hernandez, O. Rojas-Espinosa, R. Chacon-Salinas, S. Estrada-Parra, and I. Estrada-Garcia. 2009. Neutrophil extracellular traps are induced by Mycobacterium tuberculosis. *Tuberculosis* 89: 29-37.

103. Appelberg, R., A. G. Castro, S. Gomes, J. Pedrosa, and M. T. Silva. 1995. Susceptibility of beige mice to Mycobacterium avium: role of neutrophils. *Infection and immunity* 63: 3381-3387.

104. Pedrosa, J., B. M. Saunders, R. Appelberg, I. M. Orme, M. T. Silva, and A. M. Cooper. 2000. Neutrophils play a protective nonphagocytic role in systemic Mycobacterium tuberculosis infection of mice. *Infection and immunity* 68: 577-583.

105. Silva, M. T., M. N. Silva, and R. Appelberg. 1989. Neutrophil-macrophage cooperation in the host defence against mycobacterial infections. *Microbial pathogenesis* 6: 369-380.

106. Tan, B. H., C. Meinken, M. Bastian, H. Bruns, A. Legaspi, M. T. Ochoa, S. R. Krutzik, B. R. Bloom, T. Ganz, R. L. Modlin, and S. Stenger. 2006. Macrophages acquire neutrophil granules for antimicrobial activity against intracellular pathogens. *Journal of immunology* 177: 1864-1871.

107. Blomgran, R., and J. D. Ernst. 2011. Lung neutrophils facilitate activation of naive antigen-specific CD4+ T cells during Mycobacterium tuberculosis infection. *Journal of immunology* 186: 7110-7119.

108. Blomgran, R., L. Desvignes, V. Briken, and J. D. Ernst. 2012. Mycobacterium tuberculosis inhibits neutrophil apoptosis, leading to delayed activation of naive CD4 T cells. *Cell host & microbe* 11: 81-90.

109. Lowe, D. M., P. S. Redford, R. J. Wilkinson, A. O'Garra, and A. R. Martineau. 2012. Neutrophils in tuberculosis: friend or foe? *Trends in immunology* 33: 14-25.

110. Appelberg, R. 2007. Neutrophils and intracellular pathogens: beyond phagocytosis and killing. *Trends in microbiology* 15: 87-92.

111. Maglione, P. J., and J. Chan. 2009. How B cells shape the immune response against Mycobacterium tuberculosis. *European journal of immunology* 39: 676-686.

112. Torrado, E., J. J. Fountain, R. T. Robinson, C. A. Martino, J. E. Pearl, J. Rangel-Moreno, M. Tighe, R. Dunn, and A. M. Cooper. 2013. Differential and site specific impact of B cells in the protective immune response to Mycobacterium tuberculosis in the mouse. *PloS one* 8: e61681.

113. Kozakiewicz, L., Y. Chen, J. Xu, Y. Wang, K. Dunussi-Joannopoulos, Q. Ou, J. L. Flynn, S. A. Porcelli, W. R. Jacobs, Jr., and J. Chan. 2013. B cells regulate neutrophilia during Mycobacterium tuberculosis infection and BCG vaccination by modulating the interleukin-17 response. *PLoS pathogens* 9: e1003472.

114. Behar, S. M. 2013. Antigen-specific CD8(+) T cells and protective immunity to tuberculosis. *Advances in experimental medicine and biology* 783: 141-163.

115. Behar, S. M., C. C. Dascher, M. J. Grusby, C. R. Wang, and M. B. Brenner. 1999. Susceptibility of mice deficient in CD1D or TAP1 to infection with Mycobacterium tuberculosis. *The Journal of experimental medicine* 189: 1973-1980.

116. Sousa, A. O., R. J. Mazzaccaro, R. G. Russell, F. K. Lee, O. C. Turner, S. Hong, L. Van Kaer, and B. R. Bloom. 2000. Relative contributions of distinct MHC class I-dependent cell populations in protection to tuberculosis infection in mice. *Proceedings of the National Academy of Sciences of the United States of America* 97: 4204-4208.

117. Mogues, T., M. E. Goodrich, L. Ryan, R. LaCourse, and R. J. North. 2001. The relative importance of T cell subsets in immunity and immunopathology of airborne Mycobacterium tuberculosis infection in mice. *The Journal of experimental medicine* 193: 271-280.

118. Turner, J., C. D. D'Souza, J. E. Pearl, P. Marietta, M. Noel, A. A. Frank, R. Appelberg, I. M. Orme, and A. M. Cooper. 2001. CD8- and CD95/95L-dependent mechanisms of resistance in mice with chronic pulmonary tuberculosis. *American journal of respiratory cell and molecular biology* 24: 203-209.

119. Woodworth, J. S., Y. Wu, and S. M. Behar. 2008. Mycobacterium tuberculosis-specific CD8+ T cells require perforin to kill target cells and provide protection in vivo. *Journal of immunology* 181: 8595-8603.

120. Saunders, B. M., and C. Cheers. 1995. Inflammatory response following intranasal infection with Mycobacterium avium complex: role of T-cell subsets and gamma interferon. *Infection and immunity* 63: 2282-2287.

121. Appelberg, R., A. G. Castro, J. Pedrosa, R. A. Silva, I. M. Orme, and P. Minoprio. 1994. Role of gamma interferon and tumor necrosis factor alpha during T-cell-independent and -dependent phases of Mycobacterium avium infection. *Infection and immunity* 62: 3962-3971.

122. Schutz, C., G. Meintjes, F. Almajid, R. J. Wilkinson, and A. Pozniak. 2010. Clinical management of tuberculosis and HIV-1 co-infection. *The European respiratory journal* 36: 1460-1481.

123. Saunders, B. M., A. A. Frank, I. M. Orme, and A. M. Cooper. 2002. CD4 is required for the development of a protective granulomatous response to pulmonary tuberculosis. *Cellular immunology* 216: 65-72.

124. Florido, M., A. M. Cooper, and R. Appelberg. 2002. Immunological basis of the development of necrotic lesions following Mycobacterium avium infection. *Immunology* 106: 590-601.

125. Reiley, W. W., M. D. Calayag, S. T. Wittmer, J. L. Huntington, J. E. Pearl, J. J. Fountain, C. A. Martino, A. D. Roberts, A. M. Cooper, G. M. Winslow, and D. L. Woodland. 2008. ESAT-6-specific CD4 T cell responses to aerosol Mycobacterium tuberculosis infection are initiated in the mediastinal lymph nodes. *Proceedings of the National Academy of Sciences of the United States of America* 105: 10961-10966.

126. Zhu, J., H. Yamane, and W. E. Paul. 2010. Differentiation of effector CD4 T cell populations (*). *Annual review of immunology* 28: 445-489.

127. Larson, R. P., S. Shafiani, and K. B. Urdahl. 2013. Foxp3(+) regulatory T cells in tuberculosis. *Advances in experimental medicine and biology* 783: 165-180.

128. Bustamante, J., S. Boisson-Dupuis, L. Abel, and J. L. Casanova. 2014. Mendelian susceptibility to mycobacterial disease: genetic, immunological, and clinical features of inborn errors of IFN-gamma immunity. *Seminars in immunology* 26: 454-470.

129. Cooper, A. M., A. D. Roberts, E. R. Rhoades, J. E. Callahan, D. M. Getzy, and I. M. Orme. 1995. The role of interleukin-12 in acquired immunity to Mycobacterium tuberculosis infection. *Immunology* 84: 423-432.

130. Cooper, A. M., J. Magram, J. Ferrante, and I. M. Orme. 1997. Interleukin 12 (IL-12) is crucial to the development of protective immunity in mice intravenously infected with mycobacterium tuberculosis. *The Journal of experimental medicine* 186: 39-45.

131. Castro, A. G., R. A. Silva, and R. Appelberg. 1995. Endogenously produced IL-12 is required for the induction of protective T cells during Mycobacterium avium infections in mice. *Journal of immunology* 155: 2013-2019.

132. Flynn, J. L., M. M. Goldstein, K. J. Triebold, J. Sypek, S. Wolf, and B. R. Bloom. 1995. IL-12 increases resistance of BALB/c mice to Mycobacterium tuberculosis infection. *Journal of immunology* 155: 2515-2524.

133. Doherty, T. M., and A. Sher. 1998. IL-12 promotes drug-induced clearance of Mycobacterium avium infection in mice. *Journal of immunology* 160: 5428-5435.

134. Gallegos, A. M., J. W. van Heijst, M. Samstein, X. Su, E. G. Pamer, and M. S. Glickman. 2011. A gamma interferon independent mechanism of CD4 T cell mediated control of M. tuberculosis infection in vivo. *PLoS pathogens* 7: e1002052.

135. Sakai, S., K. D. Kauffman, M. A. Sallin, A. H. Sharpe, H. A. Young, V. V. Ganusov, and D. L. Barber. 2016. CD4 T Cell-Derived IFN-gamma Plays a Minimal Role in Control of Pulmonary Mycobacterium tuberculosis Infection and Must Be Actively Repressed by PD-1 to Prevent Lethal Disease. *PLoS pathogens* 12: e1005667.

136. Sallin, M. A., K. D. Kauffman, C. Riou, E. Du Bruyn, T. W. Foreman, S. Sakai, S. G. Hoft, T. G. Myers, P. J. Gardina, A. Sher, R. Moore, T. Wilder-Kofie, I. N. Moore, A. Sette, C. S. Lindestam Arlehamn, R. J. Wilkinson, and D. L. Barber. 2018. Host resistance to pulmonary Mycobacterium tuberculosis infection requires CD153 expression. *Nature microbiology*.

137. Florido, M., M. Borges, H. Yagita, and R. Appelberg. 2004. Contribution of CD30/CD153 but not of CD27/CD70, CD134/OX40L, or CD137/4-1BBL to the optimal induction of protective immunity to Mycobacterium avium. *Journal of leukocyte biology* 76: 1039-1046.

138. Walker, J. A., and A. N. J. McKenzie. 2018. TH2 cell development and function. *Nature reviews. Immunology* 18: 121-133.

139. Roy, E., J. Brennan, S. Jolles, and D. B. Lowrie. 2008. Beneficial effect of anti-interleukin-4 antibody when administered in a murine model of tuberculosis infection. *Tuberculosis* 88: 197-202.

140. North, R. J. 1998. Mice incapable of making IL-4 or IL-10 display normal resistance to infection with Mycobacterium tuberculosis. *Clinical and experimental immunology* 113: 55-58.

141. Jung, Y. J., R. LaCourse, L. Ryan, and R. J. North. 2002. Evidence inconsistent with a negative influence of T helper 2 cells on protection afforded by a dominant T helper 1 response against Mycobacterium tuberculosis lung infection in mice. *Infection and immunity* 70: 6436-6443.

142. Pagan, A. J., and L. Ramakrishnan. 2018. The Formation and Function of Granulomas. *Annual review of immunology* 36: 639-665.

143. Das, S., and S. Khader. 2017. Yin and yang of interleukin-17 in host immunity to infection. *F1000Research* 6: 741.

144. Gopal, R., L. Monin, S. Slight, U. Uche, E. Blanchard, B. A. Fallert Junecko, R. Ramos-Payan, C. L. Stallings, T. A. Reinhart, J. K. Kolls, D. Kaushal, U. Nagarajan, J. Rangel-Moreno, and S. A. Khader. 2014. Unexpected role for IL-17 in protective immunity against hypervirulent Mycobacterium tuberculosis HN878 infection. *PLoS pathogens* 10: e1004099.

145. Segueni, N., E. Tritto, M. L. Bourigault, S. Rose, F. Erard, M. Le Bert, M. Jacobs, F. Di Padova, D. P. Stiehl, P. Moulin, D. Brees, S. D. Chibout, B. Ryffel, M. Kammuller, and V. F. Quesniaux. 2016. Controlled Mycobacterium tuberculosis infection in mice under treatment with anti-IL-17A or IL-17F antibodies, in contrast to TNFalpha neutralization. *Scientific reports* 6: 36923.

146. Umemura, M., A. Yahagi, S. Hamada, M. D. Begum, H. Watanabe, K. Kawakami, T. Suda, K. Sudo, S. Nakae, Y. Iwakura, and G. Matsuzaki. 2007. IL-17-mediated regulation of innate and acquired immune response against pulmonary Mycobacterium bovis bacille Calmette-Guerin infection. *Journal of immunology* 178: 3786-3796.

147. Okamoto Yoshida, Y., M. Umemura, A. Yahagi, R. L. O'Brien, K. Ikuta, K. Kishihara, H. Hara, S. Nakae, Y. Iwakura, and G. Matsuzaki. 2010. Essential role of IL-17A in the formation of a mycobacterial infection-induced granuloma in the lung. *Journal of immunology* 184: 4414-4422.

148. Cruz, A., A. G. Fraga, J. J. Fountain, J. Rangel-Moreno, E. Torrado, M. Saraiva, D. R. Pereira, T. D. Randall, J. Pedrosa, A. M. Cooper, and A. G. Castro. 2010. Pathological role of interleukin 17 in mice subjected to repeated BCG vaccination after infection with Mycobacterium tuberculosis. *The Journal of experimental medicine* 207: 1609-1616.

149. Khader, S. A., G. K. Bell, J. E. Pearl, J. J. Fountain, J. Rangel-Moreno, G. E. Cilley, F. Shen, S. M. Eaton, S. L. Gaffen, S. L. Swain, R. M. Locksley, L. Haynes, T. D. Randall, and A. M. Cooper. 2007. IL-23 and IL-17 in the establishment of protective pulmonary CD4+ T cell responses after vaccination and during Mycobacterium tuberculosis challenge. *Nature immunology* 8: 369-377.

150. Cruz, A., S. A. Khader, E. Torrado, A. Fraga, J. E. Pearl, J. Pedrosa, A. M. Cooper, and A. G. Castro. 2006. Cutting edge: IFN-gamma regulates the induction and expansion of IL-17-producing CD4 T cells during mycobacterial infection. *Journal of immunology* 177: 1416-1420.

151. Condos, R., W. N. Rom, Y. M. Liu, and N. W. Schluger. 1998. Local immune responses correlate with presentation and outcome in tuberculosis. *American journal of respiratory and critical care medicine* 157: 729-735.

152. Lowe, D. M., A. K. Bandara, G. E. Packe, R. D. Barker, R. J. Wilkinson, C. J. Griffiths, and A. R. Martineau. 2013. Neutrophilia independently predicts death in tuberculosis. *The European respiratory journal* 42: 1752-1757.

153. Keller, C., R. Hoffmann, R. Lang, S. Brandau, C. Hermann, and S. Ehlers. 2006. Genetically determined susceptibility to tuberculosis in mice causally involves accelerated and enhanced recruitment of granulocytes. *Infection and immunity* 74: 4295-4309.

154. Eruslanov, E. B., I. V. Lyadova, T. K. Kondratieva, K. B. Majorov, I. V. Scheglov, M. O. Orlova, and A. S. Apt. 2005. Neutrophil responses to Mycobacterium tuberculosis infection in genetically susceptible and resistant mice. *Infection and immunity* 73: 1744-1753.

155. Petrofsky, M., and L. E. Bermudez. 1999. Neutrophils from Mycobacterium avium-infected mice produce TNF-alpha, IL-12, and IL-1 beta and have a putative role in early host response. *Clinical immunology* 91: 354-358.

156. Zhang, X., L. Majlessi, E. Deriaud, C. Leclerc, and R. Lo-Man. 2009. Coactivation of Syk kinase and MyD88 adaptor protein pathways by bacteria promotes regulatory properties of neutrophils. *Immunity* 31: 761-771.

157. O'Garra, A., P. S. Redford, F. W. McNab, C. I. Bloom, R. J. Wilkinson, and M. P. Berry. 2013. The immune response in tuberculosis. *Annual review of immunology* 31: 475-527.

158. Redford, P. S., P. J. Murray, and A. O'Garra. 2011. The role of IL-10 in immune regulation during M. tuberculosis infection. *Mucosal immunology* 4: 261-270.

159. Ehlers, S., and U. E. Schaible. 2012. The granuloma in tuberculosis: dynamics of a host-pathogen collusion. *Frontiers in immunology* 3: 411.

160. Davis, J. M., and L. Ramakrishnan. 2009. The role of the granuloma in expansion and dissemination of early tuberculous infection. *Cell* 136: 37-49.

161. Torrado, E., and A. M. Cooper. 2010. IL-17 and Th17 cells in tuberculosis. *Cytokine & growth factor reviews* 21: 455-462.

162. Shaler, C. R., C. N. Horvath, M. Jeyanathan, and Z. Xing. 2013. Within the Enemy's Camp: contribution of the granuloma to the dissemination, persistence and transmission of Mycobacterium tuberculosis. *Frontiers in immunology* 4: 30.

163. Smith, D., H. Hansch, G. Bancroft, and S. Ehlers. 1997. T-cell-independent granuloma formation in response to Mycobacterium avium: role of tumour necrosis factor-alpha and interferon-gamma. *Immunology* 92: 413-421.

164. Flynn, J. L., M. M. Goldstein, J. Chan, K. J. Triebold, K. Pfeffer, C. J. Lowenstein, R. Schreiber, T. W. Mak, and B. R. Bloom. 1995. Tumor necrosis factor-alpha is required in the protective immune response against Mycobacterium tuberculosis in mice. *Immunity* 2: 561-572.

165. Lousada, S., M. Florido, and R. Appelberg. 2006. Regulation of granuloma fibrosis by nitric oxide during Mycobacterium avium experimental infection. *International journal of experimental pathology* 87: 307-315.

166. Adams, D. O. 1974. The structure of mononuclear phagocytes differentiating in vivo. I. Sequential fine and histologic studies of the effect of Bacillus Calmette-Guerin (BCG). *The American journal of pathology* 76: 17-48.

167. Cronan, M. R., R. W. Beerman, A. F. Rosenberg, J. W. Saelens, M. G. Johnson, S. H. Oehlers, D. M. Sisk, K. L. Jurcic Smith, N. A. Medvitz, S. E. Miller, L. A. Trinh, S. E. Fraser, J. F. Madden, J. Turner, J. E. Stout, S. Lee, and D. M. Tobin. 2016. Macrophage Epithelial Reprogramming Underlies Mycobacterial Granuloma Formation and Promotes Infection. *Immunity* 45: 861-876.

168. Helming, L., and S. Gordon. 2009. Molecular mediators of macrophage fusion. *Trends in cell biology* 19: 514-522.

169. Herrtwich, L., I. Nanda, K. Evangelou, T. Nikolova, V. Horn, Sagar, D. Erny, J. Stefanowski, L. Rogell, C. Klein, K. Gharun, M. Follo, M. Seidl, B. Kremer, N. Munke, J. Senges, M. Fliegauf, T. Aschman, D. Pfeifer, S. Sarrazin, M. H. Sieweke, D. Wagner, C. Dierks, T. Haaf, T. Ness, M. M. Zaiss, R. E. Voll, S. D. Deshmukh, M. Prinz, T. Goldmann, C. Holscher, A. E. Hauser, A. J. Lopez-Contreras, D. Grun, V. Gorgoulis, A. Diefenbach, P. Henneke, and A. Triantafyllopoulou. 2016. DNA Damage Signaling Instructs Polyploid Macrophage Fate in Granulomas. *Cell* 167: 1264-1280 e1218.

170. Adams, D. O. 1976. The granulomatous inflammatory response. A review. *The American journal of pathology* 84: 164-192.

171. Algood, H. M., J. Chan, and J. L. Flynn. 2003. Chemokines and tuberculosis. *Cytokine & growth factor reviews* 14: 467-477.

172. Russell, D. G., P. J. Cardona, M. J. Kim, S. Allain, and F. Altare. 2009. Foamy macrophages and the progression of the human tuberculosis granuloma. *Nature immunology* 10: 943-948.

173. Santucci, P., F. Bouzid, N. Smichi, I. Poncin, L. Kremer, C. De Chastellier, M. Drancourt, and S. Canaan. 2016. Experimental Models of Foamy Macrophages and Approaches for Dissecting the Mechanisms of Lipid Accumulation and Consumption during Dormancy and Reactivation of Tuberculosis. *Frontiers in cellular and infection microbiology* 6: 122.

174. Peyron, P., J. Vaubourgeix, Y. Poquet, F. Levillain, C. Botanch, F. Bardou, M. Daffe, J. F. Emile, B. Marchou, P. J. Cardona, C. de Chastellier, and F. Altare. 2008. Foamy macrophages from tuberculous patients' granulomas constitute a nutrient-rich reservoir for M. tuberculosis persistence. *PLoS pathogens* 4: e1000204.

175. Caire-Brandli, I., A. Papadopoulos, W. Malaga, D. Marais, S. Canaan, L. Thilo, and C. de Chastellier. 2014. Reversible lipid accumulation and associated division arrest of Mycobacterium avium in lipoprotein-induced foamy macrophages may resemble key events during latency and reactivation of tuberculosis. *Infection and immunity* 82: 476-490.

176. Groom, J. R., and A. D. Luster. 2011. CXCR3 in T cell function. *Experimental cell research* 317: 620-631.

177. Florido, M., A. S. Goncalves, R. A. Silva, S. Ehlers, A. M. Cooper, and R. Appelberg. 1999. Resistance of virulent Mycobacterium avium to gamma interferon-mediated antimicrobial activity suggests additional signals for induction of mycobacteriostasis. *Infection and immunity* 67: 3610-3618.

178. Roach, D. R., A. G. Bean, C. Demangel, M. P. France, H. Briscoe, and W. J. Britton. 2002. TNF regulates chemokine induction essential for cell recruitment, granuloma formation, and clearance of mycobacterial infection. *Journal of immunology* 168: 4620-4627.

179. Florido, M., and R. Appelberg. 2007. Characterization of the deregulated immune activation occurring at late stages of mycobacterial infection in TNF-deficient mice. *Journal of immunology* 179: 7702-7708.

180. Mohan, V. P., C. A. Scanga, K. Yu, H. M. Scott, K. E. Tanaka, E. Tsang, M. M. Tsai, J. L. Flynn, and J. Chan. 2001. Effects of tumor necrosis factor alpha on host immune response in chronic persistent tuberculosis: possible role for limiting pathology. *Infection and immunity* 69: 1847-1855.

181. Keane, J., S. Gershon, R. P. Wise, E. Mirabile-Levens, J. Kasznica, W. D. Schwieterman, J. N. Siegel, and M. M. Braun. 2001. Tuberculosis associated with infliximab, a tumor necrosis factor alpha-neutralizing agent. *The New England journal of medicine* 345: 1098-1104.

182. Keane, J. 2005. TNF-blocking agents and tuberculosis: new drugs illuminate an old topic. *Rheumatology* 44: 714-720.

183. Askling, J., C. M. Fored, L. Brandt, E. Baecklund, L. Bertilsson, L. Coster, P. Geborek, L. T. Jacobsson, S. Lindblad, J. Lysholm, S. Rantapaa-Dahlqvist, T. Saxne, V. Romanus, L. Klareskog, and N. Feltelius. 2005. Risk and case characteristics of tuberculosis in rheumatoid arthritis associated with tumor necrosis factor antagonists in Sweden. *Arthritis and rheumatism* 52: 1986-1992.

184. Shaikha, S. A., K. Mansour, and H. Riad. 2012. Reactivation of Tuberculosis in Three Cases of Psoriasis after Initiation of Anti-TNF Therapy. *Case reports in dermatology* 4: 41-46.

185. Kim, M. J., H. C. Wainwright, M. Locketz, L. G. Bekker, G. B. Walther, C. Dittrich, A. Visser, W. Wang, F. F. Hsu, U. Wiehart, L. Tsenova, G. Kaplan, and D. G. Russell. 2010.

Caseation of human tuberculosis granulomas correlates with elevated host lipid metabolism. *EMBO molecular medicine* 2: 258-274.

186. Orme, I. M. 1998. The immunopathogenesis of tuberculosis: a new working hypothesis. *Trends in microbiology* 6: 94-97.
187. Kramnik, I., and G. Beamer. 2016. Mouse models of human TB pathology: roles in the analysis of necrosis and the development of host-directed therapies. *Seminars in immunopathology* 38: 221-237.
188. Via, L. E., P. L. Lin, S. M. Ray, J. Carrillo, S. S. Allen, S. Y. Eum, K. Taylor, E. Klein, U. Manjunatha, J. Gonzales, E. G. Lee, S. K. Park, J. A. Raleigh, S. N. Cho, D. N. McMurray, J. L. Flynn, and C. E. Barry, 3rd. 2008. Tuberculous granulomas are hypoxic in guinea pigs, rabbits, and nonhuman primates. *Infection and immunity* 76: 2333-2340.
189. Harper, J., C. Skerry, S. L. Davis, R. Tasneen, M. Weir, I. Kramnik, W. R. Bishai, M. G. Pomper, E. L. Nuermberger, and S. K. Jain. 2012. Mouse model of necrotic tuberculosis granulomas develops hypoxic lesions. *The Journal of infectious diseases* 205: 595-602.
190. Cardoso, M. S., T. M. Silva, M. Resende, R. Appelberg, and M. Borges. 2015. Lack of the Transcription Factor Hypoxia-Inducible Factor 1alpha (HIF-1alpha) in Macrophages Accelerates the Necrosis of Mycobacterium avium-Induced Granulomas. *Infection and immunity* 83: 3534-3544.
191. Cortez, V. S., M. L. Robinette, and M. Colonna. 2015. Innate lymphoid cells: new insights into function and development. *Current opinion in immunology* 32: 71-77.
192. Rochman, Y., R. Spolski, and W. J. Leonard. 2009. New insights into the regulation of T cells by gamma(c) family cytokines. *Nature reviews. Immunology* 9: 480-490.
193. Spits, H., D. Artis, M. Colonna, A. Diefenbach, J. P. Di Santo, G. Eberl, S. Koyasu, R. M. Locksley, A. N. McKenzie, R. E. Mebius, F. Powrie, and E. Vivier. 2013. Innate lymphoid cells–a proposal for uniform nomenclature. *Nature reviews. Immunology* 13: 145-149.
194. Eberl, G., M. Colonna, J. P. Di Santo, and A. N. McKenzie. 2015. Innate lymphoid cells. Innate lymphoid cells: a new paradigm in immunology. *Science* 348: aaa6566.
195. Artis, D., and H. Spits. 2015. The biology of innate lymphoid cells. *Nature* 517: 293-301.
196. Klose, C. S., and D. Artis. 2016. Innate lymphoid cells as regulators of immunity, inflammation and tissue homeostasis. *Nature immunology* 17: 765-774.
197. Spits, H., J. H. Bernink, and L. Lanier. 2016. NK cells and type 1 innate lymphoid cells: partners in host defense. *Nature immunology* 17: 758-764.

198. Diefenbach, A., M. Colonna, and S. Koyasu. 2014. Development, differentiation, and diversity of innate lymphoid cells. *Immunity* 41: 354-365.

199. Xu, W., R. G. Domingues, D. Fonseca-Pereira, M. Ferreira, H. Ribeiro, S. Lopez-Lastra, Y. Motomura, L. Moreira-Santos, F. Bihl, V. Braud, B. Kee, H. Brady, M. C. Coles, C. Vosshenrich, M. Kubo, J. P. Di Santo, and H. Veiga-Fernandes. 2015. NFIL3 orchestrates the emergence of common helper innate lymphoid cell precursors. *Cell reports* 10: 2043-2054.

200. Firth, M. A., S. Madera, A. M. Beaulieu, G. Gasteiger, E. F. Castillo, K. S. Schluns, M. Kubo, P. B. Rothman, E. Vivier, and J. C. Sun. 2013. Nfil3-independent lineage maintenance and antiviral response of natural killer cells. *The Journal of experimental medicine* 210: 2981-2990.

201. Cortez, V. S., A. Fuchs, M. Cella, S. Gilfillan, and M. Colonna. 2014. Cutting edge: Salivary gland NK cells develop independently of Nfil3 in steady-state. *Journal of immunology* 192: 4487-4491.

202. Boulenouar, S., J. M. Doisne, A. Sferruzzi-Perri, L. M. Gaynor, J. Kieckbusch, E. Balmas, H. W. Yung, S. Javadzadeh, L. Volmer, D. A. Hawkes, K. Phillips, H. J. Brady, A. L. Fowden, G. J. Burton, A. Moffett, and F. Colucci. 2016. The Residual Innate Lymphoid Cells in NFIL3-Deficient Mice Support Suboptimal Maternal Adaptations to Pregnancy. *Frontiers in immunology* 7: 43.

203. Cortez, V. S., and M. Colonna. 2016. Diversity and function of group 1 innate lymphoid cells. *Immunology letters* 179: 19-24.

204. Klose, C. S., M. Flach, L. Mohle, L. Rogell, T. Hoyler, K. Ebert, C. Fabiunke, D. Pfeifer, V. Sexl, D. Fonseca-Pereira, R. G. Domingues, H. Veiga-Fernandes, S. J. Arnold, M. Busslinger, I. R. Dunay, Y. Tanriver, and A. Diefenbach. 2014. Differentiation of type 1 ILCs from a common progenitor to all helper-like innate lymphoid cell lineages. *Cell* 157: 340-356.

205. Constantinides, M. G., B. D. McDonald, P. A. Verhoef, and A. Bendelac. 2014. A committed precursor to innate lymphoid cells. *Nature* 508: 397-401.

206. Colonna, M. 2018. Innate Lymphoid Cells: Diversity, Plasticity, and Unique Functions in Immunity. *Immunity* 48: 1104-1117.

207. Spits, H. 2015. TOX sets the stage for innate lymphoid cells. *Nature immunology* 16: 594-595.

208. Eberl, G., J. P. Di Santo, and E. Vivier. 2015. The brave new world of innate lymphoid cells. *Nature immunology* 16: 1-5.

209. Klose, C. S., E. A. Kiss, V. Schwierzeck, K. Ebert, T. Hoyler, Y. d'Hargues, N. Goppert, A. L. Croxford, A. Waisman, Y. Tanriver, and A. Diefenbach. 2013. A T-bet gradient controls the fate and function of CCR6-RORgammat+ innate lymphoid cells. *Nature* 494: 261-265.

210. Bernink, J. H., L. Krabbendam, K. Germar, E. de Jong, K. Gronke, M. Kofoed-Nielsen, J. M. Munneke, M. D. Hazenberg, J. Villaudy, C. J. Buskens, W. A. Bemelman, A. Diefenbach, B. Blom, and H. Spits. 2015. Interleukin-12 and -23 Control Plasticity of CD127(+) Group 1 and Group 3 Innate Lymphoid Cells in the Intestinal Lamina Propria. *Immunity* 43: 146-160.

211. Silver, J. S., J. Kearley, A. M. Copenhaver, C. Sanden, M. Mori, L. Yu, G. H. Pritchard, A. A. Berlin, C. A. Hunter, R. Bowler, J. S. Erjefalt, R. Kolbeck, and A. A. Humbles. 2016. Inflammatory triggers associated with exacerbations of COPD orchestrate plasticity of group 2 innate lymphoid cells in the lungs. *Nature immunology* 17: 626-635.

212. Ohne, Y., J. S. Silver, L. Thompson-Snipes, M. A. Collet, J. P. Blanck, B. L. Cantarel, A. M. Copenhaver, A. A. Humbles, and Y. J. Liu. 2016. IL-1 is a critical regulator of group 2 innate lymphoid cell function and plasticity. *Nature immunology* 17: 646-655.

213. Neill, D. R., S. H. Wong, A. Bellosi, R. J. Flynn, M. Daly, T. K. Langford, C. Bucks, C. M. Kane, P. G. Fallon, R. Pannell, H. E. Jolin, and A. N. McKenzie. 2010. Nuocytes represent a new innate effector leukocyte that mediates type-2 immunity. *Nature* 464: 1367-1370.

214. Saunders, B. M., and C. Cheers. 1996. Intranasal infection of beige mice with Mycobacterium avium complex: role of neutrophils and natural killer cells. *Infection and immunity* 64: 4236-4241.

215. Florido, M., R. Appelberg, I. M. Orme, and A. M. Cooper. 1997. Evidence for a reduced chemokine response in the lungs of beige mice infected with Mycobacterium avium. *Immunology* 90: 600-606.

216. Junqueira-Kipnis, A. P., A. Kipnis, A. Jamieson, M. G. Juarrero, A. Diefenbach, D. H. Raulet, J. Turner, and I. M. Orme. 2003. NK cells respond to pulmonary infection with Mycobacterium tuberculosis, but play a minimal role in protection. *Journal of immunology* 171: 6039-6045.

217. Feng, C. G., M. Kaviratne, A. G. Rothfuchs, A. Cheever, S. Hieny, H. A. Young, T. A. Wynn, and A. Sher. 2006. NK cell-derived IFN-gamma differentially regulates innate resistance and neutrophil response in T cell-deficient hosts infected with Mycobacterium tuberculosis. *Journal of immunology* 177: 7086-7093.

218. Florido, M., M. Correia-Neves, A. M. Cooper, and R. Appelberg. 2003. The cytolytic activity of natural killer cells is not involved in the restriction of Mycobacterium avium growth. *International immunology* 15: 895-901.

Chapter II

INNATE IFN-γ-PRODUCING CELLS DEVELOPING IN THE ABSENCE OF IL-2 RECEPTOR COMMON γ-CHAIN

The Journal of Immunology, 2017, 199: 1429-1439.

The Journal of Immunology

Innate IFN-γ–Producing Cells Developing in the Absence of IL-2 Receptor Common γ-Chain

Mariana Resende,*,† Marcos S. Cardoso,* Ana R. Ribeiro,* Manuela Flórido,*,1 Margarida Borges,*,2 António Gil Castro,† Nuno L. Alves,* Andrea M. Cooper,‡,3 and Rui Appelberg*

IFN-γ is known to be predominantly produced by lymphoid cells such as certain subsets of T cells, NK cells, and other group 1 innate lymphoid cells. In this study, we used IFN-γ reporter mouse models to search for additional cells capable of secreting this cytokine. We identified a novel and rare population of nonconventional IFN-γ–producing cells of hematopoietic origin that were characterized by the expression of Thy1.2 and the lack of lymphoid, myeloid, and NK lineage markers. The expression of IFN-γ by this population was higher in the liver and lower in the spleen. Furthermore, these cells were present in mice lacking both the *Rag2* and the common γ-chain (γc) genes ($Rag2^{-/-}\gamma c^{-/-}$), indicating their innate nature and their γc cytokine independence. $Rag2^{-/-}\gamma c^{-/-}$ mice are as resistant to *Mycobacterium avium* as $Rag2^{-/-}$ mice, whereas $Rag2^{-/-}$ mice lacking IFN-γ are more susceptible than either $Rag2^{-/-}$ or $Rag2^{-/-}\gamma c^{-/-}$. These lineage-negative $CD45^{+}/Thy1.2^{+}$ cells are found within the mycobacterially induced granulomatous structure in the livers of infected $Rag2^{-/-}\gamma c^{-/-}$ animals and are adjacent to macrophages that expressed inducible NO synthase, suggesting a potential protective role for these IFN-γ–producing cells. Accordingly, Thy1.2-specific mAb administration to infected $Rag2^{-/-}\gamma c^{-/-}$ animals increased *M. avium* growth in the liver. Overall, our results demonstrate that a population of $Thy1.2^{+}$ non-NK innate-like cells present in the liver expresses IFN-γ and can confer protection against *M. avium* infection in immunocompromised mice. ***The Journal of Immunology*****, 2017, 199: 000–000.**

Interferon-γ is a proinflammatory cytokine that plays a major role in protective immune responses against intracellular pathogens. Upon infection, phagocytes will respond by producing cytokines such as IL-12 and IL-18, which will induce NK cells and invariant NK T cells to release IFN-γ during the innate phase of the immune response. At later stages, $CD4^{+}$ and $CD8^{+}$ T cells are primed to produce IFN-γ and contribute to pathogen clearance (reviewed in Ref. 1). The major cellular targets of IFN-γ are mononuclear phagocytes that are activated to upregulate Ag processing and presentation pathways, lysosomal activity, and reactive species production, which in turn mediate the microbicidal effect (1, 2). IFN-γ is also responsible for inducing leukocyte recruitment to the infection site and generation of granulomatous lesions, such as the ones induced by mycobacterial infections (1), wherein the newly recruited leukocytes are able to produce more IFN-γ as well as other cytokines that will directly act on the infected cells. Ab-mediated or genetic ablation of IFN-γ signaling severely compromises the in vivo assembly of granulomas in mycobacterial infections (3–5). Complete lack of IFN-γ signaling, such as found in gene-deleted mice, leads to an increased susceptibility to infection relative to that seen when only IFN-γ–producing T cells are lacking (6–9). NK cells are efficient producers of IFN-γ (1, 10) and have been associated with IFN-γ–mediated protection, particularly in the absence of T cells (11, 12). However, mice that lack B and T cells, NK cells, and the other innate lymphoid cells (ILCs), as a result of the deletion of the Rag enzyme required for TCR and BCR recombination and the IL-2R common γ-chain (γc), are more resistant to *Chlamydia pneumoniae* than $Rag1^{-/-}$IFN-$\gamma^{-/-}$double-knockout mice (13). In addition, the authors showed that both $Rag1^{-/-}$ and $Rag1^{-/-}\gamma c^{-/-}$ express equivalent levels of *Ifng* mRNA and protein in infected lungs. These data suggest, therefore, the existence of an additional cellular source of IFN-γ. Indeed, several reports propose the existence of nonconventional IFN-γ–producing cells. Infection with

*IBMC – Instituto de Biologia Molecular e Celular and i3S – Instituto de Investigação em Saúde, Universidade do Porto, 4200-135 Porto, Portugal; †Life and Health Sciences Research Institute (ICVS), School of Health Sciences, University of Minho and ICVS/3B's – PT Government Associate Laboratory, 4170 Braga/Guimarães, Portugal; and ‡Trudeau Institute, Saranac Lake, NY 12983

[1]Current address: Mycobacterial Research Group, Centenary Institute of Cancer Medicine and Cell Biology, Newtown, NSW, Australia.

[2]Current address: UCIBIO/REQUIMTE, Departamento de Ciências Biológicas, Laboratório de Bioquímica, Faculdade de Farmácia da Universidade do Porto, Porto, Portugal.

[3]Current address: Department of Infection, Immunity and Inflammation, University of Leicester, Leicester, U.K.

ORCIDs: 0000-0003-4835-3035 (M.R.); 0000-0003-0150-7359 (M.S.C.); 0000-0001-6035-4095 (M.B.); 0000-0002-1567-8389 (N.L.A.); 0000-0001-6050-3863 (A.M.C.); 0000-0002-9447-0665 (R.A.).

Received for publication October 7, 2016. Accepted for publication June 11, 2017.

This work was supported by a structured program on bioengineered therapies for infectious diseases and tissue regeneration (Grant NORTE-01-0145-FEDER-000012) supported by Norte Portugal Regional Operational Programme (NORTE 2020, under the Portugal 2020 Partnership Agreement, through the European Regional Development Fund); by Fundo Europeu de Desenvolvimento Regional funds through the COMPETE 2020 – Operacional Programme for Competitiveness and Internationalisation, Portugal 2020; by Portuguese funds through Fundação para a Ciência e a Tecnologia/Ministério da Ciência (FCT), Tecnologia e Inovação in the framework of the project "Institute for Research and Innovation in Health Sciences" (Grant POCI-01-0145-FEDER-007274); by the Trudeau Institute, Inc.; and by FCT Grant SFRH/BD/89871/2012 (to M.R.).

Address correspondence and reprint requests to Mariana Resende, Instituto de Biologia Molecular e Celular, Universidade do Porto, Rua Alfredo Allen 208, 4200-135 Porto, Portugal. E-mail address: mrsilva@ibmc.up.pt

The online version of this article contains supplemental material.

Abbreviations used in this article: γc, γ-chain; dpi, day postinfection; ILC, innate lymphoid cell; ILCp, ILC progenitor; iNOS, inducible NO synthase; qPCR, quantitative PCR; Yeti, YFP-enhanced transcript for IFN-γ.

www.jimmunol.org/cgi/doi/10.4049/jimmunol.1601701

Escherichia coli or *Listeria monocytogenes* induces IFN-γ production by splenic innate B cells, which in turn promotes an innate response against these bacteria (14). Human oral epithelial cells have also been shown to produce IFN-γ upon in vitro infection with *Candida albicans* (15). Expression or secretion of IFN-γ has been detected in peritoneal or splenic macrophages and in bone marrow–derived macrophages or dendritic cells after in vitro stimulation with IL-12/IL-18 or infection with different pathogens (*C. pneumoniae*, *Salmonella typhimurium*) (16–21). However, a more detailed study revealed that the lack of purity of the myeloid cells casts doubt upon macrophages as the source of the IFN-γ (22, 23). More recently, work from Sturge et al. (24) identified peritoneal neutrophils as an IL-12–independent source of IFN-γ in response to *Toxoplasma gondii*.

To identify novel cellular sources of IFN-γ, we used reporter mouse models and describe in this article a rare population of IFN-γ–expressing CD45$^+$ Thy1.2$^+$ cells that are of nonlymphoid, nonmyeloid, and non-NK lineage. Moreover, we provide experimental evidence that these cells are functionally relevant, conferring protection against *M. avium* infection in the liver of lymphopenic Rag2$^{-/-}$γc$^{-/-}$ (lacking both the *Rag2* and the common γc genes) mice.

Materials and Methods

Animals

YFP-enhanced transcript for IFN-γ (Yeti) mice were crossed with C57BL/6.Rag1$^{-/-}$ mice at the Trudeau animal house facilities. Yeti mice were generated by the introduction of an IRES–enhanced YFP construct after the stop codon of IFN-γ and is under the control of a bovine growth hormone polyA tail (25). The IFN-γ reporter with endogenous polyA tail (Great) mice (C57BL/6 background) have the IFN-γ-IRES-enhanced YFP reporter cassette under the control of the endogenous *ifng* 3′ untranslated region and polyA tail (25). All procedures involving live animals were performed in accordance with the Guide for Care and Use of Laboratory Animals of the National Institutes of Health, and individual procedures were approved by the Trudeau Institute Animal Care and Use Committee.

C57BL/6.IFN-γ$^{-/-}$ mice were purchased from Jackson Laboratories (Bar Harbor, ME), and C57BL/6.Rag2$^{-/-}$ mice were obtained from the Centre de Développement des Techniques Avancées pour l'expérimentation animale (Orleans, France). The two strains were crossed at Instituto de Biologia Molecular e Celular animal facilities to obtain double-mutant mice. Double-knockout mice were screened by performing PCR with IFN-γ gene-specific primers (according to Jackson Laboratories) from genomic DNA extracted from an ear clipping and by performing flow cytometric analysis of blood samples to detect lymphopenic mice. Mice deficient in both Rag2 and the common γc (B6.Rag2$^{-/-}$.γc$^{-/-}$) were provided by Dr. J. di Santo. Animal care procedures were in accordance with institutional guidelines. This study was previously approved by the Portuguese National Authority for Animal Health–Direcção Geral de Veterinária.

Infection and Ab administration

Mice were infected with *Mycobacterium avium* strain 2447 by injecting 10^6 CFUs i.v. At different times of infection, mice were sacrificed and the bacterial burden was determined in the major target organs, the spleen and the liver, by plating serial dilutions of tissue homogenates onto Middlebrook 7H10 medium (Difco, St. Louis, MO). In two experiments, infected Rag2$^{-/-}$γc$^{-/-}$ were injected i.p. with 0.4 mg of 30-H12 (anti-Thy1.2) or nonspecific IgG twice a week throughout 60 d of infection.

Abs

The following conjugated mAbs were used in flow cytometry: Brilliant Violet (BV) 421 anti-mouse CD11c, clone N418, Isotype Armenian hamster IgG; Pacific Blue (PB) anti-mouse Ly6G, clone 1A8, Isotype rat IgG2a, k; BV510 anti-mouse CD3, clone 17A2, Isotype rat IgG2b, k; BV510 anti-mouse/human CD11b, clone RM4-5, Isotype rat IgG2b, k; FITC CD90.2 (Thy1.2), clone 30-H12, Isotype rat IgG2b, k; FITC anti-mouse NK1.1, clone PK136, Isotype mouse IgG2a, k; FITC anti-mouse CD335 (NKp46), clone 29A1.4, Isotype rat IgG2a, k; FITC anti-mouse CD49b, clone HMα2, Isotype Armenian hamster IgG; PE anti-mouse CD11c, clone N418; Isotype Armenian Hamster IgG; PerCP/Cy5.5 anti-mouse CD19, clone 6D5; Isotype rat IgG2a, k; PerCP/Cy5.5 anti-mouse CD45, clone I3/2.3, Isotype rat IgG2b, k; PerCP/Cy5.5 anti-mouse Ly-6A/E (Sca-1), clone D7, Isotype rat IgG2a, k; PerCP/Cy5.5 anti-mouse TCRγδ, clone GL3, Isotype Armenian hamster IgG; PE/Cy7 anti-mouse/human CD11b, clone M1/70, Isotype IgG2b, k; PE/Cy7 anti-mouse CD11c, clone N418, Isotype Armenian hamster IgG; PE/Cy7 anti-mouse CD122 (IL-2Rβ), clone TM-β1, Isotype rat IgG2b, k; PE/Cy7 anti-mouse CD127 (IL-7Rα), clone A7R34, Isotype rat IgG2a, k; PE/Cy7 anti-mouse IFN-γ, clone XMG1.2, Isotype rat IgG1, k; PE/Cy7 rat IgG1, k Isotype Ctrl, clone RTK2071; allophycocyanin anti-mouse IA/IE, clone M5/114.15.2, Isotype rat IgG2b, k; allophycocyanin anti-mouse NKp46, clone 29A1.4, Isotype rat IgG2a,k; allophycocyanin anti-mouse CD49b, clone Dx5, Isotype rat IgM; Alexa Fluor 647 anti-mouse F4/80, clone BM8, Isotype rat IgG2a, k; Alexa Fluor 647 anti-mouse Ly6G, clone BM8, Isotype rat IgG2a, k; Alexa Fluor700 anti-mouse Ly6C, clone HK1.4, Isotype rat IgG2a,k; allophycocyanin/Cy7 anti-mouse CD25, clone PC61, Isotype rat IgG1,λ; allophycocyanin/Cy7 anti-mouse F4/80, clone BM8, Isotype rat IgG2a, k (all purchased from BioLegend); eFluor450 anti-mouse CD11b, clone M1/70, Isotype rat IgG2b, k; eFluor450 anti-mouse CD11c, clone N418, Isotype Armenian hamster IgG; PE anti-mouse/human RORγt, clone AFKJS-9, Isotype rat IgG2a, k; PerCP/Cy5.5 anti-mouse TCRβ, clone H57-597, Isotype Armenian hamster IgG; PE/Cy7 anti-mouse CD11b, clone M1/70, Isotype rat IgG2b, k; PE/Cy7 anti-human/mouse Tbet, clone 4B10, Isotype mouse IgG2a,k; allophycocyanin anti-mouse NK1.1, clone PK136, Isotype mouse IgG2a, k; eFluor 660 anti-mouse CD11b, clone M1/70, Isotype rat IgG2b, k; eFluor 660 CD11c, clone N418, Isotype Armenian hamster; allophycocyanin eFluor780 anti-mouse F4/80, clone BM8, Isotype rat IgG2a, k (all obtained from eBioscience); PE-Texas Red anti-mouse CD45, clone 30-F11, Isotype rat IgG2b, k (from Invitrogen); V450 anti-mouse CD4, clone RM4-5, Isotype rat IgG2a, k; V500 anti-mouse CD8a, clone 53-6.7, Isotype rat IgG2a,k; V500 anti-mouse CD90.2 (Thy1.2), clone 53-2.1, Isotype rat IgG2a, k; PE anti-mouse CD90.2 (Thy1.2), clone 53-21, Isotype rat IgG2, k (from BD Biosciences); purified NOS2 (M-19) rabbit polyclonal IgG (Santa Cruz); Alexa Fluor 488 goat anti-rat IgG (H + L); and Alexa Fluor 647 goat anti-rabbit IgG (H + L) (both from Life Technologies).

Flow cytometry

Liver and spleen cells were isolated from naive or infected animals. In brief, a single cell suspension was prepared from the spleen or liver by passing the organ through a 70-μm nylon cell strainer, followed by treatment with RBC lysis buffer. Liver cells were further subjected to a 40%:80% Percoll (GE Healthcare) gradient to isolate the mononuclear cells. Cells were washed and the number of viable cells was counted by trypan blue exclusion. For the immunofluorescence staining of cells from Rag1$^{-/-}$.Yeti and Great mice, cells were incubated for 20 min with saturating concentrations of the different combinations of the following Abs: Ly6G-PB, CD90.2-V500, CD11c-PE, CD45-PE-Texas Red, TCRβ-PerCP/Cy5.5, TCRγδ-PerCP/Cy5.5, CD19-PerCP/Cy5.5, CD11b-PE/Cy7, NK1.1-allophycocyanin, NKp46-allophycocyanin, CD49b-allophycocyanin, Ly6C-Alexa Fluor 700, F4/80-allophycocyanin eFluor780, CD11c-eFluor 450, and CD11b-e.Fluor 450. For the transcription factors analysis, after the surface staining, cells were processed for intracellular staining using the eBioscience "Transcription factor staining buffer set" according to the manufacturer's instructions and then stained for RORγ*t*-PE, and Tbet-PE/Cy7. Samples were collected using Diva software on an LSRII flow cytometer (BD Biosciences).

Cells from Rag2$^{-/-}$, Rag2$^{-/-}$γc$^{-/-}$, and Rag2$^{-/-}$ IFN-γ$^{-/-}$ mice were stained with the different combinations of the following Abs: CD4-V450, CD11c-BV421, CD3-V500, CD8-V500, CD11b-BV510, CD90.2-FITC, NK1.1-FITC, NKp46-FITC, CD49b-FITC, CD90.2-PE, CD45-PerCP/Cy5.5, Sca-1-PerCP/Cy5.5, CD122-PE/Cy7, CD127-PE-Cy7, CD11b-eFluor 660, CD11c-eFluor 660, IA/IE-allophycocyanin, F4/80-AF647, Ly6G-A6F47,CD25-allophycocyanin/Cy7, and F4/80-allophycocyanin/Cy7. For the intracellular IFN-γ flow cytometry analysis, total spleen cells or total mononuclear liver cells were stimulated with PMA, Ionomycin, and brefeldin A for 5 h at 37°C. After cell surface staining, cells were fixed with 2% paraformaldehyde and permeabilized with 0.5% saponin. Cells were then incubated with IFN-γ–PE/Cy7 or the isotype-matched control for 20 min at room temperature. After two washing steps, cells were acquired by flow cytometry in a FACSCanto II cytometer (BD Biosciences) using a BD FACSDiva software. All data were analyzed using FlowJo software (Tree Star).

Cell sorting

Liver mononuclear cells prepared as described earlier were pooled from three to four naive or infected Rag1$^{-/-}$ animals and sorted in a BD Influx, 11-color, four-laser system and separated into three different cell populations based on the expression of CD45$^+$/NK1.1$^+$NKp46$^+$CD49b$^+$/Ly6G$^-$ (NK cells), CD45$^+$/NK1.1$^-$NKp46$^-$CD49b$^-$/CD11b$^+$CD11c$^+$ (myeloid cells

expressing CD11b and/or CD11c), and $CD45^+$/$Thy1.2^+$/$NK1.1^-$$NKp46^-$$CD49b^-$/$CD11b^-$$CD11c^-$/$F4/80^-$/$Ly6G^-$ ($Thy1.2^+$/non-NK/nonmyeloid cells).

Spleen and liver mononuclear cells pooled from 10 B6.$Rag2^{-/-}\gamma c^{-/-}$ animals (either naive or infected) were sorted and separated into two different $CD45^+$ cell populations: $CD11b^+CD11c^+$ (myeloid cells expressing CD11b and/or CD11c) and $Thy1.2^+$/$CD11b^-$$CD11c^-$/$F4/80^-$/$Ly6G^-$ ($Thy1.2^+$/nonmyeloid cells). These experiments were conducted in a FACSAria using FACSDiva software. The separation purity of all experiments was always confirmed and superior to 94%. Cells were sorted into RLT buffer (RNeasy Micro Kit from Qiagen) for posterior RNA purification.

Imaging flow cytometry

Liver mononuclear cells from $Rag2^{-/-}$ or $Rag2^{-/-}\gamma c^{-/-}$ mice were prepared as described earlier and stained either for surface phenotyping or intracellular IFN-γ detection. Cellular events were acquired using the ImageStream (Amnis; EDM Millipore, Darmstadt, Germany) imaging flow cytometer, and the multiple image analysis was performed using the IDEAS software (v6.0.348, Amnis; EDM Millipore).

RNA extraction and real-time RT-PCR

Total RNA was extracted from sorted populations (RNeasy Micro kit; Qiagen) according to the manufacturer's instructions. RNA was reverse transcribed to cDNA, using the SuperScript III First-Strand Synthesis System for RT-PCR (Invitrogen) and Random Hexamers (Fermentas), and real-time PCR (iCycler iQ5; Bio-Rad) was performed using TaqMan Universal PCR Master Mix and primers specific for *Hprt*, *Ifng*, *Id2*, and *Zbtb16* (Applied Biosystems) according to the manufacturer's protocols. Triplicate samples were analyzed, and the ΔΔCt method was used to calculate relative levels of targets compared with *Hprt*. Data were analyzed using iQ5 Optical System software (Bio-Rad).

Histological and morphometric analysis

Tissues samples were fixed in buffered formalin, embedded, and processed for histology by staining with H&E. Slides were photographed using an Olympus CX31 light microscope equipped with a DP-25 camera (Imaging Software Cell^B; Olympus, Center Valley, PA). One liver section per animal with random fields selected in a blind way was analyzed. The determination of the infiltration area was done in a total tissue area ranging from 6×10^6 to 9×10^6 μm^2, corresponding to five fields analyzed in each section. To determine the liver area covered by cellular infiltrations, we used the National Institutes of Health ImageJ software program. The percentage of infiltrated area was calculated by dividing the cumulative area of cell infiltration by the total liver surface of each image.

Immunofluorescence

Liver tissues were fixed in 4% paraformaldehyde, washed in PBS, incubated for 2 h in a 30% sucrose solution and embedded in optimal cutting temperature compound (OCT), and stored at −80°C until sectioning. Tissue sections (10 μm thickness) were performed in a frozen cryostat and stored at −20°C until use. Slides were saturated in blocking solution (10% FBS, 0.1% Triton X-100 in PBS) for 1 h at room temperature. Rabbit polyclonal IgG specific for inducible NO synthase (iNOS; M-19; Santa Cruz Biotechnology) and rat monoclonal CD90.2 (Thy1.2) (53-21; BD Pharmingen) Abs were diluted in Ab dilution buffer (1% FBS, 0.1% Triton X-100 in PBS) and incubated overnight with tissue sections at 4°C. After washing, sections were incubated with Alexa 647 goat anti-rabbit IgG and Alexa Fluor 488 goat anti-rat IgG Abs (Life Technologies) for 1 h at room temperature. Sections were then counterstained and mounted with DAPI-Fluoroshield and imaged in a Leica DMI 6000B inverted microscope using the ORCA-Flash4.0 version 2 (Hamamatsu Photonics) CMOS camera. Images were further analyzed and processed using ImageJ.

Statistical analysis

Results were expressed as means ± 1 SD. Statistical significance was calculated by using the unpaired Student *t* test or the one-way ANOVA test with a Tukey posttest. A p value <0.05 was considered statistically significant.

Results

IFN-γ is expressed in nonconventional $Thy1.2^+$ cells that lack T, NK, and myeloid lineage markers

The evidence of a T cell– and NK cell–independent IFN-γ–mediated immunity was suggested before by our group (9) and others (6, 13, 26). Hence, to identify a non-T, non-NK cell source of IFN-γ, we used an IFN-γ-YFP reporter mouse (Yeti) backcrossed with $Rag1^{-/-}$ animals ($Rag1^{-/-}$.Yeti). The YFP^+ cells identified by flow cytometry were $CD45^+$, and their frequency was very high in both the livers and the spleens of naive mice (Fig. 1A). To label NK cells, we stained for three different NK cell markers, NK1.1, NKp46, and CD49b, using specific mAbs conjugated with a single fluorochrome. Most of the YFP^+ cells expressed markers of NK cells, but a minor subset of non-NK, $F4/80^-$/YFP^+ cells was additionally detected. Further analysis revealed that these latter cells lacked the myeloid marker CD11b and expressed Thy1.2. To validate these findings, we assessed *Ifng* gene expression on sorted NK cells ($NK1.1^+NKp46^+$ $CD49b^+$), myeloid cells ($CD11b^+CD11c^+$/$NK1.1^-$$NKp46^-CD49b^-$), and the $Thy1.2^+$ non-NK/non-myeloid cells ($Thy1.2^+$/$NK1.1^-$ $NKp46^-CD49b^-$/$CD11b^-$$CD11c^-$/$F4/80^-$/$Ly6G^-$) from $Rag1^{-/-}$ (nonreporter) animals (Fig. 1B). Although *ifng* gene expression was detected in NK cells, no *Ifng* expression was detected in sorted myeloid cells. The non-NK/nonmyeloid $Thy1.2^+$ cells exhibited the same levels of constitutive *ifng* gene expression as the NK cell subset (Fig. 1C), confirming the flow cytometry data. Despite the negative results for the myeloid cells, and because these cells have been reported as possible sources of IFN-γ (16–21, 24), we decided to further ascertain the capacity of myeloid cells, namely macrophages, to express IFN-γ. To do so, we subjected bone marrow–derived macrophages from C57BL/6 animals to different polarizing stimuli and tested whether the different polarizations could dictate the capacity to express IFN-γ. No *Infg* gene expression was detected in any of the macrophage subsets despite their ability to express other cytokines (Supplemental Fig. 1).

Because the IFN-γ-YFP mRNA in Yeti animals is stabilized by a bovine growth hormone polyA tail, it leads to an aberrant expression of IFN-γ (25), as confirmed in this study in the $Rag1^{-/-}$. Yeti mice, which had around 70% YFP^+ cells in the liver and 60% in the spleen (Fig. 1A). To ascertain whether our previous results were not an artifact of the Yeti mouse model, we used another reporter mouse where the IFN-γ–YFP mRNA is under control of the endogenous IFN-γ polyA tail (Great mice, IFN-γ reporter with endogenous polyA transcript) in a C57BL/6 background, that is, with no deletion of Rag. The frequency of the YFP^+ cells in this mouse model was around 17% in the liver and 2% in the spleen (Supplemental Fig. 2A). To exclude the contribution of the YFP expression of T cells, such as $CD4^+$ and $CD8^+$ T cells, NKT cells, and $TCR\gamma\delta^+$ T cells, we gated on $TCR\beta^-$/$TCR\gamma\delta^-$/$CD19^-$ cells. An even higher percentage of these cells was found to express YFP (Supplemental Fig. 2B), and a population of $Thy1.2^+$/non-NK/non-T/non-B cells was identified in the liver and spleen of Great mice (Fig. 2A). In the livers, 50% of these $Thy1.2^+$/NK^- cells expressed YFP, slightly more than the NK cells (around 40%) (Fig. 2B). In contrast, in the spleen, the frequency of YFP^+ cells within the $Thy1.2^+$/non-NK population was low (around 2%). The cell number analysis reflected these differences: despite the higher $Thy1.2^+$/non-NK cell numbers in the spleen (2.3×10^4) when compared with the liver (3.9×10^3), the number of YFP^+ cells within this population was higher in the latter (2.2×10^2 and 1.4×10^3, respectively). In contrast, the number of YFP^+/NK^+ cells was higher in the spleen (Fig. 2C). Further, analysis of these $Thy1.2^+$ non-NK cells revealed that, in addition to being $F4/80^-$, they also lacked the expression of CD11b, CD11c, and Ly6G, confirming their nonmyeloid origin, and a small subset of these cells (17.7% in the liver and 33.4% in the spleen) express Ly6C, whereas the rest do not (Fig. 2D). Despite the substantial difference in YFP expression, both the liver and the spleen populations had a similar phenotype. Moreover, the majority of the $Thy1.2^+$/non-NK cells in the liver expressed T-bet (~72%), a

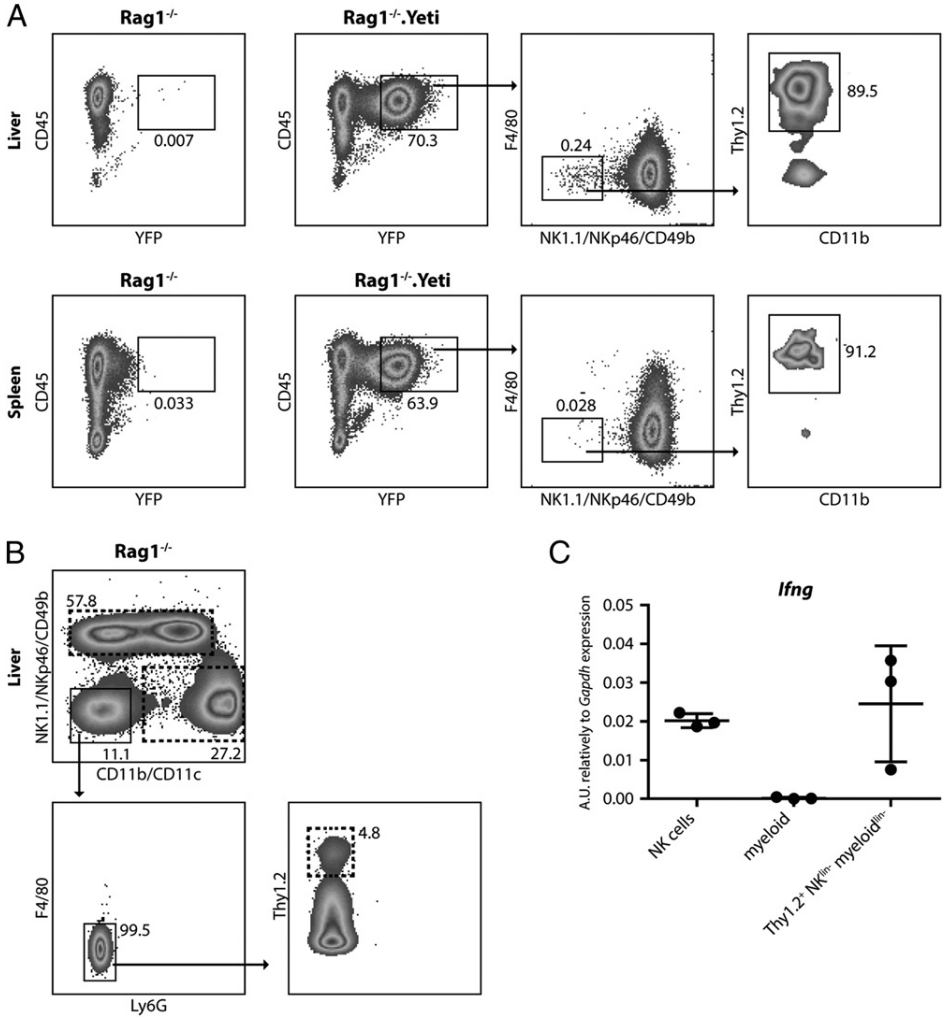

FIGURE 1. Identification of nonconventional IFN-γ–expressing Thy1.2$^+$ cells with a non-T and non-NK phenotype in Rag$^{-/-}$Yeti mice. (**A**) YFP expression of mononuclear liver cells (upper panel) or spleen cells (lower panel) from IFN-γ-YFP reporter mice with a Rag background. Gates with the respective cell frequencies are depicted. Rag1$^{-/-}$ animals were used as control for the YFP expression. Representative data of four independent experiments with at least three mice per group. (**B**) Flow cytometric sorting strategy of mononuclear liver cells from Rag1$^{-/-}$ mice. Cells were first gated on CD45$^+$ and then gated according to the scheme. Sorted populations are indicated by the gates in dashed lines. Cell frequencies are indicated next to each gate. (**C**) NK cells (NK1.1$^+$NKp46$^+$CD49b$^+$), myeloid cells (CD11b$^+$CD11c$^+$/NK1.1$^-$NKp46$^-$CD49b$^-$), and Thy1.2+NK^{lin-}myeloid^{lin-} (NK1.1$^-$NKp46$^-$CD49b$^-$/CD11b$^-$CD11c$^-$/F4/80$^-$/Ly6G$^-$/Thy1.2$^+$) were sorted, and expression of the *Ifng* gene was determined by qPCR. Values are normalized to *Gapdh* expression. Each point represents data for RNA pooled from three to four livers. Data represent the mean ± SD from three different experiments.

master regulator in IFN-γ–producing cells, and a small fraction of these cells expressed RORγt, in contrast with NK cells, which were all T-bet$^+$ and RORγt$^-$ (Fig. 2E). The spleen presented a similar transcription factor pattern, although the frequency of T-bet$^+$ cells was much lower, paralleling the lower YFP expression.

CD45$^+$ Thy1.2$^+$ cells with a non-T, non-NK, and nonmyeloid phenotype are found in common γc-deficient mice

We then asked whether the development of nonconventional IFN-γ–expressing Thy1.2$^+$ cells depended on the common γc component of the IL-2 family of receptors required for the signaling to several ILs such as IL-7 and IL-15 necessary for the development of T cells, B cells, NK cells, and all the other ILCs. To do so, we used IFN-γ nonreporter Rag2$^{-/-}$γc$^{-/-}$ mice and consistently detected the presence of the Thy1.2$^+$/non-NK/nonmyeloid population in the liver and the spleen (Fig. 3A). The absence of CD68 expression confirmed their nonmyeloid origin (Supplemental Fig. 2C). To ascertain whether these cells express IFN-γ, we assessed gene expression by quantitative PCR (qPCR) on sorted Thy1.2$^+$ nonmyeloid cells and also on myeloid$^+$ (CD11b$^+$ and/or CD11c$^+$) cells from both the liver and the spleen (Fig. 3B). A significant expression of the *Ifng* gene was detected in sorted Thy1.2$^+$ nonmyeloid cells in the liver, whereas no *Ifng* expression was detected in the spleen. These findings are in agreement with the very low levels of IFN-γ–YFP detected by cytometry in the spleens of the Great reporter mice (Fig. 2B, 2C) and support the existence of these cells in the absence of reporter gene insertion in the *Ifng* locus. No *Ifng* gene expression was detected on myeloid cells (Fig. 3B), but it was found in sorted NK cells from Rag2$^{-/-}$ mice (Supplemental Fig. 3A).

To better characterize the Thy1.2$^+$/non-NK/nonmyeloid population present in both Rag2$^{-/-}$γc$^{-/-}$ and Rag2$^{-/-}$ mice (see Supplemental Fig. 2D for the gating strategy), we performed a comparative analysis in these cells of markers that are associated with NK cells, lymphoid tissue inducer cells, and other ILCs. The results showed that these cells did not express CD122 (IL-2Rβ), a

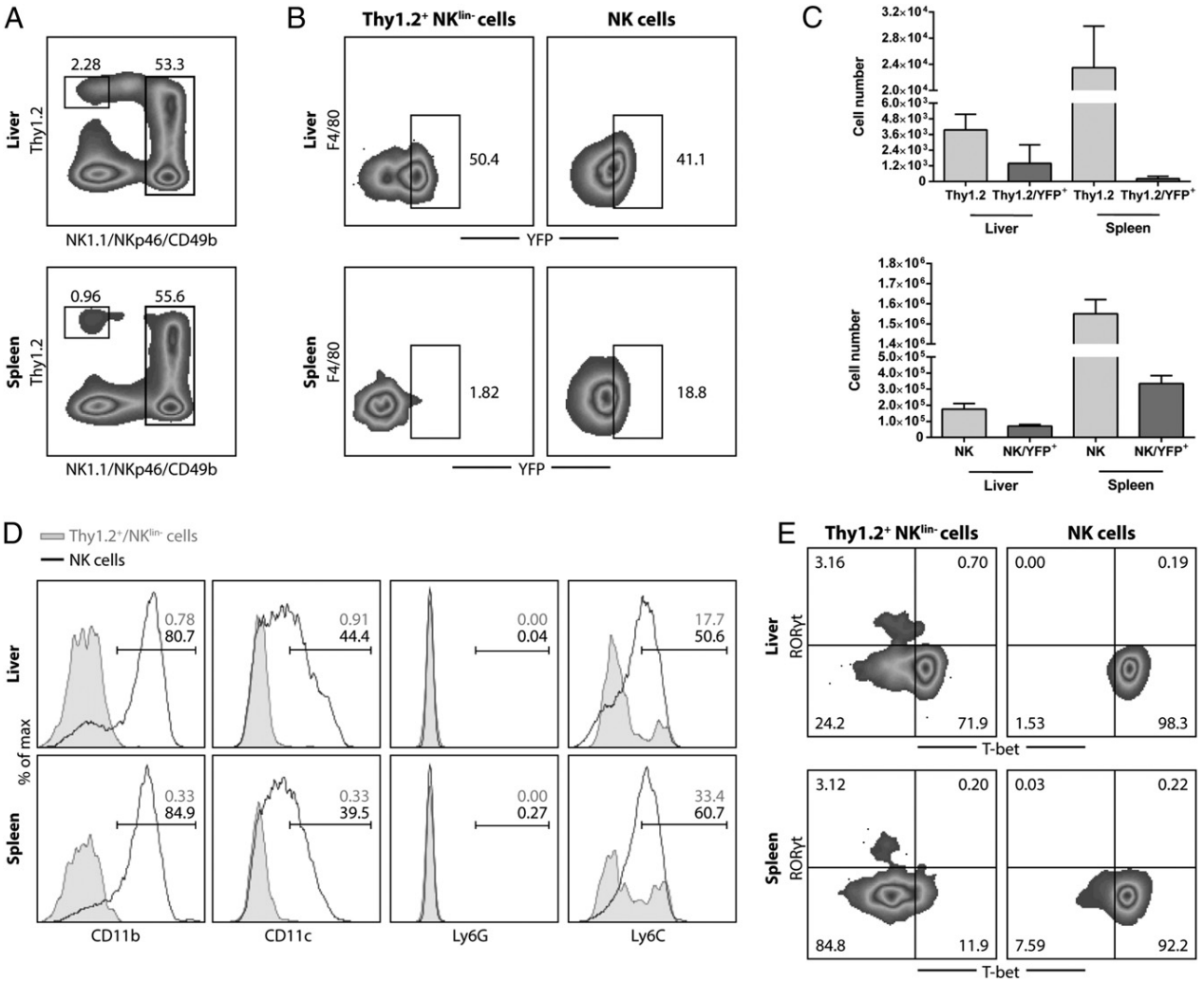

FIGURE 2. Identification of IFN-γ–expressing Thy1.2$^+$ cells lacking T, NK, or myeloid cell markers in the livers (upper panels) and spleens (lower panels) of Great mice. (**A**) Expression of Thy1.2 and NK (NK1.1/NKp46/CD49b) markers in cells from YFP-IFN-γ reporter Great mice gated on CD45$^+$/TCRβ$^-$TCRγδ$^-$CD19$^-$ cells. (**B**) YFP expression on gated Thy1.2$^+$NK$^-$ cells and NK$^+$ cells. (**C**) Number of total Thy1.2$^+$NK$^-$ cells and YFP$^+$/Thy1.2$^+$NK$^-$ cells (upper panel), and total NK cells and YFP$^+$/NK cells (lower panel). (**D**) Histograms of CD11b, CD11c, Ly6G, Ly6C expression on Thy1.2$^+$NK$^-$ cells (tinted gray) and NK$^+$ cells (black line). The frequencies of positive cells for each cell marker are indicated in each graph shaded as the corresponding histogram. (**E**) T-bet and RORγt expression on Thy1.2$^+$NK$^-$ cells and NK$^+$ cells from the liver (upper panel) and the spleen (lower panel). Data are representative from five different experiments with at least three mice each.

marker of NK cell precursors, and a fraction of them expressed MHC class II. Moreover, the majority of these cells express CD127 (IL-7Rα) and Sca-1, with a small fraction expressing low levels of CD25 (Fig. 3C). Further analysis revealed that these cells lacked CD3 and CD8, and in the absence of the γc chain they expressed CD4 (Supplemental Fig. 2E). Interestingly, the expression of both CD127 and CD4 were lower when the γc chain signaling was present (Rag2$^{-/-}$ mouse). In fact, the CD4 expression was totally abolished in cells of the liver of Rag2$^{-/-}$ mice. We next assessed the expression of *Id2* and *Zbtb16* (encoding for Id2 and PLZF, respectively) in sorted CD45$^+$/Thy1.2$^+$/nonmyeloid cells of Rag2$^{-/-}$γc$^{-/-}$ mice. As a control, we used NK cells sorted from Rag2$^{-/-}$ mice (Supplemental Fig. 2F). Despite some variability between experiments, we observed that Rag2$^{-/-}$γc$^{-/-}$ Thy1.2$^+$ cells expressed *Id2* in equivalent levels to the Rag2$^{-/-}$ NK cells. Interestingly, *Zbtb16* mRNA was specifically detected in Rag2$^{-/-}$γc$^{-/-}$ Thy1.2$^+$ liver cells and poorly expressed in the spleen. As expected, NK cells did not express *Zbtb16* mRNA (Supplemental Fig. 2F).

The lack of IFN-γ, but not of the common γc, exacerbated the infection and compromised the development of granulomas in a Rag-deficient background

To assess the biological relevance of this rare population of IFN-γ–producing Thy1$^+$ cells, we used a model of *M. avium* infection. We have previously shown that susceptibility of SCID mice to *M. avium* could be exacerbated by the Ab-mediated neutralization of IFN-γ, suggesting an innate source for this cytokine (9). Single-Ab depletions of NK cell subsets (e.g., asialo-GM1$^+$ or Thy1$^+$) were ineffective at achieving the same exacerbation but were incomplete in their ability to deplete NK cells in SCID mice, suggesting a redundant role for different populations of innate cells in the small but statistically significant protection afforded by IFN-γ in the absence of T cells (9). In this study, we found increased bacterial loads in the livers and spleens of B6.IFN-γ$^{-/-}$ mice compared with the C57BL/6 control, as well as in the Rag2$^{-/-}$ IFN-γ$^{-/-}$ double-knockout animals when compared with the Rag2$^{-/-}$ mice (Fig. 4A, Supplemental Fig. 4A). In contrast, Rag2$^{-/-}$γc$^{-/-}$ animals were as able to control the bacterial proliferation

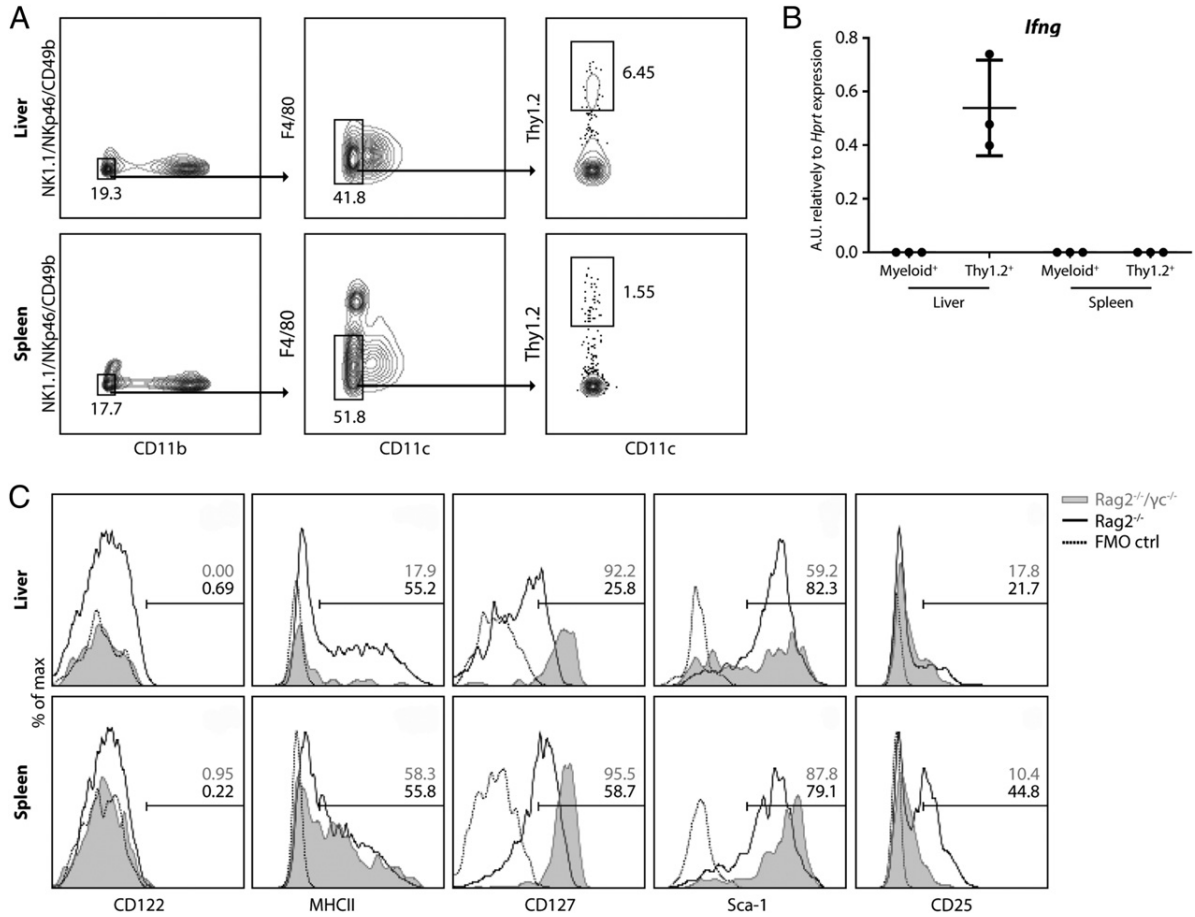

FIGURE 3. Identification of IFN-γ–expressing Thy1.2$^+$ cells in mice lacking Rag-2 and IL-2Rγc. (**A**) CD45$^+$ liver (upper panel) and spleen (lower panel) cells from Rag2$^{-/-}$γc$^{-/-}$ mice were phenotypically characterized for their expression of CD11b, CD11c, F4/80, Ly6G, and Thy1.2 according to the strategy shown. The frequency of these cells is represented next to the respective gates. (**B**) Myeloid$^+$ (CD11b$^+$/CD11c$^+$) cells and Thy1.2$^+$ myeloid$^-$ (CD11b$^-$/CD11c$^-$/F4/80$^-$/Ly6G$^-$) cells were sorted from Rag2$^{-/-}$γc$^{-/-}$ livers and spleens, and the *Ifng* gene expression was determined by qPCR. Values are normalized to *Hprt* expression. Reactions were run in triplicate. Each point represents the analysis of mRNA pooled from 10 animals. Data represent the mean ± SD from three different experiments. (**C**) Representative histograms of CD122, MHC-II, CD127, Sca-1, and CD25 expression on Thy1.2$^+$/NK$^-$/myeloid$^-$ liver (upper panel) and spleen (lower panel) cells, and from Rag2$^{-/-}$γc$^{-/-}$ (tinted gray) and Rag2$^{-/-}$ mice (black line). The frequencies of positive cells for each cell marker determined according to the fluorescence minus one control (FMO ctrl) are indicated in each graph shaded as the corresponding histogram. Data are representative of four different experiments with at least four mice each.

as Rag2$^{-/-}$ mice (Fig. 4A, Supplemental Fig. 4B). Because both mice lack T cells and Rag2$^{-/-}$γc$^{-/-}$ are further devoid of NK cells and other ILCs, these data suggest that IFN-γ may be produced by cells other than T cells, NK cells, or other ILC1 subsets as well. The differences in the bacterial loads of both organs between the strains devoid of T cells were evident only at 60 d postinfection (dpi), a time point concomitant with the observation of granulomatous lesions in these models. At 30 dpi, cell infiltrations were only detected in the C57BL/6 and the B6.IFN-γ$^{-/-}$ (although the latter with a much lower number) (data not shown). In addition, the lower CFU values observed particularly in the spleens of the different Rag-deficient strains 30 dpi as compared with the Rag-sufficient strains were due to a lower inoculum implantation at the start of the infection because of the very small size of the organ in these animals.

Granuloma assembly is highly dependent on IFN-γ production and is one of the main histopathological features of mycobacterial infections. C57BL/6 mice showed the largest cell infiltration areas, and their granulomas were well developed. The number of lesions in infected IFN-γ$^{-/-}$ or Rag2$^{-/-}$IFN-γ$^{-/-}$ mouse liver controls was smaller and lacked the prototypical organization of the inner macrophage core. Instead, they just consisted of lymphoid cell accumulations (Fig. 4B, 4C). In contrast, the livers of infected Rag2$^{-/-}$ and Rag2$^{-/-}$γc$^{-/-}$ mice showed granulomatous structures with a well-developed macrophage core and higher number of lesions (Fig. 4B, 4C).

Despite the extremely low number of the Thy1.2$^+$/non-NK cells in naive Rag2$^{-/-}$γc$^{-/-}$ mice, their number increased sharply during the course of the infection, with a 10-fold increase in the liver and a 20-fold increase in the spleen at 60 d of infection (Fig. 5A). Strikingly, these cells could be found by immunofluorescence microscopy within the granulomatous lesions in the liver adjacent to macrophages that expressed iNOS, an enzyme known to be induced by IFN-γ (Fig. 5B) and that was also found to be induced in the livers of infected Rag2$^{-/-}$ mice (data not shown). Next, we measured IFN-γ protein in liver and spleen mononuclear cells stimulated with PMA/Ionomycin and brefeldin A (Fig. 5C). Thy1.2$^+$/non-NK liver cells (upper panel) either from infected Rag2$^{-/-}$γc$^{-/-}$ or Rag2$^{-/-}$ mice presented equivalent IFN-γ$^+$ frequencies (around 17%). In contrast, spleen Thy1.2$^+$/non-NK cells (lower panel) did not express significant amounts of IFN-γ. We also used imaging flow cytometry to measure and detect IFN-γ$^+$ cells within the Thy1.2$^+$/non-NK population from both animal models (representative images for IFN-γ$^+$ and IFN-γ$^-$ cells are

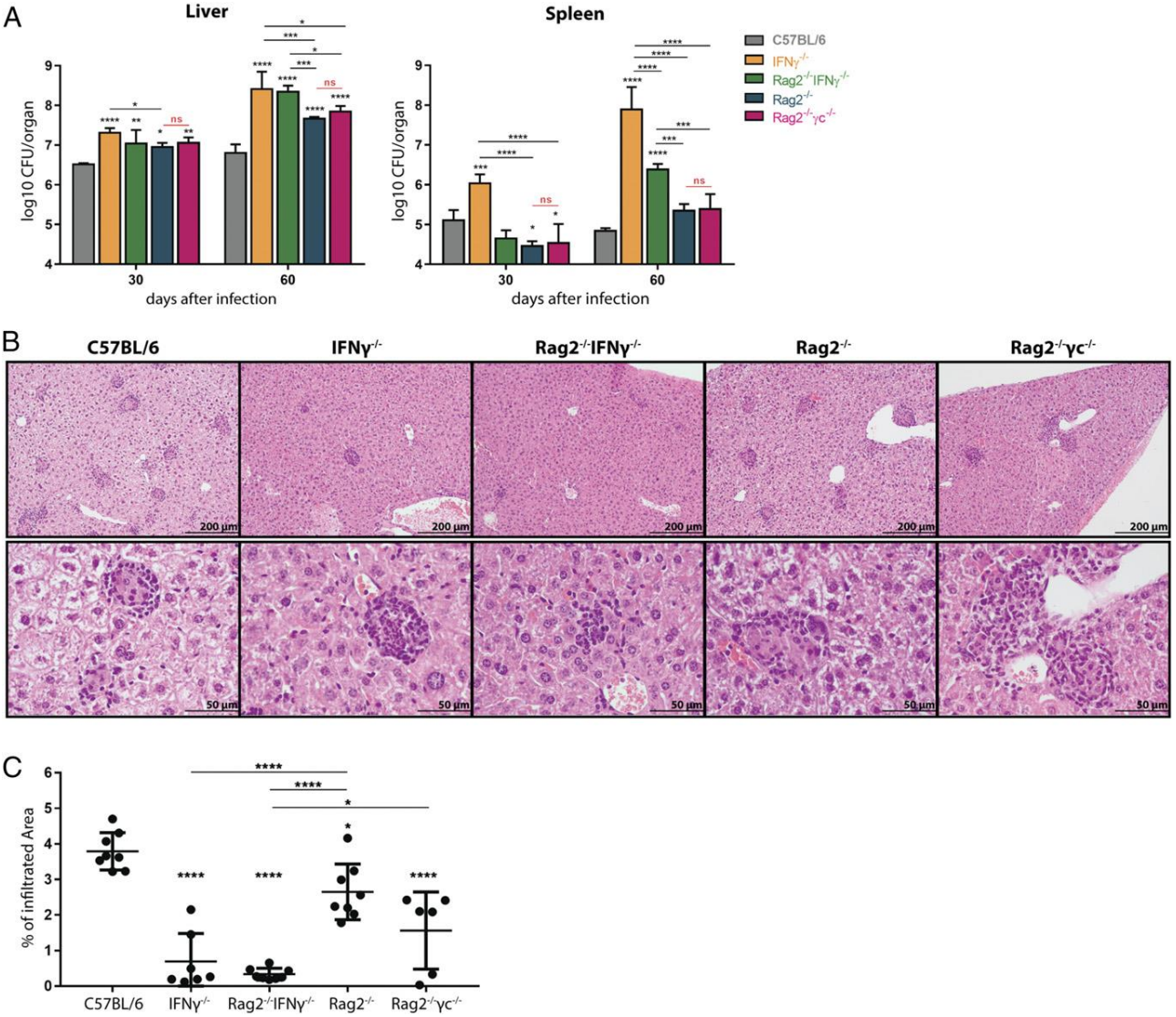

FIGURE 4. The lack of IFN-γ, but not of the common γc, exacerbates the infection in a Rag-knockout background. (**A**) *M. avium 2447* burden in the spleen and liver of C57BL/6, IFN-$\gamma^{-/-}$, Rag2$^{-/-}$IFN-$\gamma^{-/-}$, Rag2$^{-/-}$, and Rag2$^{-/-}\gamma c^{-/-}$ mice infected i.v. for 30 or 60 d. Data represent the mean CFUs ± SD from at least five mice per group of one of three experiments. (**B**) Representative histology of liver sections stained with H&E from mice infected for 60 d. Photos were taken with a light microscope Olympus CX31 with a DP-25 camera using the Imaging Software Cell^B. Pictures are shown with original magnification ×10 and ×40 in the upper and lower panels, respectively. (**C**) Percentage of infiltrated area in the livers of the indicated mice 60 dpi. Data represent the mean ± SD from six to eight mice per group. Each point represents one liver section. The statistical analysis of the differences between mutant mice and the C57BL/6 control group is shown above each column. Additional comparisons between other groups are indicated by horizontal bars. The *p* value was determined by a one-way ANOVA test with a Tukey multiple comparisons posttest (*$p < 0.05$, **$p < 0.01$, ***$p < 0.001$, ****$p < 0.0001$).

shown in Fig. 5D). As control, IFN-γ was also detected in NK cells from Rag2$^{-/-}$-infected mice (Fig. 5C, 5D). These findings are in accordance with the data obtained with the IFN-γ reporter animals (Figs. 1A, 2B) and the *Ifng* gene expression in the sorted Thy1.2$^+$ /non-NK cells (Fig. 3B, Supplemental Fig. 3B) from Rag2$^{-/-}\gamma c^{-/-}$ mice, and they indicate that Thy1.2$^+$/non-NK cells can provide an immediate source of IFN-γ under steady and infection conditions.

Thy1.2$^+$ cells of Rag2$^{-/-}\gamma c^{-/-}$ mice have a protective role during M. avium *infection in the liver*

To assess whether Thy1.2$^+$/non-NK cells displayed a protective role in lymphopenic mice infected with *M. avium*, particularly in the liver, where they express IFN-γ more abundantly, we depleted the Thy1.2 population in infected Rag2$^{-/-}\gamma c^{-/-}$ mice using mAbs (clone 30-H12). The depletion was conducted over 60 d of infection and confirmed by flow cytometry (Fig. 6A). Although no differences in the bacterial proliferation were observed in the spleens of anti-Thy1.2–treated versus control animals, the Ab depletion reverted the 2-fold decrease in liver mycobacterial loads observed in Rag2$^{-/-}\gamma c^{-/-}$ mice when compared with an IFN-γ–deficient host (Fig. 6B). These results suggest that the Thy1.2$^+$ IFN-γ–producing cells can functionally participate in the immune response against *M. avium*.

Discussion

The most important producers of IFN-γ in the mammalian organism are T lymphocytes and NK cells. B cells, epithelial cells, but more consistently myeloid cells, such as macrophages, DCs, and neutrophils, have also been reported as capable of producing this cytokine (14–21, 24). Recently, ILCs distinct from NK cells

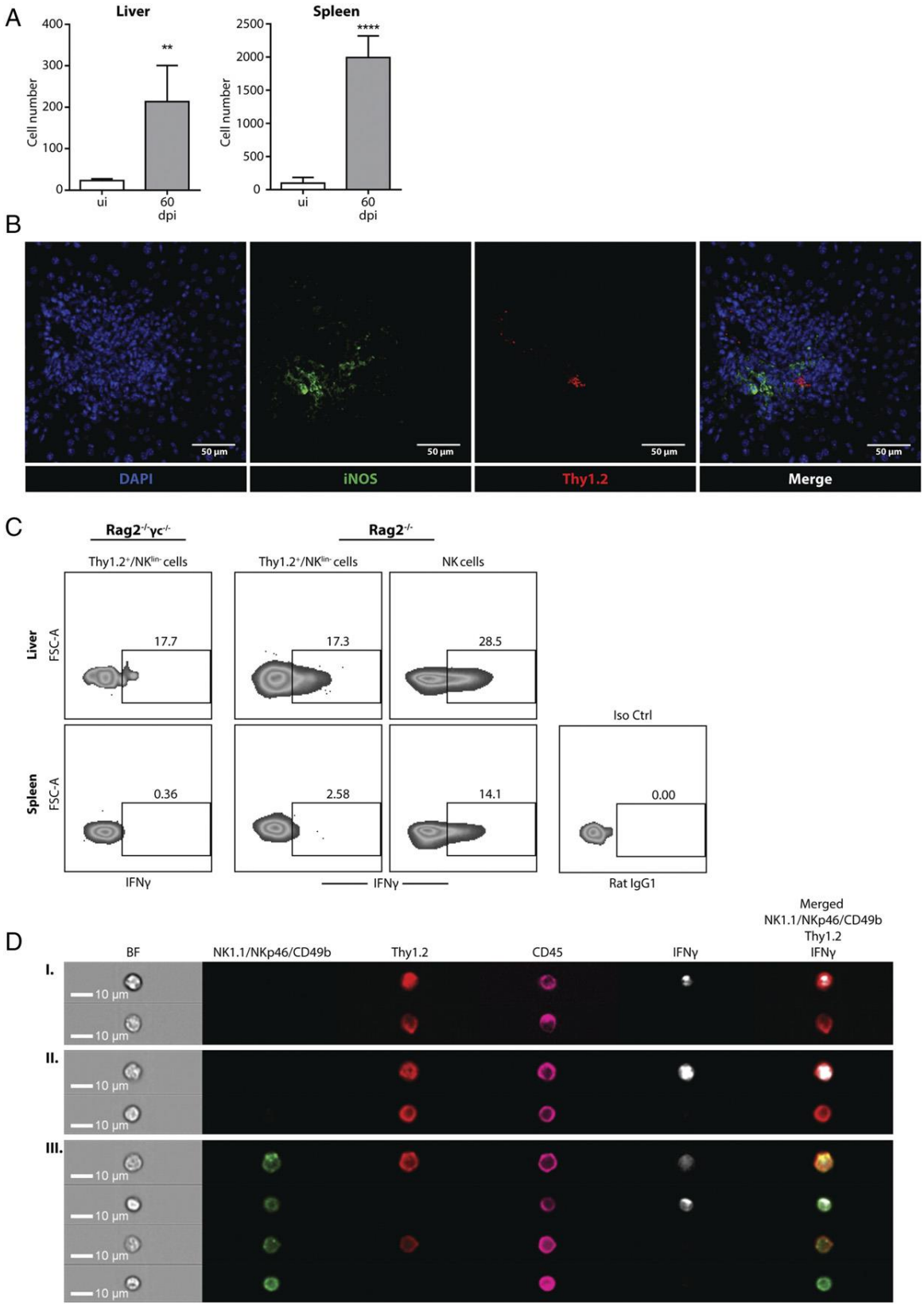

FIGURE 5. IFN-γ–expressing Thy1.2$^+$ cells and iNOS expression in granuloma macrophages from Rag2$^{-/-}$γc$^{-/-}$-infected mice. (**A**) Number of Thy1.2$^+$ myeloid$^-$ cells in uninfected (ui) or *M. avium*–infected livers and spleens from Rag2$^{-/-}$γc$^{-/-}$ mice 60 dpi. Data represent the mean ± SD from at least five mice per group. (**B**) Thy1.2 and iNOS expression in granuloma-like structures of the liver at 60 dpi. Photos were taken with an inverted microscope LEICA DMI 6000B with the ORCA-Flash4.0 version 2 (Hamamatsu Photonics) CMOS camera. (**C**) Intracellular IFN-γ expression in CD45$^+$ Thy1.2$^+$/NK$^-$/myeloid$^-$ liver (upper panel) and spleen (lower panel) cells from both Rag2$^{-/-}$γc$^{-/-}$ and Rag2$^{-/-}$ mice and in CD45$^+$NK$^+$ cells from Rag2$^{-/-}$ mice after 30 d of infection. Isotype control for IFN-γ is shown in spleen CD45$^+$/Thy1.2$^+$/NK$^-$/myeloid$^-$ cells from (*Figure legend continues*)

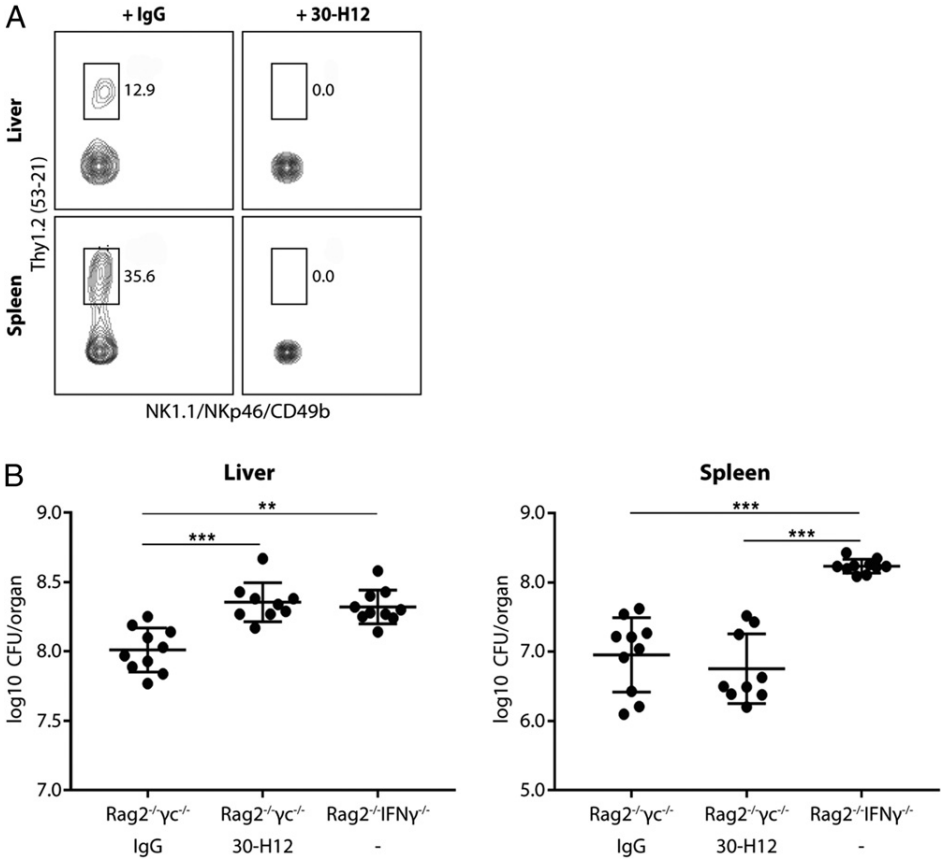

FIGURE 6. Depletion of Thy1.2$^+$ cells reduces bacterial proliferation in the livers of Rag2$^{-/-}$γc$^{-/-}$animals. (**A**) Thy1.2 cell frequency in liver cells (upper panel) and spleen cells (lower panel) from *M. avium*–infected Rag2$^{-/-}$γc$^{-/-}$ animals treated with either IgG or anti-Thy1.2 Ab (clone 30-H12) during the course of infection. A different clone of Thy1.2 was used to identify the frequency of depleted Thy1.2 cells (clone 53-21). (**B**) Bacterial loads of *M. avium* were assessed 60 dpi in Rag2$^{-/-}$γc$^{-/-}$ animals treated either with IgG or 30-H12 (anti-Thy1.2 Ab) during the course of infection. As a positive control, the bacterial loads of infected Rag2$^{-/-}$IFN-γ$^{-/-}$ mice were assessed in parallel. Each dot represents one animal. Data represent the mean ± SD from two experiments. Both experiments were performed with four to five mice per group. The *p* value was determined by a one-way ANOVA test with a Tukey multiple comparisons posttest (**$p < 0.01$, ***$p < 0.001$).

and named type 1 and type 3 ILCs were shown to express IFN-γ and to participate in the response to infection and inflammation (27–29). Based on our previous work, where we found T cell– and NK cell–independent IFN-γ–mediated immunity (9), we used IFN-γ reporter mice to look for additional IFN-γ–producing cells. Using flow cytometry, we found a small population of CD45$^+$ Thy1.2$^+$ non-T, non-B, non-NK, and nonmyeloid cells that expressed YFP in two distinct reporter strains. The IFN-γ–YFP expression by these cells was particularly evident in the liver, whereas in the spleen the expression was rather low. A cellular population with a similar phenotype was found in nonreporter Rag-deficient mice. These latter cells expressed IFN-γ as confirmed by qPCR. These cells were also found in mice that lack both the expression of Rag and the common γc of the IL-2R. Because the latter is required for the generation of NK cells and all the other ILCs, further studies should address whether this new population may represent a distinct or precursor lineage of innate-like cells. In contrast, the fact that these cells are CD127$^+$ (IL-7Rα$^+$) and are present in very small numbers in the absence of γc suggests that the signaling via the IL-7Rα/γc heterodimer may be important for their development. Supporting this hypothesis are the increased numbers of these cells in immune-competent mice (C57BL/6.Great), where the presence of γc allows the signaling via IL-7Rα. Alternatively, the IL-7Rα could form a heterodimer complex with the thymic stromal lymphopoietin receptor for thymic stromal lymphopoietin signaling, as shown during the induction of Th2 responses (30, 31). A further possibility is that the cells found in Rag2$^{-/-}$ mice are heterogeneous and represent additional populations, which may include ILC subsets requiring γc signaling and therefore are absent in the Rag2$^{-/-}$γc$^{-/-}$ mutant mice. Finally, it is possible that the population of Thy1.2$^+$ cells found in the double-mutant mice may represent the precursors of γc-dependent cells blocked in their development because of the lack of γc signaling. This last hypothesis is supported by the fact that Rag2$^{-/-}$γc$^{-/-}$ Thy1.2$^+$ cells express *Id2* mRNA. Moreover, these cells express *Zbtb16* (encoding for PLZF), particularly in the liver. PLZF was described as being expressed in a precursor stage of ILC, an ILC progenitor (ILCp) that gives rise to all ILCs, except lymphoid tissue inducer cells and NK cells, and described as Lin$^-$ Id2$^+$IL-7Rα$^+$CD25$^-$α$_4$β$_7^+$ cells (27, 32, 33). Klose and colleagues

Rag2$^{-/-}$γc$^{-/-}$ animals. Data are from one representative independent experiment out of three. (**D**) Images of IFN-γ$^+$ or IFN-γ$^-$ liver cells taken using a Flow Imager camera. The selected images are representative of the CD45$^+$/Thy1.2$^+$/NK$^-$/myeloid$^-$ cells from Rag2$^{-/-}$γc$^{-/-}$ (**I**) and Rag2$^{-/-}$ (**II**) animals, and CD45$^+$NK$^+$ cells from Rag2$^{-/-}$ mice (**III**). The *p* value was determined by a one-way ANOVA test with a Tukey multiple comparisons posttest (**$p <$ 0.01, ****$p < 0.0001$).

(27) have shown that although some ILC lineages are dependent on IL-7R signaling, common lymphoid progenitor and ILCp bone marrow numbers were only slightly reduced in IL-7Rα$^{-/-}$ animals. Importantly, the ILCp were mainly found in mucosal organs such as the small intestine and the liver, and were sparse in the spleen.

It is evident that the Rag2$^{-/-}$γc$^{-/-}$ Thy1.2^{+} cells identified in this article are phenotypically different in the liver and the spleen. Whether they belong to the same lineage is also unclear. It is not unusual for a certain cell type to differ phenotypically according to the microenvironment where it resides. Significant variations of the same ILC subset within different organs have been reported. For instance, Cortez and colleagues (34) reported a distinct subset of ILC1 in the salivary glands that shares features between ILC1 and NK cells. Their work also highlights how the particular microenvironment of the salivary glands can impact the ILC development. Robinette et al. (35) show that the discrimination between ILC1 and NK cells can be trickier in the spleen than the liver, because of the fact that these cells express different surface markers in these organs.

To understand the physiological relevance of the IFN-γ–producing Thy1.2^{+}/non-NK cells, we explored their role in an experimental *M. avium* infection model because the control of this opportunistic pathogen is strictly dependent on IFN-γ (3–5, 36, 37). In the absence of T cells, the major producers of IFN-γ, Rag-deficient mice were still more resistant than mice lacking both Rag and IFN-γ, suggesting a T cell–independent source of this molecule. We also observed that both Rag2$^{-/-}$ and Rag2$^{-/-}$γc$^{-/-}$ mice were able to control the bacterial growth more efficiently than Rag2$^{-/-}$IFN-γ$^{-/-}$ mice. These results exclude NK cells as the sole source of IFN-γ in the absence of T cells and suggest the existence of a redundant source for this cytokine. During *M. avium* infection, we observed an increase in the numbers of a novel CD45^{+}Thy1.2^{+} non-NK and nonmyeloid IFN-γ–producing population of cells. The ability of these infected cells to produce IFN-γ protein was also confirmed by intracellular staining after PMA/Ionomycin stimulation. Importantly, these cells were found to localize within granulomatous lesions in the liver in the vicinity of cells staining positive for iNOS, which is most frequently induced by IFN-γ. Further, Thy1.2-specific mAb-mediated cell depletion increased the pathogen growth in the liver of Rag2$^{-/-}$γc$^{-/-}$ mice to the levels of Rag2$^{-/-}$IFN-γ$^{-/-}$ animals while reducing the cell infiltration area. Together, our data demonstrate that this nonconventional population of IFN-γ–producing cells accumulates in the liver, within the granuloma, and mediates improved control of bacterial growth. These cells were not frequent in the spleen, and their depletion did not affect the bacterial burden in this organ, supporting a liver-specific action of Thy1.2^{+} cells in response to mycobacterial infection. We cannot exclude the possibility that the control of bacterial proliferation observed in Rag2$^{-/-}$γc$^{-/-}$ mice might also rely on IFN-γ–independent compensatory mechanisms such as TNF production. In the spleen, Thy1.2^{+}/non-NK cells produce minute amounts of IFN-γ, suggesting the involvement of another protective mechanism. The fact that Thy1.2 depletion in the infected Rag2$^{-/-}$γc$^{-/-}$ animals did not affect the bacterial proliferation control in the spleens also supports this hypothesis. It is still possible that other cells may secrete IFN-γ and compensate for the removal of these CD45^{+}Thy1.2^{+} non-NK, nonmyeloid cells in the spleen. Macrophages, dendritic cells, or PMNs may be responsible for the splenic production of IFN-γ as described in other infection models (18–21). However, we failed to detect such cytokine production in these myeloid cells by either the use of reporter mice or by qPCR of sorted populations. The regulation of IFN-γ expression in these cells is likely different and not constitutive, as is found in ILCs. Thus, the lack of detection in myeloid cells by qPCR may relate to inadequate triggering stimuli or kinetic constraints.

Taken together, our study reveals a unique subset of innate IFN-γ–producing cells that develops in the absence of IL-2R common γc. The lower amounts of IFN-γ expressed by cells other than T cells, NK cells, or other ILCs in the spleen compared with the liver may explain why these cells were never detected before. In addition, the majority of the studies exploring in vivo responses to infection and the specific role of different cell populations have been done with spleen cells. In fact, there are very few studies exploring the different liver cell populations using flow cytometry and, to our knowledge, this is the first work to unveil the cellular expression of IFN-γ by nonconventional cells in the liver. Thus, our work has identified a new cell subset capable of producing IFN-γ constitutively and with a protective role toward *M. avium* infection in an immune-compromised mouse model.

Acknowledgments

We thank Catarina Leitão, Catarina Meireles, Sofia Lamas, and Maria Gómez Lázaro for all the technical help.

Disclosures

The authors have no financial conflicts of interest.

References

1. Schoenborn, J. R., and C. B. Wilson. 2007. Regulation of interferon-gamma during innate and adaptive immune responses. *Adv. Immunol.* 96: 41–101.
2. Boehm, U., T. Klamp, M. Groot, and J. C. Howard. 1997. Cellular responses to interferon-gamma. *Annu. Rev. Immunol.* 15: 749–795.
3. Cooper, A. M., D. K. Dalton, T. A. Stewart, J. P. Griffin, D. G. Russell, and I. M. Orme. 1993. Disseminated tuberculosis in interferon gamma gene-disrupted mice. *J. Exp. Med.* 178: 2243–2247.
4. Flynn, J. L., J. Chan, K. J. Triebold, D. K. Dalton, T. A. Stewart, and B. R. Bloom. 1993. An essential role for interferon gamma in resistance to *Mycobacterium tuberculosis* infection. *J. Exp. Med.* 178: 2249–2254.
5. Flórido, M., A. S. Gonçalves, R. A. Silva, S. Ehlers, A. M. Cooper, and R. Appelberg. 1999. Resistance of virulent *Mycobacterium avium* to gamma interferon-mediated antimicrobial activity suggests additional signals for induction of mycobacteriostasis. *Infect. Immun.* 67: 3610–3618.
6. Johnson, L. L., F. P. VanderVegt, and E. A. Havell. 1993. Gamma interferon-dependent temporary resistance to acute *Toxoplasma gondii* infection independent of CD4+ or CD8+ lymphocytes. *Infect. Immun.* 61: 5174–5180.
7. Scharton-Kersten, T., H. Nakajima, G. Yap, A. Sher, and W. J. Leonard. 1998. Infection of mice lacking the common cytokine receptor gamma-chain (gamma (c)) reveals an unexpected role for CD4+ T lymphocytes in early IFN-gamma-dependent resistance to *Toxoplasma gondii*. *J. Immunol.* 160: 2565–2569.
8. Rottenberg, M. E., A. C. Gigliotti Rothfuchs, D. Gigliotti, C. Svanholm, L. Bandholtz, and H. Wigzell. 1999. Role of innate and adaptive immunity in the outcome of primary infection with *Chlamydia pneumoniae*, as analyzed in genetically modified mice. *J. Immunol.* 162: 2829–2836.
9. Flórido, M., M. Correia-Neves, A. M. Cooper, and R. Appelberg. 2003. The cytolytic activity of natural killer cells is not involved in the restriction of *Mycobacterium avium* growth. *Int. Immunol.* 15: 895–901.
10. Martín-Fontecha, A., L. L. Thomsen, S. Brett, C. Gerard, M. Lipp, A. Lanzavecchia, and F. Sallusto. 2004. Induced recruitment of NK cells to lymph nodes provides IFN-gamma for T(H)1 priming. *Nat. Immunol.* 5: 1260–1265.
11. Scharton, T. M., and P. Scott. 1993. Natural killer cells are a source of interferon gamma that drives differentiation of CD4+ T cell subsets and induces early resistance to *Leishmania major* in mice. *J. Exp. Med.* 178: 567–577.
12. Sher, A., I. P. Oswald, S. Hieny, and R. T. Gazzinelli. 1993. *Toxoplasma gondii* induces a T-independent IFN-gamma response in natural killer cells that requires both adherent accessory cells and tumor necrosis factor-alpha. *J. Immunol.* 150: 3982–3989.
13. Rothfuchs, A. G., M. R. Kreuger, H. Wigzell, and M. E. Rottenberg. 2004. Macrophages, CD4+ or CD8+ cells are each sufficient for protection against *Chlamydia pneumoniae* infection through their ability to secrete IFN-gamma. *J. Immunol.* 172: 2407–2415.
14. Bao, Y., X. Liu, C. Han, S. Xu, B. Xie, Q. Zhang, Y. Gu, J. Hou, L. Qian, C. Qian, et al. 2014. Identification of IFN-γ-producing innate B cells. *Cell Res.* 24: 161–176.
15. Rouabhia, M., G. Ross, N. Pagé, and J. Chakir. 2002. Interleukin-18 and gamma interferon production by oral epithelial cells in response to exposure to *Candida albicans* or lipopolysaccharide stimulation. *Infect. Immun.* 70: 7073–7080.
16. Schindler, H., M. B. Lutz, M. Röllinghoff, and C. Bogdan. 2001. The production of IFN-gamma by IL-12/IL-18-activated macrophages requires STAT4 signaling and is inhibited by IL-4. *J. Immunol.* 166: 3075–3082.

17. Rothfuchs, A. G., D. Gigliotti, K. Palmblad, U. Andersson, H. Wigzell, and M. E. Rottenberg. 2001. IFN-alpha beta-dependent, IFN-gamma secretion by bone marrow-derived macrophages controls an intracellular bacterial infection. *J. Immunol.* 167: 6453–6461.
18. Kirby, A. C., U. Yrlid, and M. J. Wick. 2002. The innate immune response differs in primary and secondary *Salmonella* infection. *J. Immunol.* 169: 4450–4459.
19. Stober, D., R. Schirmbeck, and J. Reimann. 2001. IL-12/IL-18-dependent IFN-gamma release by murine dendritic cells. *J. Immunol.* 167: 957–965.
20. Lugo-Villarino, G., R. Maldonado-Lopez, R. Possemato, C. Penaranda, and L. H. Glimcher. 2003. T-bet is required for optimal production of IFN-gamma and antigen-specific T cell activation by dendritic cells. *Proc. Natl. Acad. Sci. USA* 100: 7749–7754.
21. Fukao, T., D. M. Frucht, G. Yap, M. Gadina, J. J. O'Shea, and S. Koyasu. 2001. Inducible expression of Stat4 in dendritic cells and macrophages and its critical role in innate and adaptive immune responses. *J. Immunol.* 166: 4446–4455.
22. Schleicher, U., A. Hesse, and C. Bogdan. 2005. Minute numbers of contaminant CD8+ T cells or CD11b+CD11c+ NK cells are the source of IFN-gamma in IL-12/IL-18-stimulated mouse macrophage populations. *Blood* 105: 1319–1328.
23. Bogdan, C., and U. Schleicher. 2006. Production of interferon-gamma by myeloid cells–fact or fancy? *Trends Immunol.* 27: 282–290.
24. Sturge, C. R., A. Benson, M. Raetz, C. L. Wilhelm, J. Mirpuri, E. S. Vitetta, and F. Yarovinsky. 2013. TLR-independent neutrophil-derived IFN-γ is important for host resistance to intracellular pathogens. *Proc. Natl. Acad. Sci. USA* 110: 10711–10716.
25. Reinhardt, R. L., H. E. Liang, K. Bao, A. E. Price, M. Mohrs, B. L. Kelly, and R. M. Locksley. 2015. A novel model for IFN-γ-mediated autoinflammatory syndromes. *J. Immunol.* 194: 2358–2368.
26. Rottenberg, M. E., A. Gigliotti Rothfuchs, D. Gigliotti, M. Ceausu, C. Une, V. Levitsky, and H. Wigzell. 2000. Regulation and role of IFN-gamma in the innate resistance to infection with *Chlamydia pneumoniae*. *J. Immunol.* 164: 4812–4818.
27. Klose, C. S., M. Flach, L. Möhle, L. Rogell, T. Hoyler, K. Ebert, C. Fabiunke, D. Pfeifer, V. Sexl, D. Fonseca-Pereira, et al. 2014. Differentiation of type 1 ILCs from a common progenitor to all helper-like innate lymphoid cell lineages. *Cell* 157: 340–356.
28. Buonocore, S., P. P. Ahern, H. H. Uhlig, I. I. Ivanov, D. R. Littman, K. J. Maloy, and F. Powrie. 2010. Innate lymphoid cells drive interleukin-23-dependent innate intestinal pathology. *Nature* 464: 1371–1375.
29. Sonnenberg, G. F., L. A. Monticelli, M. M. Elloso, L. A. Fouser, and D. Artis. 2011. CD4(+) lymphoid tissue-inducer cells promote innate immunity in the gut. *Immunity* 34: 122–134.
30. Mazzucchelli, R., and S. K. Durum. 2007. Interleukin-7 receptor expression: intelligent design. *Nat. Rev. Immunol.* 7: 144–154.
31. He, R., and R. S. Geha. 2010. Thymic stromal lymphopoietin. *Ann. N. Y. Acad. Sci.* 1183: 13–24.
32. Diefenbach, A., M. Colonna, and C. Romagnani. 2017. The ILC world revisited. *Immunity* 46: 327–332.
33. Eberl, G., M. Colonna, J. P. Di Santo, and A. N. McKenzie. 2015. Innate lymphoid cells. Innate lymphoid cells: a new paradigm in immunology. *Science* 348: aaa6566.
34. Cortez, V. S., L. Cervantes-Barragan, M. L. Robinette, J. K. Bando, Y. Wang, T. L. Geiger, S. Gilfillan, A. Fuchs, E. Vivier, J. C. Sun, et al. 2016. Transforming growth factor-β signaling guides the differentiation of innate lymphoid cells in salivary glands. *Immunity* 44: 1127–1139.
35. Robinette, M. L., A. Fuchs, V. S. Cortez, J. S. Lee, Y. Wang, S. K. Durum, S. Gilfillan, M. Colonna, L. Shaw, B. Yu, et al 2015. Transcriptional programs define molecular characteristics of innate lymphoid cell classes and subsets. *Nat. Immunol.* 16: 306–317.
36. Appelberg, R., A. G. Castro, J. Pedrosa, R. A. Silva, I. M. Orme, and P. Minóprio. 1994. Role of gamma interferon and tumor necrosis factor alpha during T-cell-independent and -dependent phases of *Mycobacterium avium* infection. *Infect. Immun.* 62: 3962–3971.
37. Smith, D., H. Hänsch, G. Bancroft, and S. Ehlers. 1997. T-cell-independent granuloma formation in response to *Mycobacterium avium*: role of tumour necrosis factor-alpha and interferon-gamma. *Immunology* 92: 413–421.

Supplemental Information

Innate gamma interferon-producing cells developing in the absence of interleukin-2 receptor common gamma chain

Mariana Resende, Marcos S. Cardoso, Ana R. Ribeiro, Manuela Flórido, Margarida Borges, A. Gil Castro, Nuno L. Alves, Andrea M. Cooper, Rui Appelberg.

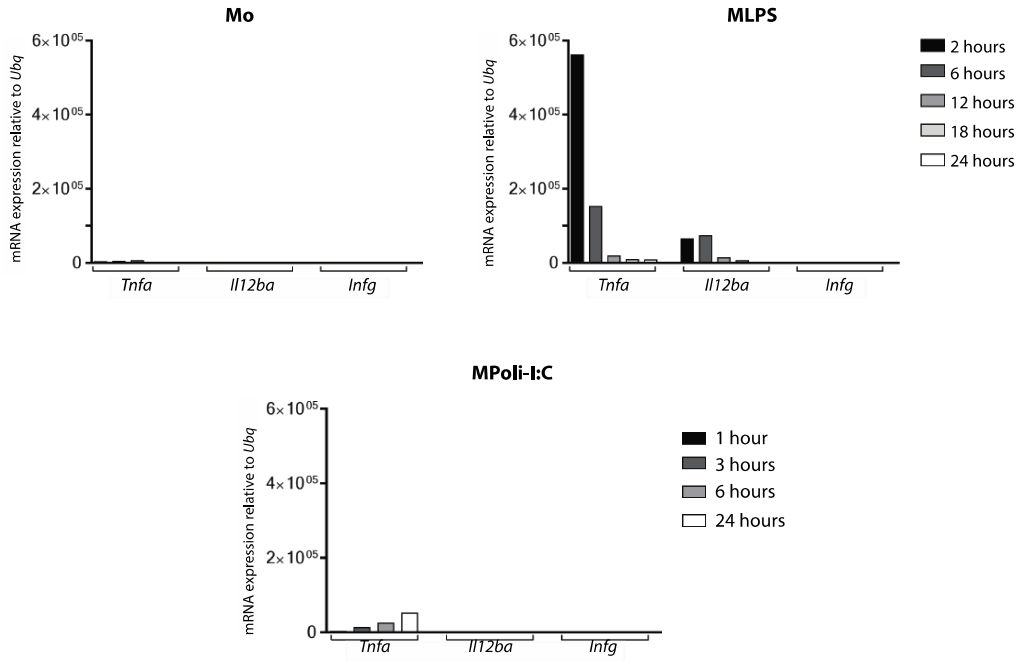

Supplemental Figure 1. Bone Marrow derived macrophages from C57Bl/6 mice were stimulated with different conditions in order to polarize them in different subsets: Mo (no stimuli); MLPS (stimulated with LPS); and MPoly-I:C (stimulated with Poly-I:C) and the *Tnfa*, *Il12ba* and *Ifng* gene expression was quantified by qPCR. Values are normalized to *Ubq* expression.

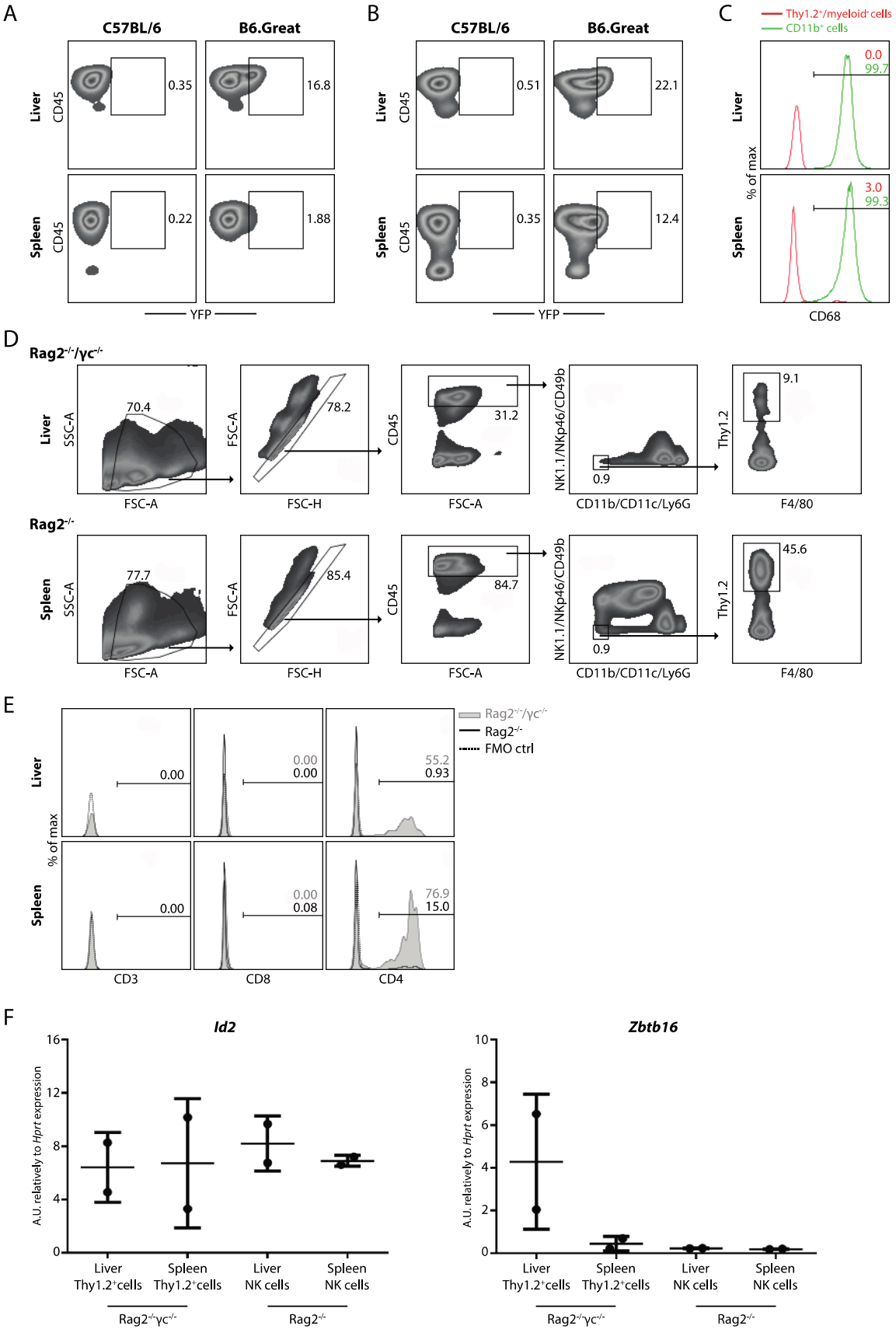

Supplemental Fig. 2

Supplemental Figure 2. Liver cells (upper panels) and spleen cells (lower panels) from YFP-IFNγ reporter Great mice: **(A)** YFP expression on single cells; **(B)** YFP expression on cells previously gated on $TCR\beta^{-}TCR\gamma\delta^{-}CD19^{-}$. YFP frequency is indicated next to the gates. Data is representative from five different experiments with at least 3 mice each. **(C)** CD68 intracellular staining in $Thy1.2^{+}$/$myeloid^{-}$ (red) and myeloid cells ($CD11b^{+}/CD11c^{+}$) of $Rag2^{-/-}/\gamma c^{-/-}$ mice livers (upper panel) and spleens (lower panel). Data are representative from two different experiments with at least 3 mice each. **(D)** Gating strategy to identify $Thy1.2^{+}/NK^{-}/myeloid^{-}$ liver cells in both $Rag2^{-/-}/\gamma c^{-/-}$ (upper panel) and $Rag2^{-/-}$ (lower panel) mice. Cell frequencies are indicated next to the gates **(E)** Representative histograms of CD3, CD4 and CD8 expression on $Thy1.2^{+}/NK^{-}/myeloid^{-}$ liver cells (upper panel) and spleen cells (lower panel) from $Rag2^{-/-}/\gamma c^{-/-}$ mice (tinted gray) and $Rag2^{-/-}$ mice (black line). The frequencies of positive cells for each cell marker determined according to the fluorescence minus one control (FMO ctrl) are indicated in each graph shaded as the correspondng histogram. Data is representative of four different experiments with at least 4 mice each. **(F)** $CD45^{+}$/ $Thy1.2^{+}$/$myeloid^{-}$ cells were sorted from from $Rag2^{-/-}/\gamma c^{-/-}$ livers and spleens for *Id2* and *Zbtb16* gene expression determination by qPCR. Each point represents mRNA pooled from ten animals. Cells were sorted using the same gating strategy as for Fig. 3B. As a positive control $CD45^{+}/NK^{+}$ cells from $Rag2^{-/-}$ livers and spleens were used. For the latter, each point represents mRNA pooled from three animals. Values are normalized to *Hprt* expression. Reactions were run in triplicate. Data represent the mean ± SD from two different experiments.

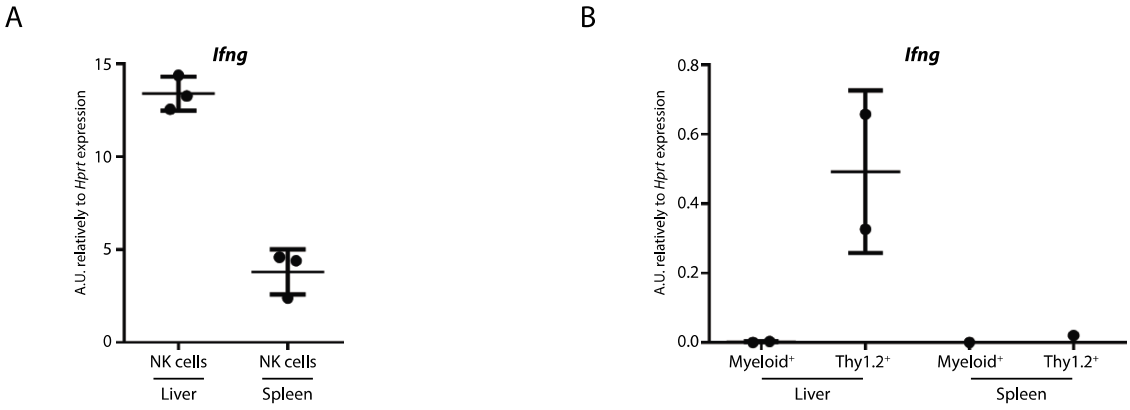

Supplemental Figure 3. Expression of the *Ifng* gene determined by qPCR in **(A)** sorted NK cells from Rag2$^{-/-}$ and **(B)** sorted Thy1.2^{+}/myeloid^{-} cells and myeloid^{+} cells isolated from livers and spleens of Rag2$^{-/-}$/γc$^{-/-}$ mice at 15dpi. Cells were sorted using the same gating strategy as for Fig. 3B. Values are normalized to *Hprt* expression. Reactions were run in triplicate. Each point represents mRNA pooled from three animals (A) or from ten animals (B). Data represent the mean ± SD from two different experiments for the liver. One experiment was performed for the spleen.

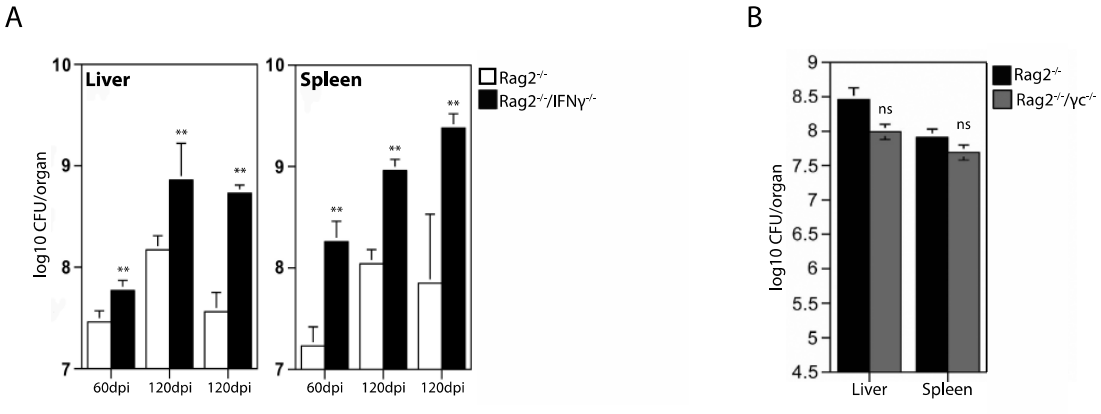

Supplemental Figure 4. (A) *M. avium* burden in the liver, spleen and lung of Rag2$^{-/-}$ and Rag2$^{-/-}$/IFNγ$^{-/-}$ mice infected for 60 days or 120 days (two independent experiments). **(B)** *M. avium* burden in the liver, spleen and lung of Rag2$^{-/-}$ and Rag2$^{-/-}$/γc$^{-/-}$ mice infected for 60 days. Differences in bacterial loads between groups are indicated. The *p* value was determined by a Student's t test (**p< 0.01, ns = not significant). Four or five mice per group were used in all experiments.

Chapter III

TNF-MEDIATED COMPENSATORY IMMUNITY TO *MYCOBACTERIUM AVIUM* IN THE ABSENCE OF MACROPHAGE ACTIVATION BY IFN-γ

Ongoing work

TNF-mediated compensatory immunity to *Mycobacterium avium* in the absence of macrophage activation by IFN-γ

M. Resende[1,2], M. S. Cardoso[1], R. Fróis-Martins[1], M. Borges[3], M. B. Jordan[4], A. Gil Castro[2], R. Appelberg[1]

[1] I3S – Instituto de Investigação e Inovação em Saúde, Universidade do Porto, Portugal/ IBMC – Instituto de Biologia Molecular e Celular, Universidade do Porto, Portugal

[2] Life and Health Sciences Research Institute (ICVS), School of Health Sciences, University of Minho/ ICVS/3B's – PT Government Associate Laboratory, Braga/Guimarães, Portugal

[3] Faculty of Pharmacy, University of Porto, Portugal

[4] Department of Pediatrics, Cincinnati Children's Hospital Medical Center/University of Cincinnati College of Medicine, Cincinnati, OH 45229, USA

Abstract

Granuloma formation is a hallmark of several infectious diseases, including those caused by *Mycobacterium sp*. These structures assembled under the influence of IFN-γ and TNF-α result in the accumulation of inflammatory cells. Whether or not IFN-γ has to act directly on macrophages to establish the organization of the granuloma remains elusive. MIIG mice have macrophages, monocytes and dendritic cells that are unresponsive to IFN-γ. During the response to *M. avium*, we observed that although IFN-$\gamma^{-/-}$ mice present an exacerbated infection, the same is not true for MIIG animals, where the same levels of protection as the wild type (WT) animals were observed in the liver and partial protection in the spleen. Unlike IFN-$\gamma^{-/-}$ mice, MIIG mice still develop well defined granulomas suggesting that IFN-γ-mediated macrophage activation is not required for granuloma assembly. This work also shows that MIIG animals exhibit increased cell recruitment with higher $CD4^+$ T cell numbers as well as increased IFN-γ and TNF-α expression, suggesting that TNF-α may have a role on protection and may compensate the lack of macrophage response to IFN-γ in the MIIG model. Moreover MIIG infected mice also exhibit increased macrophage recruitment with increased production of reactive oxygen species (ROS) and increased iron accumulation within the granulomas. Importantly, TNF-α-genetically ablated MIIG mice (MIIG.TNF-$\alpha^{-/-}$) exhibited increased bacterial burdens following *M. avium* infection. This increased susceptibility was accompanied by a reduction of ROS production and lack of iron

accumulation. While reduced iron accumulation was also observed in TNF-$\alpha^{-/-}$ infected mice, the reduction of ROS production was only observed in MIIG.TNF-$\alpha^{-/-}$. These results suggest that in the absence of IFN-γ signaling in macrophages, TNF-α has a compensatory protective role against *M. avium* infection.

Introduction

Gamma interferon (IFN-γ) was identified as the major macrophage-activating cytokine over three decades ago (1, 2). The subsequent discovery of human primary immunodeficiencies leading to defects in IFN-γ production or responsiveness (3) as well as the generation of mice with genetic disruption of either the IFN-γ or of its receptor genes provided evidence of the importance of this cytokine in mediating resistance to multiple intracellular microbes (4). IFN-γ-induced macrophage activation leads to the enhanced expression of antimicrobial mechanisms namely the induction of the enzymes responsible for the production of oxygen and nitrogen reactive species, small GTPases involved in vacuolar maturation and autophagy, amino-acid degrading systems and iron sequestration mechanisms (reviewed in ref. (5)). Although IFN-γ acts on multiple cell types in addition to the macrophage, there is an implicit inference that its protective effect during infection by intracellular pathogens, in particular those that proliferate inside the macrophage, is related to its ability to activate the latter phagocyte.

One of the most frequent opportunistic infections in human patients with a defect in the IL-12/IFN-γ axis is that caused by *Mycobacterium avium* (3). Indeed IFN-γ is able to promote the control of *M. avium* growth in cultured mouse primary macrophages (6). Moreover in mouse models, neutralization of IFN-γ or a genetic IFN-γ deficiency leads to increased susceptibility to infection by *M. avium*, as well as a profound impairment in granuloma assembly (7, 8). The granuloma structure is central for mycobacterial containment. It develops around infected macrophages, which upon activation induce the accumulation of different cell populations promoting interactions between innate and adaptive immune cells (9). Hence IFN-γ plays a fundamental role in host resistance both as a key activator of macrophage microbicidal molecules and as a requisite for granuloma development. Therefore, resistance to infection by *M. avium* and other intracellular microbes is believed to be mostly associated with IFN-γ-mediated macrophage activation.

The specific function of IFN-γ-mediated macrophage activation cannot be assessed in vivo with mice deficient for IFN-γ or its receptor, nor with antibody depletion strategies as the

response of all cell types to the cytokine is affected. Here we studied the course of infection by *M. avium* in transgenic mice with macrophages that are unresponsive to IFN-γ (Macrophages Insensitive to Interferon Gamma, MIIG (10)). We show that these mice exhibit protective responses that are dependent on IFN-γ but independent of its ability to activate macrophages. We also demonstrate that in the absence of IFN-γ signaling in macrophages, TNF-α can exert a compensatory mechanism promoting bacterial growth control.

Materials and Methods

Animals

C57BL/6 (WT) and every mice used in the experiments were bred at I3s/IBMC, Portugal. C57BL/6 mice with macrophages insensitive to IFN-γ (MIIG) were provided by Dr Michael B. Jordan, C57BL/6.IFN-$\gamma^{-/-}$ (IFN-$\gamma^{-/-}$) were purchased from the Jackson Laboratories (Bar Harbor, ME), and C57BL/6.TNF-$\alpha^{-/-}$ (TNF-$\alpha^{-/-}$) were purchased from B&K Universal (East Yorkshire, United Kingdom). The latter were crossed with MIIG mice to obtain MIIG.TNF-$\alpha^{-/-}$ mice. Animal care procedures were in accordance with institutional guidelines. This study was previously approved by the Portuguese National Authority for Animal Health – Direcção Geral de Veterinária.

In vivo infection

Mice were intravenously infected with 10^6 CFUs of *Mycobacterium avium* strain 2447 and were sacrificed at different time points after infection. Bacterial burdens in the major target organs, the spleen and the liver, were determined by plating serial dilutions of tissue homogenates onto Middlebrook 7H10 medium (Difco, St Louis, MO).

Histological and morphometric analysis

Liver samples were fixed in buffered formalin, embedded, and processed for histology by staining with H&E or Perl's. Slides were photographed using an Olympus CX31 light microscope equipped with a DP-25 camera (Imaging Software Cell^B; Olympus, Center Valley, PA). To determine the liver area occupied by cellular infiltrations, five random fields of each H&E stained liver slide were selected in a blind way. For the analysis we used the National Institutes of Health ImageJ software program. The percentage of infiltrated area was calculated by dividing the cumulative area of cell infiltration by the total liver surface of each image.

Immunofluorescence

Liver tissues were fixed in 4% paraformaldehyde, washed in PBS, incubated for 2 h in a 30% sucrose solution and embedded in optimal cutting temperature compound (OCT), and stored at -80°C until sectioning. Tissue sections (10 μm thickness) were performed in a frozen cryostat and stored at -20°C until use. Slides were saturated in blocking solution (10% FBS, 0.1% Triton X-100 in PBS) for 1 h at room temperature. Rabbit polyclonal IgG specific for inducible NO synthase (iNOS; M-19; Santa Cruz Biotechnology) or anti-Ferritin Heavy Chain 1 (FTH1, clone D1D4; Cell Signaling Technology) were diluted in Ab dilution buffer (1% FBS, 0.1% Triton X-100 in PBS) and incubated overnight with tissue sections at 4°C. After washing, sections were incubated with Alexa 488 goat anti-rabbit IgG Ab (Life Technologies) for 1 h at room temperature. Sections were then counterstained and mounted with DAPI-Fluoroshield and imaged in a Leica DMI 6000B inverted microscope using the ORCA-Flash4.0 version 2 (Hamamatsu Photonics) CMOS camera. Images were further analyzed and processed using ImageJ.

Protein extraction and western blot

Mouse liver homogenates were lysed in RIPA buffer with proteases inhibitors and heat denatured in reducing sample buffer. Proteins were separated in 10% polyacrylamide gels and transferred onto nitrocellulose membranes. Nonspecific binding was blocked with 5% milk in TBST (Tris-buffered saline, 0.1% Tween 20), and membranes were probed with primary antibodies against FTH1 (1:1000; D1D4, Cell Signaling Technology) and β-actin (1:4000; ac8227, abcam) followed by incubation with HRP-conjugated anti-rabbit IgG secondary antibody (1:10000; Molecular Probes) and developed by Clarity Western ECL Substrate (Bio-Rad).

Flow Cytometry

Single cell suspensions from the liver or spleen of naïve or infected mice were prepared by passing the organs through a 70-μm nylon cell strainer. Erythrocytes were excluded by subjecting cells to a treatment with RBC lysis buffer. To isolate liver mononuclear cells, these cells were subjected to a 40%:80% Percoll (GE Healthcare) gradient. Liver and spleen cells were washed and the number of viable cells was counted by trypan blue exclusion. For surface immunofluorescence staining, cells were incubated for 20 min with saturating combinations of the different Abs. For intracellular cytokine analysis, cells were previously stimulated with 8 μg/mL of *M. avium* antigens followed by Brefeldin A incubation. After cell surface staining, cells

were fixed with 2% paraformaldehyde and permeabilized with 0.5% saponin. Cells were then incubated with the cytokine Abs for 20 min at room temperature. After two washing steps, cells were acquired in a FACSCanto II cytometer (BD Biosciences) using a BD FACSDiva software. Data were analyzed using FlowJo software (Tree Star).

Abs for flow cytometry

The conjugated mAbs used in flow cytometry are listed in table 1

Table1. List of Abs used for Flow Cytometry

Ab-Fluorochrome	Clone	Isotype	Manufacturer
CD3-FITC	145-2C11	Ar Ham IgG1, k	BD Biosciences
CD3-APC	145-2C11	Ar Ham IgG	Biolegend
CD4-V450	RM4-5	Rat IgG2a, k	BD Biosciences
CD8-V500	53-6.7	Rat IgG2a, k	BD Biosciences
CD11b-BV510	M1/70	Rat IgG2b, k	BD Biosciences
CD11c-BV421	N418	Ar Ham IgG	Biolegend
CD19-FITC	6D5	Rat IgG2a, k	Biolegend
CD19-APC	6D5	Rat IgG2a, k	Biolegend
CD44-PE	IM7	Rat IgG2b, k	BD Biosciences
CD45-PerCP/Cy5.5	I3/2.3	Rat IgG2b, k	Biolegend
F4/80-APC/Cy7	BM8	Rat IgG2a, k	Biolegend
IA/IE-FITC	M5/114.15.2	Rat IgG2b, k	Biolegend
IFN-γ-PE/Cy7	XMG1.2	Rat IgG1, k	Biolegend
Ly6C-PE	HK1.4	Rat IgG2c,k	Biolegend
Ly6G-FITC	1A8	Rat IgG2a,k	Biolegend
Ly6G-APC	1A8	Rat IgG2a, k	Biolegend
NK1.1-FITC	PK136	Mouse IgG2a, k	Biolegend
NK1.1-PE/Cy7	PK136	Mouse IgG2a, k	eBioscience
TNF-α-PerCP/Cy5.5	MP6-XT22	Rat IgG1, k	Biolegend

Cell Sorting

Spleen and liver mononuclear cells were prepared as described earlier. Cells were acquired in a FACSAria using FACSDiva software (BD Biosciences) and sorted into three different macrophage subsets. Briefly after debris and doublets exclusion, cells were gated in the

$CD45^{+}CD11b^{high}CD11c^{-}Ly6G^{-}$ population, and separated accordingly the high, intermediated and low expression of Ly6C. Cells were sorted into the RLT lysis buffer (RNeasy Micro Kit; Qiagen) for posterior RNA purification.

RNA extraction and real-time qPCR

Total RNA was extracted from sorted cell populations (RNeasy Micro kit; Qiagen) according to the manufacturer's instructions. RNA was reverse transcribed to cDNA using the NZY First-strand cDNA synthesis kit (nzytech). Real-time quantitative PCR were run in duplicate for each sample on a Bio-Rad My Cycler iQ5 (Bio-Rad). Primer sequences for each gene are listed in table 2. The resulting RT product was expanded using the Syber Green Supermix (Bio-Rad). The results were analyzed and the ΔΔCt method was used to calculate relative levels of targets compared with *Hprt*. Data were analyzed using iQ5 Optical System software (Bio-Rad).

Table 2. List of primers used for quantitative PCR

Gene	Forward sequence	Reverse Sequence
Hprt	agatgggaggccatcacattgt	atgtcccccgttgactgatcat
Il1b	tctttcccgtggaccttc	cagcaggttatcatcatcatcc
Tnfa	cctgtagcccacgtcgtag	gggagtagacaaggtacaaccc
Cybb	ggattggagtcacgcccttt	caggtctgcaaaccactcaaag
Ncf1	tgtggagaagagcgagagc	tcgtcgggactgtcaagg

Cellular oxidative stress detection

Spleen and liver mononuclear cells were stained with myeloid markers as described in the flow cytometry section. For oxidative stress detection, cells were incubated for 30 min at 37°C with the fluorescent probe CellROX Deep Red Reagent (ThermoFisher) or with ROS-ID Superoxide detection kit (Enzo). After two washing steps, cells were acquired in a FACSCanto II cytometer (BD Biosciences) using a BD FACSDiva software. Data were analyzed using FlowJo software (Tree Star).

In vivo reactive oxygen species detection

After shaving the ventral fur, anesthetized mice were intraperitoneally injected with 25mg/Kg of the chemiluminescent probe L-012 (Wako Pure Chemical Industry). Images were taken immediately using an IVIS Lumina LT system (Perkin Elmer) for 15 min at one minute intervals. Quantification of the luminescence signal intensity was performed using the Living Image

software (Perkin Elmer). The liver was defined as a region of interest (ROI). The total flux (photons/s) and average radiance (photons/sec/cm^2/steradian) within the ROI were automatically calculated. ROI background signal was obtained from imaging non-infected mice that received L-012 as described above. The average radiance background signals of the respective ROIs were subtracted to the respective average radiance measured on infected animals.

Statistical analysis

Results were expressed as means ±SD. Statistical significance was calculated using the unpaired Student t test or the one-way ANOVA test with a Tukey posttest. A p value <0.05 was considered statistically significant.

Results

Control of *M. avium* replication and granuloma development in the absence of IFN-γ-mediated macrophage activation.

To assess the need for IFN-γ-dependent macrophage activation for the control of *M. avium* infections we used MIIG mice which express a dominant non-functional IFN-γ-R1 chain under the control of the CD68 promoter making macrophages, monocytes, DCs and mast cells unable to respond to IFN-γ (10). MIIG mice together with C57BL/6 and IFN-γ$^{-/-}$ animals were intravenously infected with *M. avium* 2447 and the bacterial burdens in the liver and the spleen, the major target organs of the infection, were assessed at different time points. IFN-γ$^{-/-}$ mice exhibited exacerbated bacterial loads in both organs when compared to wild-type C57Bl/6 animals (Fig. 1), confirming the pivotal role of this cytokine for the control of the infection. However MIIG mice, which produce IFN-γ but lack IFN-γ-mediated macrophage activation, were able to control the bacterial replication better than the IFN-γ$^{-/-}$ mice (Fig. 1). In the liver, MIIG mice were able to control the infection to the same extent as the C57BL/6 animals until day 60 post-infection and had lower burdens at day 130 post-infection. In the spleen, MIIG animals were able to control the *M. avium* proliferation until 60 days after infection. However at later time points (130dpi) they exhibited increased bacterial burdens when compared to the C57BL/6 animals (Fig. 1). These results clearly show that mice with impaired IFN-γ signaling in macrophages are able to fully control the bacterial proliferation in the liver and partially in the spleen.

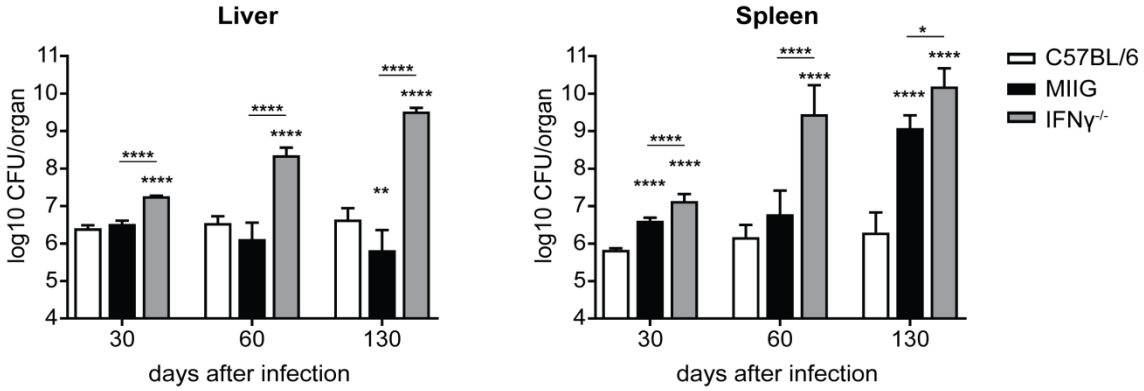

Figure 1. Lack of IFN-γ-mediated macrophage activation does not fully impair antimycobacterial response. *M. avium* 2447 burden in the liver and the spleen of C57BL/6, MIIG and IFN-$\gamma^{-/-}$ mice at days 30, 60 and 130 post-infection. Data represent the mean CFUs ± SD from at least five mice per group of one out of three experiments. The statistical analysis of the differences between mutant mice and the C57BL/6 control group is shown above each column. Additional comparisons between others groups are indicated by horizontal lines. The *p* value was determined by a one-way ANOVA test with a Tukey multiple comparisons posttest (*p< 0.05, **p< 0.01, ****p< 0.0001).

The development of granulomas is a hallmark of mycobacterial infections. The absolute requirement of IFN-γ for the assembly of these structures was already demonstrated (chapter II of this thesis (11) and (12)). However, previous work with a highly virulent strain of *M. avium* has shown that granulomas develop normally in the absence of macrophage activation by IFN-γ (13). Here we found similar results with the less virulent 2447 strain. At 60 dpi, and in contrast to IFN-$\gamma^{-/-}$ mice, MIIG mice exhibit well developed granulomata, with a core of epithelioid macrophages surrounded by a well-defined lymphocytic cuff (Fig. 2A). When compared to C57BL/6, granulomas in MIIG mice were larger and in higher number leading to an increased percentage of infiltrated area (Fig. 2A, 2B). To confirm the lack of IFN-γ signaling in macrophages we performed an iNOS staining in infected liver tissues at 60 dpi since the induction of this enzyme in macrophages is known to be dependent on the activation by IFN-γ (14). As shown in figure 2C granulomas in MIIG mice did not exhibit iNOS^{+} macrophages.

Taken together these results show that IFN-γ-mediated macrophage activation is not absolutely-required for *M. avium* proliferation control or for granuloma assembly in the liver. This suggests that in order to control *M. avium* replication and promote granuloma assembly in MIIG mice, IFN-γ is targeting cells other than macrophages or DCs, and/or an IFN-γ-independent mechanism is compensating for the lack of IFN-γ-macrophage signaling.

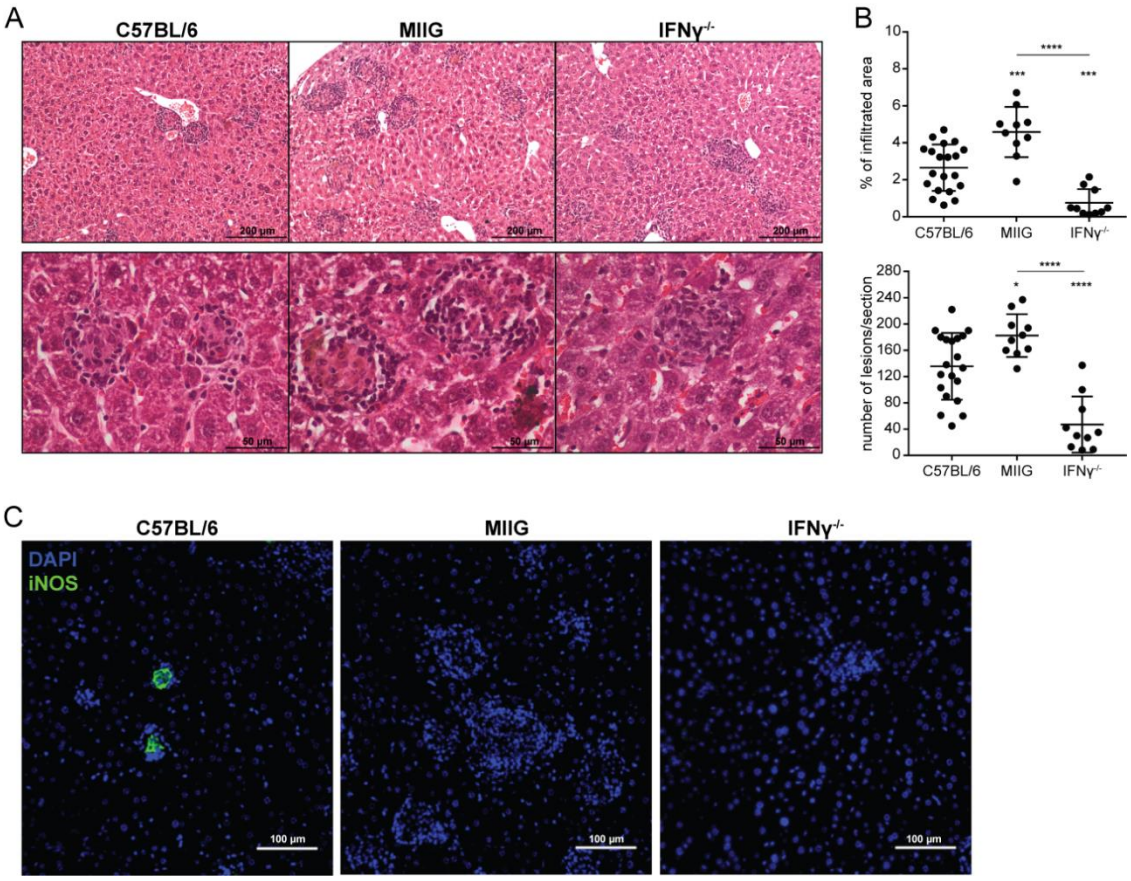

Figure 2. IFN-γ-mediated macrophage activation is not required for granuloma assembly. C57BL/6, MIIG and IFN-γ$^{-/-}$ mice were intravenously infected with *M. avium* 2447 for 60 days. **(A)** Representative liver sections stained with H&E. **(B)** Percentage of the infiltrated area and quantification of the number of lesions per liver section. Data represent the mean ± SD from at least 10 mice per group. Each point represents one liver section. The statistical analysis of the differences between mutant mice and the C57BL/6 control group is shown above each column. Additional comparisons between others groups are indicated by horizontal lines. The *p* value was determined by a one-way ANOVA test with a Tukey multiple comparisons posttest (*$p<$ 0.05, ***$p<$ 0.001, ****$p<$ 0.0001). **(C)** Representative iNOS expression in granulomas of the liver.

M. avium infected MIIG mice exhibited increased macrophage and CD4$^+$ T cell recruitment.

To identify the cell populations being recruited into the lesions in infected MIIG mice, we performed flow cytometric analysis of different lymphoid and myeloid populations. We began by showing that there were no differences in these populations in naïve C57BL6 and MIIG animals. Both groups of non-infected mice showed similar numbers of total mononuclear liver and spleen cells (Fig. 3A). No differences in cell numbers were detected among myeloid cells, namely neutrophils, DCs and macrophages (Fig. 3B for gating strategy) in both the liver and the spleen (Fig. 3C). Likewise no differences were observed in the numbers of B cells, CD4$^+$ and CD8$^+$ T cells between the two mouse strains (Fig. 3D for gating strategy, and Fig. 3E).

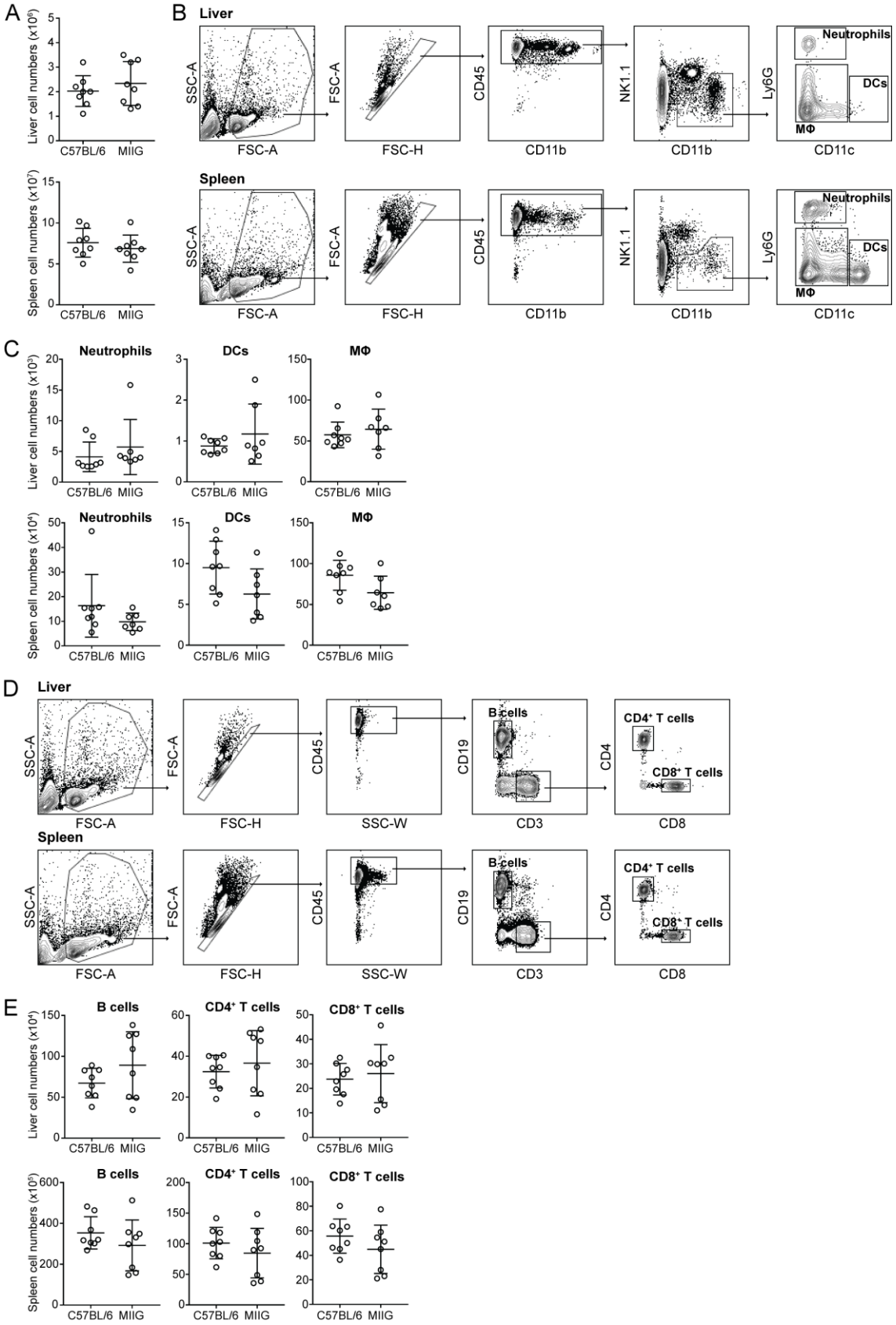

Figure 3. Naïve C57BL/6 and MIIG mice display similar myeloid and lymphoid cell populations. **(A)** Total cell numbers of uninfected C57BL/6 and MIIG livers (upper panel) and spleens (lower panel). **(B)** Gating strategy to identify the myeloid populations: neutrophils, DCs and macrophages (Mϕ) and **(C)** the respective cell numbers in the

liver and the spleen (upper and lower panels, respectively). **(D)** Gating strategy to identify the lymphoid populations: B cells, $CD4^+$ and $CD8^+$ T cells, and **(E)** the respective cell numbers in the liver and the spleen (upper and lower panels, respectively). Each point represents one animal. Data represent the mean ± SD from seven to eight mice per group. The statistical analysis was performed with an unpaired student's t test. No statistical differences between the groups were detected.

We chose to study the *M. avium*-induced effects in the hosts at 60dpi since this is a time point where both C57BL/6 and MIIG animals present equivalent bacterial burdens in the organs studied (Fig. 1) thus normalizing the stimuli for the inflammatory response in the two strains. Upon infection we observed that mononuclear liver and total spleen cells were increased in infected MIIG mice when compared both with uninfected animals (Ui) and with infected C57BL/6 mice (Fig. 4A).

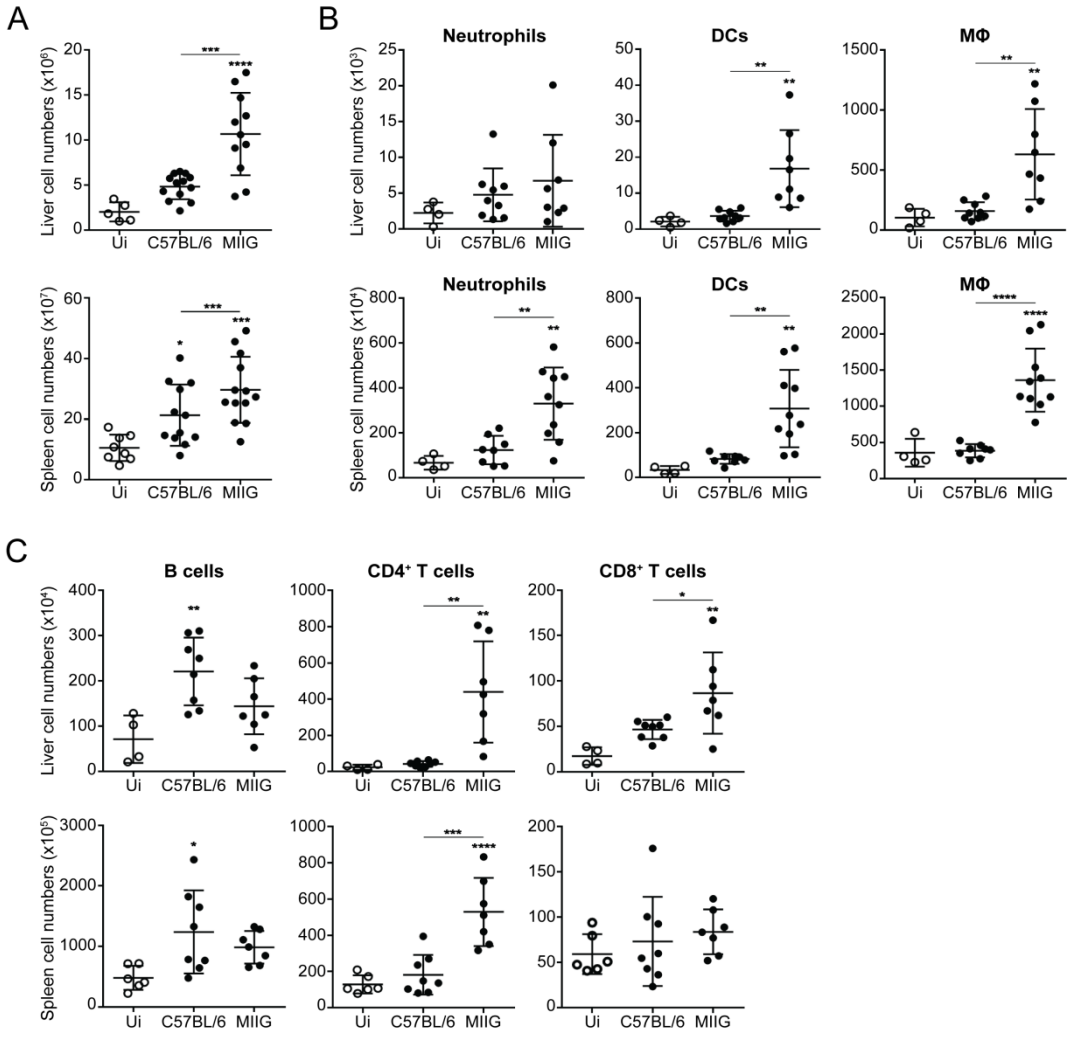

Figure 4. *M. avium* infected MIIG mice exhibit increased leukocyte accumulation. A pool of C57BL/6 and MIIG uninfected (Ui) mice was used for comparison purposes with the infected mice at 60 dpi. **(A)** Total numbers of live cells were determined based on trypan blue exclusion in livers and spleens (upper and lower panel, respectively).

(B) Myeloid and **(C)** lymphoid liver and spleen cell numbers were determined based on the flow cytometric data. Each point represents one animal. Data represent the mean ± SD from at least four uninfected and seven infected mice per group of two experiments out of four. The statistical analysis of the differences between infected groups and the Ui control group is shown above each column. Additional comparisons between others groups are indicated by horizontal lines. The *p* value was determined by a one-way ANOVA test with a Tukey multiple comparisons posttest (*$p < 0.05$, **$p < 0.01$, ***$p < 0.001$, ****$p < 0.0001$).

To identify the different myeloid and lymphoid cell populations, the gating strategy showed in Fig. 3B and 3D, respectively, was used in infected animals. In the liver there were no differences in neutrophil numbers but both DCs and macrophages were increased 4-fold in MIIG infected mice when compared to infected C57BL/6 mice (Fig. 4B). In the spleen all three myeloid populations were increased 3-fold in MIIG infected animals when compared to the infected C57BL/6 control animals (Fig. 4B). No differences in B cell numbers were found between the two infected mouse strains (Fig 4C). Importantly when compared to the infected C57BL/6, $CD4^+$ T cells from infected MIIG mice presented a 10-fold increase in the liver and a 5-fold increase in the spleen. $CD8^+$ T cell numbers were also increased in the infected MIIG livers compared to infected C57BL/6 but not in the spleens (Fig. 4C).

M. avium infection induced increased numbers of TNF-α-producing $CD4^+$ T cells in MIIG animals.

We next evaluated the capacity of T cells from infected mice to produce IFN-γ and TNF-α after *ex vivo* restimulation with *M. avium* antigens. While $CD8^+$ T cells had poor capacity to express these cytokines under these experimental conditions, $CD4^+$ T cells from MIIG mice had increased capacity to express IFN-γ and TNF-α in both the liver and the spleen when compared to the infected C57BL/6 control group (Fig. 5A). The increase in TNF-α-producing $CD4^+$ T cells was mostly due to the IFN-γ^+TNF-α^+ double producing (DP) cells (Fig. 5A, 5B). The increased capacity of MIIG $CD4^+$ T cells to express these cytokines resulted in a 20-fold increase in the total numbers of IFN-γ^+ $CD4^+$ T cells and a 45-fold increase in the total numbers TNF-α^+ $CD4^+$ T cells, when compared with the infected C57BL/6 mice. These fold changes were similar in the liver and the spleen (Fig. 5C).

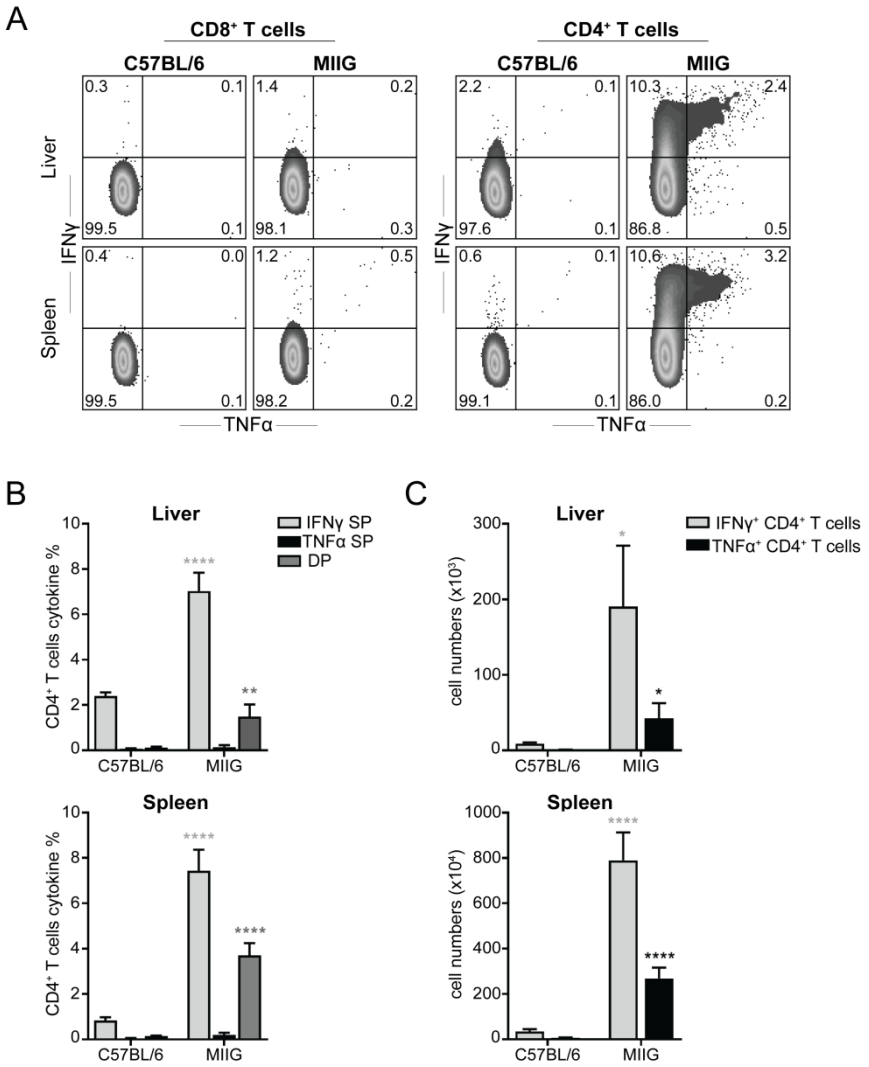

Figure 5. CD4⁺ T cells from infected MIIG animals have increased capacity to express IFN-γ and TNF-α. Intracellular IFN-γ and TNF-α expression in CD8⁺ and CD4⁺ liver (upper panels) and spleen (lower panels) T cells from both C57BL/6 and MIIG mice after 60 days of infection. **(A)** IFN-γ and TNF-α producing cells gated on CD8⁺ or CD4⁺ T cells. **(B)** Frequencies of IFN-γ and TNF-α single and double producers (SP and DP, respectively) in CD4⁺ T cells. **(C)** Cell numbers of total IFN-γ- and TNF-α-producing CD4⁺ T cells. Data represent the mean ± SD from at least seven animals per group. The statistical analysis of the differences between MIIG mice and the C57BL/6 control group is shown above the respective MIIG column. The p value was determined by an unpaired student's t test (*$p< 0.05$, **$p< 0.01$, ****$p< 0.0001$).

M. avium induced increased *Tnfa* and *Il1b* gene expression in MIIG Ly6C^{low} macrophages.

MIIG mice have impaired IFN-γ signaling in macrophages, monocytes and DCs, but as macrophages are the main target cells of mycobacteria, we focused on this cell population in order to unveil the consequences of the lack of IFN-γ-mediated cell activation during the immune

response to *M. avium* infection. Liver and spleen macrophage populations as defined before (Fig. 3B) were further divided into four different subsets according to Ly6C and F4/80 expression (Fig. 6A). Similar numbers of the different subsets were found in both organs in uninfected (Ui) mice despite the Ly6C^{int}F4/80^{-} subset was the least represented subset (Fig. 6B). After 60 days of infection no significant alterations were detected in control C57Bl/6 animals whereas almost all macrophage subsets were increased in both organs from MIIG mice when compared with the infected C57BL/6 (Fig. 6B). Among them, the Ly6C^{high} subset in MIIG animals was recruited in higher numbers, with a 4.7-fold increase in the liver and a 3-fold increase in the spleen. Ly6C^{int}F4/80^{-} cells from infected MIIG mice exhibited nearly a 4.5-fold increase in both organs, and Ly6C^{low} subset from infected MIIG animals were increased 3 times over the infected C57BL/6 in both organs. The exception was the Ly6C^{int}F4/80^{+} macrophage subset in the liver. This subset is mostly comprised by Kupffer cells, the liver resident macrophages. Hence it was not surprising that, when compared with the Ui group, this particular liver subset was not increased upon infection in either of the mouse strains. On the other hand, Ly6C^{int}F4/80^{+} cells from the spleen of infected MIIG mice were 3.6 times increased over the infected WT (Fig. 6B).

Different macrophage subsets expressing different amounts of Ly6C are known to have different inflammatory profiles (15). To analyze the gene expression of these populations, we sorted three different macrophage subsets expressing high, intermediate or low levels of Ly6C, from livers and spleens of C57BL/6 and MIIG mice after 60 days of infection (Fig. 6 C, for the sorting scheme). Given the low cell numbers of the liver Ly6C^{int}F4/80^{+} subset (Kuppfer cells) we decided to sort just one population of Ly6C^{int} macrophages (comprising both the F4/80 positive and negative cells). The *Il1b* and *Tnfa* gene expression for each one of these macrophage subsets was analyzed by qPCR (Fig 6D, 6E). In liver Ly6C^{high} cells isolated from MIIG mice the *Il1b* and *Tnfa* gene expression was slightly reduced when compared to the C57BL/6 controls. The opposite was observed for spleen Ly6C^{high} cells, with both genes being expressed in higher levels in MIIG cells. Interestingly, higher *Il1b* and *Tnfa* gene expression was observed in MIIG Ly6C^{int} and Ly6C^{low} cells in both organs. These results were particularly evident in the liver Ly6C^{low} population where MIIG cells exhibited a 30-fold increase of *Il1b* and a 7.5-fold increase of *Tnfa* expression over that found in C57BL/6 Ly6C^{low} cells (Fig. 6D, 6E).

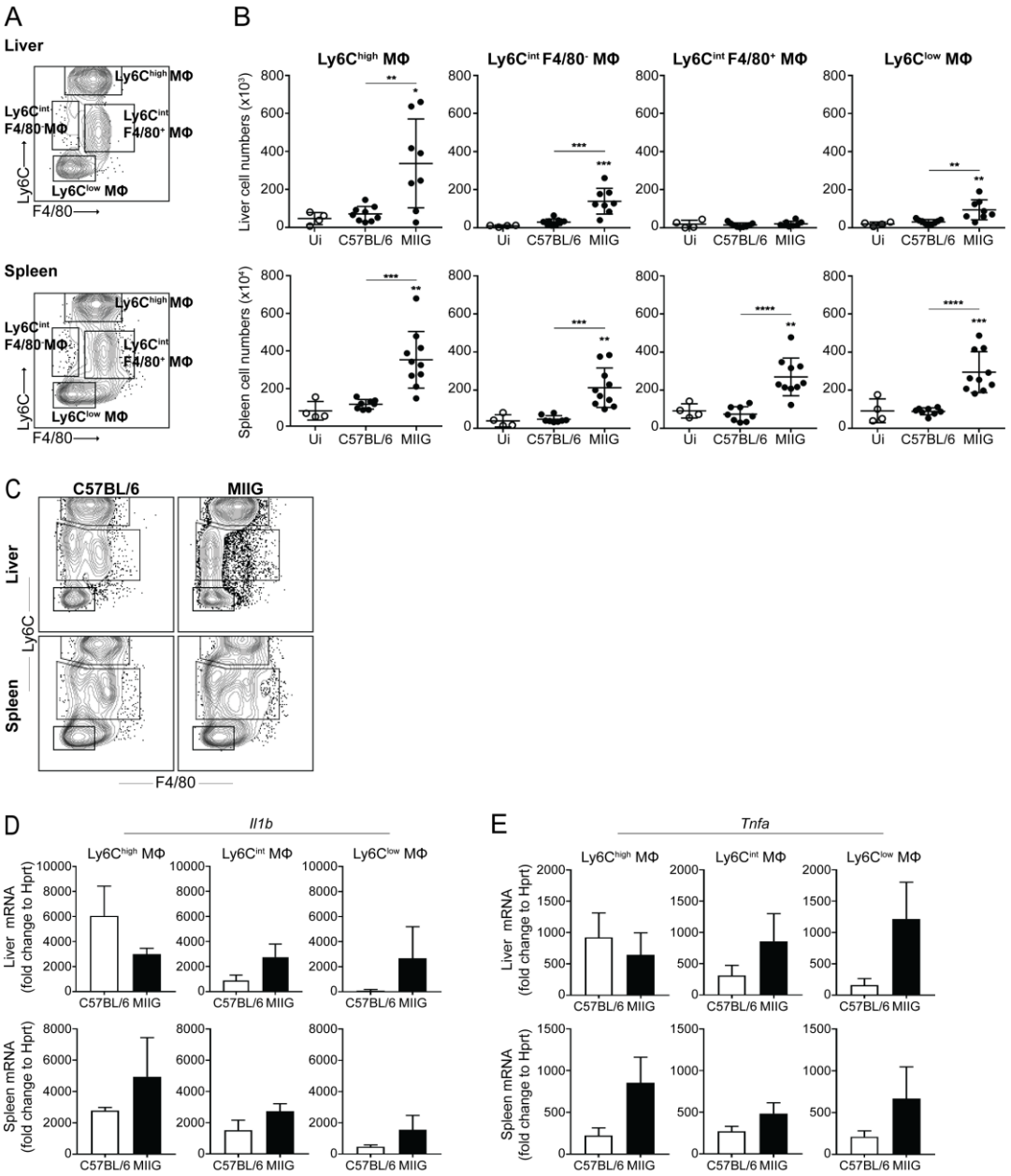

Figure 6. Ly6C^{low} macrophages from infected MIIG mice express increased levels of *Tnfa* and *Il1b* mRNA. **(A)** Gating scheme of the four different macrophage subsets according to the expression of Ly6C and F4/80 in both the liver and the spleen. **(B)** Cell numbers of the respective macrophage subsets from uninfected (Ui) and infected mice (C57BL/6 and MIIG) at 60dpi. Each point represents one animal. Data represent the mean ± SD from at least four uninfected and eight infected mice per group of two experiments out of four. The statistical analysis of the differences between infected groups and the Ui control group is shown above each column. Additional comparisons between others groups are indicated by horizontal lines. The *p* value was determined by a one-way ANOVA test with a Tukey multiple comparisons posttest (*$p< 0.05$, **$p< 0.01$, ***$p< 0.001$, ****$p< 0.0001$). **(C)** Sorting strategy of the three different macrophage subsets with high, intermediate or low expression of Ly6C from the livers and spleens of *M. avium*-infected C57BL/6 and MIIG mice at 60 dpi. **(D)** *Il1b* and **(E)** *Tnfa* gene expression of the indicated sorted Ly6C macrophage subsets were determined by qPCR. Values are normalized to *Hprt* expression. Reactions were run in duplicated and represent the mean ± SD from three individual mice per group of one experiment.

Macrophages from infected MIIG animals showed increased ROS production.

Previous data from our group have shown that the superoxide secretion by macrophages in *M. avium* infected mice is dependent on TNF-α (16). As MIIG animals are able to control the bacterial growth and also exhibit increased levels of *Tnfa*, we hypothesized that the oxidative burst could be increased in these animals and be at least partially responsible for the control of *M. avium* replication. Therefore we injected infected mice with a ROS luminescent probe that allows ROS production measurement in live animals. The liver was defined as a Region of interest (ROIs-red circle) and the luminescence signal within it was quantified. Signal quantification showed that in the liver, infected MIIG mice express more ROS than infected C57BL/6 (Fig. 7A, 7B). The same is evident when liver MIIG luminesce signal is compared with Rag$^{-/-}$IFN-γ$^{-/-}$ mice suggesting that the increased ROS production only occurs when IFN-γ signaling is impaired in macrophages and not when it is totally abrogated.

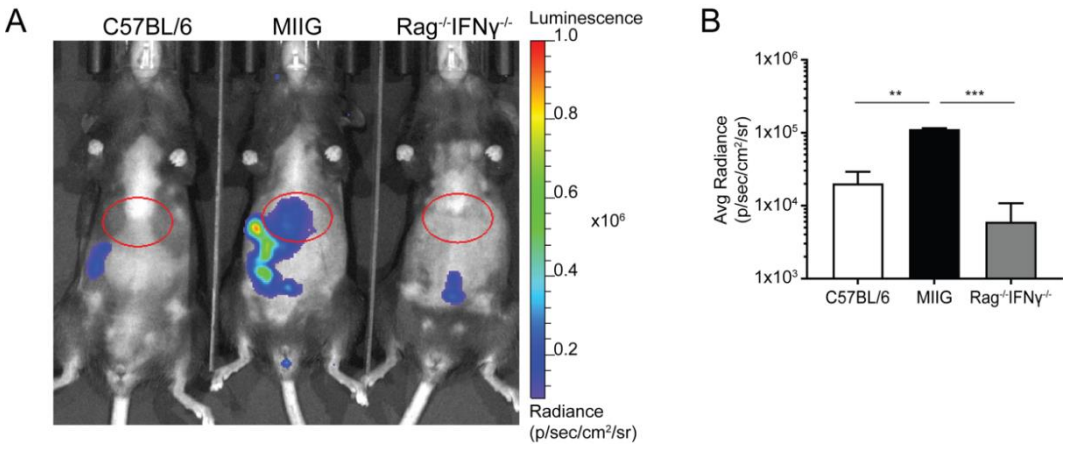

Figure 7. *M.avium*-infected MIIG mice exhibit increased ROS expression in vivo. **(A)** *In vivo* imaging of animals injected with L-012. The probe was injected into the peritoneal cavity of C57BL/6, MIIG and Rag$^{-/-}$.IFN-γ$^{-/-}$ mice after 60 days of infection. Images represent the luminescence obtained 7 min after L-012 injection, with the defined Regions of Interest (ROIs) used for quantitative analysis. **(B)** Quantification of the luminescence signal in average radiance (photons/s/cm2/steradian) of the previous defined ROIs at 7 min after L-012 injection. Data represent the mean ± SD from two animals per group from each of two independent experiments. The *p* value was determined by a one-way ANOVA test with a Tukey multiple comparisons posttest (**p< 0.01, ***p< 0.001).

In order to explore the source of *M. avium*–induced ROS production in MIIG mice, we assessed the mRNA expression of two phox subunits from the NOX2 family of NADPH oxidases: *Cybb* encoding for gp91, and *Ncf1*, encoding for p47, a membrane and a cytosolic subunit respectively. After 60 days of infection, despite the elevated levels of *Cybb* and *Ncf1* in liver and

spleen Ly6C^{high} macrophages, there were no major differences in the mRNA expression of this population between MIIG and C57BL/6 mice (Fig. 8A, 8B). Importantly, although the mRNA levels of both subunits were lower the in the Ly6C^{int} and Ly6C^{low} cells when compared to the Ly6C^{high} population, both *Cybb* and *Ncf1* gene expression was increased in MIIG Ly6C^{int} and Ly6C^{low} macrophages when compared to their C57BL/6 counterparts. This was particularly evident in Ly6C^{low} cells isolated from the liver of infected MIIG mice where *Cybb* gene expression presented a 30-fold increase and *Ncf1* gene expression a 7-fold increase over the respective C57BL/6 controls (Fig. 8A, 8B).

Using a fluorescent probe (CellROX), total ROS expression in specific myeloid cell populations was also measured by flow cytometry (Fig. 8C). Neutrophils from the liver and spleen of infected MIIG and C57BL/6 mice expressed high and equivalent amounts of ROS. DCs from infected MIIG animals expressed higher amounts of ROS, particularly in the liver, as compared to cells from infected controls. Concerning the three Ly6C macrophage subsets, despite the high levels of ROS in the Ly6C^{high} subsets, there were no differences between the two mouse strains. On the other hand ROS expression in both liver and spleen cells from MIIG animals was increased in Ly6C^{int} and Ly6C^{low} populations over the C57BL/6 corresponding subsets (Fig. 8C). Taken together these flow cytometry data is in agreement with the gene expression data (Fig. 8A, 8B). The ROS^{+} and ROS^{-} cell numbers for each macrophage subset was determined based on the flow cytometric data. In infected MIIG mice the recruitment of the different Ly6C macrophage subsets into the liver and spleen was mainly comprised of ROS-producing cells (CellROX^{+}) (Fig 8D).

To assure that the increased ROS production in infected MIIG mice was originated from NOX2 activation as suggested by the *Cybb* and *Ncf1* mRNA expression (Fig. 8A, 8B), we used a fluorescent probe specific for superoxide. Neutrophils from both organs produced equivalent amounts of superoxide in the two mouse strains (Fig. 8E). On the other hand, DCs from MIIG mice produced higher amounts of superoxide than DCs from C57BL/6 animals. This result was more evident in the liver than the spleen. The broad fluorescence spectrum of this probe blocked the use of other fluorophores at the same time. Hence we could not distinguish between the different Ly6C macrophage subsets, and could only analyze the probe fluorescence in total macrophages. Superoxide was produced in higher levels by macrophages from infected MIIG mice. The differences in superoxide production between the two mouse strains were most striking in the liver (Fig 8E).

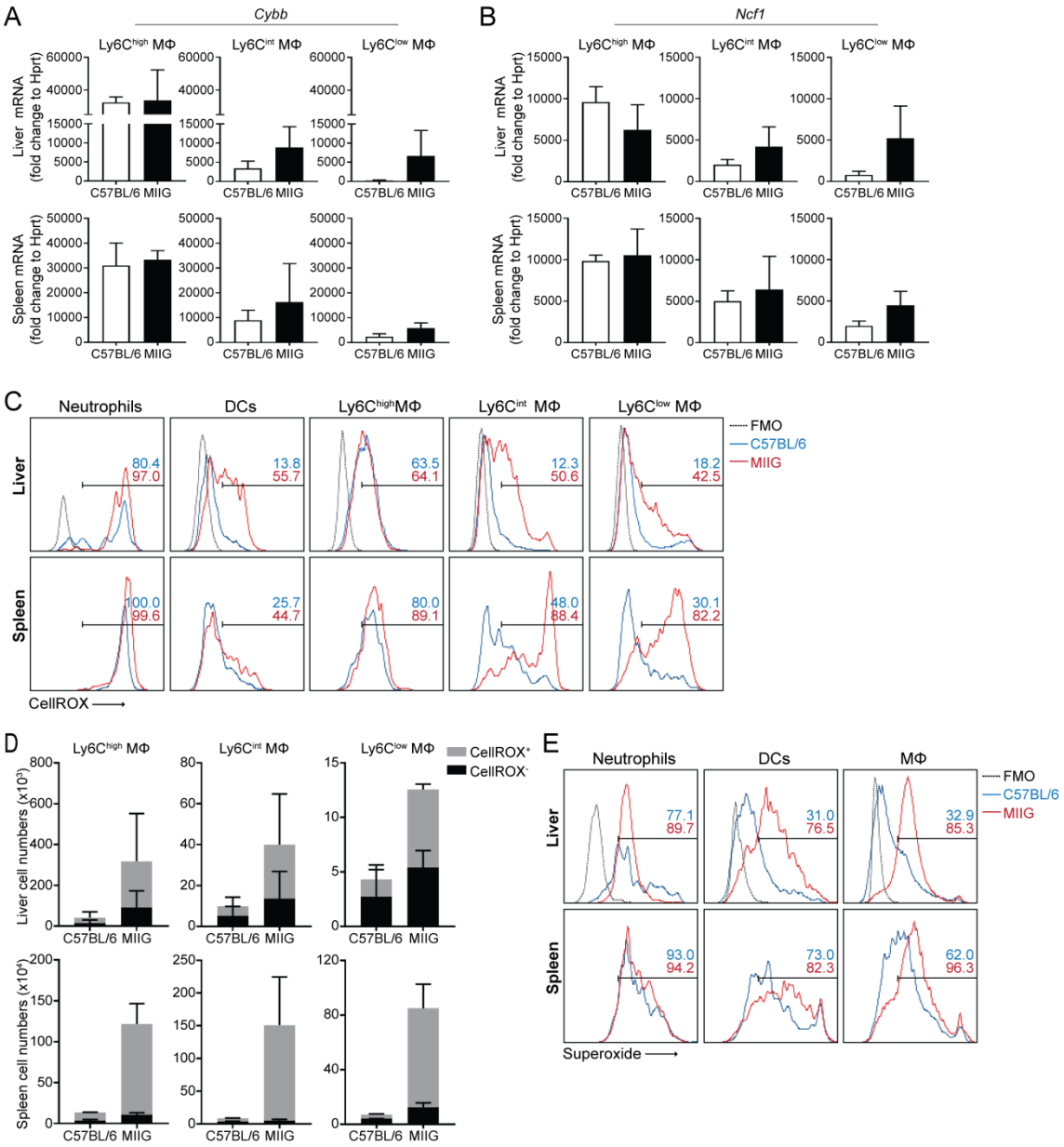

Figure 8. Ly6C^{int} and Ly6C^{low} macrophages from MIIG mice exhibit increased ROS expression at 60 dpi. **(A)** *Cybb* and **(B)** *Ncf1* gene expression in the three different Ly6C sorted macrophage populations from infected animals as determined by qPCR. Values are normalized to *Hprt* expression. Reactions were run in duplicated and represent the mean ± SD from three mice per group of one experiment. **(C)** Representative histograms of liver (upper panel) and spleen (lower panel) CellROX expression obtained by flow cytometric analysis on the indicated myeloid cell subsets from 60dpi C57BL/6 (blue) and MIIG animals (red). **(D)** Cell number quantification of CellROX positive and negative cells within each Ly6C macrophage subset in both the liver and spleen as determined by the previous flow cytometric analysis. **(E)** Representative histograms of superoxide expression in the indicated myeloid cell subsets from the liver and spleen of C57BL/6 (blue) and MIIG (red) mice at 60 dpi as obtained by flow cytometry. The frequencies of positive cells for both CellROX and Superoxide were determined according to the fluorescence minus one (FMO) and are indicated in each histogram shaded with the corresponding blue or red color. Histograms displayed in (C) and (E) are representative of three animals per group from two independent experiments. Data showed in (D) represent the mean ± SD from three animals per group of two independent experiments.

MIIG mice exhibited extensive iron accumulation within granuloma macrophages.

Both TNF-α and ROS are tightly involved in iron metabolism (17, 18). A Perl's staining of liver sections from infected mice revealed an increased iron content in macrophages from infected MIIG animals that was not observed in C57BL/6 livers neither in the livers of IFN-$\gamma^{-/-}$ animals (Fig. 9). This result suggests that iron accumulation within the granulomas only occurs when IFN-γ signaling in macrophages is impaired and not when it is fully abrogated.

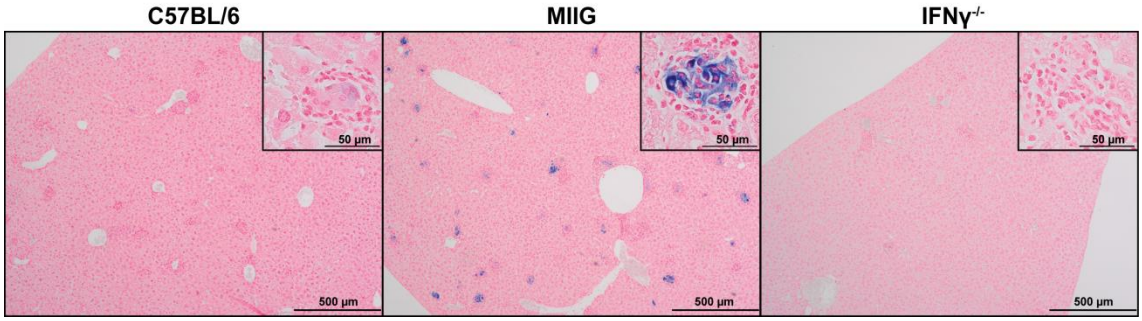

Figure 9. MIIG mice exhibit high iron content in the granuloma macrophages. Representative Perl's stained liver sections from mice infected for 60 days. A representative granuloma structure for group is displayed with a higher magnification in the right upper quadrant of the respective image.

Ferritin is the main iron storage protein in the cell (17). To assess whether ferritin was involved in the increased iron accumulation in infected MIIG mice, we stained liver sections with an antibody for the ferritin heavy chain (FTH1). Granulomas from infected C57BL/6 and MIIG mice exhibited high ferritin content (Fig. 10A). To quantify the FTH1 expression we performed a western blot in total liver extracts, but no differences between the two infected strains were observed (Fig. 10B). To exclude that cells other than mononuclear cells, namely hepatocytes, were diluting the detection of FTH1 expression, we performed a western blot with isolated mononuclear liver cell extracts. Again no differences in the FTH1 expression were observed between infected MIIG and C57BL/6 mice (Fig. 10C). This result shows that the strong iron accumulation in the granulomas of infected MIIG mices is not associated with increased ferritin expression.

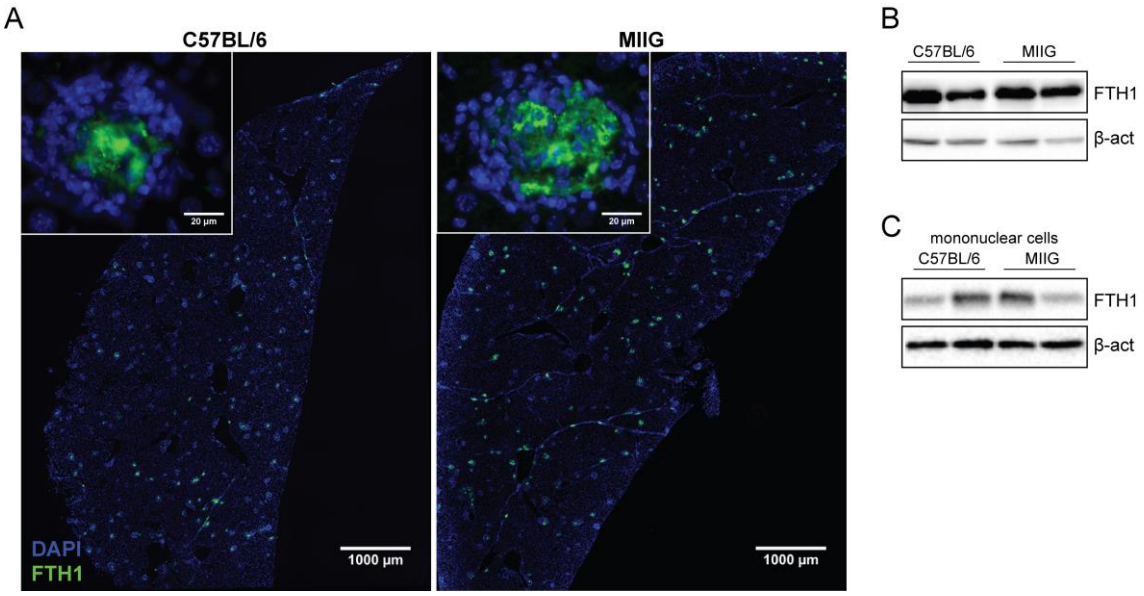

Figure 10. Iron accumulation in granulomas from MIIG mice does not associate with increased Ferritin H expression. **(A)** FTH1 expression (green) counterstained with DAPI (blue) in liver sections of C57BL/6 and MIIG mice at 60dpi. A representative granuloma structure is displayed with a higher magnification in the left upper quadrant of the corresponding image. **(B-C)** Western blots for FTH1. Representative blots from **(B)** total liver extracts and **(C)** mononuclear liver cells of infected C57BL/6 and MIIG mice. Data is representative of four mice per group from one experiment.

TNF-α has a pivotal role in the control of *M. avium* proliferation in MIIG mice by compensating the lack of IFN-γ-mediated macrophage activation.

The control of *M. avium* growth and the development of granuloma structures in MIIG mice, together with the high TNF-α expression that was accompanied by increased ROS production and iron accumulation led us to hypothesize that TNF-α could be compensating for the lack of IFN-γ signaling in macrophages. To assess this hypothesis we crossed MIIG mice with TNF-$\alpha^{-/-}$ animals obtaining MIIG.TNF-$\alpha^{-/-}$ mice. Previous work from our lab has shown that TNF-$\alpha^{-/-}$ mice can control *M. avium* 2447 proliferation with almost similar efficacy as wild type animals. The same work also showed that TNF-$\alpha^{-/-}$ animals get moribund and succumb around 7 to 8 weeks after infection with *M. avium* 2447. This early death was not associated with increased bacterial burdens and was related to granuloma desintegration (19). For this reason the study of the response of MIIG.TNF-$\alpha^{-/-}$ animals to *M. avium* 2447 infection was performed at 48 dpi, a time point when TNF-$\alpha^{-/-}$ infected mice still appear healthy. The analysis of the bacterial burden revealed increased *M. avium* proliferation in the liver and spleen of MIIG.TNF-$\alpha^{-/-}$ mice when

compared with C57BL/6, MIIG or even with TNF-$\alpha^{-/-}$ mice (Fig. 11). TNF-$\alpha^{-/-}$ animals presented only slightly higher bacterial burdens than C57BL/6 mice (Fig. 11) as previously described (19).

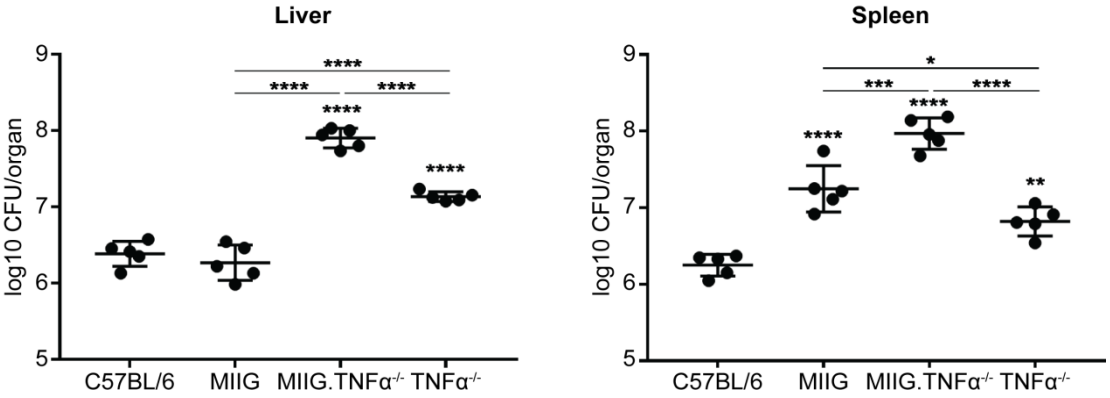

Figure 11. The lack of TNF-α in MIIG animals impairs bacterial proliferation control. Liver and spleen bacterial loads of *M. avium* infected C57BL/6, MIIG, MIIG.TNF-$\alpha^{-/-}$ and TNF-$\alpha^{-/-}$ mice at 48 dpi. Data represent the mean CFUs ± SD from five mice per group of one representative out of two experiments. The statistical analysis of the differences between mutant mice and the C57BL/6 control group is shown above each column. Additional comparisons between others groups are indicated by horizontal lines. The *p* value was determined by a one-way ANOVA test with a Tukey multiple comparisons posttest (*$p< 0.05$, **$p< 0.01$, ***$p< 0.001$, ****$p< 0.0001$).

Unlike infected MIIG mice, neither MIIG.TNF-$\alpha^{-/-}$ or TNF-$\alpha^{-/-}$ infected mice showed any detectable iron accumulation in the granulomas from the liver (Fig. 12A). The CellROX flow cytometer analysis in myeloid cells from the livers and spleens of infected mice revealed no major differences in ROS expression for the Ly6C^{high} macrophages subset among the four mice groups. In the particular case of neutrophils, both mouse strains lacking TNF-α exhibited reduced ROS expression. For all the other cell populations MIIG.TNF-$\alpha^{-/-}$ but not TNF-$\alpha^{-/-}$ mice exhibited impaired ROS expression. In fact TNF-$\alpha^{-/-}$ animals were able to express equivalent levels of ROS as the C57BL/6 group in the latter populations (Fig. 12B). Again, Ly6C^{int} and Ly6C^{low} macrophages from the liver and spleen of infected MIIG mice produced high amounts of ROS (Fig. 8C and 12B). Taken together these data suggests that the high levels of TNF-α detected in the liver and spleen of infected MIIG (Fig. 5 and 6E) mice is required for the increased ROS production. Finally, the increase in cell recruitment/accumulation in MIIG mice was not reverted in the liver of the double transgenic MIIG.TNF-$\alpha^{-/-}$ mice at 48 dpi (Fig. 12C). In fact MIIG animals exhibited higher cell numbers in the absence of TNF-α suggesting that the increased cellular accumulation is independent of this cytokine.

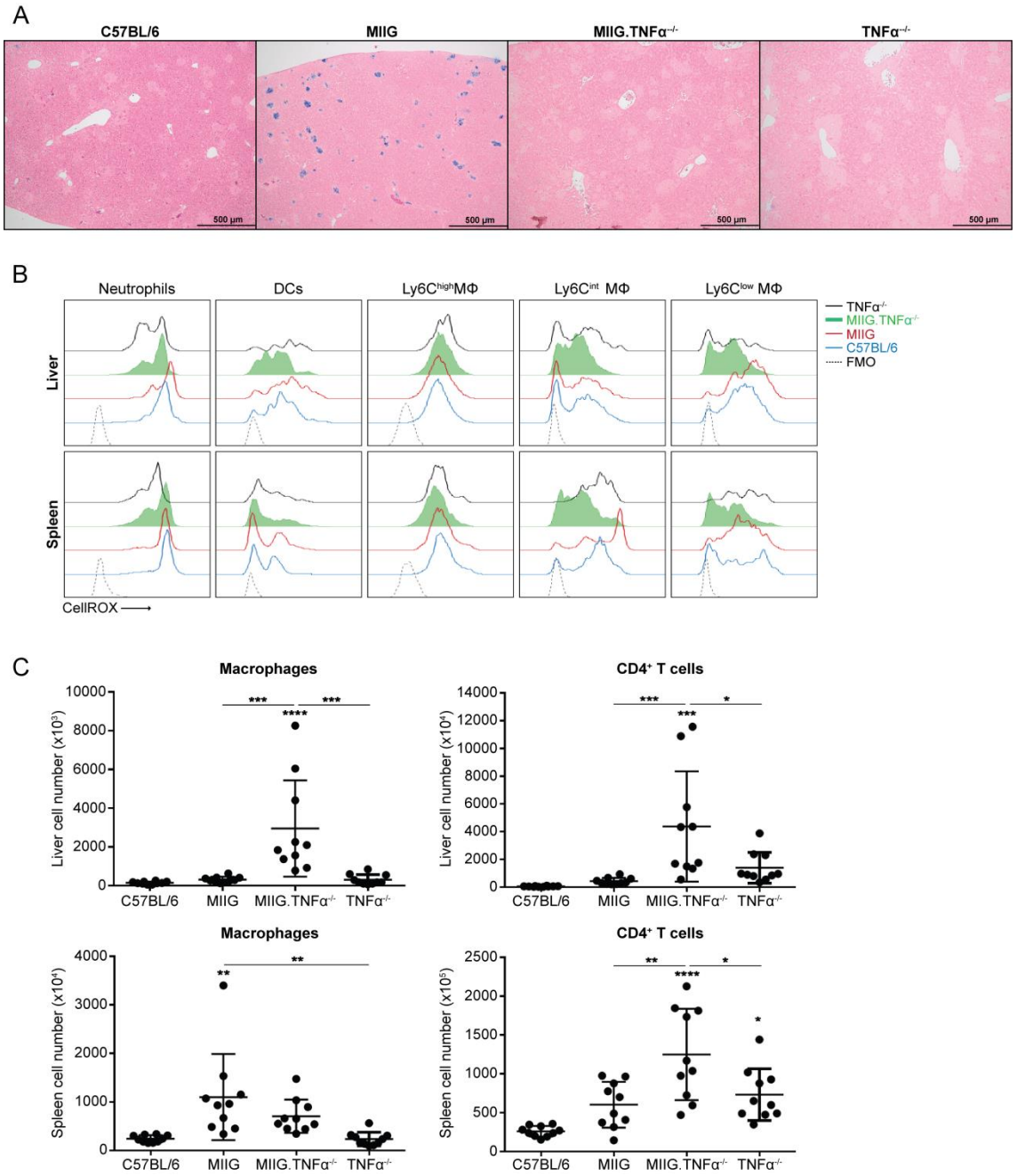

Figure 12. TNF-α compensates for the lack of IFN-γ signaling in macrophages. **(A)** Representative Perl's staining of liver sections from the indicated mice infected for 48 days. **(B)** Representative histograms of CellROX expression in the indicated myeloid cell subsets from the liver and spleen (upper and lower panel, respectively) from C57BL/6 (blue), MIIG (red), MIIG.TNF-$\alpha^{-/-}$ (tinted green) and TNF-$\alpha^{-/-}$ (black) mice after 48 days of infection. FMO is indicated in each histogram in dashed black line. Data is representative of three animals per group from one experiment. **(C)** Macrophages and CD4$^+$ T cell numbers in infected mice at 48 dpi. Each point represents one animal. Data represent the mean ± SD from ten mice from two experiments. The statistical analysis of the differences between mutant mice and the C57BL/6 control group is shown above each column. Additional comparisons between others groups are indicated by horizontal lines. The *p* value was determined by one-way ANOVA test with a Tukey multiple comparisons posttest (*$p< 0.05$, **$p< 0.01$, ***$p< 0.001$, ****$p< 0.0001$).

Discussion

The impact of IFN-γ-dependent resistance to intracellular pathogens has been widely attributed to its action on macrophages, particularly in the case of pathogens that have this cell as their main target. However, the specific role of IFN-γ-dependent macrophage activation has not been properly assessed in vivo. Therefore we used MIIG mice, whose macrophages are insensitive to IFN-γ (10), in a *M. avium* infection model. As in other mycobacteria, the complete lack of IFN-γ signaling during *M. avium* infections leads not only to an uncontrolled growth of the bacteria (7, 20, 21) but also to a deregulation in granuloma development (8, 22, 23). In the *M. avium* infection model and despite the increased susceptibility in the absence of IFNγ, these mice do no succumb to infection (7, 8). Hence, this bacterium is a more suitable model to assess the impact of IFN-γ-macrophage mediated activation, particularly because it allows studying its effect in a chronic stage. Our results clearly showed that the drastic phenotype observed in the total absence of IFN-γ cannot be explained solely by an impaired IFNγ-signaling in macrophages. Despite the lack of IFN-γ-mediated macrophage activation, MIIG animals were able to control *M. avium* proliferation. This was particularly evident in the liver throughout the entire studied course of the infection (up to 130 dpi), while in the spleens the ability to restrict bacterial replication was decreased at later time points. The MIIG transgenic mouse has neutrophils that can respond to IFN-γ. Indeed at 130 dpi we observed a prominent increase of these cells in spleens of MIIG mice (43-fold increase over the infected WT -data not shown) that was not observed in the livers. This result suggests that the uncontrolled bacterial proliferation specifically observed in the spleen at later time points might rely in an excessive neutrophilic inflammatory response.

The contrasting effects of a complete lack of IFN-γ and the MIIG genotype may be explained by the action of IFN-γ in cells other than the macrophage. A major defect in IFN-γ-deficient mice that was not present in MIIG mice was the recruitment of mononuclear phagocytes to form a granuloma. Our data thus show that granuloma organization with the recruitment of macrophages is associated with resistance. This structuring of the granuloma does not require macrophages activated by IFN-γ but is dependent on the production of this cytokine. Which other cells may be responding to IFN-γ to mediate recruitment of leukocytes, in particular monocytes into the nascent granuloma was not yet identified. Lymphocytes, on the other hand, were able to establish small foci in the absence of IFN-γ production implying that their recruitment is regulated in a distinct fashion to that of mononuclear phagocytes. The increased lymphocyte recruitment

occurring in the absence of IFN-γ and in the MIIG genotype also takes place in iNOS gene-disrupted mice (24, 25). Indeed, IFN-γ-mediated macrophage activation has been shown to impact on the survival and function of T cells within the granuloma namely through the induction of iNOS and massive NO secretion (24, 26). We observed a dramatic increase in the accumulation of $CD4^+$ T cells in the granulomas of MIIG mice as compared to C57BL/6 animals. $CD4^+$ T cells in MIIG mice were also better able to produce cytokines such as IFN-γ and TNF-α the latter being almost absent in T cells from C57BL/6 mice. Moreover macrophages from MIIG mice also exhibit increased *Tnfa* gene expression which together with the high amounts of TNF-α^+CD4^+T cells suggests that this cytokine might play a protective role that otherwise is not observable in the infection of C57BL/6 mice where the TNF-α expression is basal. Indeed the increased production of TNF was shown to underlie the resistance in MIIG mice. Our data show that in the absence of IFN-γ-macrophage signaling, TNF-α expression is particularly required for the control of *M. avium* growth, which suggests TNF-α production as a compensatory mechanism in MIIG infected mice. TNF-α has a well-known protective role during mycobacterial infections. It enhances mycobacterial killing exhibiting a synergistic effect with IFN-γ (7, 27), and it has a pivotal role in regulating leukocyte recruitment and inflammation. Therefore TNF production is required both for the assembly and for the maintenance of the granuloma structure (12, 28, 29). Although in the absence of TNF-α or its receptor mice succumb to infection, in *M. avium* infection this death is not associated with increased bacterial numbers but is consistent with the disintegration of the granuloma structure (19, 30). The basis of TNF-α-induced mycobacterial growth control *in vivo*, and the causes underlying its capacity to maintain the granulomata are not clear. TNF-α is directly involved in iron and in oxidative metabolism (17, 18) and both pathways have a direct role in bacterial proliferation control. Our data show that TNF-α is an effective ROS inducer and promotes iron storage within the cell, suggesting that the compensatory effects of TNF-α in the absence of IFN-γ-macrophage signaling might be mediated by these two TNF–induced pathways. Moreover both pathways are interconnected as iron can contributes to the formation of more toxic ROS through the Fenton reaction (17).

Our results revealed that iron accumulates extensively in the macrophages within the granuloma from the MIIG mice, where TNF-α is extensively produced. No detectable accumulation of iron was observed in TNF-α gene-disrupted mice while in the C57BL/6 animals, where the levels of TNF are rather low, iron accumulation was scarce. TNF is a known inducer of the ferritin H gene, which encodes for the heavy chain of ferritin, the main iron storage protein of

the cell (31, 32). However, despite the elevated levels of TNF-α in the MIIG animals, iron accumulation within granuloma macrophages was not correlated with increased Ferritin H expression. *M. avium* can use iron from its host to proliferate (33), thus it seems peculiar that MIIG animals are able to control bacterial growth despite the elevated iron content. For such event to occur we reason that the vast majority of iron needs to be stored in iron storage proteins, being unavailable to the bacteria residing in the phagolysosome. Ferritin is capable of storing up to 4500 atoms of ferric iron (34) hence we hypothesize that despite the lack of increased ferritin levels, the high iron content in MIIG infected livers may be explained by differences in the number of iron atoms stored within this protein complex. Ferritin is composed by subunits of heavy (H) and light (L) chains. The H chain subunit is involved in the oxidation of Fe^{2+} to Fe^{3+}, the non-toxic iron form, whereas the L chain is devoid of catalytic activity (35). Although the H:L ratio is usually constant within a cell, it has been described that in chronic iron overload situations an increase in the L subunits mRNA occurs (36). In our work we only assessed the expression of the Ferritin H chain, hence we cannot exclude a possible increase in the L chain expression in MIIG infected animals.

In contrast to mycobacterial species, which are known to be susceptible to host's iron deprivation, the growth of other pathogens such as *Brucella abortus* and some *Leishmania spp* are decreased by host's iron overload. In both cases, pathogen proliferation control is associated to oxidative burst (37-39). In *M. avium* infected MIIG mice, ROS production was also augmented and its expression was associated with increased TNF-α production. The main sources of cellular ROS are mitochondria and NADPH oxidases (NOXs) (40, 41). TNF-α expression have been implicated in both: TNF-α was shown to induce phosphorylation of p47phox, a subunit of the NOX2 family (42); while in a *M. marinum*-infected zebrafish model it was shown that TNF excess induces mitochondrial ROS (43). Here we observed that MIIG macrophages, specifically the $Ly6C^{int}$ and $Ly6C^{low}$ subsets, produce increased amounts of ROS, particularly superoxide, upon infection. These macrophage subsets exhibit increased expression of genes encoding for $p47^{phox}$ and $gp91^{phox}$, suggesting that NOX2 is associated with the increased respiratory burst in MIIG infected mice. Nevertheless the additional involvement of mitochondrial ROS cannot be excluded. Supporting the role for TNF-α as a ROS inducer after *M. avium* infection, is the fact that: (1) the high TNF producer strain (MIIG) exhibit the highest levels of ROS; (2) TNF-$\alpha^{-/-}$ animals produce slightly lower ROS than the C57BL/6 which expresses very low levels of TNF-α. Importantly in MIIG.TNF-$\alpha^{-/-}$ infected mice, ROS production was diminished. Taken together our data suggest

that while both IFN-γ and TNF-α are ROS inducers and have synergistic effects, TNF-α plays a major role in macrophage respiratory burst. Notably we observe that mice with impaired respiratory burst (MIIG.TNF-$\alpha^{-/-}$) were not able to control *M. avium* growth. This result suggests a protective role for TNF-α-induced ROS production evidenced in the absence of IFN-γ-mediated macrophage activation. Indeed TNF-α-induced ROS production has been shown to be able to control *M. avium* proliferation in in vitro models (16) but not in vivo. Given the low levels of TNF-α production in mouse wild type strains such as C57BL/6, we speculate that in such cases the ability of macrophages to trigger the respiratory burst is minimal, and therefore it has been difficult to associate ROS production to the control of *M. avium* growth in vivo.

One other aspect of *M. avium* infected MIIG animals is the undetectable induction of NO production, which may also contribute to the increased iron and ROS content observed here. It is known that iNOS derived nitric reactive species have a direct impact on cell iron content. NO can activate the transcription factor nuclear factor erythroid 2-related factor 2 (Nrf2) which induces the expression of ferroportin-1 a major cellular iron exporter, hence reducing iron intracellular content. In a *Salmonella* infection mouse model, Nairz and colleagues have shown that iNOS deficiency results in macrophagic iron overload due to a defect in the Nrf2-induced ferroportin-1 expression (44). Given the lack of IFN-γ signaling, macrophages from MIIG animals are also deficient in iNOS expression, which can explain the iron overload in these cells, most probably due to a defect on Nfr2. Additionally, Nrf2 induces the transcription of the anti-oxidant-responsive element (ARE) gene (45), being essential for the multiple antioxidant defense systems of the cell. In fact the loss of Nfr2 increases several types of cellular ROS (46, 47). Overall this plausible defect in NO-induced Nfr2 expression in MIIG mice together with the excess of TNF-α might underlie the increased iron and ROS content observed in *M. avium* infected MIIG mice. Despite the lack of NO production, infected MIIG.TNF-$\alpha^{-/-}$ double mutants do not showed any detectable iron accumulation, also observable in the TNF-$\alpha^{-/-}$ mice. This phenotype is most probably due to a direct effect of the lack of TNF-α, known to be required for the *Fth* mRNA expression.

Our data clearly show that in the absence of IFN-γ-mediated macrophage activation, TNF-α emerges as a key player in the control of bacterial replication. However how these cytokines impact the different subpopulations of macrophages in a *M. avium* infection context is not known. We observed that neither TNF-α nor IFN-γ impacts the ability of Ly6C^{high} monocytes/macrophages to produce ROS. The Ly6C^{high} monocyte subset is known to be rapidly

recruited from the bone marrow to the inflamed tissues, where they end up differentiating into inflammatory macrophages (48). Although these cells are characterized by a proinflammatory phenotype, as we observed in chronically *M. avium* infected C57BL/6 mice, in MIIG mice the excess of TNF-α only impacted the Ly6C intermediate and low macrophage subsets with a clear increase of ROS production. Monocytes/Macrophages lacking Ly6C are described as an intravascular population with a main function of patrolling the endothelium (48, 49). Although still a matter of debate, increasing evidence suggest that Ly6C^{high} monocytes can differentiate into Ly6C^{low} monocytes (50-53). In a murine liver fibrosis model, Ramachandran and colleagues characterized a Ly6C^{high}-derived Ly6C^{low} macrophage population with a restorative phenotype and increased expression of matrix metalloproteinases, such as MMP-9 (54). This particular metalloproteinase is known to be induced during mycobacterial infections and required for macrophage recruitment and tissue remodeling contributing to tight and well-organized granuloma structures (55). It is also reported that in vitro addition of exogenous TNF-α induces MMP-9 production in macrophages whereas neutralizing this cytokine inhibits BCG-induced MMP9 production (56). Given the well-structured MIIG granulomata with a significant core of macrophages, we wonder whether MMP-9 might play a role in its development. Finally whether the increased numbers of Ly6C^{low} macrophages in MIIG infected animals arise from the Ly6C^{high} population remains an open question. Our data suggests that the pro-inflammatory phenotype observed in the Ly6C^{low} macrophages from *M. avium*-infected MIIG mice might be of the utmost relevance to the host immune response, and that TNF-α plays a major role in inducing this particular phenotype on Ly6C^{low} macrophages.

In summary, the genetic MIIG model used here allowed us to clarify the specific role that IFN-γ exerts over the macrophage. Upon *M. avium* infection we found a particular phenotype in MIIG animals that could not be seen in the genetic-disrupted IFN-γ mice due to the lack of signaling cells other than the macrophage. Hence in the absence of IFN-γ-mediated macrophage activation, mice are still able to control *M. avium* growth and to develop well-structured granulomata. Our results show that TNF-α increased production is the main mechanism responsible for this protection, which also correlates with an increase of ROS production and iron accumulation in macrophages. Nevertheless we cannot exclude the potential role that the excess of IFN-γ on MIIG infected mice might play on cells other than macrophages, particularly on its impact in the granuloma development. Overall this work shows an unequivocal role for TNF-α in the control of mycobacterial growth in the absence of IFN-γ-macrophage mediated activation.

References

1. Nathan, C. F., H. W. Murray, M. E. Wiebe, and B. Y. Rubin. 1983. Identification of interferon-gamma as the lymphokine that activates human macrophage oxidative metabolism and antimicrobial activity. *The Journal of experimental medicine* 158: 670-689.
2. Schreiber, R. D., J. L. Pace, S. W. Russell, A. Altman, and D. H. Katz. 1983. Macrophage-activating factor produced by a T cell hybridoma: physiochemical and biosynthetic resemblance to gamma-interferon. *Journal of immunology* 131: 826-832.
3. Casanova, J. L., and L. Abel. 2002. Genetic dissection of immunity to mycobacteria: the human model. *Annual review of immunology* 20: 581-620.
4. Schroder, K., P. J. Hertzog, T. Ravasi, and D. A. Hume. 2004. Interferon-gamma: an overview of signals, mechanisms and functions. *Journal of leukocyte biology* 75: 163-189.
5. MacMicking, J. D. 2012. Interferon-inducible effector mechanisms in cell-autonomous immunity. *Nature reviews. Immunology* 12: 367-382.
6. Appelberg, R., and I. M. Orme. 1993. Effector mechanisms involved in cytokine-mediated bacteriostasis of Mycobacterium avium infections in murine macrophages. *Immunology* 80: 352-359.
7. Appelberg, R., A. G. Castro, J. Pedrosa, R. A. Silva, I. M. Orme, and P. Minoprio. 1994. Role of gamma interferon and tumor necrosis factor alpha during T-cell-independent and -dependent phases of Mycobacterium avium infection. *Infection and immunity* 62: 3962-3971.
8. Florido, M., A. S. Goncalves, R. A. Silva, S. Ehlers, A. M. Cooper, and R. Appelberg. 1999. Resistance of virulent Mycobacterium avium to gamma interferon-mediated antimicrobial activity suggests additional signals for induction of mycobacteriostasis. *Infection and immunity* 67: 3610-3618.
9. Ehlers, S., and U. E. Schaible. 2012. The granuloma in tuberculosis: dynamics of a host-pathogen collusion. *Frontiers in immunology* 3: 411.
10. Lykens, J. E., C. E. Terrell, E. E. Zoller, S. Divanovic, A. Trompette, C. L. Karp, J. Aliberti, M. J. Flick, and M. B. Jordan. 2010. Mice with a selective impairment of IFN-gamma signaling in macrophage lineage cells demonstrate the critical role of IFN-gamma-

activated macrophages for the control of protozoan parasitic infections in vivo. *Journal of immunology* 184: 877-885.

11. Resende, M., M. S. Cardoso, A. R. Ribeiro, M. Florido, M. Borges, A. G. Castro, N. L. Alves, A. M. Cooper, and R. Appelberg. 2017. Innate IFN-gamma-Producing Cells Developing in the Absence of IL-2 Receptor Common gamma-Chain. *Journal of immunology* 199: 1429-1439.
12. Smith, D., H. Hansch, G. Bancroft, and S. Ehlers. 1997. T-cell-independent granuloma formation in response to Mycobacterium avium: role of tumour necrosis factor-alpha and interferon-gamma. *Immunology* 92: 413-421.
13. Appelberg, R., D. Moreira, P. Barreira-Silva, M. Borges, L. Silva, R. J. Dinis-Oliveira, M. Resende, M. Correia-Neves, M. B. Jordan, N. C. Ferreira, A. J. Abrunhosa, and R. Silvestre. 2015. The Warburg effect in mycobacterial granulomas is dependent on the recruitment and activation of macrophages by interferon-gamma. *Immunology* 145: 498-507.
14. Nathan, C., and Q. W. Xie. 1994. Regulation of biosynthesis of nitric oxide. *The Journal of biological chemistry* 269: 13725-13728.
15. Auffray, C., M. H. Sieweke, and F. Geissmann. 2009. Blood monocytes: development, heterogeneity, and relationship with dendritic cells. *Annual review of immunology* 27: 669-692.
16. Sarmento, A., and R. Appelberg. 1996. Involvement of reactive oxygen intermediates in tumor necrosis factor alpha-dependent bacteriostasis of Mycobacterium avium. *Infection and immunity* 64: 3224-3230.
17. Cassat, J. E., and E. P. Skaar. 2013. Iron in infection and immunity. *Cell host & microbe* 13: 509-519.
18. Brandes, R. P., N. Weissmann, and K. Schroder. 2014. Nox family NADPH oxidases: Molecular mechanisms of activation. *Free radical biology & medicine* 76: 208-226.
19. Florido, M., and R. Appelberg. 2007. Characterization of the deregulated immune activation occurring at late stages of mycobacterial infection in TNF-deficient mice. *Journal of immunology* 179: 7702-7708.
20. Cooper, A. M., D. K. Dalton, T. A. Stewart, J. P. Griffin, D. G. Russell, and I. M. Orme. 1993. Disseminated tuberculosis in interferon gamma gene-disrupted mice. *The Journal of experimental medicine* 178: 2243-2247.

21. Flynn, J. L., J. Chan, K. J. Triebold, D. K. Dalton, T. A. Stewart, and B. R. Bloom. 1993. An essential role for interferon gamma in resistance to Mycobacterium tuberculosis infection. *The Journal of experimental medicine* 178: 2249-2254.

22. Pearl, J. E., B. Saunders, S. Ehlers, I. M. Orme, and A. M. Cooper. 2001. Inflammation and lymphocyte activation during mycobacterial infection in the interferon-gamma-deficient mouse. *Cellular immunology* 211: 43-50.

23. Murray, P. J., R. A. Young, and G. Q. Daley. 1998. Hematopoietic remodeling in interferon-gamma-deficient mice infected with mycobacteria. *Blood* 91: 2914-2924.

24. Gomes, M. S., M. Florido, T. F. Pais, and R. Appelberg. 1999. Improved clearance of Mycobacterium avium upon disruption of the inducible nitric oxide synthase gene. *Journal of immunology* 162: 6734-6739.

25. Lousada, S., M. Florido, and R. Appelberg. 2006. Regulation of granuloma fibrosis by nitric oxide during Mycobacterium avium experimental infection. *International journal of experimental pathology* 87: 307-315.

26. Ehlers, S., S. Kutsch, J. Benini, A. Cooper, C. Hahn, J. Gerdes, I. Orme, C. Martin, and E. T. Rietschel. 1999. NOS2-derived nitric oxide regulates the size, quantity and quality of granuloma formation in Mycobacterium avium-infected mice without affecting bacterial loads. *Immunology* 98: 313-323.

27. Bekker, L. G., S. Freeman, P. J. Murray, B. Ryffel, and G. Kaplan. 2001. TNF-alpha controls intracellular mycobacterial growth by both inducible nitric oxide synthase-dependent and inducible nitric oxide synthase-independent pathways. *Journal of immunology* 166: 6728-6734.

28. Flynn, J. L., M. M. Goldstein, J. Chan, K. J. Triebold, K. Pfeffer, C. J. Lowenstein, R. Schreiber, T. W. Mak, and B. R. Bloom. 1995. Tumor necrosis factor-alpha is required in the protective immune response against Mycobacterium tuberculosis in mice. *Immunity* 2: 561-572.

29. Ehlers, S., S. Kutsch, E. M. Ehlers, J. Benini, and K. Pfeffer. 2000. Lethal granuloma disintegration in mycobacteria-infected TNF-Rp55-/- mice is dependent on T cells and IL-12. *Journal of immunology* 165: 483-492.

30. Ehlers, S., J. Benini, S. Kutsch, R. Endres, E. T. Rietschel, and K. Pfeffer. 1999. Fatal granuloma necrosis without exacerbated mycobacterial growth in tumor necrosis factor

receptor p55 gene-deficient mice intravenously infected with Mycobacterium avium. *Infection and immunity* 67: 3571-3579.

31. Torti, S. V., E. L. Kwak, S. C. Miller, L. L. Miller, G. M. Ringold, K. B. Myambo, A. P. Young, and F. M. Torti. 1988. The molecular cloning and characterization of murine ferritin heavy chain, a tumor necrosis factor-inducible gene. *The Journal of biological chemistry* 263: 12638-12644.
32. Miller, L. L., S. C. Miller, S. V. Torti, Y. Tsuji, and F. M. Torti. 1991. Iron-independent induction of ferritin H chain by tumor necrosis factor. *Proceedings of the National Academy of Sciences of the United States of America* 88: 4946-4950.
33. Dhople, A. M., M. A. Ibanez, and T. C. Poirier. 1996. Role of iron in the pathogenesis of Mycobacterium avium infection in mice. *Microbios* 87: 77-87.
34. Theil, E. C. 1987. Ferritin: structure, gene regulation, and cellular function in animals, plants, and microorganisms. *Annual review of biochemistry* 56: 289-315.
35. Sammarco, M. C., S. Ditch, A. Banerjee, and E. Grabczyk. 2008. Ferritin L and H subunits are differentially regulated on a post-transcriptional level. *The Journal of biological chemistry* 283: 4578-4587.
36. Leggett, B. A., L. M. Fletcher, G. A. Ramm, L. W. Powell, and J. W. Halliday. 1993. Differential regulation of ferritin H and L subunit mRNA during inflammation and long-term iron overload. *Journal of gastroenterology and hepatology* 8: 21-27.
37. Jiang, X., and C. L. Baldwin. 1993. Iron augments macrophage-mediated killing of Brucella abortus alone and in conjunction with interferon-gamma. *Cellular immunology* 148: 397-407.
38. Bisti, S., G. Konidou, J. Boelaert, M. Lebastard, and K. Soteriadou. 2006. The prevention of the growth of Leishmania major progeny in BALB/c iron-loaded mice: a process coupled to increased oxidative burst, the amplitude and duration of which depend on initial parasite developmental stage and dose. *Microbes and infection / Institut Pasteur* 8: 1464-1472.
39. Vale-Costa, S., S. Gomes-Pereira, C. M. Teixeira, G. Rosa, P. N. Rodrigues, A. Tomas, R. Appelberg, and M. S. Gomes. 2013. Iron overload favors the elimination of Leishmania infantum from mouse tissues through interaction with reactive oxygen and nitrogen species. *PLoS neglected tropical diseases* 7: e2061.

40. Holmstrom, K. M., and T. Finkel. 2014. Cellular mechanisms and physiological consequences of redox-dependent signalling. *Nature reviews. Molecular cell biology* 15: 411-421.

41. Dan Dunn, J., L. A. Alvarez, X. Zhang, and T. Soldati. 2015. Reactive oxygen species and mitochondria: A nexus of cellular homeostasis. *Redox biology* 6: 472-485.

42. Dewas, C., P. M. Dang, M. A. Gougerot-Pocidalo, and J. El-Benna. 2003. TNF-alpha induces phosphorylation of p47(phox) in human neutrophils: partial phosphorylation of p47phox is a common event of priming of human neutrophils by TNF-alpha and granulocyte-macrophage colony-stimulating factor. *Journal of immunology* 171: 4392-4398.

43. Roca, F. J., and L. Ramakrishnan. 2013. TNF dually mediates resistance and susceptibility to mycobacteria via mitochondrial reactive oxygen species. *Cell* 153: 521-534.

44. Nairz, M., U. Schleicher, A. Schroll, T. Sonnweber, I. Theurl, S. Ludwiczek, H. Talasz, G. Brandacher, P. L. Moser, M. U. Muckenthaler, F. C. Fang, C. Bogdan, and G. Weiss. 2013. Nitric oxide-mediated regulation of ferroportin-1 controls macrophage iron homeostasis and immune function in Salmonella infection. *The Journal of experimental medicine* 210: 855-873.

45. Itoh, K., T. Chiba, S. Takahashi, T. Ishii, K. Igarashi, Y. Katoh, T. Oyake, N. Hayashi, K. Satoh, I. Hatayama, M. Yamamoto, and Y. Nabeshima. 1997. An Nrf2/small Maf heterodimer mediates the induction of phase II detoxifying enzyme genes through antioxidant response elements. *Biochemical and biophysical research communications* 236: 313-322.

46. Harada, N., M. Kanayama, A. Maruyama, A. Yoshida, K. Tazumi, T. Hosoya, J. Mimura, T. Toki, J. M. Maher, M. Yamamoto, and K. Itoh. 2011. Nrf2 regulates ferroportin 1-mediated iron efflux and counteracts lipopolysaccharide-induced ferroportin 1 mRNA suppression in macrophages. *Archives of biochemistry and biophysics* 508: 101-109.

47. Schieber, M., and N. S. Chandel. 2014. ROS function in redox signaling and oxidative stress. *Current biology : CB* 24: R453-462.

48. Auffray, C., D. Fogg, M. Garfa, G. Elain, O. Join-Lambert, S. Kayal, S. Sarnacki, A. Cumano, G. Lauvau, and F. Geissmann. 2007. Monitoring of blood vessels and tissues by a population of monocytes with patrolling behavior. *Science* 317: 666-670.

49. Hanna, R. N., L. M. Carlin, H. G. Hubbeling, D. Nackiewicz, A. M. Green, J. A. Punt, F. Geissmann, and C. C. Hedrick. 2011. The transcription factor NR4A1 (Nur77) controls bone marrow differentiation and the survival of Ly6C- monocytes. *Nature immunology* 12: 778-785.

50. Yona, S., K. W. Kim, Y. Wolf, A. Mildner, D. Varol, M. Breker, D. Strauss-Ayali, S. Viukov, M. Guilliams, A. Misharin, D. A. Hume, H. Perlman, B. Malissen, E. Zelzer, and S. Jung. 2013. Fate mapping reveals origins and dynamics of monocytes and tissue macrophages under homeostasis. *Immunity* 38: 79-91.

51. Dal-Secco, D., J. Wang, Z. Zeng, E. Kolaczkowska, C. H. Wong, B. Petri, R. M. Ransohoff, I. F. Charo, C. N. Jenne, and P. Kubes. 2015. A dynamic spectrum of monocytes arising from the in situ reprogramming of CCR2+ monocytes at a site of sterile injury. *The Journal of experimental medicine* 212: 447-456.

52. Mildner, A., J. Schonheit, A. Giladi, E. David, D. Lara-Astiaso, E. Lorenzo-Vivas, F. Paul, L. Chappell-Maor, J. Priller, A. Leutz, I. Amit, and S. Jung. 2017. Genomic Characterization of Murine Monocytes Reveals C/EBPbeta Transcription Factor Dependence of Ly6C(-) Cells. *Immunity* 46: 849-862 e847.

53. Lessard, A. J., M. LeBel, B. Egarnes, P. Prefontaine, P. Theriault, A. Droit, A. Brunet, S. Rivest, and J. Gosselin. 2017. Triggering of NOD2 Receptor Converts Inflammatory Ly6C(high) into Ly6C(low) Monocytes with Patrolling Properties. *Cell reports* 20: 1830-1843.

54. Ramachandran, P., A. Pellicoro, M. A. Vernon, L. Boulter, R. L. Aucott, A. Ali, S. N. Hartland, V. K. Snowdon, A. Cappon, T. T. Gordon-Walker, M. J. Williams, D. R. Dunbar, J. R. Manning, N. van Rooijen, J. A. Fallowfield, S. J. Forbes, and J. P. Iredale. 2012. Differential Ly-6C expression identifies the recruited macrophage phenotype, which orchestrates the regression of murine liver fibrosis. *Proceedings of the National Academy of Sciences of the United States of America* 109: E3186-3195.

55. Taylor, J. L., J. M. Hattle, S. A. Dreitz, J. M. Troudt, L. S. Izzo, R. J. Basaraba, I. M. Orme, L. M. Matrisian, and A. A. Izzo. 2006. Role for matrix metalloproteinase 9 in granuloma formation during pulmonary Mycobacterium tuberculosis infection. *Infection and immunity* 74: 6135-6144.

56. Quiding-Jarbrink, M., D. A. Smith, and G. J. Bancroft. 2001. Production of matrix metalloproteinases in response to mycobacterial infection. *Infection and immunity* 69: 5661-5670.

Chapter IV

HIF-1α ACTIVITY IN THE MYELOID COMPARTMENT REGULATES PULMONARY INFLAMMATION AND SUSCEPTIBILITY TO *MYCOBACTERIUM TUBERCULOSIS* INFECTION

Submitted

HIF-1α activity in the myeloid compartment regulates pulmonary inflammation and susceptibility to *Mycobacterium tuberculosis* infection

Mariana Resende,[*, †, ‡, §,1] Catarina M. Ferreira,[*, †,1] Ana Margarida Barbosa,[*, †] Marcos S. Cardoso,[‡, §] Jeremy Sousa,[‡, §] Ricardo Silvestre,[*, †] António G. Castro,[*, †] Rui Appelberg,[‡, §] and Egídio Torrado,[*, †, ¶]

[*]Life and Health Sciences Research Institute (ICVS), School of Medicine, University of Minho, Braga, Portugal.

[†]ICVS/3B's - PT Government Associate Laboratory, Braga/Guimarães, Portugal.

[‡]i3S - Instituto de Investigação e Inovação em Saúde, Universidade do Porto, Portugal.

[§]IBMC – Instituto de Biologia Molecular e Celular, Universidade do Porto, Porto, Portugal.

[1]Contributed equally

[¶]Corresponding author

Abstract

The transcription factor hypoxia inducible factor -1 alpha (HIF-1α) has emerged as an important regulator of myeloid cell response and function in hypoxic and inflammatory microenvironments. As such, HIF-1α plays critical roles in regulating the immune response and control of multiple infections. In this regard, recent data has shown that mice deficient in HIF-1α in the myeloid compartment (mHIF-1α$^{-/-}$) are acutely susceptible to a high dose aerosol *Mycobacterium tuberculosis* (Mtb) infection. As severe phenotypes such as this underlie the deregulation of immune pathways essential to control tuberculosis (TB), it is critical to define the mechanisms by which HIF-1α coordinates immunity to TB.

In this work, we analyzed the progression of Mtb infection in mHIF-1α$^{-/-}$ mice upon high and low dose aerosol Mtb challenge. Our data show that mHIF-1α$^{-/-}$ are indeed more susceptible to Mtb infection, with reduced survival and increased lung bacterial burdens, but only at late stages of infection and upon high dose aerosol infection. The enhanced susceptibility of mHIF-1α$^{-/-}$ mice was associated with enhanced pulmonary inflammation, but not with defective T cell activation or expression of type 1 immunity. Instead, we found that deficiency in myeloid HIF-1α activity

prompts a microenvironment that sustains chronic Th17 responses, with important immunopathological consequences to the host.

These data support the hypothesis that HIF-1α activity coordinates the response of myeloid cells during TB to prevent excessive leukocyte recruitment and immunopathological consequences to the host.

Introduction

Tuberculosis (TB), caused by *Mycobacterium tuberculosis* (Mtb), is still a world health problem and a priority for infectious disease research. In 2016 alone, an estimated 10.4 million people fell ill with TB and over 1.5 million died of the disease, placing TB as the ninth leading cause of death worldwide (1). To meet the WHO goals of ending the global epidemic of TB by 2035, additional tools to improve diagnosis, drug therapy, and new vaccine strategies need to become available so that TB incidence can fall faster (2). However, to succeed in these fronts it is critical that we identify the constituents of protective immunity to TB and the mechanisms that determine protection or pathogenesis upon Mtb infection.

One of the most distinctive pathological hallmarks of the host response to Mtb infection is the development of granulomas (3). Although these histological structures play critical roles in controlling infection, in humans and some animal models, some granulomas suffer extensive remodeling and undergo central necrosis (caseous necrosis), a critical process for the pathogenesis and dissemination of Mtb infection (3). Recent data show that, unlike solid granulomas, necrotic granulomas are hypoxic (4-6) and that hypoxia induces the upregulation of host matrix metalloproteinases resulting in extensive lung destruction (6). As such, necrotic granulomas are associated with more severe forms of TB disease, as they compromise lung integrity and facilitate bacterial spread (6). Therefore, recent efforts have gone into further understanding the role of hypoxia and its pathological consequences to the host during TB.

Hypoxia-inducible factor (HIF)-1 is an heterodimeric transcription factor consisting of an oxygen-labile alpha subunit (HIF-1α) and a constitutively stable beta subunit (HIF-1β), that play a crucial role in the adaptation of immune cells to hypoxia (7, 8). Indeed, under hypoxic microenvironments HIF-1α is stabilized and dimerizes with HIF-1β to form a complex capable of binding to the DNA activating multiple target genes (7). This event results in the expression of hypoxia-inducible proteins, which include the vascular endothelial growth factor (9), erythropoietin (10), and glycolytic enzymes and glucose transporters (11, 12). As such, HIF-1α stabilization

promotes the metabolic shift of immune cells to aerobic glycolysis, and therefore their adaptation to hypoxic microenvironments (13). However, it is now recognized that inflammatory stimuli can also induce HIF-1α stabilization independently of hypoxia. Specifically, the inflammatory cytokines TNF and IL-1β promote HIF-1α accumulation through an NF-kB-dependent mechanism (14-16). Bacteria and bacterial components, such as LPS, can also induce HIF-1α under normoxic conditions through different mechanisms (17-20). Therefore, HIF-1α plays critical roles during infectious and inflammatory diseases by regulating the adaptation of immune cells to hypoxic and inflammatory microenvironments (7).

A growing body of evidence now suggests that HIF-1α is a central coordinator of the effector response of both myeloid and lymphoid cells. Specifically in myeloid cells, HIF-1α has been shown to be essential in the recruitment and production of inflammatory mediators (21, 22). In lymphoid cells, this transcription factor prompts the differentiation of Th17 cells (23), the expression of cytolytic molecules by $CD8^+$ T cells (24) and the production of IL-10 by B cells (25). As such, HIF-1α plays essential roles in the control of multiple infections, including those caused by Group A *Streptococcus* (22), *Pseudomonas aeruginosa* (26), *Escherichia coli* (27), and mycobacteria (28-30). Specifically to mycobacteria, a recent report using a mouse model of *Mycobacterium avium* infection that develops granuloma necrosis has shown that HIF-1α activity plays a central role in preventing the earlier emergence of granuloma necrosis (30). While this same mouse model does not develop necrotic granulomas upon aerosol Mtb infection, a recent study has suggested a central role of HIF-1α in coordinating the activation of macrophages by IFN-γ (29). Indeed, the transcriptional response of Mtb-infected macrophages to IFN-γ was partially dependent on HIF-1α, and mice deficient in this transcription factor in the myeloid compartment (mHIF-$1\alpha^{-/-}$) were acutely susceptible to high-dose Mtb infection (29). The enhanced susceptibility of mHIF-$1\alpha^{-/-}$ mice to Mtb infection was associated with a reduced production of nitric oxide (29), product of the reaction catalyzed by inducible Nitric Oxide Synthase (iNOS, coded by *Nos2*), a key effector molecule of the macrophage antimycobacterial response (28, 29). These data are interesting because mHIF-$1\alpha^{-/-}$ mice were acutely susceptible to Mtb infection, despite displaying only a reduced expression of iNOS (29). Notably, in addition to the direct bactericidal activity of nitric oxide, this molecule also regulates the inflammatory response via nitrosilation of NLRP3 (31) or inhibition of NF-kB (28). As such, the role of HIF-1α during TB may be not only in coordinating the response of infected macrophages to IFN-γ, but also in regulating the pulmonary inflammatory response.

Acute susceptibility to Mtb infection is generally associated with the deregulation of critical immune pathways such as the IL-12/IFNγ-axis, TNF or MyD88/IL-1β deficiency (32). Previous data showing that mHIF-1α$^{-/-}$ mice were acutely susceptible to Mtb infection (29) suggest a key role for HIF-1α in orchestrating protective immune responses to TB. These data warrants further investigation on the role of HIF-1α in TB. Therefore, in this work we sought to determine if the acute susceptibility of mHIF-1α$^{-/-}$ mice to TB was associated with the dose of infection or a consequence of unregulated pulmonary inflammation. To do this, we challenged mHIF-1α$^{-/-}$ mice with a high or low dose of Mtb through the aerosol route and followed the progression of infection. We found that HIF-1α activity in the myeloid compartment is required for long-term containment of Mtb infection. Indeed, mHIF-1α$^{-/-}$ mice displayed increased lung bacterial burdens, but only upon high dose infection and at late stages of infection. Despite this, mHIF-1α$^{-/-}$ did not have deficient type 1 immunity, but had increased pulmonary inflammation and chronic Th17 responses.

These data show that HIF-1α activity coordinates the response of myeloid cells during TB to prevent the influx of leukocytes and restraint inflammatory responses that have important immunopathological consequences to the host.

Materials and Methods

Mice

Mice deficient in HIF-1α in the myeloid compartment (Hif1a$^{fl/fl}$-LysMcre$^{+/+}$, hereafter referred to as mHIF-1α$^{-/-}$) were obtained by crossing single transgenic mice originally obtained from the Jackson Laboratory (Bar Harbor). C57BL/6 (B6) mice were originally from Charles River Laboratory (Barcelona, Spain). All mice used in this study were bred and maintained at the ICVS animal facility. Experimental animals were age and sex matched and used between the ages of 8 and 12 weeks.

All procedures involving live animals were carried out in accordance with the European Directive 86/609/EEC, approved by the *Subcomissão de Ética para as Ciências da Vida e da Saúde* (SECVS 074/2016) and the Portuguese National Authority *Direcção Geral de Veterinária*.

Mtb aerosol infections and bacterial load determination

The Mtb strain H37Rv (originally from the Trudeau Institute) was grown in Proskauer Beck medium containing 0.05% Tween 80 to the mid-log phase and frozen at -80°C until used. For aerosol infections, subject animals were exposed to Mtb using a Glas-Col airborne infection system, as previously described (33). The data presented in this work are a composite of two independent experiments wherein a low dose setting (which delivered 75±5.77 CFU in experiment 1 and 80±16.33 CFU in experiment 2) and high dose setting (which delivered 512±30.95 CFU in experiment 1 and 528±4.03 in experiment 2), were used.

At 60 and 120 days post-infection, infected mice were killed by CO_2 asphyxiation and target organs were aseptically excised and individually homogenized in PBS. The organ homogenates were serially diluted in PBS and plated onto Middlebrook 7H11 agar (BD Biosciences). CFU were counted after 3 weeks of incubation at 37°C.

Lymphocyte isolation for flow cytometry

Aseptically excised lungs were sectioned with two sterile scalpels and incubated at 37°C for 30 min with collagenase D (0.7mg/mL, Sigma). The reaction was stopped with 10 ml of DMEM (Gibco), and the lungs were disrupted into a single cell suspension by passage through a 70-μm nylon cell strainer (BD Biosciences). After centrifugation, the cell-free suspensions were aliquoted and frozen at -80°C until the concentration of cytokines were determined using ELISA kits (Thermo Fisher Scientific), following the manufacturer's instructions. Lung single cell suspensions were treated with erythrocyte lysis buffer (0.87% of NH_4Cl) and processed over a 40:80% percoll (GE Healthcare) gradient. The resulting cell suspension was washed twice and counted.

For flow cytometry analysis, lung single cell suspensions were stained with fluorochrome-conjugated antibodies for 30 min on ice. For intracellular cytokine detection, cells were cultured in 5 μg/ml of ESAT-6_{1-20} peptide for 1.5 h before 10 μg/ml of Brefeldin A (Sigma) was added to the culture for 3.5 more h. After surface stained, cells were fixed with 2% paraformaldehyde for 20 min, permeabilized and stained for 30 min on ice. Antibodies specific for MHC-II (M5/114.15.2), Siglec-F (E50-2440), Ly6C (HK1.4), CD11b (M1/70), CD103 (E27), F4/80 (BM8), CD24 (M1/69), CD45 (30-F11), CD11c (N418), CD64 (X54-5/7.1), Ly6G (1A8), CD45 (30-F11), CD3 (145-2C11), CD44 (IM7), CD4 (GK1.5), IL-17 (TC11-18H10.1), IFN-γ (XMG1.2) and TNF-α (MP6-XT22) were from BD biosciences, Biolegend or eBioscience. Samples were acquired on a LSRII flow cytometer (BD Biosciences) with Diva Software. Data were analyzed

using FlowJo software (TreeStar). The total number of cells for each population was determined based on the percentage of cells determined by flow cytometry and the total number of cells per lung.

Histology and immunohistochemistry

The apical lobe of each lung was inflated with 4% paraformaldehyde, embedded in paraffin, and sectioned in 2-3 μm thickness slices before stained with hematoxylin-eosin (H&E) or Zhiel-Neelsen.

For immunohistochemistry staining, tissue sections were deparaffinized with xylene and rehydrated in sequential steps from absolute ethanol to distilled water. Antigens were then retrieved using Antigen Retrieval Solution (DAKO) in a 96°C pre-warmed water bath for 30 min. Endogenous peroxidases were inhibited with 3% hydrogen peroxide in methanol for 10 min at RT. Samples were incubated overnight at 4°C with rabbit anti-mouse iNOS primary antibody (sc-650, Santa Cruz Biotechnology). Slides were then incubated with a biotinylated horse anti-rabbit secondary antibody (BA-1100, Vector Laboratories) for 1h at RT, followed by Horseradish peroxidase-conjugated streptavidin (S2438, Sigma) for 30 min. Slides were finally incubated with DAB (DAKO) for 10 min and counterstained with hematoxylin.

Images were captured using an Olympus BX61 microscope and recorded with a digital camera (DP70) using the cell^P software. Image analysis and stain density was performed using Fiji (ImageJ) software, as previously described (34, 35).

Real Time RT-PCR

Total RNA was extracted using triple TRIzol (Thermo Fisher Scientific) according to the manufacturer's instructions. cDNA was generated from 1 mg RNA using the GRS cDNA Synthesis Master Mix (Grisp) following the manufacturer's instructions. The resultant cDNA template was used to quantify the expression of target genes by real-time PCR (Bio-Rad CFX96 Real-Time System with C1000 Thermal Cycler), and normalized to Ubiquitin mRNA levels using the ΔCt method. Target gene mRNA expression was quantified using SYBR green (Thermo Scientific) and specific oligonucleotides (Invitrogen) for:

Arg1 (F: 5'-TTTTAGGGTTACGGCCGGTG-3';R: 5'-CCTCGAGGCTGTCCTTTTGA-3'),

Cxcl1 (F: 5'-AGCTTGAAGGTGTTGCCCTCAG-3'; R: 5´-AGCTTCAGGGTCAAGGCAAGC-3')

Cxcl2 (F: 5'-CCCAGACAGAAGTCATAGCCAC-3'; R: 5'-CTTCCGTTGAGGGACAGCAG-3'),

Cxcl9 (F: 5'-TGTGGAGTTCGAGGAACCCT-3'; R: 5'-AGTCCGGATCTAGGCAGGTT-3'),

Cxcl10 (F: 5'-TCATCCTGCTGGGTCTGAGT-3'; R: 5'-ATCGTGGCAATGATCTCAACAC-3');
Cxcl11 (F: 5'-CAGCTGCTCAAGGCTTCCTTA-3'; R: 5'-TCTCTGCCATTTTGACGGCT-3'),
Fizz1 (F: 5'-CCCTGCTGGGATGACTGCTA-3'; R: 5'-CAGTGGTCCAGTCAACGAGT-3'),
Il6 (F: ACACATGTTCTCTGGGAAATCGT; R: AAGTGCATCATCGTTGTTCATACA),
Il23a (F: CGTATCCAGTGTGAAGATGGTTGT; R: GCTCCCCTTTGAAGATGTCAGA),
Irgm1 (F: 5'-GCTCGAAGACCAGAAGCTGA-3'; R: 5'-GAGCAGCCTGATCCAGAGGA-3'),
Nos2 (F: 5'-CTGGGAGCGCTCTAGTGAAG-3'; R: 5'-CGATGCACAACTGGGTGAAC-3'),
Ubq (F: 5'-TGGCTATTAATTATTCGGTCTGCAT-3'; R: 5'-GCAAGRGGCTAGAGTGCAGAGTAA-3'),
Ym1 (F: 5'-GAAGCTCTCCAGAGCAATCCT-3'; R: 5'-GTAGGAAGATCCCAGCTGTACG-3').

Statistical analysis

Data sets represent the composite of a total of two independent experiments. In each experiment, at least four animals were used per experimental group. Statistical differences between experimental groups were determined using unpaired student's *t* test with a Welch correction. Inherently logarithmic data from bacterial growth was transformed for statistical analysis. Differences were considered significant for $p \leq 0.05$ and represented as *, $p \leq 0.05$; **, $p \leq 0.01$; ***, $p \leq 0.001$; and ****, $p \leq 0.0001$.

Results

mHIF-1α$^{-/-}$ mice are more susceptible to high dose aerosol Mtb infection

In previous studies, mice deficient in HIF-1α in the myeloid compartment (mHIF-1α$^{-/-}$) displayed acute susceptibility with increased bacterial burdens and reduced survival when infected through the aerosol route with a high dose of Mtb Erdman strain (29). Since acute susceptibility to TB occurs only in humans and mice under severe immunocompromising conditions, including TNF blockade, deficiency in MyD88 or IL-12/IFN-γ axis, we wanted to clarify the role of HIF-1α in TB and determine the mechanism underlying the acute susceptibility of mHIF-1α$^{-/-}$ mice.

We began by comparing the progression of Mtb infection between B6 WT and mHIF-1α$^{-/-}$ mice after high dose aerosol infection. We found that that mHIF-1α$^{-/-}$ mice are indeed more susceptible to Mtb infection (Fig. 1A). However, mHIF-1α$^{-/-}$ mice only began to show signs of illness and decreased survival after day 150 post-infection (Fig. 1A), which contrasts with the acute susceptibility previously reported (29). Therefore, to determine if the susceptibility of mHIF-1α$^{-/-}$

mice is dose-dependent, we decided to compare bacterial burdens in B6 and mHIF-1$\alpha^{-/-}$ mice after challenge with a high or low dose aerosol infection. We found similar bacterial burdens in both B6 and HIF-1α deficient mice at days 60 and 120 post-infection after low dose aerosol infection (Fig. 1B). After high dose infection, bacterial burdens were also similar in both groups at day 60 post infection (Fig. 1B). However, by day 120 post-infection mHIF-1$\alpha^{-/-}$ mice displayed a 0.88 $\log_{10}$ increase in bacterial burdens in the lung, whereas no differences were found in the spleen and liver (Fig. 1B).

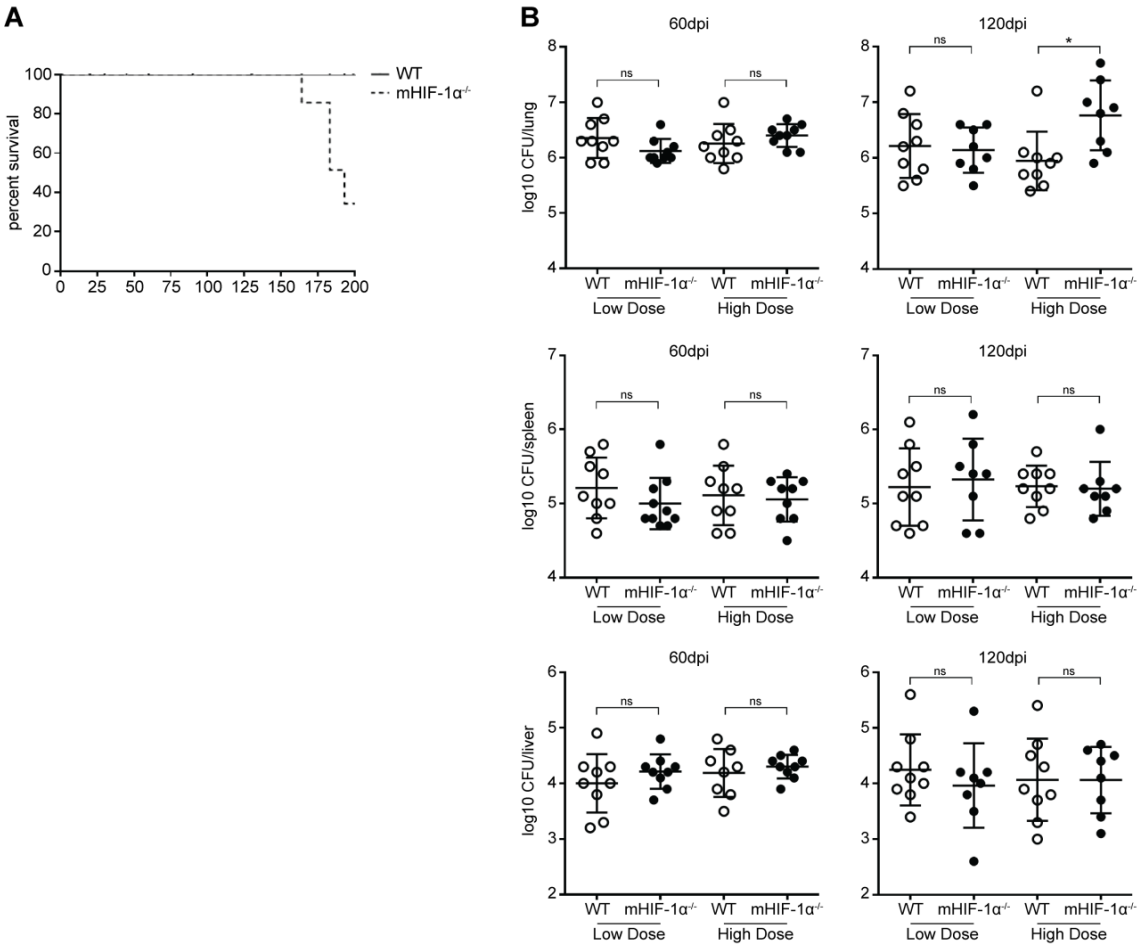

Figure 1. mHIF-1$\alpha^{-/-}$ mice are more susceptible to chronic Mtb infection. **(A)** Survival of B6 and mHIF-1$\alpha^{-/-}$ mice challenged with a high dose of Mtb infection via the aerosol route. Data represent 10 animals per group. **(B)** Mice were challenged either with a low or high dose Mtb infection via the aerosol route. At 60 and 120 days post-infection, bacterial burdens were assessed in the lungs, spleens and livers. Data represent the mean CFU ± SD from two independent experiments with at least 9 mice per group. Statistical significance was calculated by using unpaired student's *t* test with a Welch correction (*p<0.05; ns, not significant).

These data show that mHIF-1$\alpha^{-/-}$ mice are more susceptible to chronic Mtb infection, displaying reduced survival and higher lung bacterial burdens, but only after high dose aerosol

infection and at late stages of the infection. This susceptibility is more pronounced after high dose aerosol infection and during the late stages of the infection.

Myeloid HIF-1α activity regulates pulmonary inflammation during Mtb infection

mHIF-1α$^{-/-}$ mice display impaired myeloid cell function and migration to sites of inflammation (21, 22). Therefore, we wanted to determine if mHIF-1α$^{-/-}$ mice had altered influx of cells to the lungs following Mtb infection. To do this, we began analyzing the histological sections of Mtb-infected lungs at day 60 and 120 post-infection. Despite the increased lung bacterial burdens of mHIF-1α$^{-/-}$ mice challenged with a high dose (Fig. 1B), microscopic analysis of the lungs' histological sections revealed that mHIF-1α$^{-/-}$ mice had increased inflammatory infiltrates at both time-points analyzed and irrespective of the dose of infection (Fig. 2A).

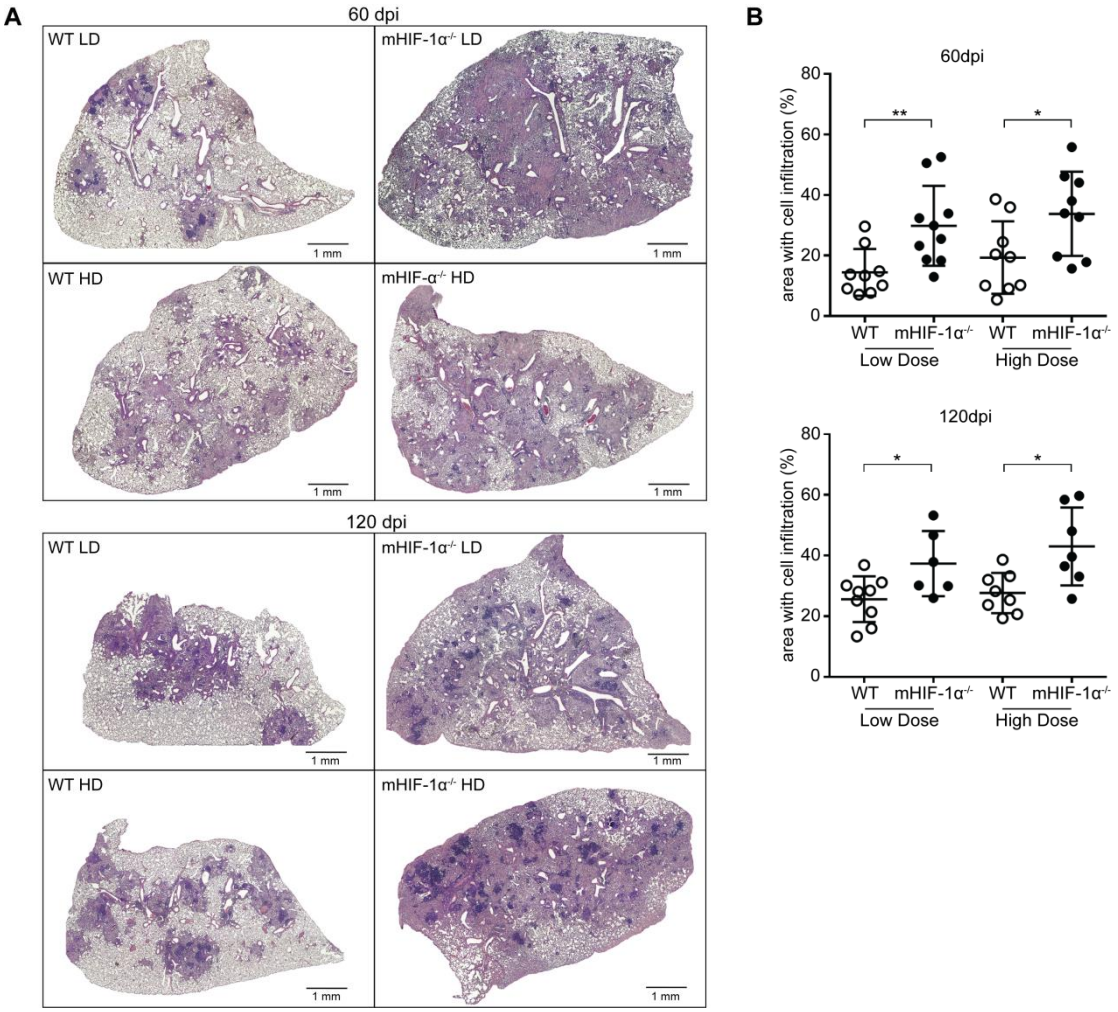

Figure 2. HIF-1α activity in the myeloid compartment regulates pulmonary inflammation during chronic Mtb infection. B6 and mHIF-1α$^{-/-}$ mice were challenged with either a low dose (LD) or high dose (HD) Mtb infection via the aerosol route. **(A)** Representative H&E lung sections at 60 and 120 days post-infection. **(B)** Percentage of the infiltrated area in the lungs at 60 and 120 days post-infection. Individual data points represent one lung section. Data

represent the mean ± SD from two independent experiments with at least 9 mice per group. Statistical significance was calculated by using unpaired student's *t* test with a Welch correction (*$p<0.05$; **$p<0.01$).

These data were confirmed upon measuring the areas of inflammation showing that there was a clear and reproducible increase in cellular infiltrates in mHIF-1$\alpha^{-/-}$ when compared to B6 mice (Fig. 2B). These data suggest that, HIF-1α activity in the myeloid compartment impacts pulmonary inflammation upon aerosol Mtb infection.

We next quantified the cellular composition of the inflammatory infiltrates using flow cytometry, as depicted in Supplemental Fig. 1. We focused our analysis at day 60 post-infection and found that, in accordance with the increased pulmonary inflammation of mHIF-1$\alpha^{-/-}$ mice there were more CD45^{+} cells in the lungs of these mice, both after low and high dose Mtb infection (Fig. 3). Therefore, we next assessed the accumulation of different myeloid populations in the lungs of Mtb-infected mice using multiparametric flow cytometry analysis (36, 37). We began determining the number of neutrophils in Mtb-infected B6 and mHIF-1$\alpha^{-/-}$ mice, as neutrophil accumulation is associated with more aggressive TB disease (38, 39). In accordance with the increased inflammatory foci shown above, mHIF-1$\alpha^{-/-}$ mice displayed a modest increased accumulation of neutrophils in the lungs (Fig. 3). Despite this increase, there was no altered expression of the neutrophil-recruiting chemokines *Cxcl1* and *Cxcl2* (Supplemental Fig. 2). Additionally, the number of CD11b^{-} and CD103^{+} DC, and interstitial macrophages were also increased (Fig. 3). Interestingly, resident monocytes were the only population that was increased in mHIF-1$\alpha^{-/-}$ mice after high dose infection, but not after low dose infection (Fig. 3). Finally, no differences were found in alveolar macrophages or inflammatory monocytes (Fig. 3) between both groups of mice. When we analyzed these populations at day 120 post-infection, we found similar a similar profile in both B6 and mHIF-1$\alpha^{-/-}$ Mtb-infected mice (not depicted). These data show that the absence of HIF-1α in the myeloid compartment has profound, but transient, implications in the accumulation of myeloid cells in the lungs of Mtb-infected mice.

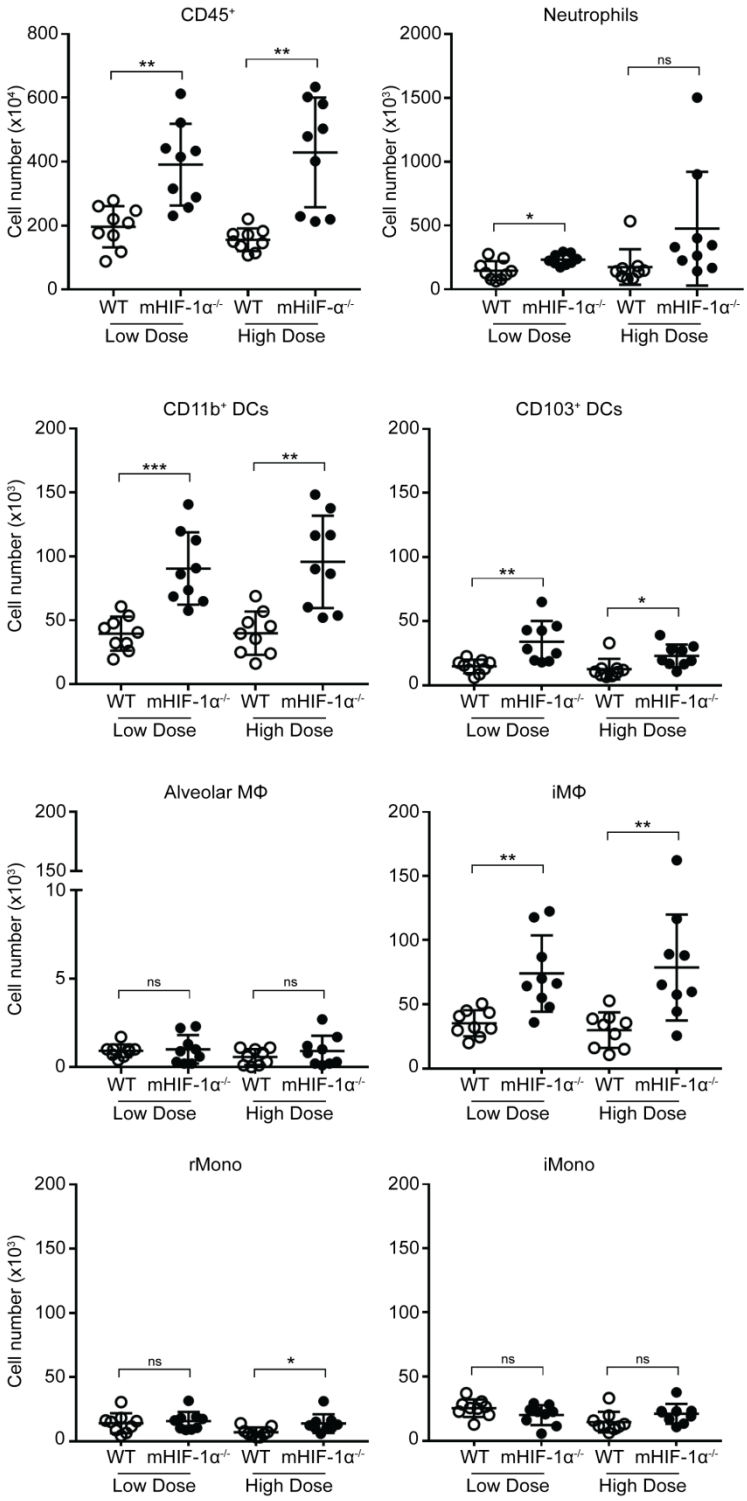

Figure 3. HIF-1α activity in the myeloid compartment regulates the accumulation of inflammatory cells in the lungs of Mtb infected mice. B6 and mHIF-1α$^{-/-}$ mice were challenged with either a low dose or a high dose Mtb infection and the different cell populations were assessed by flow cytometry at 60 days post-infection. Individual data point represent one animal. Data represent the mean ± SD of two independent experiments with at least 9 mice per group. Statistical significance was calculated by using unpaired student's *t* test with a Welch correction (*p<0.5; **p<0.01, ***p<0.01; ns, not significant).

Transient reduction of lung iNOS in mHIF-1α$^{-/-}$ mice upon high dose Mtb infection

HIF-1α has been shown to play a central role in the control of TB by coordinating the response of macrophages to IFN-γ (29). In vitro studies further suggested that the role of HIF-1α was mediated, at least in part, through the induction of *Nos2* expression and iNOS activity (28). Therefore, we determined the levels of iNOS in the lungs Mtb-infected B6 and mHIF-1α$^{-/-}$ mice at both day 60 and 120 post-infection, by immunohistochemistry (Fig. 4A). Microscopic analysis revealed a less intense and more diffuse staining of iNOS within the granulomas of mHIF-1α$^{-/-}$ mice, particularly at day 60 post-infection (Fig. 4A).

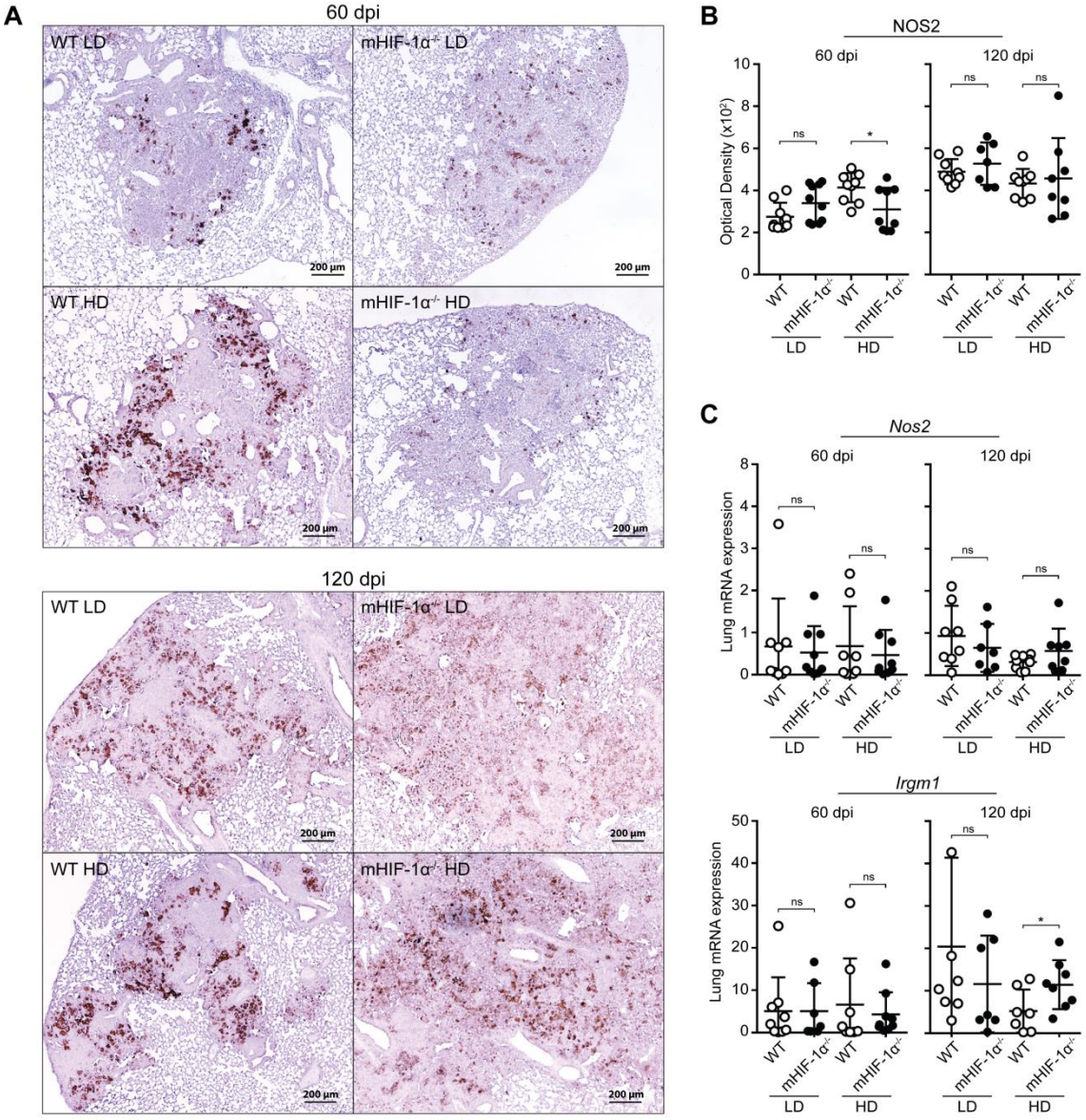

Figure 4. Transient decrease of lung iNOS in mHIF-1α$^{-/-}$ mice upon high dose Mtb infection. B6 and mHIF-1α$^{-/-}$ mice were challenged with either a low dose (LD) or a high dose (HD) Mtb infection and iNOS was assessed at 60 and 120 days post-infection. **(A)** Immunohistochemical analysis of iNOS in lung tissues of Mtb infected mice. **(B)** Optical density quantification of iNOS staining. **(C)** *Nos2* and *Irgm1* gene expression in lung tissues of Mtb infected

mice. Individual data points represent one animal. Data represent the mean ± SD of two independent experiments with ate least 9 mice per group. Statistical significance was calculated by using unpaired student's *t* test with a Welch correction (*p<0.5; ns, not significant).

However, quantitative determination of iNOS staining revealed that both B6 and mHIF-1α mice expressed similar levels of iNOS at both time points after low dose aerosol infection (Fig. 4B). Interestingly however, upon high dose Mtb infection, mHIF-1$\alpha^{-/-}$ mice expressed lower levels of iNOS when compared to B6 mice at day 60 post-infection (Fig. 4B). Despite this, *Nos2* gene expression in lung tissues was similar at both time points irrespective of the dose of infection (Fig. 4C). Furthermore, both strains of mice expressed similar levels of iNOS at day 120 post-infection (Fig. 4B-C). To determine if the expression of other IFN-γ-dependent antimycobacterial genes were altered, we measured the expression of immunity-related GTPase family M member 1 gene (*Irgm1*) that has an important role in the control of Mtb infection (40). We found similar levels of *Irgm1* expression in both groups of mice challenged with a low dose infection and a slight increase in high dose challenged mHIF-1$\alpha^{-/-}$ mice at day 120 post-infection (Fig. 4C).

With the reduction in iNOS protein observed in high dose challenged mHIF-1$\alpha^{-/-}$ mice at day 60 post-infection, we asked if in this situation macrophages were alternatively activated. In this regard, IL-10 has been shown to promote the alternative activated macrophages during TB with important consequences in the control of infection (41, 42). Therefore, we measured the expression of *Il10* mRNA in lung tissues and found similar levels of expression in both groups of mice (Fig. 5). Furthermore, the expression of several genes associated with alternative activation of macrophages, as *Arg1*, *Fizz1* and *Ym1*, was also similar between both groups of mice (Fig. 5). These data show that macrophages from mHIF-1$\alpha^{-/-}$ mice do not become alternatively activated during Mtb infection.

Taken together, these data show that HIF-1α deficiency in the myeloid compartment results in increased and altered lung inflammatory infiltrates but has no significant impact in classical macrophage activation.

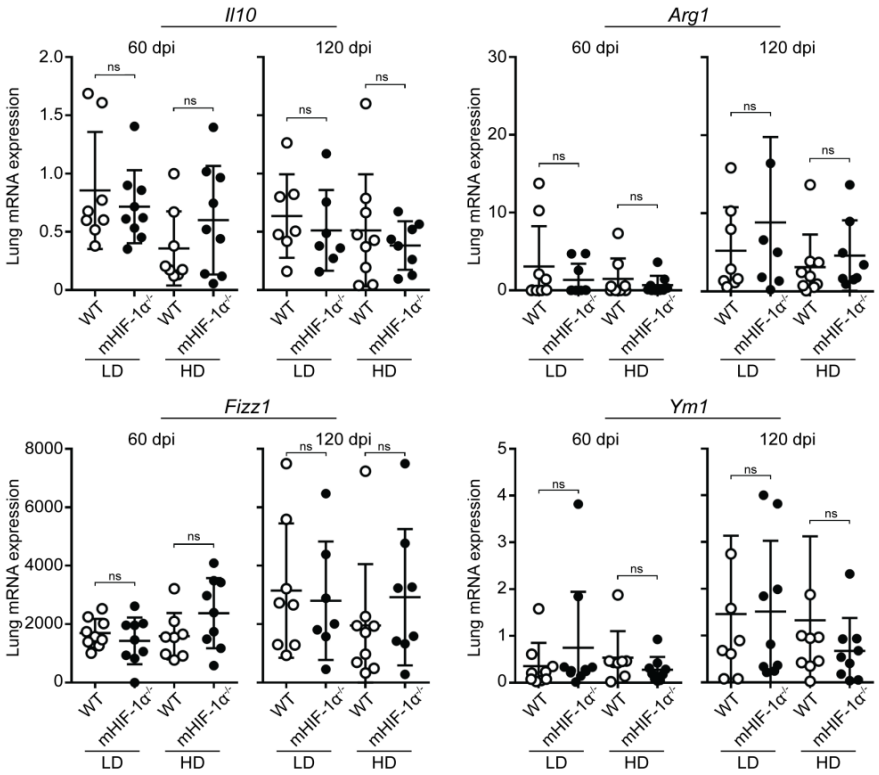

Figure 5. Myeloid HIF-1α deficiency does not promote alternative macrophage activation. *Il10*, *Arg1*, *Fizz1* and *Ym1* gene expression of lung tissue from mice infected with a low dose (LD) or a high dose (HD) Mtb infection at 60 and 120 days post-infection. Individual data points represent one animal. Data represent the mean ± SD of two independent experiments with at least 9 mice per group. Statistical significance was calculated by using unpaired student's *t* test with a Welch correction (ns, not significant).

Myeloid HIF-1α deficiency regulates the accumulation of Th1 and Th17 cells in the lungs of Mtb infected mice

Data from AIDS patients (43) and the acute susceptibility of humans and mice deficient in the IFN-γ pathway (44, 45) support the role of $CD4^+$ T cells producing IFN-γ as crucial to control Mtb infection. However, unregulated Ag-specific responses can also cause important immunopathological consequences to the host (46-48). Therefore, after determining that mHIF-$1\alpha^{-/-}$ mice had increased accumulation of myeloid cells and altered iNOS upon high dose aerosol Mtb infection, we wanted to determine if the acquired response was similar in both groups of mice.

We first quantified the total number of T cells ($CD3^+$) by flow cytometry and found that mHIF-$1\alpha^{-/-}$ mice display increased accumulation of $CD3^+$ cells in the lungs, irrespective of the dose of infection (Fig. 6A). As $CD4^+$ T cells are critical to control Mtb infection, we further analyzed the

CD4+ compartment. We began by determining the total number of CD4+ T cells in the lungs of both groups of mice and found an increased accumulation of this population in the lungs of Mtb-infected mHIF-1α$^{-/-}$ mice (Fig. 6A). To determine the cytokine response of these cells, we restimulated lung single cell suspensions with the I-A^{b}-restricted immunodominant ESAT-6$_{1-20}$ peptide (33). In keeping with the increased numbers of CD4+ T cells, and despite the similar frequency of IFN-γ+, TNF-α+, and IFN-γ+TNF-α+ CD4+ T cells between B6 and mHIF-1α$^{-/-}$ mice (Fig. 6B-C), there were increased numbers of these populations in Mtb-infected mHIF-1α$^{-/-}$ mice (Fig. 6D). Accordingly, when we measured the concentration of IFN-γ in the supernatants of lung single cell suspensions we found increased concentrations of this cytokine in mHIF-1α$^{-/-}$ mice at day 60 post-infection and irrespective of the infection dose (Fig. 6E). However, by day 120 post-infection the number of cytokine-producing cells (not depicted), and the levels of IFN-γ were similar in both groups of mice (Fig. 6F). Accordingly, the expression *Ifng* and genes upregulated by IFNγ, namely *Cxcl10* and *Cxcl11* was similar in both groups of animals, at both time points, and with the two infection doses (Supplemental Fig. 2). *Cxcl9* expression was reduced at day 60 in low dose challenged mHIF-1α$^{-/-}$ mice, but similar in both groups at day 120 post-infection (Supplemental Fig. 2).

Enhanced IL-17 responses have been associated with lung granulocytic inflammation and more severe TB disease (39, 48, 49). As there was increased inflammation and accumulation of neutrophils in the lungs of mHIF-1α$^{-/-}$ mice, we next analyzed the Ag-specific IL-17 response. In accordance with the inflammatory status of mHIF-1α$^{-/-}$ mice at 60 days post-infection, we found an increased frequency (Fig. 6B-C) and number (Fig. 6D) of Ag-specific IL-17+ cells in the lungs of mHIF-1α$^{-/-}$ mice. Despite this increase, we did not find increased expression of *Il6* or *IL23a* in the lung tissue (Supplemental Fig. 2).

These data show that HIF-1α deficiency in the myeloid compartment results in increased but differential accumulation of IFN-γ and IL-17-producing CD4+ T cells in the lungs of Mtb-infected mice.

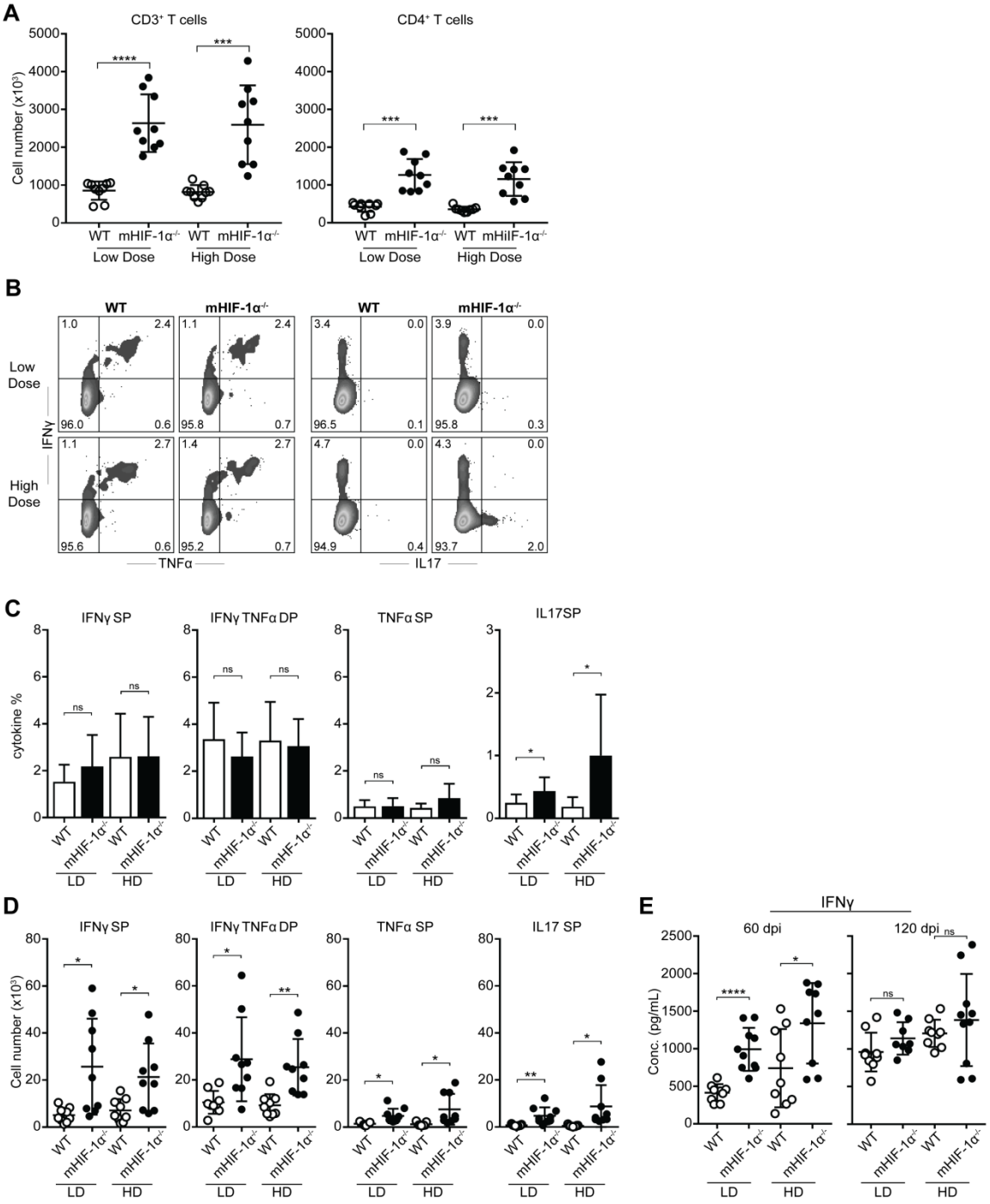

Figure 6. Myeloid HIF-1α deficiency prompts chronic Th17 responses during TB. B6 and mHIF-1α$^{-/-}$ mice were challenged with either a low dose (LD) or a high dose (HD) Mtb infection. **(A)** Lung CD3$^+$ and CD4$^+$ T cells numbers determined by flow cytometry at 60 days post-infection. **(B-D)** Lung cells were restimulated with ESAT-6$_{1-20}$ to assess the polyfunctionality of CD4$^+$ T cells. **(B)** Representative flow cytometry data of IFN-γ, TNF-α, and IL-17-expressing CD4$^+$ T cells. **(C)** Frequencies and **(D)** numbers of IFN-γ$^+$ single producers (SP), IFN-γ$^+$TNF-α$^+$ double producers (DP), TNF-α$^+$ SP and IL-17 SP CD4$^+$ T cells. **(E)** IFN-γ concentration in the supernatants of lung single cell suspensions at 60 and 120 days post-infection determined by ELISA. Individual data points represent one animal. Data represent the mean ± SD of two independent experiments with at least 9 mice per group. Statistical

significance was calculated by using unpaired student's *t* test with a Welch correction (*p<0.05; **p<0.01; ***p<0.01; ****p<0.0001; ns, not significant).

Discussion

Although the central role of HIF-1α in coordinating the response of myeloid cells in inflammatory and hypoxic environments is recognized (7), the precise mechanisms whereby this transcription factor modulates protective immunity to Mtb infection remains incompletely understood. Recent data suggest that HIF-1α plays an important role in coordinating the response of macrophages during mycobacterial infection (28-30, 50). Indeed, mice deficient in HIF-1α in the myeloid lineage were acutely susceptible to high dose aerosol Mtb challenge (29). Therefore, HIF-1α may represent a central node in coordinating the development of protective immunity to TB and, therefore, a potential target to intervene therapeutically.

In this work, we have used mice deficient in HIF-1α in the myeloid compartment (mHIF-1$\alpha^{-/-}$) to clarify the acute susceptibility of the mice to Mtb infection. We found that mHIF-1$\alpha^{-/-}$ mice were more susceptible to Mtb infection. However, our experimental approach did not reveal acute susceptible to Mtb infection even after high dose challenge, which contrast with previously published data (29). Instead, we found that mHIF-1$\alpha^{-/-}$ mice had elevated lung inflammation irrespective of the dose of infection, and only slightly elevated bacterial burdens after high dose challenge and at late stages of infection. These data, taken together with previously published data, suggest that HIF-1α activity in the myeloid lineage plays a key role in regulating pulmonary inflammation and that, the enhanced susceptibility of mHIF-1$\alpha^{-/-}$ mice to aerosol Mtb infection is a result of impaired response of macrophages to IFN-γ combined with unrestrained pulmonary inflammation. One key difference between our work and Braverman's work was the stain of Mtb used (29). While both H37Rv and Erdman are laboratory strains they differ in their in vivo grow rate and degree of inflammation induced (51). As such, the relevance of HIF-1α in the regulation of the pulmonary inflammation is likely more prominent in the high inflammatory settings induced by infection with the Mtb Erdman strain. Interestingly, despite the different pulmonary inflammation between B6 and mHIF-1$\alpha^{-/-}$ there were no major differences in bacterial burdens. Indeed, mice challenged with a low dose were able to control infection irrespective of the genetic background. These data suggest that, although lung lesions were increased in size in mHIF-1$\alpha^{-/-}$ mice, the ability of these mice to control bacterial burden was not significantly compromised and it was only at late stages of infection that bacterial burdens begin to diverge. Additionally, both B6

and mHIF-1$\alpha^{-/-}$ mice display similar bacterial burdens in spleens and livers. We speculate that this is because mHIF-1$\alpha^{-/-}$ mice mount normal Ag-specific IFN-γ responses, which are highly efficient at controlling systemic Mtb growth (52).

While our data confirmed that in the absence of HIF-1α the macrophage response is impaired, specifically in what regards iNOS, this effect was only transient and clear at day 60 post-infection when bacterial burdens where similar between B6 and mHIF-1$\alpha^{-/-}$ mice. By day 120 post-infection, the level of iNOS was similar in both groups of mice. It was only at this time-point that we found slightly increased lung Mtb burdens in mHIF-1$\alpha^{-/-}$ mice challenged with a high dose of infection. The relevance of nitric oxide during TB goes beyond its bactericidal activity, with recent data pointing to a key role in the regulation of pulmonary inflammatory responses (28, 31) and granulocytic infiltration (53), which are settings associated with TB disease severity (39). Therefore, while the reduced iNOS at day 60 post-infection is not the likely explanation for the susceptibility of mHIF-1$\alpha^{-/-}$ mice it may contribute to worsen the inflammatory response.

Additionally, we also found increased IL-17-producing $CD4^+$ T cells in the lungs of Mtb-infected mHIF-1$\alpha^{-/-}$ mice. As this population is known impact neutrophil homeostasis and recruitment which may result in severe immunopathological consequences to the host (48, 49), it is plausible that the pathological inflammation of mHIF-1$\alpha^{-/-}$ mice might be caused by the enhanced IL-17 response. In addition to inducing granulocyte recruitment, IL-17 is associated with the accumulation of myeloid-derived suppressor cells (MDSC), specifically in cancer models (54). These cells have also been described in both mice (55, 56) and humans with TB (57) and are associated with increased TB disease severity. Therefore, it is tempting to speculate that the IL-17-MDSC axis may be associated with the susceptibility of mHIF-1$\alpha^{-/-}$ mice. However, recent data suggest that IL-17 limits the accumulation of MDSC during TB (5). Additionally, we did not find suppression of the Ag-specific response as the number of IFN-γ-producing cells and levels of IFN-γ in the lung were higher in mHIF-1$\alpha^{-/-}$ mice than in control mice. Therefore, the increased accumulation of $Ly6G^{high}$ cells in mHIF-1$\alpha^{-/-}$ mice likely do not represent MDSC.

Taken together, our data support the hypothesis that the activity of HIF-1α is essential to regulate pulmonary inflammation and susceptibility to Mtb infection. Further research is important to clarify whether the pathological inflammation and susceptibility of mHIF-1$\alpha^{-/-}$ mice is a consequence of reduced iNOS activity, increased IL-17 responses or a combination of both.

One interesting aspect that our data reveled regarding the inflammatory infiltrates of mHIF-1α$^{-/-}$ mice was the increased accumulation of resident monocytes upon high dose challenge, the only setting with elevated bacterial burdens at day 120 post-infection. The function of this monocyte population (which has the CD16^{+} non-classical monocyte as their human counterpart (58)) during TB is still not well defined (59). However, TB patients have higher numbers of the CD16^{+} non-classical monocyte subset (60) that can differentiate into a DC population with reduced Ag-presenting capacities (61). Although our data support the hypothesis that the susceptibility of mHIF-1α$^{-/-}$ mice to Mtb infection is not a consequence of reduced Ag-specific responses, resident monocytes may impact protective immunity through other mechanisms.

In previous studies, macrophages deficient for HIF-1α expressed high levels of IL-10 upon in vitro Mtb infection (29). The role of IL-10 in TB has been extensively addressed (41, 42, 62-64). One of the mechanisms whereby this cytokine modulates protective immunity to TB is by promoting alternative macrophage activation resulting in impaired nitric oxide production and reduced control of Mtb infection (41). In our in vivo approach, we did not find significant differences in IL-10 expression between B6 and mHIF-1α$^{-/-}$ mice nor was there any altered expression of genes associated with alternative macrophage activation. Therefore, the absence of HIF-1α activity in myeloid cells appears to have a minimal impact in the in vivo IL-10 response during TB.

Overall, our data show that HIF-1α plays an important role in the control of Mtb infection and support the hypothesis that HIF-1α activity in myeloid cells is crucial to regulate pulmonary inflammatory responses and TB disease severity. We propose that the anti-inflammatory role of HIF-1α activity in the myeloid compartment may limit the development of hypoxia that would ensue from an exaggerated influx of leukocytes. Further research is required to clarify the mechanisms by which HIF-1α coordinates the response of myeloid cells to regulate pulmonary inflammation. Defining these mechanisms may have important implications in the design of new therapies for treatment of TB.

Acknowledgements

We thank the personnel of the ICVS animal facility and histology core for all the technical assistance. This work was supported by the project NORTE-01-0145-FEDER-000013, supported by the Northern Portugal Regional Operational Programme (NORTE 2020), under the Portugal 2020 Partnership Agreement, through the European Regional Development Fund (FEDER), and the Fundação para a Ciência e Tecnologia (FCT) through the FCT investigator grant IF/01390/2014 (to ET), IF/00021/2014 (to RS) and the PhD fellowships SFRH/BD/89871/2012 (to MR), PD/BD/137447/2018 (to CMF), and SFRH/BD/120371/2016 (to AMB).

Conflict of interest

The authors declare that the research was conducted in the absence of any commercial or financial relationships that could be construed as a potential conflict of interest.

Supplemental Figures

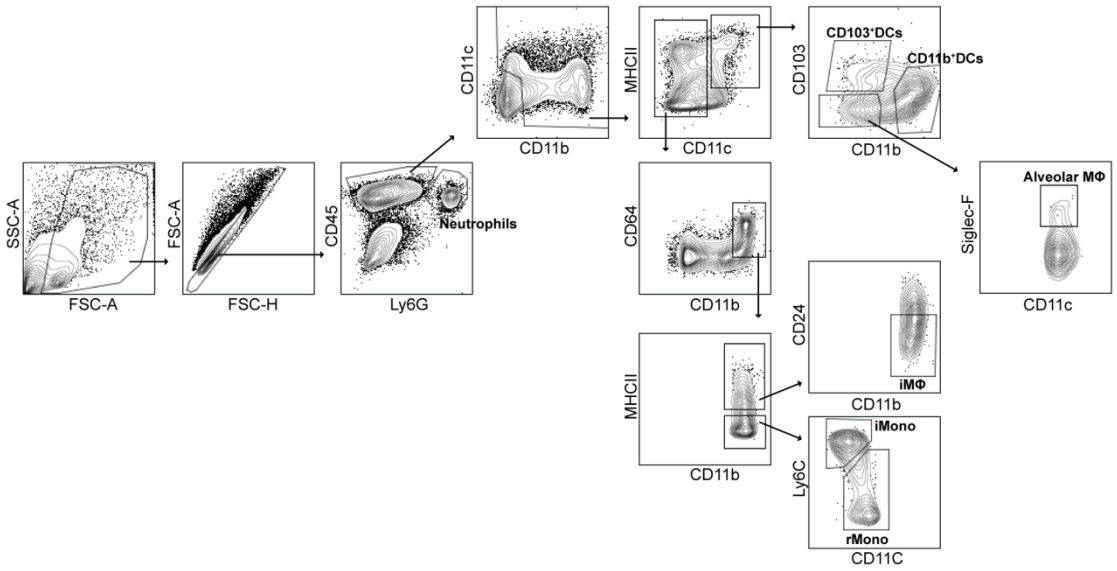

Supplemental Figure 1. Gating strategy used to identify the different lung myeloid cells

Supplemental Figure 2

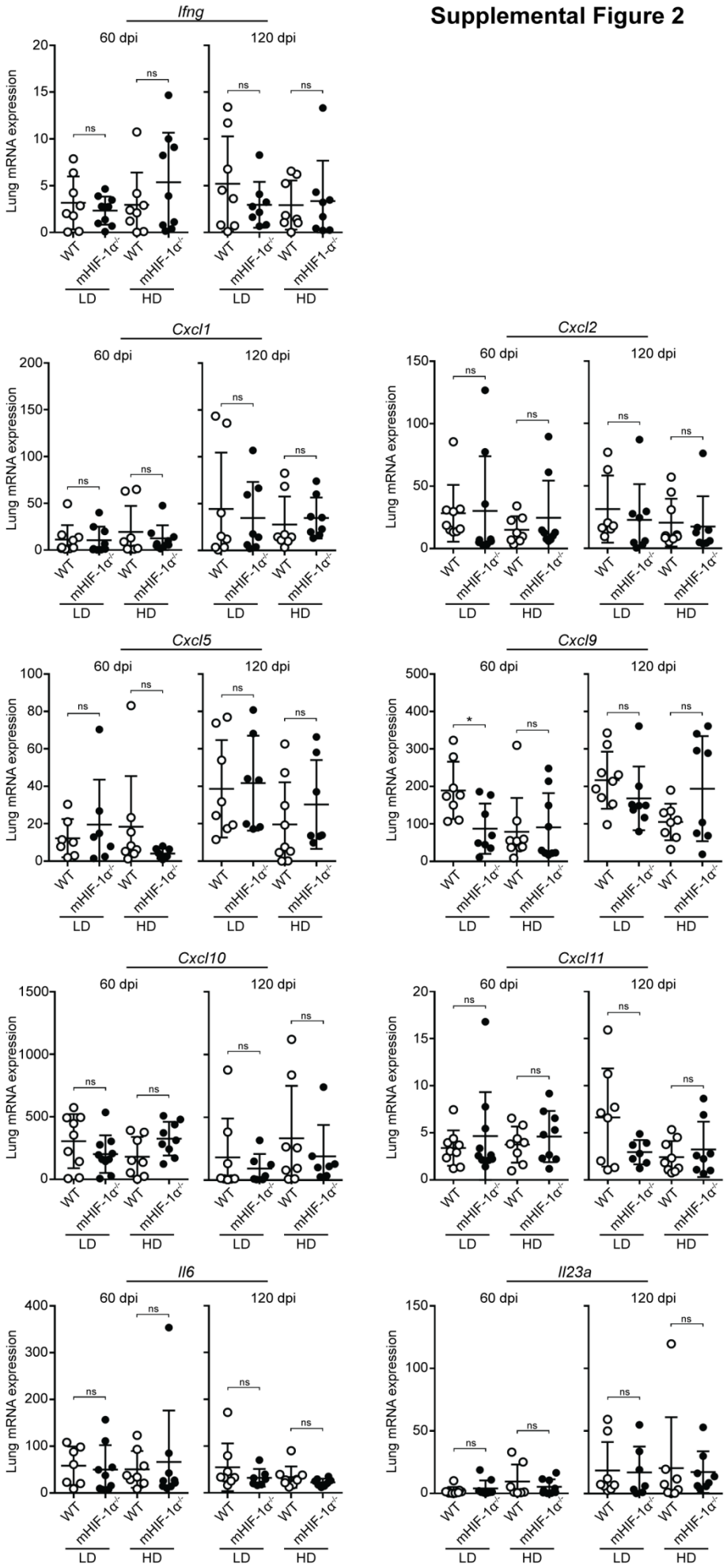

Supplemental Figure 2. Expression of *Ifng*, *Cxcl1*, *Cxcl2*, *Cxcl5*, *Cxcl9*, *Cxcl10*, *Cxcl11*, *Il6* and *Il23a* at 60 and 120 days post-infection in the lungs from B6 and mHIF-1α$^{-/-}$ mice challenged with either a low dose (LD) or a high dose (HD) Mtb infection. Individual data points represent one animal. Data represent the mean ± SD of two independent experiments with at least 9 mice per group. Statistical significance was calculated by using student's *t* test with a Welch correction (*p<0.05; ns, not significant).

References

1. Organization, W. H. 2017. Global tuberculosis report 2017; available at: www.who.int/tb/publications/global_report/en.
2. Dye, C., P. Glaziou, K. Floyd, and M. Raviglione. 2013. Prospects for tuberculosis elimination. *Annu. Rev. Public Health* 34: 271-286.
3. Orme, I. M., and R. J. Basaraba. 2014. The formation of the granuloma in tuberculosis infection. *Semin. Immunol.* 26: 601-609.
4. Via, L. E., P. L. Lin, S. M. Ray, J. Carrillo, S. S. Allen, S. Y. Eum, K. Taylor, E. Klein, U. Manjunatha, J. Gonzales, E. G. Lee, S. K. Park, J. A. Raleigh, S. N. Cho, D. N. McMurray, J. L. Flynn, and C. E. Barry, 3rd. 2008. Tuberculous granulomas are hypoxic in guinea pigs, rabbits, and nonhuman primates. *Infect. Immun.* 76: 2333-2340.
5. Domingo-Gonzalez, R., S. Das, K. L. Griffiths, M. Ahmed, M. Bambouskova, R. Gopal, S. Gondi, M. Munoz-Torrico, M. A. Salazar-Lezama, A. Cruz-Lagunas, L. Jimenez-Alvarez, G. Ramirez-Martinez, R. Espinosa-Soto, T. Sultana, J. Lyons-Weiler, T. A. Reinhart, J. Arcos, M. de la Luz Garcia-Hernandez, M. A. Mastrangelo, N. Al-Hammadi, R. Townsend, J. M. Balada-Llasat, J. B. Torrelles, G. Kaplan, W. Horne, J. K. Kolls, M. N. Artyomov, J. Rangel-Moreno, J. Zuniga, and S. A. Khader. 2017. Interleukin-17 limits hypoxia-inducible factor 1alpha and development of hypoxic granulomas during tuberculosis. *JCI insight* 2: e92973.
6. Belton, M., S. Brilha, R. Manavaki, F. Mauri, K. Nijran, Y. T. Hong, N. H. Patel, M. Dembek, L. Tezera, J. Green, R. Moores, F. Aigbirhio, A. Al-Nahhas, T. D. Fryer, P. T. Elkington, and J. S. Friedland. 2016. Hypoxia and tissue destruction in pulmonary TB. *Thorax* 71: 1145-1153.
7. Lin, N., and M. C. Simon. 2016. Hypoxia-inducible factors: key regulators of myeloid cells during inflammation. *J. Clin. Invest.* 126: 3661-3671.
8. Dengler, V. L., M. Galbraith, and J. M. Espinosa. 2014. Transcriptional regulation by hypoxia inducible factors. *Crit. Rev. Biochem. Mol. Biol.* 49: 1-15.
9. Shweiki, D., A. Itin, D. Soffer, and E. Keshet. 1992. Vascular endothelial growth factor induced by hypoxia may mediate hypoxia-initiated angiogenesis. *Nature* 359: 843-845.
10. Haase, V. H. 2013. Regulation of erythropoiesis by hypoxia-inducible factors. *Blood Rev.* 27: 41-53.

11. Hayashi, M., M. Sakata, T. Takeda, T. Yamamoto, Y. Okamoto, K. Sawada, A. Kimura, R. Minekawa, M. Tahara, K. Tasaka, and Y. Murata. 2004. Induction of glucose transporter 1 expression through hypoxia-inducible factor 1alpha under hypoxic conditions in trophoblast-derived cells. *J. Endocrinol.* 183: 145-154.

12. Kim, J. W., I. Tchernyshyov, G. L. Semenza, and C. V. Dang. 2006. HIF-1-mediated expression of pyruvate dehydrogenase kinase: a metabolic switch required for cellular adaptation to hypoxia. *Cell Metab.* 3: 177-185.

13. Roiniotis, J., H. Dinh, P. Masendycz, A. Turner, C. L. Elsegood, G. M. Scholz, and J. A. Hamilton. 2009. Hypoxia prolongs monocyte/macrophage survival and enhanced glycolysis is associated with their maturation under aerobic conditions. *J. Immunol.* 182: 7974-7981.

14. Jung, Y., J. S. Isaacs, S. Lee, J. Trepel, Z. G. Liu, and L. Neckers. 2003. Hypoxia-inducible factor induction by tumour necrosis factor in normoxic cells requires receptor-interacting protein-dependent nuclear factor kappa B activation. *Biochem. J.* 370: 1011-1017.

15. Zhou, J., T. Schmid, and B. Brune. 2003. Tumor necrosis factor-alpha causes accumulation of a ubiquitinated form of hypoxia inducible factor-1alpha through a nuclear factor-kappaB-dependent pathway. *Mol. Biol. Cell* 14: 2216-2225.

16. Jung, Y. J., J. S. Isaacs, S. Lee, J. Trepel, and L. Neckers. 2003. IL-1beta-mediated up-regulation of HIF-1alpha via an NFkappaB/COX-2 pathway identifies HIF-1 as a critical link between inflammation and oncogenesis. *FASEB J.* 17: 2115-2117.

17. Rius, J., M. Guma, C. Schachtrup, K. Akassoglou, A. S. Zinkernagel, V. Nizet, R. S. Johnson, G. G. Haddad, and M. Karin. 2008. NF-kappaB links innate immunity to the hypoxic response through transcriptional regulation of HIF-1alpha. *Nature* 453: 807-811.

18. Nishi, K., T. Oda, S. Takabuchi, S. Oda, K. Fukuda, T. Adachi, G. L. Semenza, K. Shingu, and K. Hirota. 2008. LPS induces hypoxia-inducible factor 1 activation in macrophage-differentiated cells in a reactive oxygen species-dependent manner. *Antioxid. Redox Signal.* 10: 983-995.

19. Peyssonnaux, C., P. Cejudo-Martin, A. Doedens, A. S. Zinkernagel, R. S. Johnson, and V. Nizet. 2007. Cutting edge: Essential role of hypoxia inducible factor-1alpha in development of lipopolysaccharide-induced sepsis. *J. Immunol.* 178: 7516-7519.

20. Frede, S., C. Stockmann, P. Freitag, and J. Fandrey. 2006. Bacterial lipopolysaccharide induces HIF-1 activation in human monocytes via p44/42 MAPK and NF-kappaB. *Biochem. J.* 396: 517-527.

21. Cramer, T., Y. Yamanishi, B. E. Clausen, I. Forster, R. Pawlinski, N. Mackman, V. H. Haase, R. Jaenisch, M. Corr, V. Nizet, G. S. Firestein, H. P. Gerber, N. Ferrara, and R. S. Johnson. 2003. HIF-1alpha is essential for myeloid cell-mediated inflammation. *Cell* 112: 645-657.

22. Peyssonnaux, C., V. Datta, T. Cramer, A. Doedens, E. A. Theodorakis, R. L. Gallo, N. Hurtado-Ziola, V. Nizet, and R. S. Johnson. 2005. HIF-1alpha expression regulates the bactericidal capacity of phagocytes. *J. Clin. Invest.* 115: 1806-1815.

23. Dang, E. V., J. Barbi, H. Y. Yang, D. Jinasena, H. Yu, Y. Zheng, Z. Bordman, J. Fu, Y. Kim, H. R. Yen, W. Luo, K. Zeller, L. Shimoda, S. L. Topalian, G. L. Semenza, C. V. Dang, D. M. Pardoll, and F. Pan. 2011. Control of T(H)17/T(reg) balance by hypoxia-inducible factor 1. *Cell* 146: 772-784.

24. Doedens, A. L., A. T. Phan, M. H. Stradner, J. K. Fujimoto, J. V. Nguyen, E. Yang, R. S. Johnson, and A. W. Goldrath. 2013. Hypoxia-inducible factors enhance the effector responses of CD8(+) T cells to persistent antigen. *Nat. Immunol.* 14: 1173-1182.

25. Meng, X., B. Grotsch, Y. Luo, K. X. Knaup, M. S. Wiesener, X. X. Chen, J. Jantsch, S. Fillatreau, G. Schett, and A. Bozec. 2018. Hypoxia-inducible factor-1alpha is a critical transcription factor for IL-10-producing B cells in autoimmune disease. *Nat. Commun.* 9: 251.

26. Berger, E. A., S. A. McClellan, K. S. Vistisen, and L. D. Hazlett. 2013. HIF-1alpha is essential for effective PMN bacterial killing, antimicrobial peptide production and apoptosis in *Pseudomonas aeruginosa* keratitis. *PLoS Pathog.* 9: e1003457.

27. Lin, A. E., F. C. Beasley, J. Olson, N. Keller, R. A. Shalwitz, T. J. Hannan, S. J. Hultgren, and V. Nizet. 2015. Role of Hypoxia Inducible Factor-1alpha (HIF-1alpha) in innate defense against uropathogenic *Escherichia coli* infection. *PLoS Pathog.* 11: e1004818.

28. Braverman, J., and S. A. Stanley. 2017. Nitric Oxide Modulates Macrophage Responses to Mycobacterium tuberculosis Infection through Activation of HIF-1alpha and Repression of NF-kappaB. *J. Immunol.* 199: 1805-1816.

29. Braverman, J., K. M. Sogi, D. Benjamin, D. K. Nomura, and S. A. Stanley. 2016. HIF-1alpha Is an Essential Mediator of IFN-gamma-Dependent Immunity to Mycobacterium tuberculosis. *J. Immunol.* 197: 1287-1297.

30. Cardoso, M. S., T. M. Silva, M. Resende, R. Appelberg, and M. Borges. 2015. Lack of the Transcription Factor Hypoxia-Inducible Factor 1alpha (HIF-1alpha) in Macrophages Accelerates the Necrosis of *Mycobacterium avium*-Induced Granulomas. *Infect. Immun.* 83: 3534-3544.

31. Mishra, B. B., V. A. Rathinam, G. W. Martens, A. J. Martinot, H. Kornfeld, K. A. Fitzgerald, and C. M. Sassetti. 2013. Nitric oxide controls the immunopathology of tuberculosis by inhibiting NLRP3 inflammasome-dependent processing of IL-1beta. *Nat. Immunol.* 14: 52-60.

32. Fraga, A. G., A. M. Barbosa, C. M. Ferreira, J. Fevereiro, J. Pedrosa, and E. Torrado. 2018. Immune-evasion strategies of mycobacteria and their implications for the protective immune response. *Curr. Issues Mol. Biol.* 25: 169-198.

33. Torrado, E., J. J. Fountain, M. Liao, M. Tighe, W. W. Reiley, R. P. Lai, G. Meintjes, J. E. Pearl, X. Chen, D. E. Zak, E. G. Thompson, A. Aderem, N. Ghilardi, A. Solache, K. K. McKinstry, T. M. Strutt, R. J. Wilkinson, S. L. Swain, and A. M. Cooper. 2015. Interleukin 27R regulates $CD4^+$ T cell phenotype and impacts protective immunity during M*ycobacterium tuberculosis* infection. *J. Exp. Med.* 212: 1449-1463.

34. Varghese, F., A. B. Bukhari, R. Malhotra, and A. De. 2014. IHC Profiler: an open source plugin for the quantitative evaluation and automated scoring of immunohistochemistry images of human tissue samples. *PLoS One* 9: e96801.

35. Ruifrok, A. C., and D. A. Johnston. 2001. Quantification of histochemical staining by color deconvolution. *Anal. Quant. Cytol. Histol.* 23: 291-299.

36. Misharin, A. V., L. Morales-Nebreda, G. M. Mutlu, G. R. Budinger, and H. Perlman. 2013. Flow cytometric analysis of macrophages and dendritic cell subsets in the mouse lung. *Am. J. Respir. Cell Mol. Biol.* 49: 503-510.

37. Yu, Y. R., E. G. O'Koren, D. F. Hotten, M. J. Kan, D. Kopin, E. R. Nelson, L. Que, and M. D. Gunn. 2016. A Protocol for the comprehensive flow cytometric analysis of immune cells in normal and inflamed murine non-lymphoid tissues. *PLoS One* 11: e0150606.

38. Berry, M. P., C. M. Graham, F. W. McNab, Z. Xu, S. A. Bloch, T. Oni, K. A. Wilkinson, R. Banchereau, J. Skinner, R. J. Wilkinson, C. Quinn, D. Blankenship, R. Dhawan, J. J.

Cush, A. Mejias, O. Ramilo, O. M. Kon, V. Pascual, J. Banchereau, D. Chaussabel, and A. O'Garra. 2010. An interferon-inducible neutrophil-driven blood transcriptional signature in human tuberculosis. *Nature* 466: 973-977.

39. Nandi, B., and S. M. Behar. 2011. Regulation of neutrophils by interferon-gamma limits lung inflammation during tuberculosis infection. *J. Exp. Med.* 208: 2251-2262.

40. MacMicking, J. D., G. A. Taylor, and J. D. McKinney. 2003. Immune control of tuberculosis by IFN-gamma-inducible LRG-47. *Science* 302: 654-659.

41. Torrado, E., J. J. Fountain, R. T. Robinson, C. A. Martino, J. E. Pearl, J. Rangel-Moreno, M. Tighe, R. Dunn, and A. M. Cooper. 2013. Differential and site specific impact of B cells in the protective immune response to *Mycobacterium tuberculosis* in the mouse. *PLoS One* 8: e61681.

42. Schreiber, T., S. Ehlers, L. Heitmann, A. Rausch, J. Mages, P. J. Murray, R. Lang, and C. Holscher. 2009. Autocrine IL-10 induces hallmarks of alternative activation in macrophages and suppresses antituberculosis effector mechanisms without compromising T cell immunity. *J. Immunol.* 183: 1301-1312.

43. Havlir, D. V., and P. F. Barnes. 1999. Tuberculosis in patients with human immunodeficiency virus infection. *N. Engl. J. Med.* 340: 367-373.

44. Casanova, J. L., and L. Abel. 2002. Genetic dissection of immunity to mycobacteria: the human model. *Annu. Rev. Immunol.* 20: 581-620.

45. Cooper, A. M., D. K. Dalton, T. A. Stewart, J. P. Griffin, D. G. Russell, and I. M. Orme. 1993. Disseminated tuberculosis in interferon gamma gene-disrupted mice. *J. Exp. Med.* 178: 2243-2247.

46. Barber, D. L., K. D. Mayer-Barber, C. G. Feng, A. H. Sharpe, and A. Sher. 2011. CD4 T cells promote rather than control tuberculosis in the absence of PD-1-mediated inhibition. *J. Immunol.* 186: 1598-1607.

47. Lazar-Molnar, E., B. Chen, K. A. Sweeney, E. J. Wang, W. Liu, J. Lin, S. A. Porcelli, S. C. Almo, S. G. Nathenson, and W. R. Jacobs, Jr. 2010. Programmed death-1 (PD-1)-deficient mice are extraordinarily sensitive to tuberculosis. *Proc. Natl. Acad. Sci. USA* 107: 13402-13407.

48. Cruz, A., A. G. Fraga, J. J. Fountain, J. Rangel-Moreno, E. Torrado, M. Saraiva, D. R. Pereira, T. D. Randall, J. Pedrosa, A. M. Cooper, and A. G. Castro. 2010. Pathological

role of interleukin 17 in mice subjected to repeated BCG vaccination after infection with *Mycobacterium tuberculosis*. *J. Exp. Med.* 207: 1609-1616.

49. Torrado, E., and A. M. Cooper. 2010. IL-17 and Th17 cells in tuberculosis. *Cytokine Growth Factor Rev.* 21: 455-462.

50. Elks, P. M., S. Brizee, M. van der Vaart, S. R. Walmsley, F. J. van Eeden, S. A. Renshaw, and A. H. Meijer. 2013. Hypoxia inducible factor signaling modulates susceptibility to mycobacterial infection via a nitric oxide dependent mechanism. *PLoS Pathog.* 9: e1003789.

51. Manca, C., L. Tsenova, C. E. Barry, 3rd, A. Bergtold, S. Freeman, P. A. Haslett, J. M. Musser, V. H. Freedman, and G. Kaplan. 1999. *Mycobacterium tuberculosis* CDC1551 induces a more vigorous host response in vivo and in vitro, but is not more virulent than other clinical isolates. *J. Immunol.* 162: 6740-6746.

52. Sakai, S., K. D. Kauffman, M. A. Sallin, A. H. Sharpe, H. A. Young, V. V. Ganusov, and D. L. Barber. 2016. CD4 T cell-derived IFN-gamma plays a minimal role in control of pulmonary *Mycobacterium tuberculosis* infection and must be actively repressed by PD-1 to prevent lethal disease. *PLoS Pathog.* 12: e1005667.

53. Mishra, B. B., R. R. Lovewell, A. J. Olive, G. Zhang, W. Wang, E. Eugenin, C. M. Smith, J. Y. Phuah, J. E. Long, M. L. Dubuke, S. G. Palace, J. D. Goguen, R. E. Baker, S. Nambi, R. Mishra, M. G. Booty, C. E. Baer, S. A. Shaffer, V. Dartois, B. A. McCormick, X. Chen, and C. M. Sassetti. 2017. Nitric oxide prevents a pathogen-permissive granulocytic inflammation during tuberculosis. *Nat. Microbiol.* 2: 17072.

54. Chen, X., M. J. Churchill, K. K. Nagar, Y. H. Tailor, T. Chu, B. S. Rush, Z. Jiang, E. B. Wang, B. W. Renz, H. Wang, M. C. Fung, D. L. Worthley, S. Mukherjee, and T. C. Wang. 2015. IL-17 producing mast cells promote the expansion of myeloid-derived suppressor cells in a mouse allergy model of colorectal cancer. *Oncotarget* 6: 32966-32979.

55. Obregon-Henao, A., M. Henao-Tamayo, I. M. Orme, and D. J. Ordway. 2013. Gr1(int)CD11b^{+} myeloid-derived suppressor cells in *Mycobacterium tuberculosis* infection. *PLoS One* 8: e80669.

56. Knaul, J. K., S. Jorg, D. Oberbeck-Mueller, E. Heinemann, L. Scheuermann, V. Brinkmann, H. J. Mollenkopf, V. Yeremeev, S. H. Kaufmann, and A. Dorhoi. 2014. Lung-residing myeloid-derived suppressors display dual functionality in murine pulmonary tuberculosis. *Am. J. Respir. Crit. Care Med.* 190: 1053-1066.

57. du Plessis, N., L. Loebenberg, M. Kriel, F. von Groote-Bidlingmaier, E. Ribechini, A. G. Loxton, P. D. van Helden, M. B. Lutz, and G. Walzl. 2013. Increased frequency of myeloid-derived suppressor cells during active tuberculosis and after recent *Mycobacterium tuberculosis* infection suppresses T-cell function. *Am. J. Respir. Crit. Care Med.* 188: 724-732.

58. Sprangers, S., T. J. de Vries, and V. Everts. 2016. Monocyte Heterogeneity: Consequences for Monocyte-Derived Immune Cells. *J. Immunol. Res.* 2016: 1475435.

59. Srivastava, S., J. D. Ernst, and L. Desvignes. 2014. Beyond macrophages: the diversity of mononuclear cells in tuberculosis. *Immunol. Rev.* 262: 179-192.

60. Balboa, L., M. M. Romero, J. I. Basile, C. A. Sabio y Garcia, P. Schierloh, N. Yokobori, L. Geffner, R. M. Musella, J. Castagnino, E. Abbate, S. de la Barrera, M. C. Sasiain, and M. Aleman. 2011. Paradoxical role of $CD16^{+}CCR2^{+}CCR5^{+}$ monocytes in tuberculosis: efficient APC in pleural effusion but also mark disease severity in blood. *J. Leukoc. Biol.* 90: 69-75.

61. Balboa, L., M. M. Romero, E. Laborde, Y. G. C. A. Sabio, J. I. Basile, P. Schierloh, N. Yokobori, R. M. Musella, J. Castagnino, S. de la Barrera, M. C. Sasiain, and M. Aleman. 2013. Impaired dendritic cell differentiation of CD16-positive monocytes in tuberculosis: role of p38 MAPK. *Eur. J. Immunol.* 43: 335-347.

62. Torrado, E., and A. M. Cooper. 2013. Cytokines in the balance of protection and pathology during mycobacterial infections. *Adv. Exp. Med. Biol.* 783: 121-140.

63. Redford, P. S., A. Boonstra, S. Read, J. Pitt, C. Graham, E. Stavropoulos, G. J. Bancroft, and A. O'Garra. 2010. Enhanced protection to *Mycobacterium tuberculosis* infection in IL-10-deficient mice is accompanied by early and enhanced Th1 responses in the lung. *Eur. J. Immunol.* 40: 2200-2210.

64. Moreira-Teixeira, L., P. S. Redford, E. Stavropoulos, N. Ghilardi, C. L. Maynard, C. T. Weaver, A. P. Freitas do Rosario, X. Wu, J. Langhorne, and A. O'Garra. 2017. T Cell-derived IL-10 impairs host resistance to *Mycobacterium tuberculosis i*nfection. *J. Immunol.* 199: 613-623.

Footnotes

This work was supported by the project NORTE-01-0145-FEDER-000013, supported by the Northern Portugal Regional Operational Programme (NORTE 2020), under the Portugal 2020 Partnership Agreement, through the European Regional Development Fund (FEDER), and the Fundação para a Ciência e Tecnologia (FCT) through the FCT investigator grant IF/01390/2014 (to E.T.), IF/00021/2014 (to R.S.) and the PhD fellowships SFRH/BD/89871/2012 (to M.R.), PD/BD/137447/2018 (to C.M.F.), and SFRH/BD/120371/2016 (to A.M.B.).

Abbreviations

B6, C57BL/6; CFU, Colony forming units; DC, Dendritic cells; dpi, Days post-infection; HIF-1α, Hypoxia Inducible Factor- 1alpha; HD, High dose; iNOS, inducible Nitric Oxide Synthase; LD, Low dose; Mtb, *Mycobacterium tuberculosis*; mHIF-1$\alpha^{-/-}$, myeloid restricted HIF-1α deficient mice; MDSC, Myeloid-derived Suppressor Cells; TB, tuberculosis.

Chapter V

GENERAL DISCUSSION

The data presented in this thesis include two topics related with mycobacterial-induced granulomata and pathogen proliferation control. The first topic addresses the role of IFN-γ: its requirement during innate immunity; and the impact of IFN-γ-mediated macrophage activation in the development of the immune response to mycobacterial infection. To assess these questions we have used the low virulence *M. avium* 2447 strain that despite the increased susceptibility in the absence of IFN-γ or T cell-mediated immunity, mice still succeed to get to chronic stage. We have found that innate cell sources of IFN-γ contribute to protection against *M. avium* infection in lymphopenic mice and although IFN-γ is required for the development of a mature granuloma and bacterial proliferation control, the IFN-γ-mediated macrophage activation can be dispensable. The second topic is focused on the later stages of granuloma development namely in the progression of the inflammatory process and development of central necrosis by hypoxia-induced mechanisms. We found that in Mtb infected C57BL/6 mice the hypoxia adaptor molecule Hif-1α is crucial to control pulmonary inflammation although we failed to detect necrotic lesions in its absence, unlike what was previously observed in a model of *M. avium*-induced necrotic granuloma (1).

1. IFN-γ-mediated protection

The requirement of IFN-γ for immune mediated protection in mycobacterial infections has been thoroughly demonstrated (2-4). In here we have confirmed the relevance of IFNγ both to control *M. avium* proliferation and to granuloma development (Chapter II and III). In the absence of IFNγ we observed increased *M. avium* proliferation and incipient granulomata, mostly constituted by lymphoid cell accumulations and lacking the inner macrophage core. We further observed that the deficient lymphoid accumulation was even more drastic in $Rag^{-/-}IFN\gamma^{-/-}$ -double deficient mice where one can expect to be mostly constituted by NK cells and other ILCs.

1.1. Innate sources of IFN-γ

IFN-γ is mostly produced by αβ T cells but also by γδ T cells, NKT cells, MAIT cells and by non-T cell sources as ILCs and NK cells (5). $Rag^{-/-}$ animals, which lack B cells and all T cells subsets, and $Rag^{-/-}\gamma c^{-/-}$ mice which additionally lack NK cells and ILCs were able to restrict *M. avium* proliferation to similar levels, and more efficiently than Rag mice lacking IFN-γ ($Rag^{-/-}IFN\text{-}\gamma^{-/-}$) and we could observe granuloma-like structures with an inner core of macrophages in $Rag^{-/-}\gamma c^{-/-}$ mice that were not present when IFN-γ is absent (Chapter II). Although NK cells are reported to be a pivotal IFN-γ cell source in several infection models (6, 7), our results suggest that other

innate IFN-γ-producing cells are involved in the control of *M. avium* proliferation in the Rag background. Feng and colleagues have previously reported the detection of IFN-γ, although in minimal amounts, in the supernatants of $Rag^{-/-}\gamma c^{-/-}$ splenocytes stimulated with Mtb (8). Despite the minimal capacity to produce IFN-γ, $Rag^{-/-}\gamma c^{-/-}$ mice were highly susceptible to Mtb infection with decreased survival rates and increased bacterial burdens when compared with the $Rag^{-/-}$ control group (8). The contrasting results observed by us in the response to *M. avium* infection by $Rag^{-/-}\gamma c^{-/-}$ mice must rely on the strict dependence of IFN-γ by the immune response to Mtb infection. Indeed Mtb-infected $Rag^{-/-}$ mice although more resistant, succumbed to infection only 2 weeks after $Rag^{-/-}\gamma c^{-/-}$ and $Rag^{-/-}$IFN-$\gamma^{-/-}$ mice (8). These data suggest that while minimal amounts of IFN-γ are not sufficient to induce protection to Mtb infection it appears to be enough to confer a small, albeit significant protection to *M. avium* infection. Once again this highlights the great opportunity that *M. avium* affords to study the effects of IFN-γ during the chronic response.

In the quest to search for an innate-non NK cell source of IFN-γ we first focused on myeloid cells, namely macrophages Although controversial, a significant bulk of literature point myeloid cells as innate IFN-γ producers suggesting that IFN-γ can activate macrophages in an autocrine fashion (reviewed in (9)). We searched for such cells using two IFN-γ-reporter mice (Rag.Yeti and Great mice) either before or after *M. avium* infection ranging from very early time points to 30 days post infection and failed to detect any IFN-γ-producing myeloid cell. Our data suggest that *M. avium* infection is not able to trigger IFN-γ-production by any myeloid cell, contributing to the current of thought which argues that myeloid cells are not IFN-γ producers. Indeed it has been suggested that much of the previous studies arguing for myeloid cells to be able to produce IFN-γ resulted from minute numbers of contaminating NK cells and/or different subsets of T cells (10).

1.2. IFN-γ^{+}Thy1.2^{+}/non-NK cells mediated protection

Our results have shown that a particular small population from hematopoietic origin, characterized by the expression of Thy1.2 and the absence of NK, T, and even myeloid cell markers are capable to produce IFN-γ particularly in the liver and contribute to the *M. avium* proliferation control in this organ. These cells, hereafter termed Thy1.2^{+}/non-NK cells for simplicity, were further characterized by the surface expression of Sca-1, and intermediate levels of MHCII. Despite the lack of the γc chain, these cells expressed CD127 (IL-7Rα). However, we have not explored this finding further and we do not know whether IL-7Rα might be binding to

other receptor subunit. In addition Thy1.2$^+$/non-NK cells also expressed the transcription factors *Id2* and *Zbtb16* although the latter was only detected in the liver but not in the spleen (Fig 1).

Although we were not able to identify the precise phenotype/origin of the IFN-γ-producing Thy1.2$^+$/non-NK cells, our experiments point to a population belonging to the ILC lineage, however further work is required in order to clarify it. ILCs development requires signaling either through IL-7R or IL15-R, which are impaired in the Rag$^{-/-}$γc$^{-/-}$ mice. We hypothesized that the Thy1.2$^+$ cell population found in Rag$^{-/-}$γc$^{-/-}$ animals might be an ILC precursor blocked in their development due to the lack of γc signaling. This hypothesis was strengthened by the finding of the expression of *Zbtb16* (PLZF) in the liver, known to be transiently expressed in ILCP stage of the ILC development. At the same time, the absence of PLZF in the spleen suggests that in this organ the Thy1.2$^+$/non-NK cells might not represent the same population as in the liver, or the ILC development arrest was prior to the PLZF stage. In Rag$^{-/-}$ mice, it is conceivable that the Thy1.2$^+$/non-NK cells additionally include mature ILCs since the γc signaling is not impaired in these animals.

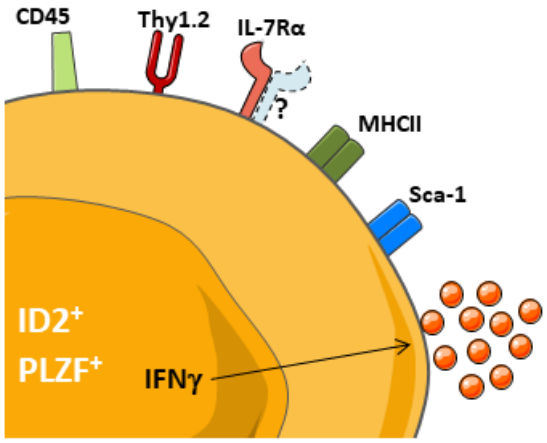

Figure 1. Schematic representation of the IFN-γ- producer Thy1.2$^+$/non-NK/non-T cells in the liver.

ILCs are definitely a heterogeneous population. Even within the same subset there can be considerable differences depending on the microenvironment as exemplified by the distinct ILC1 subset described in the salivary glands by Cortez and colleagues (11). Although the involvement of non-NK ILCs in the response to mycobacterial infections is not known, it has been described that ILC1s capable of producing high levels of IFN-γ and TNF-α contribute to resistance to the intracellular parasite *Toxopasma gondii* in the intestine (12). Given the high dependence on these two cytokines during the immune response to mycobacterial infections it would be interesting to

ascertain whether TNF-α can also be produced by the IFN-γ$^+$Thy1.2$^+$/non-NK cells and study its hypothetical contribution for the *M. avium* proliferation control in lymphopenic mice.

One important feature that differentiates NK cells from the remaining ILCs is the fact that the former are circulating cells while the latter are mostly tissue-resident cells. It has been proposed that this characteristic might provide an immediate source of IFN-γ in response to IL-12 by ILC1s while NK cells represent a delayed source of IFN-γ due to the time required for recruitment into the affected tissues (13). This was suggested to be relevant to the control of a viral infection in the liver (13) although, given the slow growing rates of most *Mycobacterium sp* one could speculate that the small delay of NK cells might not be as relevant as for the control of viral replication.

The study of ILC development is still an expanding field. There are several uncertainties particularly on the branching stages of the different ILCs subsets. Moreover the high plasticity among the different ILC subsets increases the challenge. ILC3s were reported to be able to convert into ILC1s (14) and it has recently been suggested that ILC1s can be converted back into ILC3s (15). In addition to ILC3s, ILC2s have also been described to be able to convert into IFN-γ-producers ILC1s, both in human and mouse (16-18). This conversion occurs in response to increased expression of IL-12 and IL-1β acting on ILC2s with a subsequent down-regulation of Gata-3 and up-regulation of T-bet, the IFN-γ master transcription factor (16-18). Curiously, it was through the analysis of MSDM patients with IL-12RBβ1 deficiencies which failed to convert ILC2s into ILC1s that highlighted the relevance of IL-12 for the conversion process (16). TSLP signals through the heterodimer TSLPR and IL-7Rα (19) and together with IL-25 and IL-33 drive ILC2s differentiation (20). Interestingly it has been reported that in T/B cell lineage differentiation TLSP can partially compensate for the absence of IL-7 signaling (21). In our model, the IFN-γ-producers Thy1.2$^+$/non-NK cells are IL-7Rα$^+$, and in fact this receptor is expressed in increased amounts in Rag$^{-/-}$γc$^{-/-}$ animals as compared to Rag$^{-/-}$ mice. Despite the lack of IL-7 signaling which is known to be required for the ILC2 development, it is tempting to speculate that TSLP might be signaling through the TSLPR/IL-7Rα heterodimer and driving ILC2 differentiation, which given the production of IL-12 and IL-1β by the infected macrophages (known to occur upon *M. avium* infection) could be promoting the conversion of ILC2s into the IFN-γ-producing Thy1.2$^+$/non-NK cells. The caveat of this hypothesis is the fact that we find IFN-γ-producing Thy1.2$^+$/non-NK cells in non-infected animals where the levels of IL-12 and IL-1β must be rather low. Although ILC2s are associated with the response to allergic responses and helminth infections, it is known that

TNF-α, a pro-inflammatory cytokine widely produced in the response to mycobacterial infections, can lead to increased TLSP production (22, 23). It would be interesting to know whether TSLP expression in *M. avium*-infected Rag$^{-/-}$γc$^{-/-}$ mice is increased.

In humans one of the natural routes of entry of *M. avium* is through the intestinal track which is an organ particularly enriched in ILCs, hence it would be interesting to study the effect of ILCs under such conditions. Regardless of what type of cell the IFN-γ producer Thy1.2^{+}/non-NK cell is, the most relevant conclusion taken on chapter II is the fact that very small amounts of IFN-γ seem to be enough to provide protection in the livers of immunocompromised *M. avium* infected mice.

1.3. IFN-γ mediated macrophage activation

Although IFN-γ acts on multiple cell types, the genetic MIIG model used here (chapter III) allowed us to clarify the specific role that this cytokine exerts over the macrophage, the main host cell of mycobacteria. Upon *M. avium* infection we found a protective immune response in the MIIG mouse model that could not be seen in the genetic-disrupted IFN-γ mice due to the lack of signaling in every cell of the host including the macrophage. Here we confirmed the importance of IFNγ for the resistance to *M. avium* infection (4, 24) and granuloma development (chapter II (25) and (4, 26, 27)) however we also show that both effects can be independent of the IFN-γ capacity to activate macrophages (chapter III). These results were somehow surprising. The direct microbicidal effect that IFN-γ exerts over the infected macrophages was established in the early 80's by Carl Nathan through the exogenous addition of IFN-γ to infected macrophages (28), and reproduced countless times by laboratories all over the world. Hence the direct microbicidal effect exerted by IFN-γ over infected macrophages is undeniable. Indeed MIIG mice displayed increased susceptibility over the WT controls to infection by the protozoan parasites *Leishmania major*, *Toxoplasma gondii* or *Trypanosoma cruzi*, all having macrophages as their host cell (29). On the other hand in LCMV infection that develops a host immune response with modest IFN-γ influence, MIIG and WT mice exhibited similar viral loads (29). Preliminary data from our laboratory showed that the resistance of MIIG mice to infection was not reproduced with an aerogenic infection with Mtb, which may be due to the higher dependence of IFN-γ by the host infected with Mtb over *M. avium*. In contrast to *M. avium*, Mtb proliferation control in the murine model is highly dependent on NO produced by iNOS which is mainly triggered by the action of IFN-γ on the infected macrophages, explaining the different requirement of IFN-γ by the two

mycobacterial species. Nevertheless that does not imply that any additional antimicrobial pathway that might be identified using the *M. avium* model may not be relevant in the control of other infectious agents namely Mtb.

In the liver, MIIG mice were able to restrict *M. avium* proliferation even better than WT mice at later time points, which was in contrast to what happened in the spleen. We observed that the lack of bacterial growth restriction at 120 dpi in the spleen was concomitant with an exacerbation of neutrophil numbers (not observed in the livers). At later time points neutrophils can be deleterious to the host (30) and we speculate that might be the case here since we observed greatly enlarged spleens with purulent foci. It has been shown that IL-17 can lead to neutrophil accumulation in the infected site (31, 32) hence it would be interesting to explore the role of Th17 cells in the MIIG context and whether that can underlie the differences between the liver and the spleen.

1.4. TNF-α compensatory mechanisms

The contrasting effects of a complete lack of IFNγ and the MIIG transgenic can be explained by the action of IFNγ in cells other than the macrophage and/or a compensatory mechanism developing in the latter. We found that the number of TNF-α-producing cells is drastically augmented in infected MIIG animals and that this cytokine mediates the protection observed in these animals. We observed that both iron restriction by the ferritin complex and NOX2-induced ROS were enhanced in infected MIIG mice. Our results suggest that these two antimicrobial mechanisms were induced by the increased expression of TNF-α. *M. avium* is not controlled by the iNOS-derived NO (33), and despite superoxide production has been observed by infected macrophages in vitro, its role in mycobacterial-infected mice is not clear. To understand whether NOX-induced ROS production might be mediating *M. avium* growth restriction in mice lacking IFN-γ signaling on macrophages, we aim to cross MIIG animals with phox-deficient mice. In vitro experiments have shown that ROS production by infected macrophages is dependent on TNF-α which is induced in increased amounts by low virulent strains of *M. avium* as the one used in this thesis (34, 35). Despite lacking a direct correlation, our work points the increased TNF-α expression in infected MIIG mice to be responsible for the higher ROS content on macrophages. This hypothetical anti-microbial mechanism deserves to be investigated in the future. Although in the murine model the anti-mycobacterial role of NOX2 is not obvious, in humans it is clear that deficiencies in the NOX2 complex renders them an increased susceptibility to develop mycobacterial disease (36) which suggests that ROS production can confer protection to

mycobacterial infection. It would be interesting to understand whether TNF-α can mediate the dependence of ROS for the control of the infection observed in humans.

M. avium-induced granulomata in the absence of IFN-γ-macrophage signaling is characterized by a greater number of granulomas with enlarged size reflecting the increased accumulation of both macrophages and lymphocytes which contrasts with the granulomata developed in the complete absence of IFN-γ (Fig 2). The increased cellularity observed on granulomas from MIIG mice may result from increased recruitment as well as improved survival. The latter is particularly likely as macrophages in the granulomas of MIIG mice lack the production of NO and this molecule may lead to reduced T cell responses in infected animals (33, 37).

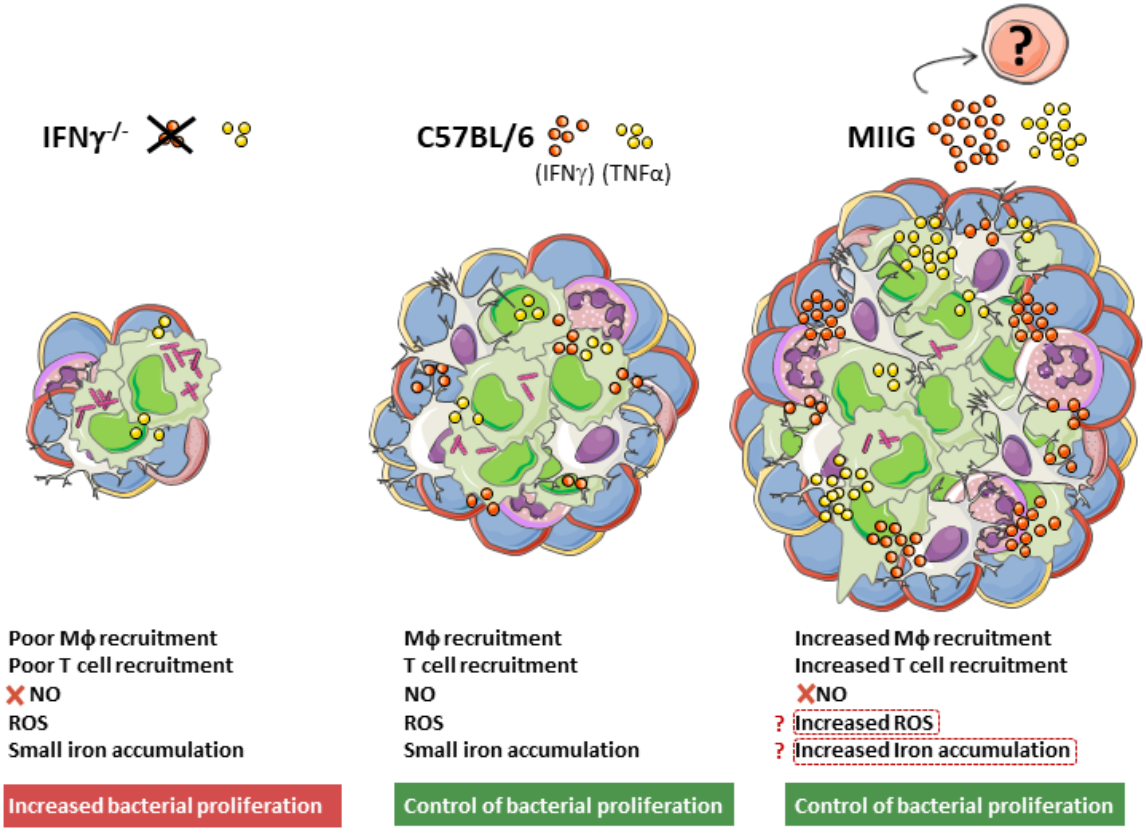

Figure 2. Schematic representation of the granulomas developed by *M. avium* -infected IFN-γ$^{-/-}$, C57BL/6 (WT) and MIIG mice. The nature of the cell population(s) responding to IFN-γ in MIG mice was not identified so far.

TNF-α is involved in promoting granuloma assembly and in the maintenance of their integrity (38, 39). As so we did observe increased granuloma cellularity in the MIIG mice, however we also observed granulomas (though less compacted) and increased cellular accumulation in the livers of MIIG mice lacking TNF-α production (MIIG.TNF-α$^{-/-}$). Unlike the induction of antimicrobial activity in macrophages, increased TNF-α production does not seem to explain the capacity to form granulomas in the absence of IFN-γ-dependent macrophage activation. Instead, the action

of IFN-γ in cells other than the macrophage might underlie the well-developed granuloma structures observed in MIIG mice. Indeed, most cells express receptors for this cytokine (40) and some may respond to it by promoting the inflammatory accumulation of mononuclear phagocytes to form granulomas. Strengthening this hypothesis, we observed that in the response to *M. avium* infection, MIIG mice lacking TNF-α production whose granulomata exhibit increased cellular accumulations, express even higher amounts of IFN-γ$^+$CD4$^+$ T cells when compared to MIIG animals (data not shown). The nature of the cell population(s) responding to IFN-γ and consequently modulating the inflammatory recruitment of the macrophages to MIIG granulomas is a subject definitely worthy to be explored. Desvignes and colleagues have already provided evidence for non-hematopoietic cells in IFN-γ-dependent immune response to mycobacteria (41). These authors found that in the absence of IFN-γR1 on non-hematopoietic cells, Mtb infected mice developed severe lung inflammation, increase bacterial loads and succumbed to infection (41).

In summary we show here that IFNγ may have multiple cell targets in addition to the macrophage during an immune response to infection and that in some instances, lack of IFNγ-mediated macrophage activation may be compensated by the action of TNF-α. Importantly we provided the unexpected result that IFN-γ-mediated macrophage activation is not pivotal for *M. avium* proliferation control nor for granuloma assembly.

2. Role of hypoxia in the development of granuloma central necrosis

Granuloma necrosis is of crucial importance for the development of mycobacterial disease, not only because it allows for the bacillus to disseminate to other tissues but because when it occurs in the lung it can promote person-to-person spread. Despite its relevance for the outcome of the disease, the mechanisms leading to the caseous granuloma are still poorly understood. It is already well established that rabbits, guinea pigs and non-human primates develop granuloma necrotic lesions similar to the ones observed in the humans, yet the vast majority of the fundamental research is done in the mouse model and most strains do not develop caseous necrosis. In the early 2000's a granuloma-inducing necrosis model in the livers of the C57BL/6 mouse using a low dose of infection of the virulent *M. avium* 25291 strain through the intravenous route was described by our group (42). Curiously using the same settings but with a higher dose of infection, mice do not develop granuloma necrosis. The correlation between the development of necrotizing granulomas and the hypoxic microenvironment was suggested long

ago, although it was only one decade ago that it was shown that granulomas from Mtb infected rabbits, guinea pigs and non-human primates are in fact under hypoxic conditions. The authors have shown the hypoxic environment by using a probe to perform direct measurements of pO_2 in the granulomas and also by immunohistochemical detection of pimonidazole that stains under severe hypoxic conditions (43).

In 2015, using the previously developed mouse model of *M. avium* infection that develops granuloma necrosis, our group has established a role for hypoxia in the development of caseous necrosis in the liver (1). Through the analysis of vascularization and quantification of HIF-1α we have shown evidence that granulomas become hypoxic before the onset of necrosis. The absence of the hypoxia adaptor molecule HIF-1α in the myeloid lineage caused earlier development of necrotic lesions in the liver which coincided with the failure to control *M. avium* proliferation (1). The formation of necrotic granulomas in the lung was established by Ehlers and colleagues through the aerogenic infection of a similar virulent strain of *M. avium* (44). The authors also found evidence of hypoxia surrounding the necrotic lesions of the *M. avium* infected lungs (45). Despite the correlation between hypoxia and granuloma necrosis in *M. avium*-infected C57BL/6 mice, granuloma necrosis in the lungs of C57BL/6 mice infected with the Mtb bacillus has never been detected, nor the involvement of hypoxia in such granulomas (43, 45). In the work developed in chapter IV we tried to assess whether manipulating the granuloma environment by using C57BL/6 mice lacking HIF-1α in the myeloid lineage (mHIF-1$\alpha^{-/-}$) we could promote central necrosis in the lungs in response to Mtb infection. mHIF-1$\alpha^{-/-}$ mice infected with the virulent H37Rv strain of Mtb exhibited strong lung inflammation but failed to develop granuloma necrosis. Moreover mHIF-1$\alpha^{-/-}$ mice were able to control Mtb proliferation during the four months of the experiment, except when infected with a high dose of Mtb and at late stages of infection where mice displayed slightly increased bacterial loads, and eventually begun to succumb around 160 dpi. Our results are in clear contradiction with what was reported by Braverman and colleagues while we were performing these experiments. Braverman has used a similar approach although using the more virulent Erdman strain of Mtb, and observed that mHIF-1$\alpha^{-/-}$ mice quickly succumb to infection (beginning to die around 25 dpi) (46). The authors have identified HIF-1α as a mediator of Mtb-induced IFN-γ response, and found the IFN-γ-induced *Nos2* transcription to be partially dependent on HIF-1α, suggesting the impairment of NO production as critical to control the infection in mHIF1$\alpha^{-/-}$ mice (46, 47). In our work *Nos2* gene expression was similar in both WT and mHIF-1$\alpha^{-/-}$ mice independently of the infection dose and

time of infection. We did detect a small and transient decrease in NOS2^{+} cells quantified through the stain density of the immunochemistry images at 60dpi in mHIF-1$\alpha^{-/-}$ mice but only when infected with high doses of Mtb. Additionally we observed that infected mHIF-1$\alpha^{-/-}$ mice exhibit a significant increase of IFN-γ production which we hypothesize that may be compensating any reduction on IFN-γ-induced *Nos2* transcription caused by the absence of HIF-1$\alpha^{-/-}$. Taken together this might justify the bacterial proliferation control observed in mHIF-1$\alpha^{-/-}$ mice. We have also detected an increase of IL-17 production by CD4^{+} T cells in the lungs of the Mtb-infected mHIF-1$\alpha^{-/-}$ mice, which may underlie the increased inflammation in their lungs as this cytokine is known to induce neutrophil recruitment (31, 48). Indeed we detected a slight increase of neutrophil numbers that may be contributing to the immunopathology observed in the infected mHIF-1$\alpha^{-/-}$ mice.

In conclusion while in the absence of mHIF-1α, Mtb-infected C57BL/6 mice did not developed granuloma necrosis, HIF-1α in the myeloid compartment is certainly required to limit cellular infiltration which under certain conditions may prevent the occurrence of granuloma central necrosis.

The different works enclosed in this thesis tackled the protective immunity to mycobacterial infections and granuloma development through different perspectives and in distinct phases of the immune response providing new insights that may be useful to devise new strategies to cope with mycobacterial infection.

3. References

1. Cardoso, M. S., T. M. Silva, M. Resende, R. Appelberg, and M. Borges. 2015. Lack of the Transcription Factor Hypoxia-Inducible Factor 1alpha (HIF-1alpha) in Macrophages Accelerates the Necrosis of Mycobacterium avium-Induced Granulomas. *Infection and immunity* 83: 3534-3544.
2. Cooper, A. M., D. K. Dalton, T. A. Stewart, J. P. Griffin, D. G. Russell, and I. M. Orme. 1993. Disseminated tuberculosis in interferon gamma gene-disrupted mice. *The Journal of experimental medicine* 178: 2243-2247.
3. Flynn, J. L., J. Chan, K. J. Triebold, D. K. Dalton, T. A. Stewart, and B. R. Bloom. 1993. An essential role for interferon gamma in resistance to Mycobacterium tuberculosis infection. *The Journal of experimental medicine* 178: 2249-2254.
4. Florido, M., A. S. Goncalves, R. A. Silva, S. Ehlers, A. M. Cooper, and R. Appelberg. 1999. Resistance of virulent Mycobacterium avium to gamma interferon-mediated antimicrobial activity suggests additional signals for induction of mycobacteriostasis. *Infection and immunity* 67: 3610-3618.
5. Schoenborn, J. R., and C. B. Wilson. 2007. Regulation of interferon-gamma during innate and adaptive immune responses. *Advances in immunology* 96: 41-101.
6. Scharton, T. M., and P. Scott. 1993. Natural killer cells are a source of interferon gamma that drives differentiation of CD4+ T cell subsets and induces early resistance to Leishmania major in mice. *The Journal of experimental medicine* 178: 567-577.
7. Sher, A., I. P. Oswald, S. Hieny, and R. T. Gazzinelli. 1993. Toxoplasma gondii induces a T-independent IFN-gamma response in natural killer cells that requires both adherent accessory cells and tumor necrosis factor-alpha. *Journal of immunology* 150: 3982-3989.
8. Feng, C. G., M. Kaviratne, A. G. Rothfuchs, A. Cheever, S. Hieny, H. A. Young, T. A. Wynn, and A. Sher. 2006. NK cell-derived IFN-gamma differentially regulates innate resistance and neutrophil response in T cell-deficient hosts infected with Mycobacterium tuberculosis. *Journal of immunology* 177: 7086-7093.
9. Frucht, D. M., T. Fukao, C. Bogdan, H. Schindler, J. J. O'Shea, and S. Koyasu. 2001. IFN-gamma production by antigen-presenting cells: mechanisms emerge. *Trends in immunology* 22: 556-560.

10. Bogdan, C., and U. Schleicher. 2006. Production of interferon-gamma by myeloid cells–fact or fancy? *Trends in immunology* 27: 282-290.

11. Cortez, V. S., L. Cervantes-Barragan, M. L. Robinette, J. K. Bando, Y. Wang, T. L. Geiger, S. Gilfillan, A. Fuchs, E. Vivier, J. C. Sun, M. Cella, and M. Colonna. 2016. Transforming Growth Factor-beta Signaling Guides the Differentiation of Innate Lymphoid Cells in Salivary Glands. *Immunity* 44: 1127-1139.

12. Klose, C. S., M. Flach, L. Mohle, L. Rogell, T. Hoyler, K. Ebert, C. Fabiunke, D. Pfeifer, V. Sexl, D. Fonseca-Pereira, R. G. Domingues, H. Veiga-Fernandes, S. J. Arnold, M. Busslinger, I. R. Dunay, Y. Tanriver, and A. Diefenbach. 2014. Differentiation of type 1 ILCs from a common progenitor to all helper-like innate lymphoid cell lineages. *Cell* 157: 340-356.

13. Weizman, O. E., N. M. Adams, I. S. Schuster, C. Krishna, Y. Pritykin, C. Lau, M. A. Degli-Esposti, C. S. Leslie, J. C. Sun, and T. E. O'Sullivan. 2017. ILC1 Confer Early Host Protection at Initial Sites of Viral Infection. *Cell* 171: 795-808 e712.

14. Klose, C. S., E. A. Kiss, V. Schwierzeck, K. Ebert, T. Hoyler, Y. d'Hargues, N. Goppert, A. L. Croxford, A. Waisman, Y. Tanriver, and A. Diefenbach. 2013. A T-bet gradient controls the fate and function of CCR6-RORgammat+ innate lymphoid cells. *Nature* 494: 261-265.

15. Bernink, J. H., L. Krabbendam, K. Germar, E. de Jong, K. Gronke, M. Kofoed-Nielsen, J. M. Munneke, M. D. Hazenberg, J. Villaudy, C. J. Buskens, W. A. Bemelman, A. Diefenbach, B. Blom, and H. Spits. 2015. Interleukin-12 and -23 Control Plasticity of CD127(+) Group 1 and Group 3 Innate Lymphoid Cells in the Intestinal Lamina Propria. *Immunity* 43: 146-160.

16. Lim, A. I., S. Menegatti, J. Bustamante, L. Le Bourhis, M. Allez, L. Rogge, J. L. Casanova, H. Yssel, and J. P. Di Santo. 2016. IL-12 drives functional plasticity of human group 2 innate lymphoid cells. *The Journal of experimental medicine* 213: 569-583.

17. Ohne, Y., J. S. Silver, L. Thompson-Snipes, M. A. Collet, J. P. Blanck, B. L. Cantarel, A. M. Copenhaver, A. A. Humbles, and Y. J. Liu. 2016. IL-1 is a critical regulator of group 2 innate lymphoid cell function and plasticity. *Nature immunology* 17: 646-655.

18. Silver, J. S., J. Kearley, A. M. Copenhaver, C. Sanden, M. Mori, L. Yu, G. H. Pritchard, A. A. Berlin, C. A. Hunter, R. Bowler, J. S. Erjefalt, R. Kolbeck, and A. A. Humbles. 2016.

Inflammatory triggers associated with exacerbations of COPD orchestrate plasticity of group 2 innate lymphoid cells in the lungs. *Nature immunology* 17: 626-635.

19. Kang, J., and M. Coles. 2012. IL-7: the global builder of the innate lymphoid network and beyond, one niche at a time. *Seminars in immunology* 24: 190-197.
20. Spits, H., D. Artis, M. Colonna, A. Diefenbach, J. P. Di Santo, G. Eberl, S. Koyasu, R. M. Locksley, A. N. McKenzie, R. E. Mebius, F. Powrie, and E. Vivier. 2013. Innate lymphoid cells–a proposal for uniform nomenclature. *Nature reviews. Immunology* 13: 145-149.
21. Chappaz, S., L. Flueck, A. G. Farr, A. G. Rolink, and D. Finke. 2007. Increased TSLP availability restores T- and B-cell compartments in adult IL-7 deficient mice. *Blood* 110: 3862-3870.
22. He, R., and R. S. Geha. 2010. Thymic stromal lymphopoietin. *Annals of the New York Academy of Sciences* 1183: 13-24.
23. Redhu, N. S., A. Saleh, A. J. Halayko, A. S. Ali, and A. S. Gounni. 2011. Essential role of NF-kappaB and AP-1 transcription factors in TNF-alpha-induced TSLP expression in human airway smooth muscle cells. *American journal of physiology. Lung cellular and molecular physiology* 300: L479-485.
24. Appelberg, R., A. G. Castro, J. Pedrosa, R. A. Silva, I. M. Orme, and P. Minoprio. 1994. Role of gamma interferon and tumor necrosis factor alpha during T-cell-independent and -dependent phases of Mycobacterium avium infection. *Infection and immunity* 62: 3962-3971.
25. Resende, M., M. S. Cardoso, A. R. Ribeiro, M. Florido, M. Borges, A. G. Castro, N. L. Alves, A. M. Cooper, and R. Appelberg. 2017. Innate IFN-gamma-Producing Cells Developing in the Absence of IL-2 Receptor Common gamma-Chain. *Journal of immunology* 199: 1429-1439.
26. Pearl, J. E., B. Saunders, S. Ehlers, I. M. Orme, and A. M. Cooper. 2001. Inflammation and lymphocyte activation during mycobacterial infection in the interferon-gamma-deficient mouse. *Cellular immunology* 211: 43-50.
27. Murray, P. J., R. A. Young, and G. Q. Daley. 1998. Hematopoietic remodeling in interferon-gamma-deficient mice infected with mycobacteria. *Blood* 91: 2914-2924.
28. Nathan, C. F., H. W. Murray, M. E. Wiebe, and B. Y. Rubin. 1983. Identification of interferon-gamma as the lymphokine that activates human macrophage oxidative

metabolism and antimicrobial activity. *The Journal of experimental medicine* 158: 670-689.

29. Lykens, J. E., C. E. Terrell, E. E. Zoller, S. Divanovic, A. Trompette, C. L. Karp, J. Aliberti, M. J. Flick, and M. B. Jordan. 2010. Mice with a selective impairment of IFN-gamma signaling in macrophage lineage cells demonstrate the critical role of IFN-gamma-activated macrophages for the control of protozoan parasitic infections in vivo. *Journal of immunology* 184: 877-885.
30. Zhang, X., L. Majlessi, E. Deriaud, C. Leclerc, and R. Lo-Man. 2009. Coactivation of Syk kinase and MyD88 adaptor protein pathways by bacteria promotes regulatory properties of neutrophils. *Immunity* 31: 761-771.
31. Cruz, A., A. G. Fraga, J. J. Fountain, J. Rangel-Moreno, E. Torrado, M. Saraiva, D. R. Pereira, T. D. Randall, J. Pedrosa, A. M. Cooper, and A. G. Castro. 2010. Pathological role of interleukin 17 in mice subjected to repeated BCG vaccination after infection with Mycobacterium tuberculosis. *The Journal of experimental medicine* 207: 1609-1616.
32. Torrado, E., and A. M. Cooper. 2010. IL-17 and Th17 cells in tuberculosis. *Cytokine & growth factor reviews* 21: 455-462.
33. Gomes, M. S., M. Florido, T. F. Pais, and R. Appelberg. 1999. Improved clearance of Mycobacterium avium upon disruption of the inducible nitric oxide synthase gene. *Journal of immunology* 162: 6734-6739.
34. Sarmento, A. M., and R. Appelberg. 1995. Relationship between virulence of Mycobacterium avium strains and induction of tumor necrosis factor alpha production in infected mice and in in vitro-cultured mouse macrophages. *Infection and immunity* 63: 3759-3764.
35. Sarmento, A., and R. Appelberg. 1996. Involvement of reactive oxygen intermediates in tumor necrosis factor alpha-dependent bacteriostasis of Mycobacterium avium. *Infection and immunity* 64: 3224-3230.
36. Bustamante, J., A. A. Arias, G. Vogt, C. Picard, L. B. Galicia, C. Prando, A. V. Grant, C. C. Marchal, M. Hubeau, A. Chapgier, L. de Beaucoudrey, A. Puel, J. Feinberg, E. Valinetz, L. Janniere, C. Besse, A. Boland, J. M. Brisseau, S. Blanche, O. Lortholary, C. Fieschi, J. F. Emile, S. Boisson-Dupuis, S. Al-Muhsen, B. Woda, P. E. Newburger, A. Condino-Neto, M. C. Dinauer, L. Abel, and J. L. Casanova. 2011. Germline CYBB mutations that

selectively affect macrophages in kindreds with X-linked predisposition to tuberculous mycobacterial disease. *Nature immunology* 12: 213-221.

37. Cooper, A. M., L. B. Adams, D. K. Dalton, R. Appelberg, and S. Ehlers. 2002. IFN-gamma and NO in mycobacterial disease: new jobs for old hands. *Trends in microbiology* 10: 221-226.

38. Smith, D., H. Hansch, G. Bancroft, and S. Ehlers. 1997. T-cell-independent granuloma formation in response to Mycobacterium avium: role of tumour necrosis factor-alpha and interferon-gamma. *Immunology* 92: 413-421.

39. Flynn, J. L., M. M. Goldstein, J. Chan, K. J. Triebold, K. Pfeffer, C. J. Lowenstein, R. Schreiber, T. W. Mak, and B. R. Bloom. 1995. Tumor necrosis factor-alpha is required in the protective immune response against Mycobacterium tuberculosis in mice. *Immunity* 2: 561-572.

40. Bach, E. A., M. Aguet, and R. D. Schreiber. 1997. The IFN gamma receptor: a paradigm for cytokine receptor signaling. *Annual review of immunology* 15: 563-591.

41. Desvignes, L., and J. D. Ernst. 2009. Interferon-gamma-responsive nonhematopoietic cells regulate the immune response to Mycobacterium tuberculosis. *Immunity* 31: 974-985.

42. Florido, M., A. M. Cooper, and R. Appelberg. 2002. Immunological basis of the development of necrotic lesions following Mycobacterium avium infection. *Immunology* 106: 590-601.

43. Via, L. E., P. L. Lin, S. M. Ray, J. Carrillo, S. S. Allen, S. Y. Eum, K. Taylor, E. Klein, U. Manjunatha, J. Gonzales, E. G. Lee, S. K. Park, J. A. Raleigh, S. N. Cho, D. N. McMurray, J. L. Flynn, and C. E. Barry, 3rd. 2008. Tuberculous granulomas are hypoxic in guinea pigs, rabbits, and nonhuman primates. *Infection and immunity* 76: 2333-2340.

44. Ehlers, S., J. Benini, H. D. Held, C. Roeck, G. Alber, and S. Uhlig. 2001. Alphabeta T cell receptor-positive cells and interferon-gamma, but not inducible nitric oxide synthase, are critical for granuloma necrosis in a mouse model of mycobacteria-induced pulmonary immunopathology. *The Journal of experimental medicine* 194: 1847-1859.

45. Aly, S., K. Wagner, C. Keller, S. Malm, A. Malzan, S. Brandau, F. C. Bange, and S. Ehlers. 2006. Oxygen status of lung granulomas in Mycobacterium tuberculosis-infected mice. *The Journal of pathology* 210: 298-305.

46. Braverman, J., K. M. Sogi, D. Benjamin, D. K. Nomura, and S. A. Stanley. 2016. HIF-1alpha Is an Essential Mediator of IFN-gamma-Dependent Immunity to Mycobacterium tuberculosis. *Journal of immunology* 197: 1287-1297.

47. Braverman, J., and S. A. Stanley. 2017. Nitric Oxide Modulates Macrophage Responses to Mycobacterium tuberculosis Infection through Activation of HIF-1alpha and Repression of NF-kappaB. *Journal of immunology* 199: 1805-1816.

48. Umemura, M., A. Yahagi, S. Hamada, M. D. Begum, H. Watanabe, K. Kawakami, T. Suda, K. Sudo, S. Nakae, Y. Iwakura, and G. Matsuzaki. 2007. IL-17-mediated regulation of innate and acquired immune response against pulmonary Mycobacterium bovis bacille Calmette-Guerin infection. *Journal of immunology* 178: 3786-3796.